9-2009

Muscular Properties and Balance Control in Older Adults

Christopher James Hasson
University of Massachusetts Amherst, cjhasson@gmail.com

MUSCULAR PROPERTIES AND BALANCE CONTROL IN OLDER ADULTS

A Dissertation Presented

by

CHRISTOPHER J. HASSON

Submitted to the Graduate School of the
University of Massachusetts Amherst in partial fulfillment
of the requirements for the degree of

DOCTOR OF PHILOSOPHY

SEPTEMBER 2009

Kinesiology

MUSCULAR PROPERTIES AND BALANCE CONTROL IN OLDER ADULTS

A Dissertation Presented

by

CHRISTOPHER J. HASSON

Approved as to style and content by:

_____
Graham E. Caldwell, Chair

_____
Richard E. A. Van Emmerik, Member

_____
Brian Umberger, Member

_____
Sundar Krishnamurty, Member

_____
Patty S. Freedson, Department Chair
Department of Kinesiology

DEDICATION

To my wonderful wife, who made anything seem possible, no matter how daunting the task. I also dedicate this dissertation to my loving parents, who have always supported my endeavors – whether wise or foolish.

ACKNOWLEDGMENTS

The work presented in this dissertation was the result of the efforts of numerous people. These include my advisors, my dissertation committee, fellow graduate students, and willing study participants. In particular, I offer my deepest appreciation to my advisor, Graham Caldwell, who provided me with years of guidance and seemingly never grew tired of editing my horrible spelling and terrible grammar. I am thankful for his extraordinary ability to find the clearest and most concise way of making a statement, which undoubtedly improved my writing and oral presentation skills. I also appreciate his attention to detail, encouraging me to only submit my very best work. I am also very thankful to have met Richard Van Emmerik, who introduced me to the area of motor control, provided me with new analysis tools, and gave me a new way to think about human movement problems. I appreciate his incredible approachability and his willingness to listen to my ideas – no matter how crazy they seem. He never fails to provide the "big picture", which was invaluable when I become lost in the details. I also thank my other dissertation committee members, including Sundar Krishnamurty, who helped me understand the way engineers think, and John Buonaccorsi, who provided assistance with the multiple regression analysis. I am indebted to my fellow lab mates. Ross Miller spent many hours collecting the dynamometer data, while Luis Rosado and Catherine Gariépy assisted with the array of balance data collections. Finally, I owe thanks to all of the study participants, especially the older subjects who endured repeated visits to the laboratory and many hours of taxing experimental procedures.

ABSTRACT

MUSCULAR PROPERTIES AND BALANCE CONTROL IN OLDER ADULTS

SEPTEMBER 2009

CHRISTOPHER J. HASSON, B.S., UNIVERSITY OF DELAWARE

M.S., BALL STATE UNIVERSITY

Ph.D., UNIVERSITY OF MASSACHUSETTS AMHERST

Directed by: Graham E. Caldwell

The goal of this dissertation was to understand the role of age-related changes in muscle mechanical properties in the control of upright posture in humans. First, a methodology for estimating subject-specific muscle properties in healthy young and older individuals was developed. Magnetic resonance and ultrasound imaging were used in conjunction with dynamometer experiments, musculoskeletal modeling, and numerical optimization to estimate the properties of the dorsiflexor and individual plantarflexor (gastrocnemius and soleus) muscles for 12 young and 12 older adults (balanced for gender). With aging there were declines in maximal isometric strength and increases in series-elastic stiffness in the male subjects, but no differences in the female subjects. Regardless of gender, there were age-related changes in the shape of the force-velocity relation, such that the older subjects produced less relative force during both concentric and eccentric muscle contractions. The second study tested the balance abilities of the same subjects under a variety of static (quiet stance, leaning forward/backward) and dynamic (swaying at preferred/imposed frequencies, maximal reaching, external perturbation) conditions. The older adults performed more poorly on most of the balance

tasks. While maximal isometric force made a smaller than expected contribution to predicting balancing ability, the force-length, force-velocity and force-extension properties of the muscles were all predictive of the age-related declines in balance control, explaining ~40% of the variance as independent predictors and ~50% when these factors were combined. Finally, a feedback-driven inverted pendulum model of postural control was developed, which incorporated realistic representations of young and old dorsiflexor and individual plantarflexor muscles using the previously estimated mechanical properties. A sensitivity analysis was performed by manipulating the properties of the plantarflexor muscles. The balancing ability of the model was most influenced by the optimal length of the contractile component and the slack length of the series elastic component of the plantarflexor muscle models. The quiet stance model highlighted the importance of the force-length relation of muscle to the stabilization of upright posture. This dissertation demonstrated that there are age-related changes in the dorsi- and plantarflexor mechanical properties, and these changes are associated with the declines in postural control that accompany aging.

TABLE OF CONTENTS

Page

ACKNOWLEDGMENTS v

ABSTRACT vi

LIST OF TABLES xii

LIST OF FIGURES xiv

CHAPTER

1. INTRODUCTION 1

    1.1 Musculotendon Mechanical Properties, Aging, and Postural Control 3
    1.2 Specific Aims 5
        1.2.1 Chapter 2: Muscle Mechanical Properties and Aging 5
        1.2.2 Chapter 3: Mechanical Properties and Postural Control 5
        1.2.3 Chapter 4: Musculoskeletal Model of Postural Control 6
    1.3 Summary 7

2. MUSCLE MECHANICAL PROPERTIES AND AGING 8

    2.1 Introduction 8
    2.2 Methods 11
        2.2.1 Overall Experimental Design 11
        2.2.2 Ultrasound Experiment 12
            2.2.2.1 Experimental Setup 12
            2.2.2.2 Protocol 13
            2.2.2.3 Video Capture and Preprocessing 14
            2.2.2.4 Tracking of Aponeurosis 14
            2.2.2.5 Data Processing 14
        2.2.3 Dynamometer Experiments 17
            2.2.3.1 Experimental Setup 17
            2.2.3.2 Protocol 18
            2.2.3.3 Data Reduction and Analysis 19
            2.2.3.4 Adjusting for Co-Activation and Torque-Angle Effects 19
        2.2.4 Magnetic Resonance Imaging (MRI) 20
            2.2.4.1 Experimental Setup 20
            2.2.4.2 Data Reduction and Analysis 20
            2.2.4.3 Plantarflexor PCSA Calculations 22
            2.2.4.4 Moment Arm Measurement 23
            2.2.4.5 Moment Arm Correction for Retinaculum Stretch 25
        2.2.5 Modeling, Simulation, and Optimization 26

2.2.5.1 Model of Musculotendon Dynamics....27
2.2.5.2 Muscle Excitation and Activation....27
2.2.5.3 Construction of Model Torque-Angle Curve....28
2.2.5.4 Construction of Model Torque-Extension Relation....28
2.2.5.5 Construction of Model Torque-Angular Velocity Curve29
2.2.5.6 Optimization Procedure....30
2.2.5.7 Muscle Model Parameter Constraints....32
2.2.5.8 Fitness Criteria (Minimizing the Cost)....33
2.2.5.8.1 Phase 1....33
2.2.5.8.2 Phase 2....35
2.2.5.9 Comparison with Experimental Data....36
2.2.5.10 Statistics....37
2.3 Results....38
2.3.1 Ultrasound Experiment....38
2.3.2 Magnetic Resonance Imaging (MRI)....41
2.3.3 Dynamometer Experiments....42
2.3.4 Modeling Results....47
2.3.4.1 General....47
2.3.4.2 Maximal Isometric Force....50
2.3.4.3 Force-Length and Slack Length....51
2.3.4.4 Force-Extension Shape Coefficients....51
2.3.4.5 Force-Velocity....53
2.3.4.6 Comparison with Experimental Data....55
2.4 Discussion....58
2.4.1 Experimental Studies....59
2.4.1.1 Ultrasound Experiments....59
2.4.1.2 Magnetic Resonance Imaging (MRI)....61
2.4.1.3 Dynamometer Experiments....62
2.4.1.3.1 Torque-Angle Properties....62
2.4.1.3.2 Torque-Velocity Properties....65
2.4.2 Individual Muscle Mechanical Properties....66
2.4.2.1 Maximal Isometric Force....66
2.4.2.2 Force-Length....70
2.4.2.3 Series Elasticity....70
2.4.2.4 Force-Velocity....72
2.4.2.5 Maximal Shortening Velocity....74
2.4.3 Limitations....75
2.4.4 Conclusions....77

3. MUSCULAR PROPERTIES AND POSTURAL CONTROL....79

3.1 Introduction....79
3.2 Methods....82
3.2.1 Overall Experimental Design....82
3.2.2 Experimental Setup....82
3.2.2.1 Ground Reaction Forces and Marker Kinematics....82

3.2.2.2 External Perturbation Backboard / Pendulum System....83
3.2.2.3 Safety Considerations....85
3.2.2.4 Sampling....86
3.2.3 Protocol....86
3.2.3.1 Quiet Stance....88
3.2.3.2 Static Leaning....88
3.2.3.3 Rhythmic Sway....88
3.2.3.4 Maximum Reaching....89
3.2.3.5 External Perturbation....89
3.2.4 Data Analysis....90
3.2.4.1 Quiet Stance and Leaning Variables....92
3.2.4.2 Rhythmic Sway Variables....93
3.2.4.3 Reaching Variables....94
3.2.4.4 External Perturbations Variables....95
3.2.5 Statistics....95
3.2.5.1 Balance Measures....95
3.2.5.2 Regression Analysis....96
3.2.5.2.1 Individual Mechanical Properties....96
3.2.5.2.2 Multiple Mechanical Properties....97
3.3 Results....99
3.3.1 Balance Measures....99
3.3.2 Regression Analysis: Individual Mechanical Properties....103
3.3.2.1 Static Balance Conditions....104
3.3.2.2 Dynamic Balance Conditions....106
3.3.3 Multiple Mechanical Properties....110
3.3.3.1 General Multiple Regression Results....110
3.3.3.2 Static Postural Tests....111
3.3.3.3 Dynamic Postural Tests....114
3.4 Discussion....118
3.4.1 Age-Related Differences in Static and Dynamic Balance Conditions....118
3.4.2 Muscle Mechanical Properties and Balance Control....121
3.4.3 Maximal Isometric Force....122
3.4.4 Stiffness of the Series Elastic Components....124
3.4.5 Force-Velocity Characteristics....128
3.4.6 Force-Length Properties....130
3.4.7 Limitations....133
3.4.8 Conclusions....134

4. MUSCULOSKELETAL MODEL OF POSTURAL CONTROL....136

4.1 Introduction....136
4.2 Methods....140
4.2.1 Overall Study Design....140
4.2.2 Skeletal Model....140
4.2.3 Foot-Floor Model....141

4.2.4 Muscle Model 141
4.2.5 Anatomical Model 142
4.2.6 Neural Controller 143
4.2.7 Equations of Motion 147
4.2.8 Optimization Procedure 147
4.2.9 Assessment of Quiet Stance Model 150
4.2.10 Sensitivity Analysis 151
4.3 Results 153
4.3.1 Assessment of Quiet Stance Model 153
4.3.2 Sensitivity Analysis 157
4.4 Discussion 169
4.4.1 Comparison of Optimized Young and Old Model Behavior 169
4.4.2 Model Sensitivity to Changes in Muscle Mechanical Properties 171
4.4.3 Different Control for Young and Older Adults? 178
4.4.4 Novel Aspects of the Postural Model 179
4.4.5 Conclusions 180

5. GENERAL DISCUSSION 182

5.1 Future Study 186
5.2 Final Thoughts 190

APPENDICES

A. ISOVELOCITY AND CO-ACTIVATION ADJUSTMENTS 191

B. MUSCLE MODEL 194

C. OPTIMIZATION COSTS AND MUSCLE PROPERTY CORRELATIONS 201

D. MULTIPLE REGRESSION MODELING PROCEDURE 203

E. QUIET STANCE INVERTED PENDULUM MODEL PROPERTIES 205

BIBLIOGRAPHY 207

LIST OF TABLES

Table		Page
2-1	Subject characteristics.	12
2-2	Parameters describing fits to experimental torque-extension data.	40
2-3	Measured individual muscle volumes, estimated physiological cross-sectional areas (PCSAs), optimal fiber lengths, and pennation angles. Values are Mean ± SD.	41
2-4	Parameters describing fits to the experimental co-activation adjusted torque-angle and torque-angular velocity data.	45
2-5	Optimized muscle mechanical properties.	49
2-6	Maximal extensions and shortening velocities.	52
2-7	Maximal isometric force (P_0) for dorsi- and plantarflexor muscles reported in the literature and the present study.	69
3-1	Balance measures for static postural tasks.	100
3-2	Balance measures for swaying.	102
3-3	Balance measures for reaching and in response to a perturbation.	103
3-4	Linear regression results for static postural variables. Only those with an overall p-value below .05 are shown.	106
3-5	Linear regression results for dynamic postural variables. . Only those with an overall p-value below .05 are shown.	109
3-6	Frequency of appearance of mechanical properties in regression models.	110
3-7	Multiple regression results for static postural tests.	113
3-8	Multiple regression results for dynamic postural tests.	117
4-1	Balance measures characterizing the performance of young and old subjects and the postural control model using sets of young and old mechanical properties	155
4-2	Differences between average mechanical properties for young and older subjects. (Data are from Chapter 2).	159

C-1 Optimization Costs……..... 201

C-2 Correlations (*R*) between muscle mechanical properties……...…. 202

D-1 Best regression models (one of each size up to 9) for predicting the mean rearward CoM position during imposed swaying based on the mechanical properties of the DF muscle.…….……..... 204

LIST OF FIGURES

Figure		Page
2-1	Methodology for measuring musculotendon series elasticity. A: Ultrasound stills from the start (left) and end (right, at MVC) of a dorsi- (top) and plantarflexion (bottom) ramped trial. The white dots indicate points of interest, including a set of reference points near the skin, and a set of points on the central aponeurosis of each muscle. The motion of the points was tracked using an automated cross-correlation algorithm. B: Example of the horizontal displacements of the set of reference points (top) and points on the central aponeurosis for a dorsiflexion trial (thick line = average). C: The visual torque-time template (left) and the actual dorsiflexion torque produced (right). D: The resulting torque vs. extension plot. A second order polynomial was fit to the torque up to 60% MVC, and then extended up to MVC (dashed line).	16
2-2	A: Example of reconstructed muscle volumes of the dorsiflexors (DF), gastrocnemius (GA), and soleus (SO). B: An axial MRI image illustrating the identification of the muscles of interest (left). Inverted image (right) C: Pixel intensity histogram showing the separation of cortical bone/tendon (I), muscle (II), and trabecular bone/adipose tissue (III).	22
2-3	Example of the calculation of the dorsiflexor (DF) and plantarflexor (PF) moment arms (MA) from a sagittal plane MRI image. The pixel intensities were inverted for clarity (right).	25
2-4	Schematic of isometric (Phase 1) and isovelocity (Phase 2) optimization flows. See text for details.	32
2-5	Second-order polynomial fits to the young (solid black lines) and older (broken gray lines) torque-extension data from the ultrasound experiments. The mean ± SD extensions at the peak torque are shown (dot and cross).	40
2-6	Average young (solid lines) and older (dashed lines) torque-angle (left) and torque-angular velocity (right) curves. For each subject group, the measured (thicker lines) and co-activation adjusted (thinner lines) are shown.	43
2-7	Equations representing the best fit between the co-activation adjusted experimental data and second-order polynomials (isometric) and rectangular hyperbolas (isovelocity) for young	

(solid black lines) and older (dashed gray lines). The solid circles positioned on the isometric curves represent the peak isometric torque. For some subjects, the peak did not occur within the subject's range of motion, in these cases the solid circle is position at the end of the range of motion. The isovelocity fits are scaled to the peak isometric torques (solid circles). 44

2-8 Interaction plots for the maximal isometric torque ($T_{0,}$ left) and the coefficient $B_{T\omega}$ for the co-activation adjusted torque-angular velocity relation (right). 46

2-9 Graphical representations of optimized muscle mechanical properties defining the shapes of the contractile-component (CC) force-length (FL) and force-velocity (FV) relations, and the series elastic component (SEC) force-extension (FΔL) relation. Properties for the dorsiflexors (DF), gastrocnemius (GA), and soleus (SO) are shown. The thin gray lines represent data from individual subjects, while the thick black lines represent the mean of the young (solid) and old (dashed) subject groups. Note that x-axis scales are different for the three muscles to allow finer resolution of the curves. 48

2-10 Effects of age, gender, and muscle on selected muscle mechanical properties. 50

2-11 Effects of changing the coefficients describing the Hill rectangular hyperbola. Left: effect of varying a/P_0 from 0.1 to 0.6 while keeping b/L_0 constant at 0.45 s^{-1}. Right: effect of varying b/L_0 from 0.02 to1.22 s^{-1} while keeping a/P_0 constant at 0.25. Both Sides: The optimal fiber length (L_0) was set to 0.15 m and the eccentric plateau was equal to 1.5 P_0. The increment between each line is 0.01. 54

2-12 Comparison between experimental net joint torque-time histories (red curves) and the net joint torques (black curves) predicted using the optimized muscle properties for a representative young and older subject. The top panels are when the dorsiflexors were acting as agonists, and the bottom panels are when the plantarflexors were agonists. The vertical lines denote periods of a constant rate of change in muscle length. 57

3-1 Subject marker setup. 83

3-2 Left: Setup for the external perturbation condition. Right: Detail of the pendulum. 85

3-3 Diagram of the experimental protocol. Numbers in parenthesis indicate total number of trials performed for each condition; numbers in brackets indicate number of trials in different sub-conditions. For the external perturbations, the number of perturbations (n) varied between subjects (see text for details). 87

3-4 Summary of balance measures (right side) computed for the different postural conditions (left side). Abbreviations: CoP (center of pressure), CoM (center of mass), TtC (time-to-contact).....92

3-5 Hypothetical regression results between a muscle property (MP) and a balance measure (BM) for young (Y) and older (O) subject groups. See text for details. 97

3-6 Representative young (left) and older (right) subject anterior-posterior center of mass (black lines) and center of pressure (red lines oscillating around black center of mass lines) for the different postural conditions. From top to bottom: quiet stance, forward lean, backward lean, imposed swaying (preferred swaying is not shown), maximum forward reach, and sequential external perturbations (the solid circles indicate trials in which the subjects stepped off the force platform). Positions are referenced to the ankle joint. 101

3-7 Relationships between static postural measures and muscle mechanical properties for the dorsiflexors (DFs), gastrocnemius (GA), and soleus (SO). Data sets with overall significance are outlined by a dashed rectangle. Older subjects are shown as solid circles and a solid fitted line; young subjects are represented by open triangles and a dashed fitted line. 105

3-8 Relationships between dynamic postural measures and muscle mechanical properties for the dorsiflexors (DFs), gastrocnemius (GA), and soleus (SO). Data sets with overall significance are outlined by a dashed rectangle. Older subjects are shown as solid circles and a solid fitted line; young subjects are represented by open triangles and a dashed fitted line. 108

3-9 Actual vs. predicted static balance measures using the regression models. 112

3-10 Actual vs. predicted dynamic balance measures using the regression models. 116

3-11 A schematic of the role of the series elastic slack length during upright posture using a simplified inverted pendulum model. A subject with a long (left) and short (right) series elastic slack length. 128

3-12 Top: Example of “wide” and “narrow” force-length relations, for a given operating range (“Op. Range”; vertical dashed lines). Bottom: For the wide force-length relation, the force potential changes gradually so only small inputs are needed to remain near optimal length. On the other hand, large inputs are needed to counteract the large changes in force potential when the force-length relation is narrow. 132

4-1 Schematic of the skeletal and foot-floor model. See text for details 141

4-2 Schematic of the postural control model. Subscripts DF, GA, and SO refer to the dorsiflexors, gastrocnemius, and soleus muscles, respectively. X_{CoM}: the anterior-posterior (AP) position of the body center-of-mass (CoM), X_{CoM}^{REF}: the AP position of the ankle joint center, $X_{CoM}^{Boundary}$: the AP position of the base of support boundaries, v_{CoM}: AP velocity of CoM, DtB: distance from CoM to toe or heel boundaries, depending on the CoM velocity direction (v_{CoM}), TtC_{CoM}: CoM time-to-contact to toe or heel boundaries depending on the CoM velocity direction (v_{CoM}), K_{PF}^{P}: proportional control gain for a the plantarflexors, K^{D}: derivative control gain for a given muscle (DF or PF), STIM: neural excitation signal, ACT: muscle activation, F: muscle force, d = muscle moment arm at the ankle, T: ankle torque produced by each muscle, T_{MUS}: net muscle torque produced at ankle, $T_{Passive}$: passive torque contributions, K_N: noise gain, $T_{Disturb}$: disturbance torque, T_{NET}: net ankle torque, τ_d: time delay. 146

4-3 Performance of the optimized quiet stance postural control models using muscle mechanical properties measured for young (left) and older (right) subjects. For comparison, experimental data from representative young and older male subjects are shown (top graphs). 154

4-4 Long duration behavior of the optimized young postural model (10 min). The center of pressure (red) is shown oscillating around the center of mass (black). The linear trend is shown (not including the first 10 s). 155

4-5 Lengths of the contractile components of the young (Y) and older (O) optimized quiet stance models, relative to the optimum contractile component length (dashed line) 156

4-6 Total musculotendon (thick line) and contractile component (thin line) lengths for the gastrocnemius (left) and soleus (right) muscles for the optimized young model during 20 s of quiet stance. 157

4-7 Results of the optimized young quiet stance model (top), and after each of six of the mechanical properties were independently changed to the mean value of the older subjects. The center of pressure (red) is shown oscillating around the center of mass. The models were simulated for 180 s, the first 60 s of data are not shown. For three of the mechanical properties, the model was unable to maintain balance for 180 s. See text for an explanation of nomenclature. 158

4-8 Left Panel: Center of mass (black) and center of pressure kinematics (red line oscillating around black) when the slack length was increased by 15% from the reference young value, where the model fell after about 40 s. Right Panels: Corresponding length of the GA and SO contractile components. The GA length remained within the force-length (FL) relation, while the SO began outside of the force-length (FL) relation, but moved inside right before falling forward. 160

4-9 Center of mass (black) and center of pressure (red line oscillating around black) kinematics for the simulations in which the model had qualitatively different behavior compared to the rest of the simulations. The percentages represent the amount each muscle mechanical property was changed from the young reference values, while all other model parameters remained constant. 161

4-10 Results of the sensitivity analysis for each of the muscle mechanical properties. A: Effects on the gains of the plantarflexor proportional controller). B: Effects on the gains of the derivative controllers for the dorsi- (open data points) and plantarflexor (closed data points) muscle models. The results for the optimized model using the original mechanical property values are shown as triangles. Proportional and derivative controller gains for the older parameter values are identified by square data points and horizontal lines. Note that some of the changes for the older parameters were very large; these values are indicated by horizontal lines, but do not have the data points identified. 163

4-11 Result of decreasing the strength of the plantarflexors by 42% (open square). 164

4-12 Mean center of mass (CoM) position with changes in the mechanical properties. The horizontal line with wide dashes represents the postural set point. The results from changing the properties to the older values are indicated by horizontal lines with small dashes, and where possible, are indicated by hollow squares. Note that some of the changes for the older parameters were very large; these values are indicated by horizontal lines, but do not have the data points identified. 165

4-13 Average standard deviation of the center of mass (CoM) position with changes in the mechanical properties. The results from changing the properties to the older values are indicated by dashed horizontal lines, and where possible, are indicated by hollow squares. Note that some of the changes for the older parameters were very large; these values are indicated by horizontal lines, but do not have the data points identified. 166

4-14 Mean center of mass (CoM) speed with changes in the mechanical properties. The results from changing the properties to the older values are indicated by dashed horizontal lines, and where possible, are indicated by hollow squares. Note that some of the changes for the older parameters were very large; these values are indicated by horizontal lines, but do not have the data points identified. 167

4-15 Median center of mass (CoM) frequency with changes in the mechanical properties. The results from changing the properties to the older values are indicated by dashed horizontal lines, and where possible, are indicated by hollow squares. Note that some of the changes for the older parameters were very large; these values are indicated by horizontal lines, but do not have the data points identified. 168

4-16 Left panel: schematic showing the effect of changing the series elastic component slack length (L_S) on the force-length operating range of the contractile component (CC). The optimal CC length (L_0) is indicated by the vertical dashed line. If the CC is near L_0, increasing L_S (B) will shift the CC to the ascending region of the force-length curve, while decreasing L_S (A) will shift the CC to the descending region of the force-length curve. Right panel: when the CC lengthens during forward sway, case B will be "stable" as the CC will move to a more optimal length, while case A is "unstable" as the CC will move to a less optimal length and thus the force-potential will reduce. 177

A-1 Example of the procedure for adjusting the experimental torque-angle (A) and torque-angular velocity data (C) data for a representative subject. The torque-angular velocity data were adjusted for the effects of the torque-angle relationship, based on the angle at which the peak torques occurred (B), and also adjusted for the effects of antagonistic co-contraction. See text for details……..…….... 193

B-1 Components of the musculotendon model……...……. 195

B-2 Flowchart of the musculotendon model algorithm as implemented within a simulation…… 196

B-3 Illustration of the force-extension relation…….…….... 197

B-4 Example of the exponential relation between stimulation (thick line) and activation (thin line) using hypothetical data. Δt = 0.001, τ_{Rise} = 5 ms, and τ_{Fall} = 80ms…….…….... 198

B-5 Illustration of the force-length relation. The black line is when the CC is at full activation, while the gray lines show the CC at below-maximal activation…….…….. 198

B-6 Illustration of the CC force-velocity relationship used. The black line is when the CC is fully activated at optimal fiber length, while the gray lines show the CC at sub-maximal activation and/or at a non-optimal fiber length…….… 200

C-1 Interaction plots for costs associated with isometric and isovelocity optimizations…….…… 201

E-1 The inverted pendulum model……..……. 205

CHAPTER 1

INTRODUCTION

Muscles produce force. This fact has intrigued scientists for centuries and has been the subject of hundreds of research studies. Muscles are engineering marvels, possessing an array of properties that allow a wide range of functions and tremendous adaptability. Muscles are capable of producing very small or very large levels of force. Muscles can produce force while shortening, lengthening, or at a constant length. Muscles can change the maximal amount of force that they are able to produce in response to repetitive loading. Muscles can even change their stiffness. There are no existing man-made materials that can accurately replicate the actions of human muscles, which is a testament to their complex design.

Although muscle is remarkable even in isolation, it is when multiple muscles work together that the human body's potential for movement truly becomes apparent. Humans can coordinate their muscles for extremely precise movements such as threading a needle, extremely fast movements such as throwing a baseball, or extremely forceful movements such as lifting a refrigerator. Having multiple muscles makes such a wide variety of movements possible. One important question that currently occupies the minds of movement scientists is "How is such a complex array of muscles controlled"? Answers to this question are of great value to a wide range of individuals, from clinicians rehabilitating patients to the design and control of artificial limbs.

Much is known about the control of muscles at the neural level (Basmajian and De Luca 1985). Each muscle receives inputs in the form of one or more control signals

from the central and peripheral nervous systems. These control signals arise from voluntary and involuntary activations of alpha motor neurons in the spinal cord. The motor neurons transmit the control signals in the form of electrical impulses (action potentials), which are modulated in their amplitude and frequency by recruiting more motor neurons or by causing already active motor neurons to transmit impulses more rapidly. These control signals have a direct influence on the production of force by muscles.

Thus, at the neural level the amount of "effort" required for a particular muscle is specified by only two parameters (recruitment and firing-frequency). If muscle were a simple input-output "actuator", these control signals would be the sole determinant of muscle force. The same control signals would always produce the same force level, irrespective of the current state of the musculoskeletal system. Such a control scheme may impose limitations on the ability of the human body to coordinate complex movement. Another consideration is that the transmission of control signals is not instantaneous, and requires a finite period of time depending on the conduction velocity of the motor neurons, which has been shown to increase with aging (Merletti et al. 2002).

Humans possess an additional "control system" based on the properties of the muscle-tendon units. Each muscle contains an array of geometrical and mechanical properties that alters the relationship between the input (neural control) and output (force) signals - often in beneficial ways. For example, if someone standing in line is accidentally and unexpectedly perturbed from behind, the stiffness of the postural muscles provides an instantaneous level of stabilization. Without this mechanism, delays in the transmission of the nervous signal may not reach the correct muscles in time for a

stabilizing response, as ankle tendon-tap reflex latencies have been shown to average about 35 ms in healthy individuals (Frijns et al. 1997). This is just one example of the many properties of muscle that influence how muscles are coordinated during movement.

Muscular "properties" can be separated into three areas: architectural, geometrical, and mechanical. Architectural properties of muscle consist of features that define the number and orientation of muscle fibers within a muscle, including fiber length and pennation angle. Geometrical properties refer to how a muscle is positioned within the skeleton, including the number of joints crossed and the relation between muscle length, muscle moment arm, and the angular positions of the joints crossed by the muscle. The mechanical properties of muscle are defined as the mechanical characteristics of muscle influencing force production. The amount of force produced by a muscle in response to a neural input is dependent on a number of factors: the activation level of the muscle, the length and velocity of the muscle fibers, the prior history of the state of contraction, and muscle physiological cross-sectional area. Geometrical and architectural properties are largely fixed; alterations are only possible under unusual circumstances such as tendon transfer surgery (Delp et al. 1994). Mechanical properties on the other hand, have been shown to experience change with use, disuse, injury, and age (Blanpied and Smidt 1993, Doherty and Brown 1997, Frontera et al. 2000b, Larsson et al. 1997, Ochala et al. 2004a).

1.1 Musculotendon Mechanical Properties, Aging, and Postural Control

Muscular properties have been shown to change with aging, especially beyond 60 years (Ochala et al. 2004a, Vandervoort 2002). In general, muscles become weaker

(reduction in cross-sectional area) (Narici et al. 2003), slower (lower maximal contraction velocity) (D'Antona et al. 2003), and less elastic (Ochala et al. 2004a). Changes in muscle properties seem to affect the lower limbs to a greater degree than the upper limbs (McDonagh et al. 1984). In most cases, these changes are detrimental to the functioning of the neuromuscular system, causing reductions in maximal force capability and delays in the rate of force development. These alterations may place older individuals at an increased risk for injury - especially in situations where rapid force development is needed, such as coping with a threat to postural stability.

One of the most basic requirements for the execution of many activities of daily living is the successful maintenance of posture. In comparison to younger adults, older individuals have been shown to generally have a higher amplitude of postural sway, as well as higher sway velocities and either increased or decreased sway variability, depending on the population studied (Prieto et al. 1996, Prieto et al. 1993). Older adults are generally less stable than younger adults, and are more prone to experience a fall (Shumway-Cook et al. 1997, Tinetti et al. 1988), which can result in significant injury or even death. In light of the increasing proportion of older adults in our population, fall-related injuries require the expenditure of a significant amount of time and money for rehabilitation (Titler et al. 2005).

Despite the evidence for alterations in muscle properties and postural control that occur with aging, there have been no investigations into a possible association between these changes. Therefore, the purposes of this dissertation were to: 1) Measure and compare muscle mechanical properties in young and old individuals, 2) Explore the association between age-related changes in muscle mechanical properties and postural

control, and 3) Develop and evaluate a musculoskeletal model of postural control. By investigating the muscle mechanical properties and postural control of young and old individuals, specific changes in muscle properties that directly impact muscle coordination and postural stability can be identified.

1.2 Specific Aims

1.2.1 Chapter 2: Muscle Mechanical Properties and Aging

The purpose of the first study was to describe and compare the mechanical properties of the primary muscles controlling the ankle joint in healthy young and older adults. For each participant, magnetic resonance imaging was used to determine muscle volume, physiological cross-sectional area, and moment arm length, while ultrasound imaging was used to measure series elasticity. Dynamometer experiments were performed to determine individualized relationships between joint torque, joint angle, and joint angular velocity for the ankle joint. The data from these experiments were incorporated into musculoskeletal models, where numerical optimization techniques were used to obtain subject-specific muscle mechanical properties. It was hypothesized that the optimized mechanical properties would differ with age, with the older subjects demonstrating lower maximal isometric force capabilities, stiffer elastic characteristics, and slower contractile properties.

1.2.2 Chapter 3: Mechanical Properties and Postural Control

The second study examined the relationship between age-related changes in muscle mechanical properties and postural control. The balancing abilities of the same

subjects that performed the experiments in Chapter 2 were evaluated with a series of postural tests. These included static (quiet stance, leaning) and dynamic conditions (swaying, reaching) and external perturbations. Variables related to center of pressure and center of mass motion were computed and used as measures of postural stability. It was hypothesized that the older adults would have poorer postural control than younger subjects, and these deficits would be associated with the age-related changes in muscle mechanical properties.

1.2.3 Chapter 4: Musculoskeletal Model of Postural Control

In the third study, a musculoskeletal model was developed and used to evaluate the role of muscle properties in the control of quiet stance. The model included a two-segment inverted pendulum skeletal model, a foot-floor interaction allowing movement of the foot relative to the ground, and Hill two-component muscle models representing the major ankle muscles. The model was controlled by proportional-derivative neural controllers that used time-to-contact information to send excitation signals to the muscle models, which accounted for noise and delays within the nervous system. Numerical optimization was used to find the neural controller gains that would allow the model to perform quiet stance with minimal muscular intervention. Both “young” and “old” quiet stance models were created using the mechanical properties measured in Chapter 2, and their performance was compared. A sensitivity analysis was performed to assess effects of changes in individual muscle mechanical properties on the performance of the model during quiet stance.

1.3 Summary

The central question of this dissertation is how age-related changes in muscle mechanical properties influence postural control. This question is important because muscle is responsible for transforming neural commands into muscular force, and therefore, it is crucial that we understand how this “transfer” may be altered with advancing age. This may explain why individuals become less stable with age.

CHAPTER 2

MUSCLE MECHANICAL PROPERTIES AND AGING

2.1 Introduction

Muscles possess an array of mechanical properties that influence the relationship between the neural command and the force produced. These include nonlinear dependence of active contractile force on length (force-length relation) (Gordon et al. 1966) and velocity (force-velocity relation) (Hill 1938), and a nonlinear relation between force and the elongation of series elastic structures within the muscle-tendon complex (force-extension relation) (Bahler 1967). Because muscle mechanical properties dictate how nervous system input is translated into muscle force, age-related changes in these properties may have a large impact on muscle function and movement coordination (Hof 2003). Although much is known about neural and physiological changes with aging (Delbono 2003, Doherty 2003, Porter et al. 1995b, Vandervoort 2002), less research has examined age-related changes in muscle mechanical properties. However, it has been shown that single muscle fibers (both type I and type IIA) have significantly lower maximal isometric force capabilities in older men compared to younger men (Frontera et al. 2000b). Other studies have demonstrated that single muscle fiber contraction velocity decreases in older adults (Hook et al. 2001, Korhonen et al. 2006, Larsson et al. 1997).

As an alternative to the invasive nature of *in vitro* single muscle fiber studies, researchers have also examined the mechanical properties of muscle groups *in vivo* using dynamometers to elucidate torque-angle and torque-angular velocity relations. Older subjects exhibit shifts in the torque-angular velocity relationship towards slower velocities

(Lanza et al. 2003, Poulin et al. 1992), have generally slower muscle contractile properties (Gajdosik et al. 1999), and have increased resistance to fatigue (Lanza et al. 2004). Studies investigating muscle-tendon series elasticity using a quick-release technique have shown increases in stiffness with age (Blanpied and Smidt 1993, Ochala et al. 2005, Ochala et al. 2004b), and these findings are supported by evidence from single muscle fibers (Ochala et al. 2007a). In contrast, Onambele et al. (2006) showed an age-related decrease in the stiffness of the external Achilles tendon using ultrasound. These differences may be due to measurement techniques; the quick-release technique measures the total series elasticity, including elasticity of the internal aponeurosis and elasticity within the muscle fibers (Bressler and Clinch 1975), while the ultrasound technique used by Onambele et al. measures the elasticity of the external tendon at the local measurement site (Hof 2003). Age-related increases in the series elasticity measured using the quick-release technique could be due to greater fiber stiffness per unit force (Galler and Hilber 1998, Higuchi et al. 1995, Ochala et al. 2007a), while age-related decreases in external tendon stiffness measured using ultrasound may arise from increases in elastin and type V collagen and decreases in extracellular water and mucopolysacharide content (Kjaer 2004, Tuite et al. 1997).

Although it appears that muscle properties change with aging, knowledge of how the mechanical properties of *individual* muscle-tendon complexes are altered with aging is particularly sparse. This is partly because of the difficulty in determining the force in an individual muscle *in vivo* due to the over determined nature of the human muscular system (Bernstein 1967). It is even difficult to measure the contributions of isolated agonist muscle groups due to antagonistic co-activation, which is rarely accounted for in experimental

studies (Gajdosik et al. 1999, Lanza et al. 2003, Poulin et al. 1992). These challenges can be overcome through the use of musculoskeletal models that can model the behavior of individual muscles, without employing highly invasive techniques of direct muscle force measurement (Komi et al. 1987).

Thelen (2003) performed simulated muscle contractions while altering muscular parameters to mimic age-related changes. The “aged” simulation model predicted reduced power output along with prolonged contraction and relaxation times. Of note, the parameter values used were based solely on literature sources, chosen from a range of studies and different subject populations. It is possible that the specified combination of model parameters would not exist in any single human. Nevertheless, the importance of accounting for age-related changes in muscle mechanical properties was evident, especially when considering dynamic task performance (e.g. walking) or responding to environmental influences (e.g. standing in a moving bus).

Accurate knowledge of muscle mechanical properties is important for researchers who use muscle models to estimate the contribution of individual muscle forces to the net moment at a given joint. Many studies have demonstrated that muscle model output is sensitive to the parameters defining the mechanical properties (Buchanan et al. 2004, Heine et al. 2003, Herzog 1985, Out et al. 1996, Raikova and Prilutsky 2001). Therefore, inaccurate model parameters may lead to erroneous conclusions on force distribution.

The aim of this study was to combine experimental, modeling, and optimization techniques to assess individual muscle mechanical properties in young and old adults. Magnetic resonance and ultrasound imaging were used in conjunction with isometric and isovelocity muscle contractions to obtain subject-specific estimates of the mechanical

properties of the major muscles contributing to sagittal-plane movement at the ankle joint (dorsiflexors [DF], gastrocnemius [GA], soleus [SO]). Hill-type musculotendon models were used to represent each muscle. In each model, the active contractile component (CC) produced force according to stimulation-activation, force-length, and force-velocity relations, and the passive series elastic component (SEC) responded according to its force-extension relation. The parameters representing these mechanical properties of the individual muscle models were found through a numerical optimization process for each subject. It was hypothesized that the optimized muscle model parameters would differ with age, with the older subjects demonstrating lower maximal isometric force capabilities, stiffer elastic characteristics, and slower contractile properties.

2.2 Methods

2.2.1 Overall Experimental Design

Twelve young and twelve older adults participated in the experiments. All subjects were healthy and were without musculoskeletal or neurological impairments. There were equal numbers of male and female subjects in each age group; subject characteristics are listed in Table 2-1. The older subjects were all independent community-dwellers. Subjects attended multiple experimental sessions including: 1) isometric contractions in conjunction with ultrasound measurements to determine musculotendon elasticity, 2) isometric contractions at varying ankle joint angles on a dynamometer to measure torque-angle properties, 3) isovelocity contractions at various ankle angular velocities on a dynamometer to measure torque-angular velocity properties, and 4) measurements of muscle volume, cross-sectional area, and moment arm using MRI. During the first visit each participant was

provided with an overview of the experimental procedures for the study. Participants read signed an informed consent document approved by the local University ethics committee. Physician's clearance was obtained for all older subjects.

Table 2-1. Subject characteristics.

Subject Group	N	Age (yrs)		Height (m)		Mass (kg)	
		Mean ± SD	Range	Mean ± SD	Range	Mean ± SD	Range
Young Male	6	27 ± 3	21-30	1.81 ± 0.06	1.70-1.85	76.9 ± 8.2	68.3-87.5
Young Female	6	26 ± 3	21-31	1.65 ± 0.08	1.52-1.74	57.2 ± 6.6	49.9-65.8
Old Male	6	73 ± 5	67-79	1.77 ± 0.08	1.68-1.88	91.7 ± 10.3	74.0-101.5
Old Female	6	70 ± 5	66-78	1.66 ± 0.09	1.70-1.60	72.6 ± 17.0	77.4-59.3

Note: N = number of subjects; SD = standard deviation

2.2.2 Ultrasound Experiment

2.2.2.1 Experimental Setup

To estimate the series elasticity of the dorsi- and plantarflexor muscles, ankle torque was measured as subjects performed a series of ramped maximal effort isometric contractions at a fixed ankle angle. During the contractions, the movements of the DF, GA, and SO muscles were imaged using a real-time ultrasonic scanner (Acuson 128XP) with a linear-array probe (7.5 MHz, 50 mm scanning length, B-mode [brightness mode]). A transmission gel was used for acoustic coupling. The probe was orientated along the mid-sagittal axis of each muscle. Ultrasound images were sampled at 30 Hz and saved to magnetic tape.

The isometric contractions were performed on a dynamometer (Biodex System 3, Medical Systems, Shirley, NY); participants sat in a padded chair, with their left leg extended in front of them and their right foot resting on a support. The left knee was fully

extended, and the ankle was at an angle of 90° (between the tibia and the surface of the foot plate). This position has been reported to correspond to a minimal amount of passive resistance about the ankle joint (Siegler et al. 1984). The ankle joint center was visually aligned with the center of rotation of the footplate. The foot was secured to the foot plate using Velcro straps across the dorsal surface of the foot. The torque data were sampled at 900 Hz using a personal computer. An analog pulse (0-5V step function) was used to synchronize the ultrasound video with the force data.

2.2.2.2 Protocol

During the experimental session, subjects performed a block of 5 dorsiflexion trials which was preceded (followed) by a block of 5 plantarflexion trials, with the order of the blocks randomized. Within each block, two three-second maximal voluntary contractions (MVCs) were performed while torque measurements were taken; a two-minute rest was provided between the contractions. After the MVCs, subjects performed a set of five ramped contractions while force and ultrasound measurements were taken. Over a 30-second trial, subjects were required to slowly ramp up their level of torque by following a predefined template, which was scaled as percentage of the highest force recorded during the two preliminary MVCs. The template included a green line representing the target force level, which exponentially increased from 0-30% MVC, and then increased linearly from 30 – 100 % MVC (Figure 2-1C, solid line). Red lines bounded the target force level on each side (Figure 2-1C, broken lines), which were used as guides indicating the acceptable variability at each torque level. During each trial, a black line was drawn representing the subject's applied force level (in real-time). The subjects were instructed to follow the green

line as closely as possible and, although some variation was expected, they should try to stay within the red boundary lines.

2.2.2.3 Video Capture and Preprocessing

The ultrasound video was parsed into individual trials and converted into digital format (AVI, 720 x 480 pixels) using a personal computer based video capture system (Studio MovieBox USB, Pinnacle Systems). The raw force video data were processed using custom software written in Matlab (Version 7, The MathWorks, Natick MA). The raw force data were downsampled to equal the sampling rate of the ultrasound video (30 Hz). In each trial, the ultrasound video and force data records were searched for the rising edge of the synchronization pulse, and the two measurements were synchronized by shifting the data so that the synchronization pulse occurred in the same frame.

2.2.2.4 Tracking of Aponeurosis

To compute the elongation of the DF muscle two sets of eight points were identified: a set of superficial reference points evenly spaced near the skin, and a cluster of points along on the distal portion of the central aponeurosis of the DF (Figure 2-1A). Two similar sets of points were identified for the GA and SO. Each point was automatically tracked throughout the contraction using a two-dimensional cross-correlation tracking algorithm (Loram et al. 2004).

2.2.2.5 Data Processing

The horizontal and vertical displacements of the tracked points and torque data were imported into MATLAB™ and smoothed using a Butterworth digital filter. Optimal

filter cut-off frequencies were determined by performing a residual analysis and power spectral analysis (Winter 1990). The horizontal and vertical displacements of the eight reference and eight aponeurosis points were averaged to give a single reference and aponeurosis displacement time-series (Figure 2-1B). The displacement of the reference point was subtracted from the movement of the aponeurosis point to adjust for movement of the ultrasound probe relative to the skin. The scalar magnitude of the adjusted displacement vector was computed and transformed into extension by making the displacement magnitude equal to zero at the start of the trial (at rest). A second-order polynomial was then fit to the torque vs. extension data (Figure 2-1D). This polynomial had the form:

$$T = \alpha_{T\Delta L} x^2 + \beta_{T\Delta L} x \tag{3.1}$$

where T is the net ankle joint torque, $\alpha_{T\Delta L}$ is a coefficient that controls the rate of increase of torque with increasing extension (larger values represent a stiffer relationship), $\beta_{T\Delta L}$ is a coefficient that specifies the linearity of the torque-angle relation (larger values give a more linear relation), and x is the displacement of the aponeurosis.

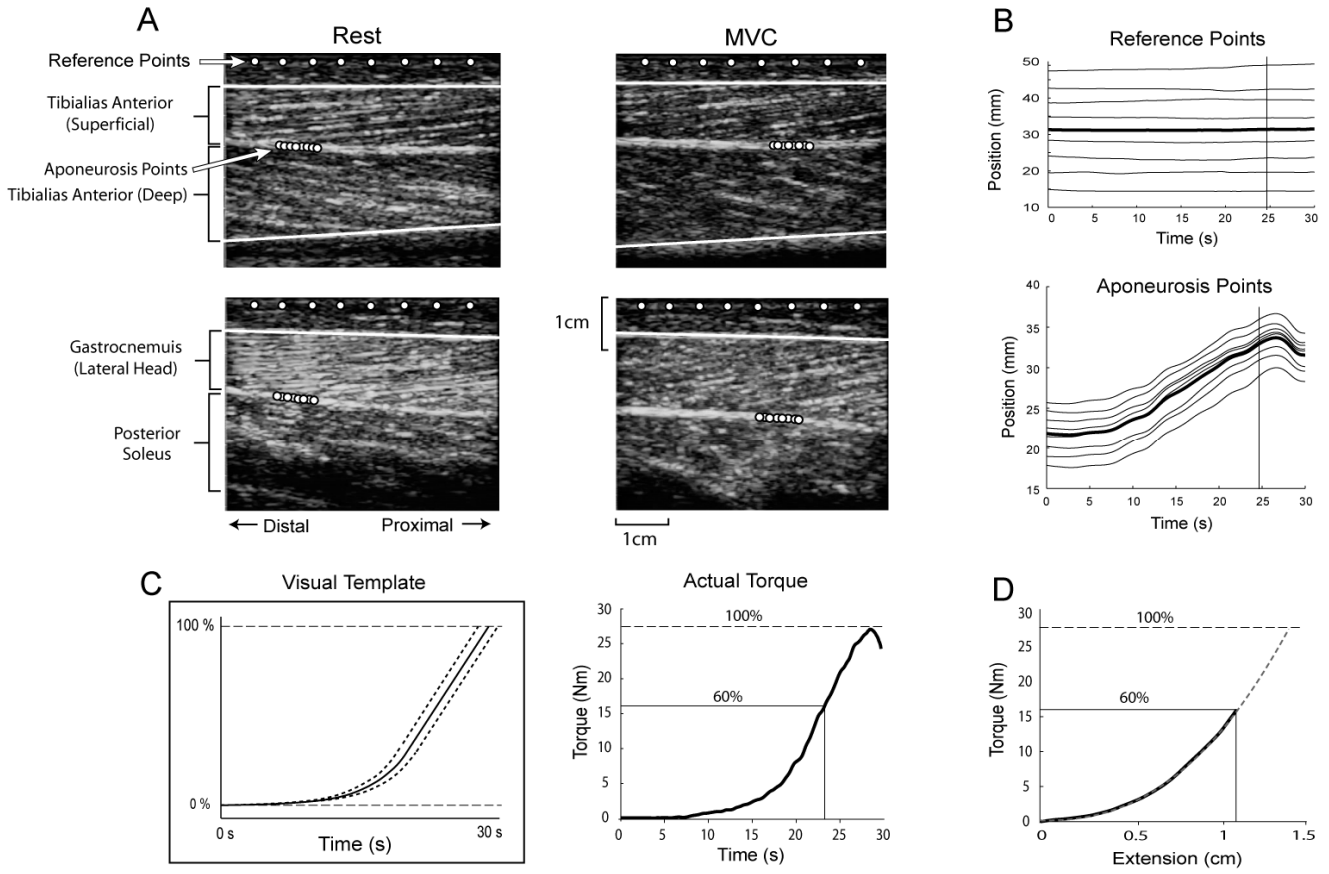

Figure 2-1. Methodology for measuring musculotendon series elasticity. A: Ultrasound stills from the start (left) and end (right, at MVC) of a dorsi- (top) and plantarflexion (bottom) ramped trial. The white dots indicate points of interest, including a set of reference points near the skin, and a set of points on the central aponeurosis of each muscle. The motion of the points was tracked using an automated cross-correlation algorithm. B: Example of the horizontal displacements of the set of reference points (top) and points on the central aponeurosis for a dorsiflexion trial (thick line = average). C: The visual torque-time template (left) and the actual dorsiflexion torque produced (right). D: The resulting torque vs. extension plot. A second order polynomial was fit to the torque up to 60% MVC, and then extended up to MVC (dashed line).

2.2.3 Dynamometer Experiments

2.2.3.1 Experimental Setup

For the determination of joint torque-angle and torque-angular velocity relations, a series of isometric and isovelocity muscle contractions were performed on the same dynamometer used for the ultrasound measurements (the dynamometer setup was the same). The torque exerted on the dynamometer and the angular displacements of the lever arm were sampled at a rate of 1000 Hz with a personal computer using a 16-bit analog-to-digital converter and custom data acquisition software.

The myoelectrical activity of the DF, GA, and SO were monitored during all isometric and isovelocity trials using bipolar pre-amplified (35x) Ag/AgCl circular surface electrodes with an interelectrode distance of 20 mm and an input impedance of > 25 MΩ at DC and >15MΩ at 100 Hz (Theraputics Unlimited, Iowa City, IA). EMG signals were further amplified (model RMG-544 amplifier / processing module; 87 dB common mode rejection ratio at 60 Hz, frequency response 20 – 4000 Hz). The gains of the individual EMG amplifier channels were adjusted for each participant to obtain the best resolution without clipping the signal. EMG data were sampled at a rate of 1000 Hz. Skin preparation for impedance minimization included shaving the electrode site, abrading the skin with an abrasive paste, and cleaning with alcohol. Electrodes were affixed along the orientation of the underlying muscle fibers.

2.2.3.2 Protocol

Maximal effort isometric and isovelocity dynamometer contractions were done on separate visits to the laboratory to minimize fatigue. For both sessions, two trials were performed at each joint angle and angular velocity. The order of the trials was randomized. A 30 s rest was provided between all trials. At the start of each session, subjects warmed up on the dynamometer by performing sub-maximal non-isovelocity contractions, and the range of motion of the ankle joint was determined and the dynamometer movement limits were set.

In the isometric session, passive joint torque was measured by having the subject relax and the dynamometer slowly (15°/s) moved the ankle joint through its entire range of motion. Maximal effort dorsiflexion trials were performed with the knee fixed at 100° (full extension = 180°), and the ankle at 70 - 110° (neutral = 90°) in 10° increments. Maximal effort plantarflexion trials were performed with the knee at 180°, and the same range of ankle angles as in the dorsiflexion condition.

In the isovelocity session, dorsiflexion and plantarflexion trials were performed with the knee fixed at 100° and 90°, respectively. Concentric trials, where the dynamometer moves at a fixed angular velocity in the same direction as the active joint torque, were performed at angular velocities of 15°/s and 30 - 240°/s in 30°/s increments. Eccentric trials, where subjects must resist against the dynamometer that is moving in the direction opposite to the active joint torque, were performed at angular velocities of -150, -60, and -30°/s.

2.2.3.3 Data Reduction and Analysis

The maximal isometric joint torque at a given ankle angle was taken as the highest torque value of the two trials, and used to construct a torque-angle relationship. For the construction of torque-angular velocity relationships, the velocity of the contractile component (rather than muscle-tendon velocity) is of interest. During the isovelocity contraction, the velocity of the contractile component is not constant and is generally unknown except for the instant at which the peak torque is achieved (or more specifically, where the slope of the torque vs. time curve is zero), where the velocity of the series elastic component is zero, and thus the contractile component velocity must equal the total muscle velocity. Therefore, for each isovelocity trial the peak torque and the corresponding joint angular velocity were used to construct a torque-angular velocity relation. For both the isometric and isovelocity data, the passive and inertial torque contributions were subtracted from the measured torque data.

2.2.3.4 Adjusting for Co-Activation and Torque-Angle Effects

Adjustments were made to the measured experimental torque-angle and torque-angular velocity data to account for antagonistic co-activation. The relationships between agonist muscle torque and the percentage of antagonist muscle co-activation were based on the data of Simoneau et al. (2005), which showed similar linear relationships for young and older adults. Adjustments were also made to the measured experimental torque-angular velocity data to account for torque-angle effects and to ensure agreement between the torque-angle and torque-angular velocity data. See Appendix A for details on these adjustments.

2.2.4 Magnetic Resonance Imaging (MRI)

2.2.4.1 Experimental Setup

Magnetic resonance images were taken of each subject's left lower leg (G.E. Sigma EchoSpeed Plus; 1.5 Tesla). Axial images were taken using a spacing of 4 mm (T1 weighted spin echo images; TR = 5000 ms, TE = 17 ms, pixel resolution 512x512, field of view 300 mm). Two sets of axial images were taken, one proximal, and one distal. A marker bead was placed on the surface of the leg so that the two image sets could be aligned. Sagittal-plane images were also taken for measurement of plantarflexor and dorsiflexor muscle moment arms.

2.2.4.2 Data Reduction and Analysis

Custom interactive software was written in MATLAB™ to identify muscle cross-sectional areas (CSAs) and to separate muscle tissue from other tissues. For each subject, the proximal and distal sets of lower-leg axial images were sorted according to the slice locations and joined together using the marker bead that was placed on the skin. This composite set of axial images was then loaded into the software for analysis. The perimeters of the anterior compartment (containing the dorsiflexors: tibialis anterior, extensor hallucis longus, extensor digitorum longus, peroneus tertius) (Gray 1973), the soleus (SO), and the medial (MG) and lateral (LG) heads of the gastrocnemius were outlined in every other slice (Figure 2-2, Left). The male data set from the online image repository for the Visible Human project was used as a primary reference (http://www.nlm.nih.gov/research/visible/visible_human.html).

The CSA of each muscle compartment in each analyzed slice (every other measured slice) was computed, multiplied by an 8 mm slice spacing (2 x 4 mm), and summed together to give muscle volumes. In pilot work, the muscles were also outlined in every slice for six young subjects. The mean absolute differences between using every slice and every other slice were 1.97, 2.61, and 1.18 cm^3 for the total volume estimates of the DF, SO, and GA (heads combined) muscles. At worst, this represented a difference of about 2%, but resulted in a significant savings in analysis time. We therefore chose to use every other slice for the muscle volume computations.

In each analyzed slice, a histogram representing the pixel intensities for the area within the leg boundary was created. The lower pixel intensities represent cortical bone and tendon; the high intensities represent trabecular bone and adipose tissue; muscle tissue lies between these intensity regions. The pixel intensity thresholds for separation of these regions were initially chosen by identifying the peak intensity (representing muscle), and then finding where the slope to either side reaches zero (Figure 2-2). The interactive MRI analysis program then colored the corresponding MRI slice, based on the chosen thresholds (bone/tendon = blue, muscle = red, adipose tissue = green). The thresholds were then manually adjusted until an optimal separation of the muscle tissue was reached.

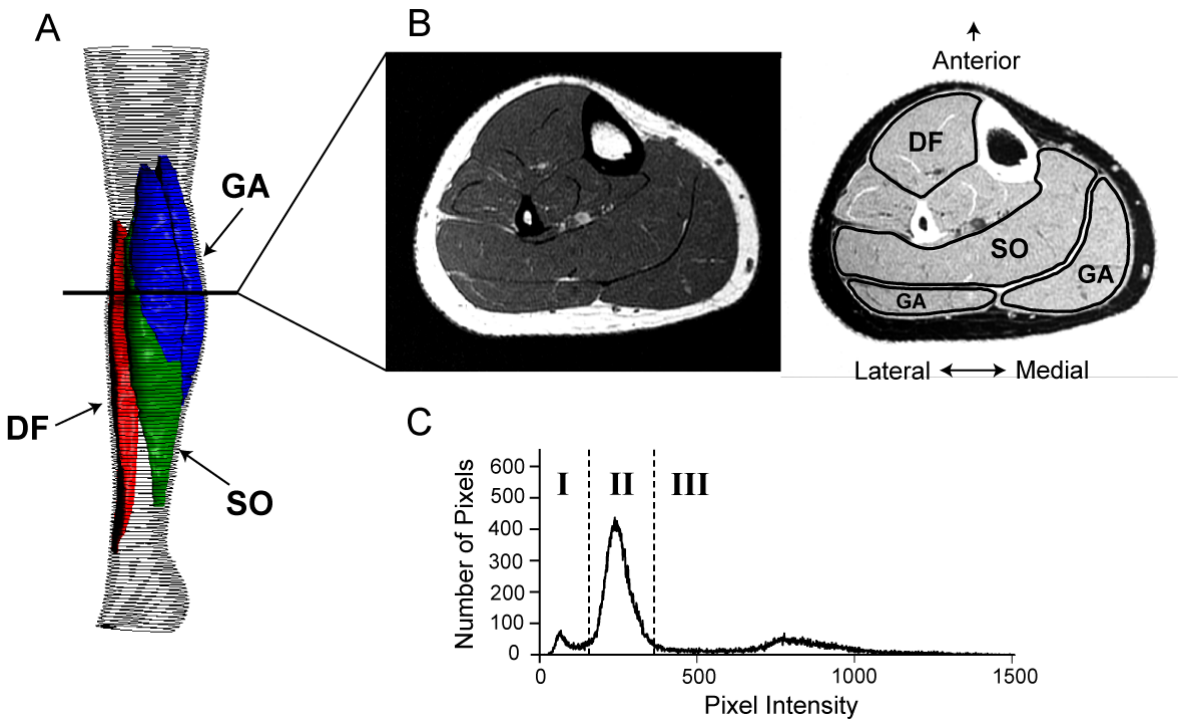

Figure 2-2. A: Example of reconstructed muscle volumes of the dorsiflexors (DF), gastrocnemius (GA), and soleus (SO). B: An axial MRI image illustrating the identification of the muscles of interest (left). Inverted image (right) C: Pixel intensity histogram showing the separation of cortical bone/tendon (I), muscle (II), and trabecular bone/adipose tissue (III).

2.2.4.3 Plantarflexor PCSA Calculations

The ratio between the optimal fiber length (MF_{OPT}) and muscle length (ML) was computed for the DF muscle (Spoor et al. 1991), and for the soleus (SO) and medial (GM) and lateral heads (GL) of the gastrocnemius (Out et al. 1996). The MF_{OPT}/ML ratios were: DF = 0.209, SO = 0.150, GM = 0.101, GL = 0.135. For each subject in the present study, the muscle length was computed at the same joint angles as used by Out et al. for their muscle length estimation (Ankle at 95°; Knee at 135°), and then multiplied by the MF_{OPT}/ML ratio, to give subject specific estimates of MF_{OPT} The muscle lengths were computed using polynomials from the SIMM anatomical model (Delp et al. 1990).

Muscle fiber pennation angles (MF_θ) were estimated by averaging the data for the three cadavers presented in Wickiewicz et al. (1983). Although MF_θ could have been estimated for some muscles from the ultrasound data, we chose to use literature values due to our limited ultrasound measurements. Mainly, ultrasound images were not obtained for the other muscles in the anterior compartment (besides the tibialias anterior), the medial head of the GA, and for the SO. Therefore MF_θ could not be measured for these muscles. The GM and GL MF_{OPT} and MF_θ values estimated from the literature were then averaged to give a combined estimate for the gastrocmenius (GA). Physiological cross-sectional areas (PCSAs) was computed for the DF, SO, and GA muscles as

$$PCSA = \frac{M_{VOL}}{MF_{OPT}} \cos MF_\theta \tag{3.2}$$

where M_{VOL} is the volume of the contractile tissue determined from the MRI data. The relative PCSA ($PCSA_{REL}$), relating the SO and GA PCSAs, was computed as

$$PCSA_{REL} = \frac{PCSA_{SO}}{PCSA_{GA}} \tag{3.3}$$

2.2.4.4 Moment Arm Measurement

The shapes of the muscle moment arm vs. ankle flexion-extension angle relationships for the DF, GA, and SO muscles were based on a SIMM (Delp et al. 1990) musculoskeletal model of the lower leg. The individual muscle moment arm relationships for the lateral and medial heads of GA and the SO were averaged together, giving an average moment arm vs. ankle flexion-extension relation for the Achilles tendon. This

average moment arm was used for both the GA and SO muscle models. The average percent difference between the “average” moment arm relation and the individual muscle relations was 1.96%.

MRI was used to obtain a series of sagittal-plane images of the ankle joint. An interactive computer program was written for identification of muscle moment arms. The following were identified on the MRI image (Figure 2-3), based on the methods of Rugg et al. (1990): 1) the ankle joint center, 2) the lines of action of the DF and Achilles tendons (for PF muscles), and 3) shank and foot segments. The DF and GA/SO moment arms were measured as the perpendicular distance from the lines of action and the joint center. The ankle angle was computed between the shank and foot segments. This measurement process (loading the blank MRI image, and then identifying the joint center, lines of action, segments, and moment arms) was repeated three times by the same investigator. The moment arms and corresponding joint angles were then averaged together. For each subject, the average moment arm and ankle angle values were used to scale the moment arm vs. ankle flexion-extension angle relationships from SIMM.

Figure 2-3. Example of the calculation of the dorsiflexor (DF) and plantarflexor (PF) moment arms (MA) from a sagittal plane MRI image. The pixel intensities were inverted for clarity (right).

2.2.4.5 Moment Arm Correction for Retinaculum Stretch

It has been demonstrated that the moment arm of the DF muscles become greater with increases in muscular force, due to the stretching of retinaculum (Maganaris et al. 1999). Using the data presented in Maganaris et al., we calculated the average moment arm increase across four different ankle angles from rest to MVC (as a percentage of the subjects' resting moment arm lengths) as 35.6 ± 4.3%. To account for these changes in the DF moment arm for the subjects in our study, we assumed that our subjects would show similar changes, in terms of the percentage change in the moment arms as a function for the force expressed across the tendon. We assumed a linear relation between

the increase in moment arm and the force expressed across the tendon. The amount of DF moment arm increase at MVC was $\left(\uparrow MA_{MVC}\right)$computed as

$$\uparrow MA_{MVC} = \uparrow MA_{REF} * MA_0 \tag{3.4}$$

where $\uparrow MA_{REF} = 0.356$ (Maganaris et al. 1999) and MA_0 is the resting DF moment arm (measured from MRI data for each subject). The amount of moment arm increase at a given DF muscle force level $\left(\uparrow MA\right)$ was determined by

$$\uparrow MA = \uparrow MA_{MVC}\left(\frac{P}{P_0}\right) \tag{3.5}$$

$$\text{If } \uparrow MA > \uparrow MA_{MVC}, \text{ then } \uparrow MA = MA_{MVC} \tag{3.6}$$

where P is the force generated by the DF muscle, and P_0 is the maximal isometric force of the DF (computed in the muscle model, see below).

2.2.5 Modeling, Simulation, and Optimization

From the experimental data analysis, the dorsi- and plantarflexor torque-angle, torque-extension, and torque-angular velocity relationships were obtained. The desired mechanical properties governing the force-length and force-velocity relations of *individual* muscles were found by optimizing the performance of a musculoskeletal model to match the experimental data. The values that are found for each subject through the optimization procedure were constrained by the subject's experimentally measured muscle properties, allowing each set of muscle properties to be tailored to the individual subjects.

2.2.5.1 Model of Musculotendon Dynamics

The dynamics of the DF, GA, and SO muscle-tendon units were represented by Hill-type models (Hill 1938). Each muscle model incorporated a contractile component and a series elastic component, and was similar in concept to that used by Soest and Bobbert (1993). The behavior of the contractile component was characterized by nonlinear stimulation-activation, force-length, and force-velocity relationships. The behavior of the series elastic component was represented by a nonlinear force-extension relationship. A detailed explanation of the muscle model can be found in Appendix B.

2.2.5.2 Muscle Excitation and Activation

We assumed that there were no age-related differences in the ability of subjects to maximally excite their muscles, in either the isometric or isovelocity trials (Klass et al. 2005). Therefore, for the isometric simulations, muscle excitation and activation was assumed to always be maximal; for the isovelocity simulations, muscle excitation was assumed to start at zero and then instantaneously increase and remain at a maximum level (100%). The timing of this step increase in muscle excitation was determined by visual inspection of rectified EMG data recorded during the experimental isovelocity simulations. A threshold of 3 standard deviations above the baseline EMG level was used as a guide to identify excitation onsets. The muscle excitation time histories were converted to muscle activation (see Appendix B) using an exponential with a time constant of 15 ms for rising activation (Winters 1995).

2.2.5.3 Construction of Model Torque-Angle Curve

For each subject, torque-angle relations were constructed as part of the optimization process (Figure 2-4A). Construction of a single model torque-angle curve entailed multiple simulations, with each simulation occurring at the same ankle angle as the experimental data for a given subject. Simulations were performed separately - one for the dorsiflexors (DF) and one for the plantarflexors (GA & SO). Based on the experimental isometric joint angles, the musculotendon lengths were calculated using a scaled SIMM model. In each simulation, the contractile component of each muscle model was initially at rest (zero force). The contractile component was then maximally stimulated for 3 s. The force that the contractile component produced at the end of this isometric simulation was multiplied by the muscle's muscle moment arm, giving the ankle joint torque. In the two-muscle model case (plantarflexion) the two muscle torques were summed. This gave a single point on the torque-angle curve. This procedure was repeated at all joint angles tested, resulting in a model torque-angle curve. The model torque-angle curve did not have antagonistic muscle contributions, and was therefore compared to the co-activation-adjusted experimental data (which accounted for this).

2.2.5.4 Construction of Model Torque-Extension Relation

In conjunction with the dorsi- and plantarflexion model isometric simulations, calculations were performed to construct a model torque-extension relation (Figure 2-4B). For each subject the aponeurosis extension data (Δl_{SEC}) from the block of 5 experimental torque-extension ultrasound trials were averaged together and input to the

series elastic component force-extension equation (used in the muscle model), which was solved for the forces generated by the contractile component of each muscle (P_0):

$$P = \frac{{P_0}^2\left(\frac{2\alpha \cdot l_{SEC}}{l_{SEC}^0} - 2\alpha + \beta\right)^2 - {P_0}^2\beta^2}{4{P_0}^2\alpha} \tag{3.7}$$

where α and β are the coefficients defining the series elastic force-extension relation, L_S is the series elastic component slack length, P_0 is the maximal isometric force, and l_{SEC} is the length of the series elastic component, computed as $l_{SEC} = L_S + \Delta l_{SEC}$. For dorsiflexion, the forces predicted in the DF muscle were multiplied by the estimated DF moment arm (corrected for retinaculum stretch), giving an estimate of the torque produced by the DF muscles, producing a model dorsiflexor torque-extension relation. For plantarflexion, the forces predicted for the GA and SO muscles were multiplied by the estimated Achilles tendon moment arm, giving estimates for the torque contributions from the GA and SO muscles. These plantarflexor torques were summed, giving a model plantarflexor torque-extension relation.

2.2.5.5 Construction of Model Torque-Angular Velocity Curve

The simulations used to construct the model torque-angular velocity relation (Figure 2-4C) was similar to that described for the torque-angle data; however, non-isometric conditions were simulated and the experimental EMG data were used to specify the timing of the onset of muscle excitation. This was done because the subjects' muscles may not be fully activated in the high-velocity trials (Bobbert and van Ingen Schenau 1990). The peak joint torque throughout each simulation was taken, yielding a single

point on the torque-angular velocity curve. Multiple simulations were performed at different joint angular velocities (corresponding to the experimental velocities) to make up a complete curve based on the given set of muscular parameters.

2.2.5.6 Optimization Procedure

For each subject, a genetic algorithm (Storn and Price 1995) was used to find the combination of muscle model parameters that minimized the differences between predicted model and experimental data (torque-angle and torque-angular velocity). We chose to use a genetic algorithm because it has been shown that gradient-based optimization methods do not always converge due to the highly nonlinear characteristics of musculoskeletal models (Pandy et al. 1992, van Soest and Casius 2003). At the start of each optimization an initial population was created; each population member possessed a set of "genes", which in our case, consisted of the parameters defining the behavior of the muscle models (the genetic makeup of each member in the initial population was chosen randomly). The number of population members in each generation was equal to ten times the number of parameters (genes). The "fitness" of each member was determined by performing a set of isometric and isovelocity simulations, and computing the difference between the model and experimental data. Smaller differences corresponded to members with higher fitness levels, which had a greater chance to pass their genes (muscle properties) to the next generation. Random mutations in the genes allow the optimization to move "uphill", preventing the procedure from getting "stuck" in local minima (a non-optimal solution). This process repeats, generation after generation, until all of the population members have similar genes (model parameters), no further

changes are observed, and a maximally fit population is obtained (when all population members differed by less than 0.001 Nm from each other and from the latest optimal solution value).

Two optimizations were performed for each muscle group (dorsi- and plantarflexor). The optimization procedures are summarized in Figure 2-4. The first of optimizations (Phase 1) found an optimal set of isometric muscle model parameters, including: one parameter specifying the maximal isometric contractile component force (P_0), two specifying the contractile component force-length relation (L_0 , W), and three specifying the series elastic component force-extension relation (L_S, α, β). The second set of optimizations (Phase 2) used the previously optimized isometric parameters as inputs and found an optimal set of dynamic model parameters specifying the contractile component force-velocity relation (a/P_0 , b/L_0 , ε).

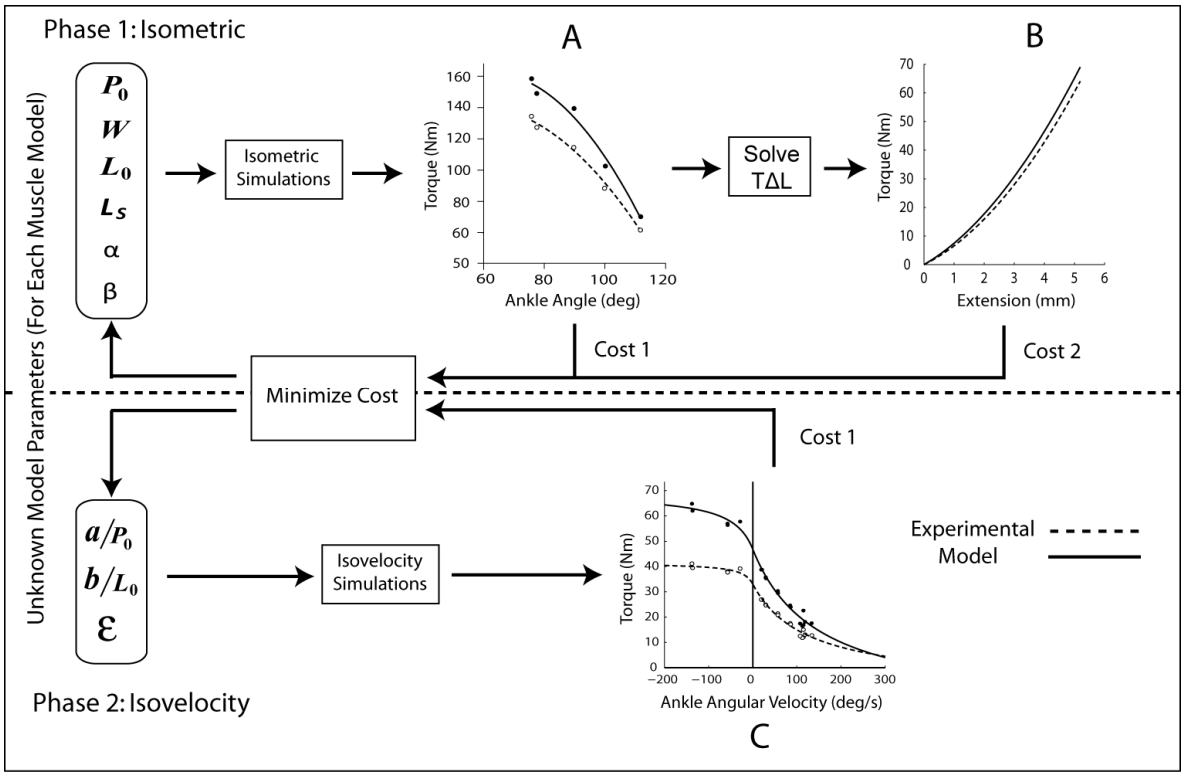

Figure 2-4. Schematic of isometric (Phase 1) and isovelocity (Phase 2) optimization flows. See text for details.

2.2.5.7 Muscle Model Parameter Constraints

For the dorsiflexion isometric optimizations (Phase 1), no restrictions were placed on the values for P_0. For the plantarflexion isometric optimizations (Phase 1), the relative PCSAs of the GA and SO muscles were used to constrain P_0 values. The PCSA ratio (SO/GA) was allowed to vary by ±15% of the value chosen for the GA. For example, if the SO PCSA was 140% greater than the GA PCSA, the SO P_0 was constrained to be 140 ± 15% of the GA P_0. The width of the force-length relationships (W) was allowed to vary between "wide" (0.6 to 1.4 L_0) and "narrow" (0.8 to 1.2 L_0) widths, representing muscles with a uniformly parallel or highly pennate architecture, respectively (Woittiez et

al. 1983). Values for the force-velocity coefficient a/P_0 were constrained to be between 0.1 and 0.6, based on the range of values reported in the literature (Bobbert and van Ingen Schenau 1990, Close 1972, Hof and Van den Berg 1981). Values for b/L_0 were constrained to be between 0.05 and 6 s^{-1} (Bobbert and van Ingen Schenau 1990). Finally, the eccentric plateau (ε) was limited to be between 1.01 and 2, which is a slightly larger range than the 1.1 to 1.8 range used by Epstein and Herzog (1998).

2.2.5.8 Fitness Criteria (Minimizing the Cost)

2.2.5.8.1 Phase 1

A maximal fitness $f\left(\vec{X}\right)$ was obtained by minimizing the costs associated with the differences between the model- and human-generated torque-angle ($C_{T\theta}$) and torque-extension data ($C_{T\Delta L}$), respectively. For the plantarflexion optimizations, an additional cost was added ($C_{SO/GA}$), which was related to the deviation of the model SO and GA maximal isometric force ratio $\left(P_0^{SO}/P_0^{GA}\right)$ from the ratio of experimental PCSAs $\left(PCSA_{SO}/PCSA_{GA}\right)$ estimated from the MRI data:

$$f\left(\vec{X}\right) = C_{T\theta} + C_{T\Delta L}\left[+ C_{SO/GA}\right] \tag{3.8}$$

where $\vec{X}$ is the vector of isometric model parameters (one vector for each muscle):

$$\vec{X} = \left[P_0, L_0, L_S, \alpha, \beta\right] \tag{3.9}$$

A second order polynomial was fit to the model generated torque-angle $\left(T\theta\right)$ data points, and the polynomial was evaluated at 1° ankle angle increments over the same range of joint angles as the experimental torque-angle data. Similarly, a second-order polynomial was fit to the model torque-extension $\left(T\Delta L\right)$ data, and evaluated at 1% increments from

zero to 60% of the series elastic component slack length. The Phase 1 costs were equal to the root-mean-squared difference between the model and experimental *evaluated* data:

$$C_{T\theta} = \sqrt{\sum_{i=1}^{N} \left(T_{\theta_i}^{MOD} - T_{\theta_i}^{EXP}\right)^2} \tag{3.10}$$

$$C_{T\Delta L} = \sqrt{\sum_{i=1}^{N} \left(T_{T\Delta L_i}^{MOD} - T_{T\Delta L_i}^{EXP}\right)^2} \tag{3.11}$$

where $T_{\theta_i}$is the maximal isometric torque at joint angle i, $T_{T\Delta L_i}$ is the torque produced at series elastic componenet extension i, and N is equal to the number of evaluated data points. The superscripts MOD and EXP represent data from the evaluated fits for the model and experimental data, respectively. For $C_{T\theta}$, N depended on each subject's ankle range of motion, for $C_{T\Delta L}$, N was always 60. The additional cost for the plantarflexion optimizations was given by:

$$C_{SO/GA} = \frac{PCSA_{SO}}{PCSA_{GA}} - \frac{P_0^{SO}}{P_0^{GA}} \tag{3.12}$$

which penalized the model for choosing maximal isometric forces for the SO and GA that were different from the measured ratio between the SO and GA PCSAs. This cost discouraged the optimization from setting the maximal isometric force of one plantarflexor muscle very high, and setting the value for other plantarflexor very low (within the ±15% range).

2.2.5.8.2 Phase 2

For the second optimization, a maximal fitness was obtained by minimizing two functions. The first was associated with the differences between equations fit to the model and experimental torque-angular velocity data (see next paragraph; $C_{T\omega}^{1}$), and the second was associated with the deviation of the model data points from a fitted equation $\left(C_{T\omega}^{2}\right)$:

$$f\left(\vec{X}\right)=C_{T\omega}^{1}+C_{T\omega}^{2} \tag{3.13}$$

where the parameters for each muscle model include:

$$\vec{X}=\left[a/P_0\,,b/L_0\,,\varepsilon\right] \tag{3.14}$$

A rectangular hyperbola fit to the concentric (Hill 1938) and eccentric (FitzHugh 1977) portions of the model torque-angular velocity data over the interval -200°/s (eccentric) to 300°/s (concentric). The Phase 2 cost was equal to the root-mean-squared difference between the model and experimental torque-angular velocity fits at 1°/s intervals:

$$C_{T\omega}^{1}=\sqrt{\sum_{i=1}^{N}\left(T_{\omega_i}^{MOD}-T_{\omega_i}^{EXP}\right)^2} \tag{3.15}$$

where $T_{\omega_i}$is the maximal torque produced during the constant angular velocity period for velocity i. For the isovelocity simulations N is equal to the number of evaluated data points (N = 500). The second cost was equal to the root-mean-squared difference between the fitted model data $\left(T_{\omega_i}^{MOD}\right)$ and the model data points $\left(\hat{T}_{\omega_i}^{MOD}\right)$:

$$C_{T\omega}^{2}=\sqrt{\sum_{i=1}^{n}\left(T_{\omega_i}^{MOD}-\hat{T}_{\omega_i}^{MOD}\right)^2} \tag{3.16}$$

where n is equal to the number of model-generated data points.

2.2.5.9 Comparison with Experimental Data

For the purposes of this study, the most important type of validity is “predictive validity”. This relates to how well the model, once tailored to an individual subject, predicts the performance of the subject. For a given subject, the optimization procedure fit a series of discrete joint torque data points, which were based on events occurring during the isometric and isovelocity dynamometer trials. The model should give a reasonable prediction of the time-course of net joint torque changes - given experimental joint angle, joint angular velocity, and muscle excitation time histories. Ideally, these inputs should come from data that were not used in the optimization process. Lacking such independent data, the next best thing is to use the isovelocity dynamometer data, and compare the entire time-course of joint torque changes that the model predicts with the experimentally measured data. The latter procedure was used in the present study.

To compare the net joint torque time-series predicted from the optimized model with the experimental data, the model must be modified to include the effects of antagonistic co-contraction, since the original experimental data included these antagonistic contributions (which were accounted for in the original optimizations). To this end, isovelocity dorsiflexion and plantarflexion simulations were performed; however, each simulation included antagonist muscle models. The excitation levels of the antagonistic muscles was set to be a percentage of the agonist muscles, using the same linear equations as used to adjust the experimental torque-angle and torque-angular velocity data for co-activation in the original optimizations (Appendix A).

2.2.5.10 Statistics

The main purpose of the statistical analysis was to test whether there were age-related differences in the various experimental measures (ultrasound, MRI, dynamometer data) and the predicted muscle mechanical properties for the different muscles. Effects of gender were also considered.

All statistical analyses were done with R (R Version 2.8.1, Foundation for Statistical Computing) (2008). Normality was assessed graphically using quantile-quantile plots; data that were not normally distributed were transformed by rank-ordering. For the analysis of the experimental dynamometer data and the optimized muscle property data, MANOVAs were first performed to assess overall main effects and interactions. These were followed by separate three-way ANOVAs (age x gender x muscle) on each of the dependent variables, with two levels for the muscle factor (DF & PF) for the dynamometer data and three levels (DF, GA, & SO) for the muscle property data. The dependent variables for the dynamometer experiments included three variables describing the torque-angle relationship: the peak torque (T_0), the ankle angle at which the peak torque occurred, and the width of the torque-angle relationship, and three variables describing the torque-angular velocity relationship: $A_{T\omega}$ and $B_{T\omega}$ shape coefficients, and the eccentric torque plateau (T_{ECC}). Note that this data analysis focused on the co-activation adjusted data for comparison to the optimized individual muscle mechanical properties; although results for the non-co-activation adjusted data will be presented graphically. The dependent variables for the mechanical properties predicted from the optimization included nine properties for each muscle:

$P_0, W, L_0, L_S, \alpha, \beta, a/P_0, b/L_0, \varepsilon.$

For assessment of the series elasticity data measured in the ultrasound experiments, separate three-way ANOVAs was performed with age, gender, and muscle (DF and PF) as factors and the maximum aponeurosis extension, maximum torque, and coefficients describing the shape of the torque-extension relation as the dependent variables ($\alpha_{T\Delta L}$, $\beta_{T\Delta L}$). For the analysis of data measured from the MRI experiments, separate three-way ANOVAs (age x gender x muscle [DF, GA, SO]) were performed with PCSA, total muscle volume, and muscle-only volume as dependent variables. Four-way ANOVAs were performed to assess differences in the net optimization costs; the independent factors included age, gender, muscle (DF or PF) and contraction type (isometric or isovelocity).

Effect sizes for the ANOVAs were determined using Cohen's *f* statistic (Cohen 1969). Although the effect sizes will not be discussed explicitly, they are listed in tables so that the reader can make informed interpretations of the results. Effect size measures the strength of the observed differences. For effect size a rough guide for interpreting Cohen's *f* is that for a small effect *f* = .1, a medium effect *f* = .25, and a large effect *f* = .4. Multiple comparisons were used for post-hoc analysis. A p-value of .05 was used as a guide for judging statistical significance for all tests.

2.3 Results

2.3.1 Ultrasound Experiment

The shapes of the experimental torque-extension relations are shown in Figure 2-5; the corresponding shape coefficients, maximal extensions, and maximal torques are presented in Table 2-2. Although the statistical analysis revealed significant effects of age

and muscle (discussed below), there were no main effects of gender on the maximal extension ($p = .111$), maximal torque ($p = .228$), or the shape coefficients α ($p = .286$) and β ($p = .279$).

Overall the older adults demonstrated smaller aponeurosis extensions, as there was a significant main effect of age ($p < .001$). There was also an interaction between age and muscle ($p = .015$). Here, the older subjects had significantly smaller extensions in the plantarflexors compared to the dorsiflexors ($p = .017$). On the other hand, there were no differences between the maximal extensions of the dorsi- and plantarflexors for the younger subjects ($p = .388$).

In general, compared to the older subjects, the younger subjects were able to generate larger torques (an age main effect; $p < .001$), and the plantarflexor muscles produced larger torques in both age groups (a muscle main effect; $p < .001$). There was a significant interaction between age and muscle ($p < .015$), such that the younger subjects had greater maximum torques in both dorsi- and plantarflexion, but the age-related difference was much larger for the plantarflexors ($p = .003$).

The older subjects had stiffer muscles, as there was a significant main effect of age for the shape coefficient $\alpha_{T\Delta L}$ ($p = .042$), which defines the rate of increase in stiffness with extension. On the other hand, there was no main effect of age for $\beta_{T\Delta L}$ ($p = .457$), which mainly affects the linearity of the torque-extension relation. For both coefficients $\left(\alpha_{T\Delta L}, \beta_{T\Delta L}\right)$ there were significant main effects for muscle group, such that the plantarflexors were stiffer (larger $\alpha_{T\Delta L}$; $p = .022$) and had a more linear relation (larger $\beta_{T\Delta L}$; $p < .001$).

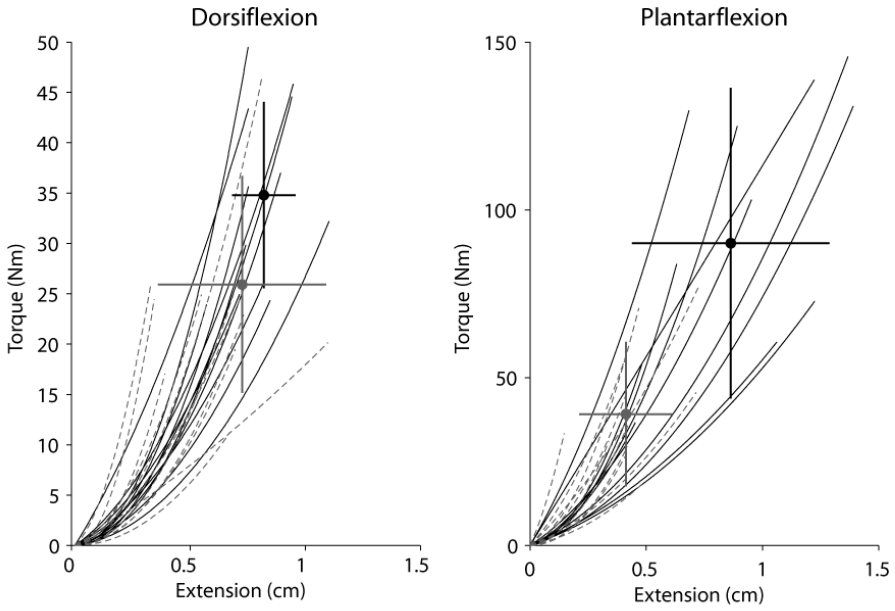

Figure 2-5. Second-order polynomial fits to the young (solid black lines) and older (broken gray lines) torque-extension data from the ultrasound experiments. The mean ± SD extensions at the peak torque are shown (dot and cross).

Table 2-2. Parameters describing fits to experimental torque-extension data.

Group	Mus.	Max. Extension (cm)	Max. Torque (Nm)	$\alpha_{T\Delta L}$ ‡	$\beta_{T\Delta L}$ ‡
Young	DF	8.4 ± 1.0	42.7 ± 5.3	4.91 x 10^5 ± 2.21 x 10^5	1096 ± 1409
Male	PF	11 ± 3.5	99.1 ± 58.6	8.35 x 10^5 ± 6.97 x 10^5	21983 ± 3554
Young	DF	8.0 ± 1.8	26.9 ± 3.4	3.86 x 10^5 ± 1.94 x 10^5	577 ± 550
Female	PF	7.8 ± 3.0	77.9 ± 30.9	8.09 x 10^5 ± 7.33 x 10^5	4641 ± 4172
Older	DF	8.5 ± 4.7	29.4 ± 14.6	5.78 x 10^5 ± 6.17 x 10^5	893 ± 815
Male	PF	3.5 ± 1.4	38.7 ± 18.2	4.64 x 10^6 ±5.58 x 10^6	1095 ± 1228
Older	DF	6.0 ± 1.8	22.4 ±3.4	8.09 x 10^5 ±6.78 x 10^5	197 ± 402
Female	PF	4.7 ± 2.0	43.6 ± 19.1	1.68 x 10^6 ±1.59 x 10^6	16298 ± 5192
Cohen's *f*		0.53	0.48	0.33	0.23
Main Effects		A	A, M	A, M	M
Interactions		A x M	A x M		

‡Coefficients describing the torque (*Nm*) vs. extension (*m*) relation: Torque = $\alpha_{T\Delta L}x^2 + \beta_{T\Delta L}x$

Significant main effects and interactions are shown for age (A), and muscle (M)

2.3.2 Magnetic Resonance Imaging (MRI)

The results of the MRI analyses are presented in Table 2-3. Male subjects had larger PCSAs, total muscle volumes, and muscle-only volumes compared with the female subjects. Significant main effects of age were found for PCSA and muscle-only volume ($p = .002$ and $p = .011$, respectively), such that the younger subjects had larger PCSAs and muscle-only volumes. Significant effects for gender and muscle were found for PCSA (gender: $p = .017$, muscle: $p < .001$), total volume (gender: $p < .001$, muscle, $p < .001$), and muscle-only volume (gender: $p < .001$, muscle, $p < .001$). Post-hoc analysis revealed significant differences between all three muscles in PCSA, total volume, and muscle-only volume ($p < .01$ for all comparisons), such that the SO had the largest values, followed by the GA, and DF.

Table 2-3. Measured individual muscle volumes, estimated physiological cross-sectional areas (PCSAs), optimal fiber lengths, and pennation angles. Values are Mean ± SD.

Group	Mus.	Total Vol. (cm^3)	Mus. Vol. (cm^3)	Opt. Fib. Len[a] (cm)	Pen. Ang.[b] (°)	PCSA (cm^2)
Young Male	DF	276 ± 32	257 ± 28	6.3 ± 0.3	5	40.7 ± 3.7
	GA	414 ± 80	397 ± 75	5.0 ± 0.3	12.5	77.5 ± 12.6
	SO	443 ± 60	424 ± 53	4.2 ± 0.2	25	91.3 ± 11.0
Young Female	DF	209 ± 48	191 ± 44	5.8 ± 0.5	5	33.2 ± 7.9
	GA	342 ± 79	326 ± 79	4.6 ± 0.4	12.5	70.2 ± 18.9
	SO	410 ± 65	390 ± 66	3.9 ± 0.4	25	91.6 ± 17.6
Older Male	DF	306 ± 55	266 ± 44	6.3 ± 0.3	5	41.9 ± 6.0
	GA	372 ± 60	306 ± 73	5.0 ± 0.2	12.5	59.7 ± 14.7
	SO	540 ± 183	406 ± 164	4.3 ± 0.2	25	86.1 ± 33.4
Older Female	DF	203 ± 36	169 ± 35	6.0 ± 0.3	5	27.9 ± 5.9
	GA	267 ± 37	224 ± 35	4.8 ± 0.2	12.5	45.4 ± 6.5
	SO	400 ± 70	349 ± 51	4.1 ± 0.2	25	77.9 ± 11.2
Cohen's *f*		0.40	0.40	-	-	0.28
Main Effects		G, M	A, G, M	-	-	A, G, M
Interactions		-	-	-	-	-

Muscle Abbreviations: DF = dorsiflexors; SO = soleus; GA = gastrocnemius
Significant main effects and interactions are shown for age (A), gender (G), and muscle (M)
[a]Optimal fiber length estimated from literature (see text for details)
[b]Based on literature (see text for details)

2.3.3 Dynamometer Experiments

The average torque angle and torque-angular velocity relations for the young and older subjects are shown in Figure 2-6, which shows the measured and co-activation adjusted data, the latter of which was used as inputs for the musculoskeletal models. To fully appreciate the variability of the data between subjects, the individual co-activation adjusted torque-angle and torque-angular velocity curves are shown in Figure 2-7. Summary statistics for the parameters describing the co-activation adjusted relations are presented in Table 2-4. The MANOVA, which considers the different parameters defining the co-activation adjusted torque-angle and torque-angular velocity relations collectively $(T_0, Width, A_{T\omega}, B_{T\omega}, T_{ECC})$, revealed a significant overall main effect for muscle group (dorsi- vs. plantarflexion; $p < .001$). No overall main effects were found for age ($p = .126$) or gender ($p = .800$).

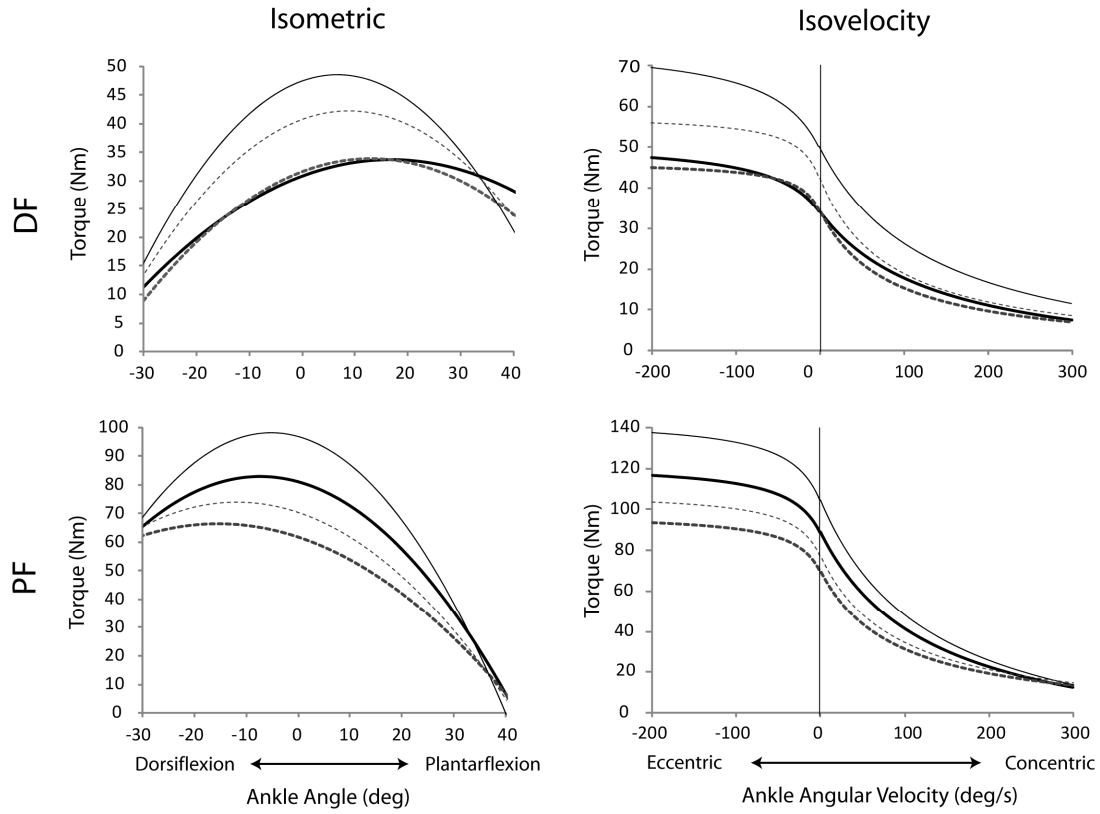

Figure 2-6. Average young (solid lines) and older (dashed lines) torque-angle (left) and torque-angular velocity (right) curves. For each subject group, the measured (thicker lines) and co-activation adjusted (thinner lines) are shown.

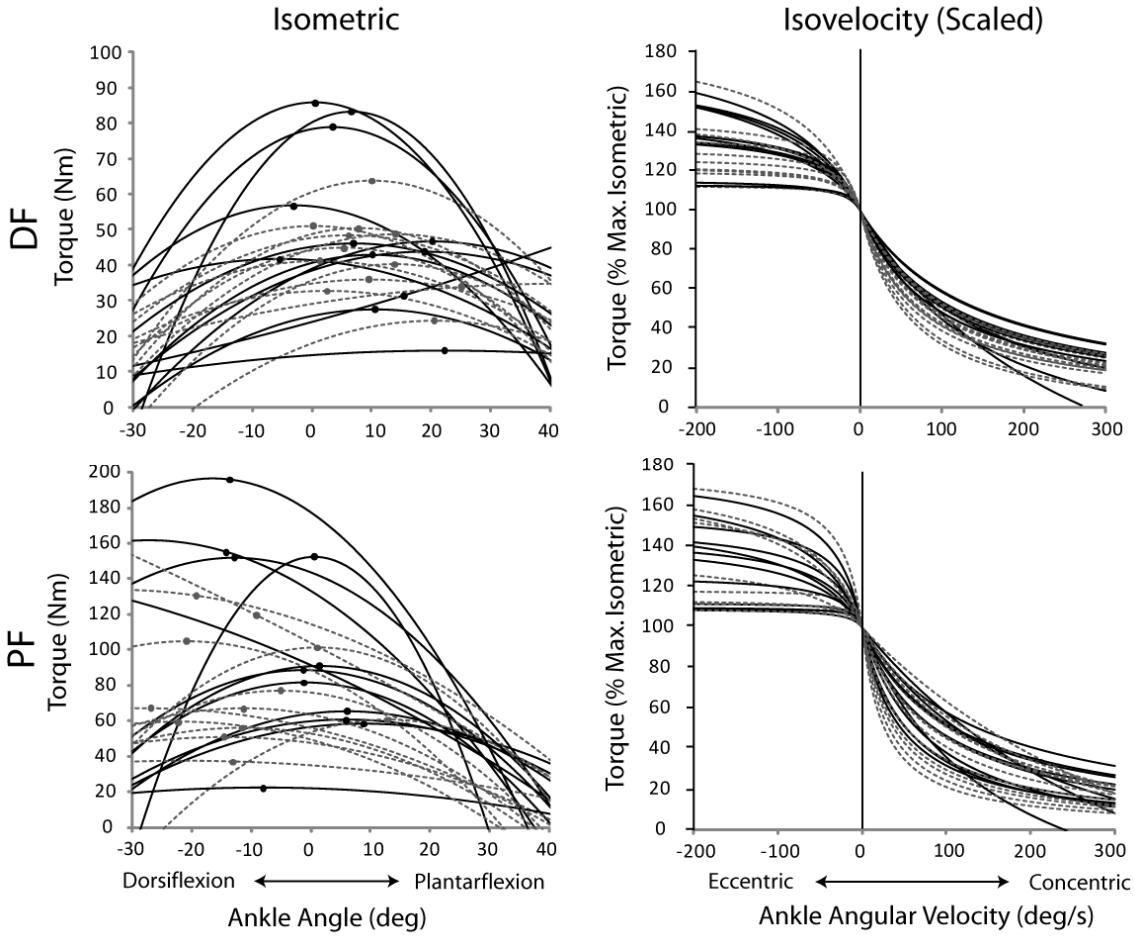

Figure 2-7. Equations representing the best fit between the co-activation adjusted experimental data and second-order polynomials (isometric) and rectangular hyperbolas (isovelocity) for young (solid black lines) and older (dashed gray lines). The solid circles positioned on the isometric curves represent the peak isometric torque. For some subjects, the peak did not occur within the subject's range of motion, in these cases the solid circle is position at the end of the range of motion. The isovelocity fits are scaled to the peak isometric torques (solid circles).

Table 2-4. Parameters describing fits to the experimental co-activation adjusted torque-angle and torque-angular velocity data.

Group	Mus.	Torque-Angle			Torque-Angular Velocity		
		T_0	Angle[a] (°)	Width (°)	$A_{T\omega}$ †	$B_{T\omega}$	T_{ECC}
Young Male	DF	61 ± 28	7 ± 9	96 ± 32	2.7 ± 6.7	117 ± 25	1.48 ± 0.31
	PF	128 ± 62	-8 ± 9	102 ± 26	14.8 ± 30.7	122 ± 61	1.33 ± 0.21
Young Female	DF	40 ± 8	11 ± 9	102 ± 13	9.9 ± 12.9	132 ± 23	1.53 ± 0.28
	PF	81 ± 26	-2 ± 15	118 ± 64	9.3 ± 15.9	91 ± 41	1.43 ± 0.27
Older Male	DF	42 ± 7	13 ± 7	111 ± 48	1.3 ± 2.0	75 ± 16	1.30 ± 0.12
	PF	74 ± 35	-12 ± 9	117 ± 33	5.2 ± 7.4	113 ± 59	1.41 ± 0.29
Older Female	DF	44 ± 14	7 ± 8	95 ± 9	0.5 ± 0.9	91 ± 17	1.39 ± 0.27
	PF	81 ± 27	-12 ± 13	110 ± 34	3.2 ± 7.6	75 ± 57	1.38 ± 0.33
Cohen's *f*		0.40	0.21	0.16	0.21	0.34	0.18
Main Effects		M	M	-	-	A	-
Interactions		A x G	-	-	-	G x M	-

Significant main effects and interactions are shown for age (A), gender (G), and muscle (M)
†Non-normal distribution.
[a]The ankle angle at which the peak torque occurred; Dorsiflexion = Negative; Plantarflexion = Positive

For the maximum isometric torque predicted from the coactivation-adjusted torque-angle curve (T_0), no significant main effect for age was found (p = .063); however, a main effect for muscle (higher torques were produced for plantarflexion; p < .001) and a significant interaction between age and gender was found (p = .040). To assist with interpretation of the interaction, interaction plots are shown in Figure 2-8 (Left). In the females, there were no differences between age groups for the dorsi- (p = .820) or plantarflexors (p = .999). In the males, although there were also no age-related differences in the dorsiflexors (p = .308), the plantarflexors were significantly stronger in the young males (p = .005) compared to the older males.

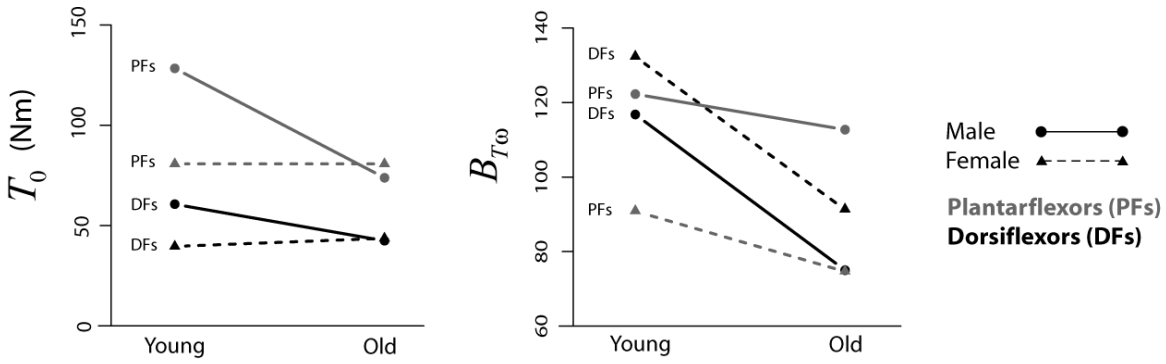

Figure 2-8. Interaction plots for the maximal isometric torque ($T_{0,}$ left) and the coefficient $B_{T\omega}$ for the co-activation adjusted torque-angular velocity relation (right).

The maximum dorsiflexion torque occurred in a plantarflexed position, and the maximum plantarflexion torque occurred in a dorsiflexed position (see Table 2-4). There was a main effect of muscle group for the angle at which the peak torque occurred; the maximum dorsi- and plantarflexion torques occurred at significantly different angles ($p < .001$). There were no effects of age ($p = .315$) or gender ($p = .954$) on the peak torque ankle angle. There were also no significant main effects for the width of the torque-angle relation with respect to age ($p = .655$), gender ($p = .909$), or muscle ($p = .244$).

There were no effects of age ($p = .533$), gender ($p = .996$), or muscle ($p = .712$) on the $A_{T\omega}$ coefficient, which is similar to the Hill a/P_0 coefficient, primarily affecting the shape of the concentric portion of the torque-angular-velocity relation (see Figure 2-11 for a schematic depicting the effects of changing the Hill coefficients). Also, for the eccentric plateau (T_{ECC}), there were no significant main effects of age ($p = .368$), gender ($p = .490$), or muscle ($p = .601$).

There was a significant main effect of age for $B_{T\omega}$, such that the value of the coefficient was greater for the younger subjects ($p = .029$). This coefficient is similar to the Hill b/L_0 coefficient, which affects the overall shape of the concentric and eccentric

portions of the torque-angular velocity curve; the larger value in the young subjects indicates a higher concentric shortening velocity and a less sharp (steep) transition between the concentric and eccentric portions of the curve. There was also a significant interaction between gender and muscle group (p = .044). Ignoring age (in the interaction), $B_{T\omega}$ was greater for plantarflexion in the male subjects, while $B_{T\omega}$ was greater for the dorsiflexors in the female subjects (Table 2-4).

2.3.4 Modeling Results

As expected, several of the muscle property parameters were correlated (see Appendix C). In particular, the maximum series elastic component extension (ΔL_{MAX}) was correlated with the coefficients defining the force-extension relation (α, β). In addition, the maximal contractile component shortening velocity (V_{MAX}) was correlated with the coefficients defining the shape of the force-velocity relation (a/P_0, b/L_0). Therefore, ΔL_{MAX} and V_{MAX} were not included in the MANOVA.

2.3.4.1 General

The optimized force-length, force-extension, and force-velocity relationships are shown in Figure 2-9. The results of the MANOVA performed on the muscle mechanical properties defining the aforementioned relationships (Table 2-5) revealed overall significant main effects for age (p = .012), gender (p = .025), and muscle (p < .001). The results from separate ANOVAs on each mechanical property follow. To assist with interpretation, variables listed in Table 2-5 with significant main effects are displayed in Figure 2-10. The individual costs for Phase 1 and 2 optimizations are in Appendix C.

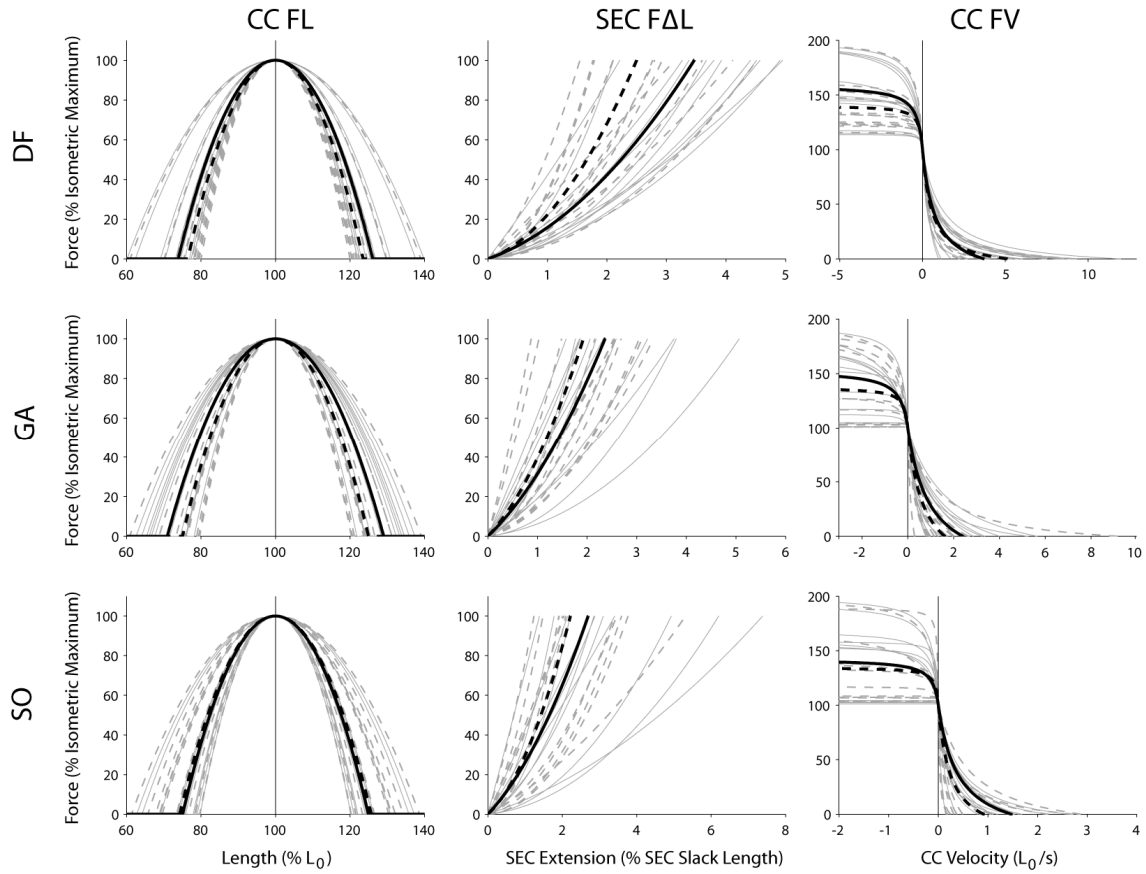

Figure 2-9. Graphical representations of optimized muscle mechanical properties defining the shapes of the contractile-component (CC) force-length (FL) and force-velocity (FV) relations, and the series elastic component (SEC) force-extension (FΔL) relation. Properties for the dorsiflexors (DF), gastrocnemius (GA), and soleus (SO) are shown. The thin gray lines represent data from individual subjects, while the thick black lines represent the mean of the young (solid) and old (dashed) subject groups. Note that x-axis scales are different for the three muscles to allow finer resolution of the curves.

Table 2-5. Optimized muscle mechanical properties.

Group	Mus.	P_0 (N)	Force-Length (FL)		Force-Extension (FΔL)			Force-Velocity (FV)		
			L_0 (cm)	$W(\%L_0)$	α	β	L_S (cm)	a/P_0 †	b/L_0 (s^{-1})	ε ‡
Young Male	DF	976 ± 403	15.4 ± 5.4	52.2 ± 11.8	370 ±165	11.6 ± 14.0	14.9 ± 3.4	0.102 ± 0.002	0.757 ± 0.309	1.58 ± 0.39
	GA	1423 ± 695	20.7 ± 7.6	58.6 ± 11.1	630 ± 299	19.2 ± 13.4	24.2 ± 7.3	0.380 ± 0.117	0.854 ± 0.554	1.42 ± 0.40
	SO	1616 ± 739	14.8 ± 9.7	53.2 ± 12.7	404 ± 284	13.3 ± 14.6	16.0 ± 4.7	0.267 ± 0.150	0.532 ± 0.587	1.31 ± 0.31
Young Female	DF	679 ± 128	14.2 ± 2.3	57.9 ± 12.4	689 ± 645	9.3 ± 6.3	14.1 ± 1.2	0.300 ± 0.230	0.736 ± 0.152	1.60 ± 0.32
	GA	873 ± 584	20.0 ± 6.7	63.4 ± 10.9	954 ± 1055	28.1 ± 23.6	21.5 ± 4.0	0.399 ± 0.151	1.011 ± 0.479	1.64 ± 0.32
	SO	1113 ± 658	13.9 ± 4.0	51.9 ± 10.5	898 ± 973	25.8 ± 23.8	13.0 ± 1.9	0.270 ± 0.136	0.258 ± 0.120	1.53 ± 0.43
Older Male	DF	623 ± 62	15.3 ± 4.6	53.6 ± 13.4	969 ± 795	15.5 ± 12.4	15.7 ± 2.7	0.105 ± 0.012	0.514 ± 0.217	1.37 ± 0.19
	GA	718 ± 149	23.0 ± 6.1	54.3 ± 14.2	1575 ± 910	10.3 ± 9.5	20.6 ± 7.4	0.395 ± 0.203	0.594 ± 0.359	1.27 ± 0.37
	SO	1053 ± 343	21.5 ± 6.0	52.5 ± 11.4	1800 ± 859	8.7 ± 14.0	11.0 ± 3.5	0.237 ± 0.128	0.270 ± 0.226	1.28 ± 0.25
Older Female	DF	721 ± 255	16.0 ± 2.0	45.2 ± 5.9	1412 ± 1237	5.0 ± 3.5	13.0 ± 2.2	0.112 ± 0.029	0.596 ± 0.210	1.44 ± 0.29
	GA	775 ± 225	23.7 ± 8.6	50.9 ± 7.8	1093 ± 590	42.2 ± 37.9	19.2 ± 7.0	0.432 ± 0.059	0.735 ± 0.311	1.48 ± 0.44
	SO	1301 ± 356	17.7 ± 4.0	57.1 ± 12.9	736 ± 529	25.2 ± 23.0	12.6 ± 3.4	0.285 ± 0.110	0.205 ± 0.154	1.41 ± 0.43
Cohen's *f*		0.43	0.24	0.21	0.47	0.25	0.22	0.19	0.27	0.30
Main Effects		A, M	-	-	A	G,M	-	M	A,M	A
Interactions		A x G	-	-	A x G	G x M	-	-	-	-

Note: Main effect and interaction abbreviations: A = Age, G = Gender, M = Muscle

Note: Muscle property abbreviations: P_0 = Maximum isometric force capability; L_0 = Optimal CC length; L_S = SEC Slack Length; W = Width of force-length relation; α, β = Coefficients defining force-extension relation; a/P_0, b/L_0 = Coefficients defining force-velocity relation; ε = eccentric force plateau

†Non-normal distribution (for DF only)

‡ Non-normal distribution (all muscles)

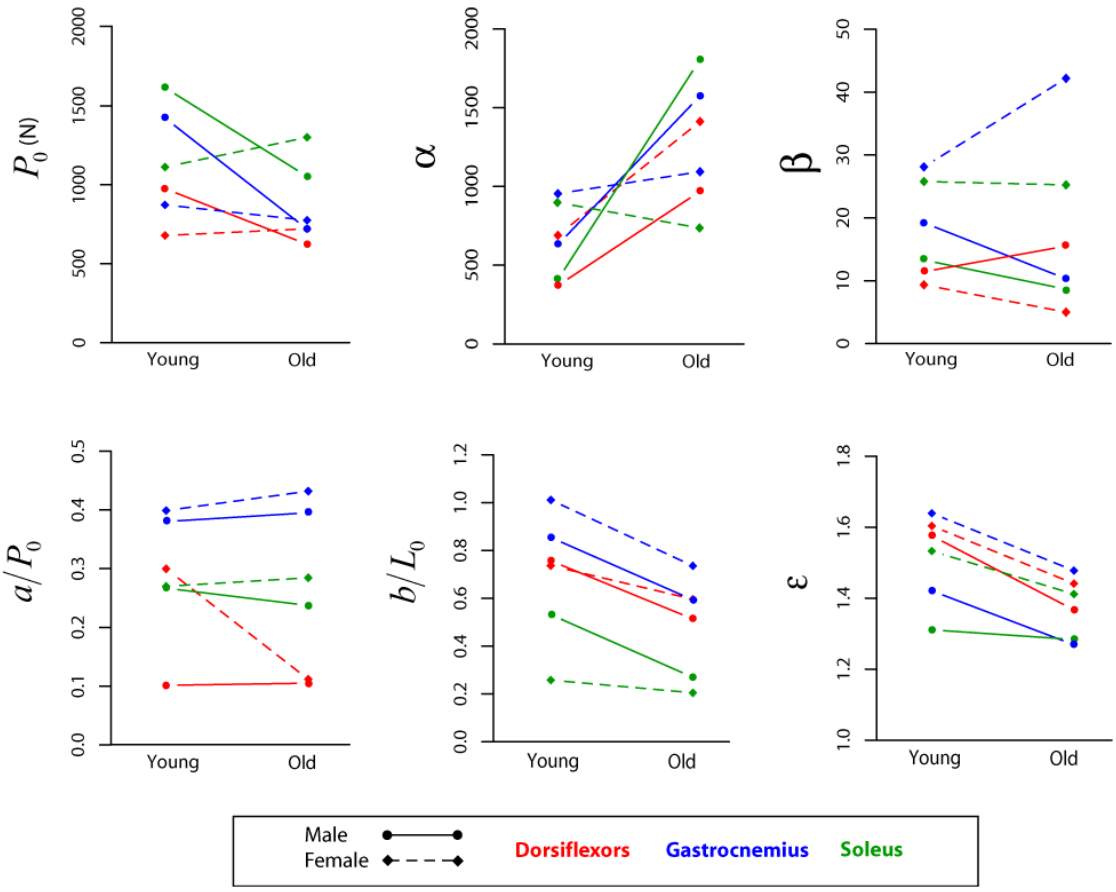

Figure 2-10. Effects of age, gender, and muscle on selected muscle mechanical properties.

2.3.4.2 Maximal Isometric Force

With aging there were declines in maximal isometric force $\left(P_0\right)$ of the male subject group, as there was a significant main effect for age (p = .019), but an interaction between age and gender (p = .006). To quantify the interaction, two-way ANOVAs were performed separately for each gender group, with Age and Muscle as factors. These showed that the older male subjects were significantly weaker than the younger males (i.e. an Age effect; p = .002). However, the young and older female subjects had similar strengths (p = .751). In

these separate ANOVAs, there were also main effects of muscle type, such that SO muscle was stronger than the DF for both the male (p = .025) and female subject (p = .015) groups.

2.3.4.3 Force-Length and Slack Length

There were no significant main effects of age on the parameters describing the force-length relation (L_0: p = .054; L_S: p = .165; W: p = .145). Nor were there any differences between the genders (L_0: p = .567; L_S: p = .275; W: p = .896) and muscles (L_0: p = .355; L_S: p = .448; W: p = .664).

2.3.4.4 Force-Extension Shape Coefficients

In general, the force-extension relations were stiffer in the older male subjects and more linear overall in the female subjects. For the α force-extension coefficient, which controls the rate of increase in stiffness (larger value = stiffer), there was a main effect of age (p = .001), such that the older subjects had larger α values (stiffer muscles). However, there was also an interaction between age and gender (p = .043), which warrants consideration. Separate two-way follow up ANOVAs (Age x Muscle for each gender group) revealed that α was greater in the older male subjects compared to the younger males (p < .001), but was not different between the young and older females (p = .432).

Overall, the female subjects had more linear force-extension relations $\left(\uparrow \beta\right)$. The statistical analysis for β revealed main effects of gender (p = .034) and muscle (p = .031), but also an interaction between gender and muscle (p = .039). There was no main effect for age (p = .986). With respect to the gender main effect, the female subjects had more linear relations, while post-hoc analysis on the muscle type main effect revealed that the GA had a significantly more linear force-extension relation than the TA muscle (p = .023). In terms

of the gender and muscle interaction, the female GA force-extension relation was more linear than the female DF (p =.006) and the male SO relations (p = .027).

In general, subjects who were young or male tended to have greater maximal series elastic component extensions (Table 2-6), as there were main effects for age (p = .009) and gender (p = .007), but not for muscle type (p = .161). There was no interaction between age and sex (p = .055). When normalized to the series elastic component slack length, there were no main effects for age (p = .072) and gender (p = .060). However, there was a main effect for muscle (p = .022); the DF extended to a greater percentage of its slack length compared to the GA muscle (p = .016)

Table 2-6. Maximal extensions and shortening velocities.

Group	Mus.	ΔL_{MAX} (mm)	$\Delta L_{MAX}(\%L_S)$	V_{MAX} (m/s)	$V_{MAX}\ (L_0/s)$
Young Male	DF	6.3 ± 2.5	4.1 ± 1.0	1.05 ± 0.38	7.5 ± 3.1
	GA	7.2 ± 2.6	3.1 ± 1.2	0.39 ± 0.14	2.4 ± 1.8
	SO	7.0 ± 3.6	4.4 ± 2.1	0.24 ± 0.15	2.4 ± 2.2
Young Female	DF	5.0 ± 1.5	3.6 ± 0.9	0.67 ± 0.56	5.0 ± 4.1
	GA	4.8 ± 1.8	2.3 ± 0.8	0.50 ± 0.18	2.9 ± 1.7
	SO	3.1 ± 6.0	2.4 ± 0.8	0.14 ± 0.06	1.1 ± 0.5
Older Male	DF	5.4 ± 3.4	3.4 ± 2.4	0.74 ± 0.29	5.0 ± 2.3
	GA	4.9 ± 1.9	2.5 ± 0.8	0.50 ± 0.51	2.6 ± 3.3
	SO	2.8 ± 1.7	2.4 ± 0.9	0.30 ± 0.25	1.5 ± 1.3
Older Female	DF	4.1 ± 1.7	3.1 ± 1.2	0.87 ± 0.31	5.6 ± 2.4
	GA	4.0 ± 2.3	2.0 ± 0.8	0.52 ± 0.22	1.7 ± 0.7
	SO	3.6 ± 1.9	3.0 ± 1.5	0.14 ± 0.13	0.7 ± 0.5
Cohen's *f*		0.51	0.36	0.11	0.18
Main Effects		A, G	M	M	M
Interactions		-	-	-	-

Note: Main effect and interaction abbreviations: A = Age, G = Gender, M = Muscle

ΔL_{MAX} = maximum series elastic component (SEC) extension in absolute units (mm)

$\Delta L_{MAX}(\%L_S)$ = maximum SEC extension as a percentage of the SEC slack length

V_{MAX} = maximum CC shortening velocity

$V_{MAX}\ (L_0/s)$ = maximum CC shortening velocity in optimal fiber lengths/s (L_0/s)

2.3.4.5 Force-Velocity

The two scaled Hill coefficients control the shape of the force-velocity relation. The first, a/P_0, primarily affects the shape of the concentric portion of the curve, such that greater values draw the curve out to higher concentric velocities (Figure 2-11). There was no significant effect of age (p = .194) or gender (p = .122) on a/P_0. However, there was a significant main effect for muscle (p < .001), with a/P_0 being the greatest for GA, followed by SO, and then the DF.

The second Hill coefficient, b/L_0, has a large influence on the overall shape of both concentric and eccentric portions of the force-velocity curve; large values tend to flatten out the curve and increase the maximal shortening velocity, while small values create a much sharper transition between concentric and eccentric sides and a decrease in the maximal shortening velocity (Figure 2-11). In contrast to a/P_0, there was a significant main effect of age for b/L_0, such that the values were greater in the younger subjects (p = .013). There was also a main effect for muscle; the values for DF and GA were both higher than SO (p < .001), however DF and GA were not different (p = .798).

There was a main effect of age (p = .047) for the eccentric plateau of the force-velocity relation (ε), such that the plateau was lower for the older subjects. There were no main effects of gender (p = .175) or muscle (p = .061).

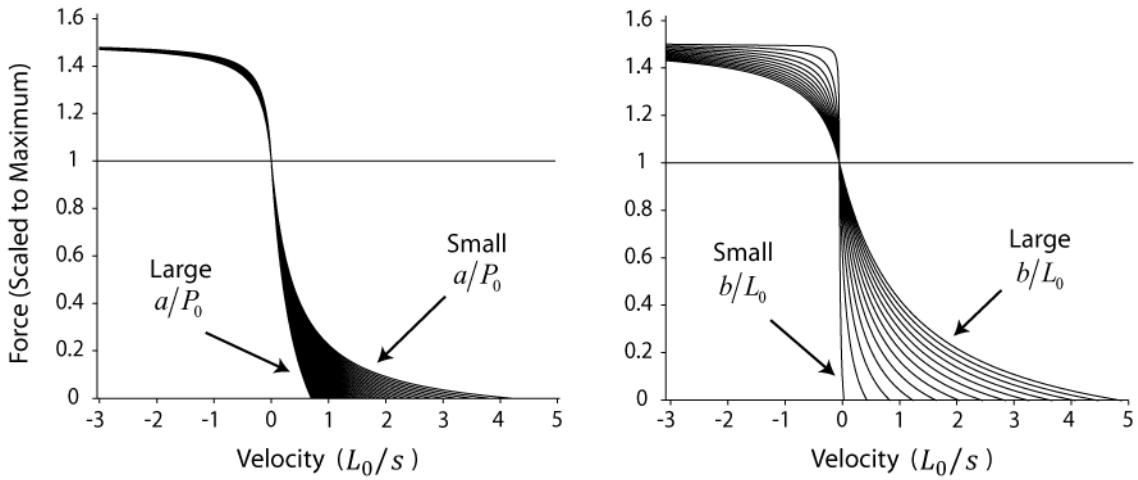

Figure 2-11. Effects of changing the coefficients describing the Hill rectangular hyperbola. Left: effect of varying a/P_0 from 0.1 to 0.6 while keeping b/L_0 constant at 0.45 s^{-1}. Right: effect of varying b/L_0 from 0.02 to1.22 s^{-1} while keeping a/P_0 constant at 0.25. Both Sides: The optimal fiber length (L_0) was set to 0.15 m and the eccentric plateau was equal to 1.5 P_0. The increment between each line is 0.01.

For the maximal CC shortening velocity ($V_{MAX,}$ Table 2-6), there was a main effect for muscle type, whether in absolute units ($p < .001$) or normalized to the optimal CC length ($p < .001$). Post-hoc analysis revealed that the DF had a higher V_{MAX} than both the GA ($p < .001$) and SO ($p < .001$). However, this result should be interpreted with caution, as the values chosen for the DF a/P_0 were up against the lower boundary (0.1) for most subjects. Smaller values for a/P_0 will lead to progressively larger V_{MAX} values. When the lower boundary was decreased beyond 0.1, the optimization chose even smaller values for a/P_0 as this gave better solutions. These improvements were only marginal though, and in this case we would only be "curve fitting", as a/P_0 values below 0.1 have not been observed in experimental studies on mammals. We did not encounter this behavior with the plantarflexor muscles, as the values chosen for a/P_0 in the optimization were well within the limits. In absolute units, the GA had a faster shortening velocity than the SO ($p = .016$).

On the other hand, this difference was not significant when expressed in relative units ($p = .277$). There were no main effects of age or gender for the maximal shortening velocity in absolute ($p = .940$ and $p = .264$, respectively) and relative units ($p = .202$ and $p = .187$, respectively).

2.3.4.6 Comparison with Experimental Data

The joint torque time histories for a representative young and older subject, as well as the results from simulations using the optimized mechanical properties, are shown in Figure 2-12. Qualitatively, the model predictions are in good agreement with the experimental data. However, there were differences in the shapes of the predicted net joint torques. Upon muscle excitation, the muscle forces/joint torques rise relatively quickly for the model, compared with the slower rise in the experimental data. This is likely based on the assumption that once the model's muscles are excited (based on the onset times of the experimental EMG data), they instantaneously rise to a maximal excitation level. However, it should be noted that although the excitation signal to the muscle increased instantaneously, the force producing capability did not due to an excitation-activation relationship with a rising time constant of 15 ms (See Appendix B). In the present study, we use the term "activation" for this force producing capability, which accounts for the various physiological delays that occur after the nervous signal ("excitation") reaches the muscle, such as the release of calcium from the sarcoplasmic reticulum. Bobbert and Van Ingen Schenau (1990) demonstrated that substantial errors could be introduced in the high-velocity isovelocity contractions when the excitation-activation relationship is not accounted for. In the present study, it is likely that some subjects did not fully excite their

muscles initially, which may be responsible for the discrepancy. However, as shown in Figure 2-12, this discrepancy usually occurs before movement, and therefore did not influence the results, as the model was not allowed to choose peak torques occurring outside the isovelocity movement period (i.e. before movement began, and after the movement ended).

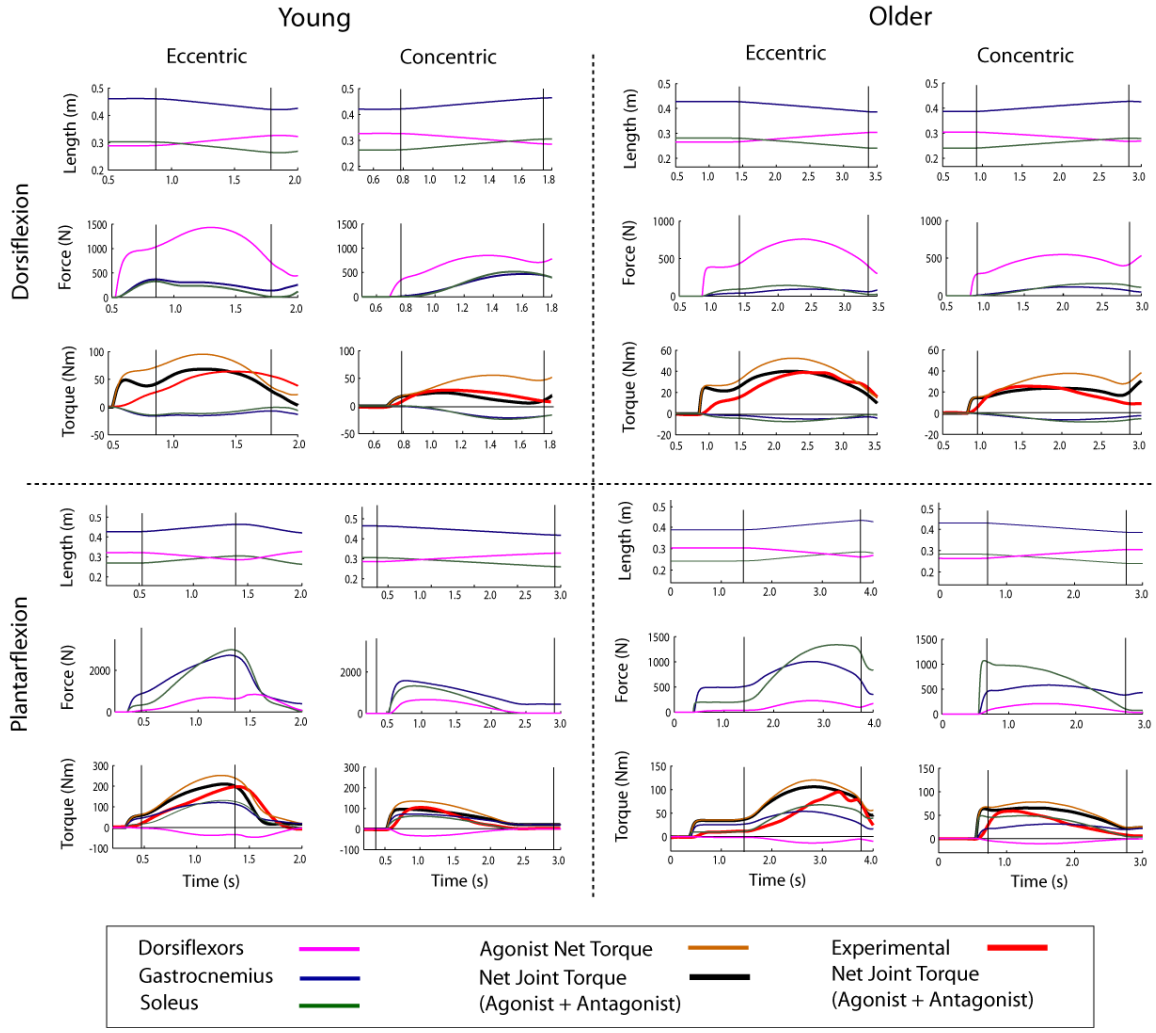

Figure 2-12. Comparison between experimental net joint torque-time histories (red curves) and the net joint torques (black curves) predicted using the optimized muscle properties for a representative young and older subject. The top panels are when the dorsiflexors were acting as agonists, and the bottom panels are when the plantarflexors were agonists. The vertical lines denote periods of a constant rate of change in muscle length.

2.4 Discussion

The main purpose of this study was to determine whether there were differences in the mechanical properties of the dorsiflexors and individual gastrocnemius and soleus plantarflexor muscles between a group of healthy young and older community-dwelling adults. In general, our hypothesis that there would be age-related decreases in the maximal isometric muscle strength, increases in series-elastic stiffness, and slower contractile properties was supported. However, only the male subjects demonstrated significant decreases in muscle strength and increases in muscle stiffness with age. With regard to the velocity-dependent properties of the muscles, there were age-related changes in the shape of the force-velocity relation in both genders, such that less relative force could be produced during both concentric and eccentric muscle contractions for all three muscles. However, the maximal shortening velocity was not different between the age groups.

To obtain these mechanical property estimates for the individual dorsi- and plantarflexor muscles, we combined experimental ultrasound, and MRI, and dynamometer data with musculoskeletal modeling and numerical optimization techniques. The modeling efforts used the experimental data as “inputs”, which were designed to constrain the outputs of the model (the muscular properties). Since the experimental measurements had a great influence on the resulting muscle property estimates, the experimental data will be discussed first, followed by a discussion of the optimized muscle mechanical properties.

2.4.1 Experimental Studies

2.4.1.1 Ultrasound Experiments

Stiffness as measured in the ultrasound experiments relates to the change in the length of the series-elastic components within a muscle with a corresponding change in joint torque. This stiffness was characterized by a second-order polynomial that was fit to the torque-extension data, which was defined by two shape coefficients. The first term $(\alpha_{T\Delta L})$ reflects the overall stiffness, such that larger values are associated with a greater rate of increase in torque as the series elastic components are stretched. The second $(\beta_{T\Delta L})$ reflects the linearity of the torque-extension relation, such that larger values are associated with a more linear rise in torque with extension. Rather than characterize the series elastic stiffness in this fashion, in terms of torque and extension, researchers have computed the series elastic stiffness as the slope of the *force*-extension relation in the linear region at high force levels, i.e. the final 10% (Kubo et al. 2003). We chose not to do this for several reasons. First, it involves estimating the moment arms to convert the measured torque to force, and second, the stiffness measures would be based on only the small, highly variable portion of the force-extension relationship at large force levels. We also did not compute Young's modulus, as these computations require assumptions concerning the length and cross-sectional area of the series-elastic components, which in reality reside in many different locations (e.g. internal and external tendon, within the cross-bridges). Finally, these scaling procedures were unnecessary, as the torque-extension data were used as inputs to a musculoskeletal model, which made its own predictions of the series elasticity (force-extension) within the individual muscle models (i.e. it was not necessary to compute Young's modulus).

The results of this study clearly demonstrated that the older individuals had stiffer $\left(\uparrow \alpha_{T\Delta L}\right)$ torque-extension relationships for both dorsi- and plantarflexor muscle groups, based on an analysis using ultrasound imaging to measure *in vivo* displacements of the internal aponeurosis. These results agree with other reports of increased plantarflexor stiffness with aging (Blanpied and Smidt 1993, Ochala et al. 2004a, Ochala et al. 2005). However, to the author's knowledge, there have not been any studies performed to determine changes in the dorsiflexor stiffness with aging.

Another overall finding was that for both age groups, the torque-extension relation was stiffer $\left(\uparrow \alpha_{T\Delta L}\right)$ and more linear $\left(\uparrow \beta_{T\Delta L}\right)$ for the plantarflexor muscles, compared with the dorsiflexors. Although data in the literature are variable, there is support for the differences between the muscle groups. For young individuals, Young's modulus has been reported to range from 530-1200 MPa for the dorsiflexors (Ito et al. 1998, Maganaris and Paul 1999), and 1108-1806 MPa for the plantarflexors (Magnusson et al. 2001); this equates to a difference of 109% for the lower end and 51% at the higher end of the range. In this study the mean $\alpha_{T\Delta L}$ for the younger subjects was twice as large for the plantarflexors compared to the dorsiflexors (a 99% difference), agreeing closely with the lower ranges in the literature.

Overall, the younger subjects reached higher maximal torque values and had greater maximum extensions than the older subjects. In the older subjects the maximum extension of the plantarflexor muscles was lower than the dorsiflexors (DF: ~7.3 vs. PF: ~4.1 mm), while the opposite was true for the younger subjects (DF: ~8.2 vs. PF: ~9.4 mm). This can be explained by the varying magnitude of the torque differences between the age groups, as

the torque performance of the older subjects was relatively close to the younger subjects in dorsiflexion, but much lower than the younger subjects in plantarflexion.

2.4.1.2 Magnetic Resonance Imaging (MRI)

MRI was used to obtain measurements of the volume of contractile material in the dorsi- and plantarflexor muscles for each young and older subject. Our analysis revealed that the muscle-only volumes and PCSAs were larger in the younger subjects, compared with the older subjects (for male and female subjects). This was expected, and supports previous studies showing reductions in muscle size with increasing age (Aniansson et al. 1980, Frontera et al. 2000a, Frontera et al. 1991), regardless of gender (Young et al. 1985, 1984) or whether the muscle is in the upper or lower extremity (Lynch et al. 1999).

There was no effect of age on total-muscle volume, which includes the muscle volumes occupied by tendon and fat. This suggests that it is important to consider the increasing amount of non-contractile tissue that appears with age, and that the size of the muscle is not necessarily predictive of the force generating capacity of a muscle (which is related to the PCSA calculated from the muscle-only volume). This is supported by studies demonstrating weak relationships between muscle cross-sectional area and strength (Sipila and Suominen 1994, Young et al. 1985). Another finding was that the total muscle volumes, the muscle-only volumes, and the PCSAs were larger in the male subjects (regardless of age), and were different between the muscles, such that the SO had the greatest volume and PCSA, followed by the GA, and finally the DF. These results are again consistent with our expectations and the literature (Wickiewicz et al. 1983).

2.4.1.3 Dynamometer Experiments

An important feature of the present study is that the dynamometer data were adjusted to account for the effects of antagonistic co-activation. The main purpose of performing this adjustment was so the torque-angle and torque-angular velocity relationships of the separate muscle groups, free from antagonistic influences, could be quantified and compared. Thus, the rest of the discussion will focus on the results for the co-activation adjusted data. This adjustment was also done for incorporation into the musculoskeletal model, which did not include antagonistic muscle contributions in the optimization algorithm.

2.4.1.3.1 Torque-Angle Properties

Overall, the maximal isometric torques measured from the co-activation adjusted dynamometer data (T_0) decreased with aging in the male subjects, but did not change in the female subjects. This suggests that there are differences between the genders with respect to the loss of joint strength with aging. For the dorsiflexors, these gender differences are supported by Kent-Braun and Ng (1999), who showed that young men were able to generate significantly more dorsiflexor torque than older men, but there were no differences between young and elderly women. In addition, Metter et al. (1997) demonstrated a greater loss in upper extremity strength for elderly men compared with elderly women. Some caution should be exercised in interpreting the gender differences found in the present study, as the gender sub-groups were relatively small (N = 6), and our findings could be related to random subject selection.

The maximal isometric torque was higher for plantarflexion than for dorsiflexion. This is consistent with the larger PCSAs that were measured for the plantarflexors. The average maximum co-activation adjusted dorsiflexor torque for the young (~50 Nm) and old (~43 Nm) subjects in the present study are higher than those reported by Lanza et al. (2003), which averaged about ~36 Nm and ~28 Nm for young and old subjects respectively (males + females). This discrepancy can be explained by antagonistic co-contraction, which was not accounted for in Lanza et al., and would cause the measured dorsiflexor torques to be underestimated. In terms of the magnitude of the difference between the age groups, the older subjects in the present study produced about 16% less torque than the older subjects, while the difference in Lanza et al. was about 21%.

The vast majority of studies in the literature reporting torque-angle data for the plantarflexors have only used male subjects. In the present study, the maximal co-activation adjusted isometric torques averaged 128 Nm and 74 Nm for young and older male subjects, respectively. Maximal isometric plantarflexion torques have been reported as ~175 Nm (Sale et al. 1982), ~166 Nm (non-dominant leg; Oberg et al. 1987), and ~210 (dominate leg; Oberg et al. 1987) for younger men, and ~120 Nm for older men (Ferri et al. 2003). Thus, the maximal plantarflexor torques of the males in the present study are lower than those in the literature, even with the co-activation adjustment (which increased the agonist torque values). There are many factors that may contribute to this discrepancy, which are related to the data collections on the dynamometer. Overestimation of the agonist torques can be caused by not fixating the upper body or from subjects “cheating” by using muscles groups other than the ones of interest (Oberg et al. 1987). In addition, subjects in

the present study used their left leg, which is likely the non-dominate leg for the majority of subjects.

A recent study by Anderson et al. (2007) measured the maximal isometric plantarflexor torques in younger and older males and females. However, their results are only reported in units that are scaled to body weight and height. For comparison with the results of the present study, the results of Anderson et al. were un-normalized based on the average subject body weights and height reported in their study. After doing these calculations, the results are somewhat curious: young males = 119 Nm and females = 102 Nm, older males = 156 Nm and females = 128. Thus, the older subjects in the Anderson et al study were stronger than the younger subjects. This is not an artifact of the un-normalization procedure, as their normalized values show the same pattern.

There were no differences between the young and older subjects with respect to the ankle angle at which the peak co-activation adjusted isometric torques occurred, but there were differences between the muscle groups. The maximum dorsiflexor torque occurred while the ankle was more plantarflexed (~9.5°, relative to a neutral ankle angle), in agreement with other studies (Belanger et al. 1983, Brown et al. 1999, Lanza et al. 2003, Marsh et al. 1981). On the other hand, the maximal plantarflexor torque occurred with the ankle in a more dorsiflexed position (~ -8.5°, relative to a neutral ankle angle), also consistent with other reports (Belanger et al. 1983, Bobbert and van Ingen Schenau 1990, Ferri et al. 2003, Sale et al. 1982).

2.4.1.3.2 Torque-Velocity Properties.

The ability of the subjects to generate torque at different eccentric and concentric angular velocities was captured by first scaling the data to account for torque-angle effects, and then fitting a rectangular hyperbola, which was the same equation that was used to describe the force-velocity relationships of the individual muscles (see Appendix B). Finally, the torque values were adjusted to account for antagonistic co-activation. There are four parameters that described the shape of this torque-angular velocity curve: T_0, $A_{T\omega}$, $B_{T\omega}$, and T_{ECC}. The discussion will focus on the latter two parameters, as the first parameter (T_0) has already been discussed, and the second ($A_{T\omega}$,), showed no differences between the age, gender, or muscle groups.

In the younger subjects, values for $B_{T\omega}$ were significantly higher than they were for the older subjects, indicating that the younger subjects tended to have larger torques during concentric contractions. The meaning of this difference is shown graphically for the force-velocity relation (for individual muscles) in Figure 2-11, which shows that larger values of the scaled "b" force-velocity coefficient $\left(b/L_0\right)$ signify higher torques across the concentric velocities (the same holds true for $B_{T\omega}$ when looking at the torque-velocity relation, since the equations are the same). It is important to note that the age-related differences in the $B_{T\omega}$ coefficient reflect differences in the scaled torque-angular velocity relation, which therefore takes into account differences in the maximal isometric torque capabilities of the subjects. These age-related differences in the concentric torque capabilities are consistent with the findings of other studies, which showed age-related declines in maximal torques across all concentric velocities (also accounting for torque-angle effects) for the dorsiflexors (Lanza et al. 2003) and knee extensors (Harries and Bassey 1990).

To the author's knowledge, previous studies have not shown gender related differences in the torque-velocity relation. However, in the present study the male subjects were able to generate more relative torque during concentric plantarflexion compared to dorsiflexion (PF $B_{T\omega}$ > DF $B_{T\omega}$), while the female subjects generated more relative torque during concentric dorsiflexion compared to plantarflexion (PF $B_{T\omega}$ < DF $B_{T\omega}$). Note that these differences are for the scaled torque-velocity data, so differences in the strengths of the male and female subjects, and between the dorsi- and plantarflexors are accounted for.

2.4.2 Individual Muscle Mechanical Properties

Collectively, there were significant changes in the individual muscle properties with aging, as well as differences between the genders and muscles. These general findings are based on the results of the multivariate analysis of variance (MANOVA) performed on the complete set of muscle properties defining the maximal isometric force (P_0), force-length (L_0, W), force-velocity $(a/P_0, b/L_0, \varepsilon)$, and force-extension (α, β, L_S) properties. Of note, is that a similar multivariate analysis on the *joint* properties (based on the dynamometer data) only revealed significant overall effects for muscle group (dorsi- or plantarflexors). *Therefore, the analysis of individual muscle properties revealed some age and gender differences that were absent at the joint level.*

2.4.2.1 Maximal Isometric Force

In broad terms, the predicted maximal isometric force (P_0) for the individual muscles was significantly lower for the older subjects, compared with the younger subjects, supporting the hypothesis that the older subjects would be weaker. This finding is

consistent with the PCSA data, which are closely associated with the maximal isometric muscle force (Gans 1982). However, some restraint should be exercised in this general interpretation, as there was an interaction between age and gender, such that the older males had significantly weaker P_0 values than the younger males, but there were no differences in strength between the young and older females. In other words, the gender-related differences in strength tended to disappear in the older subjects. Because the model data were based on the dynamometer measurements, these data are consistent with the age-related changes seen in the maximal isometric torque data.

Due to the difficulty of measuring muscle forces *in vivo*, researchers have employed a number of different methods to arrive at estimates of the maximal isometric force. A representative sampling of these studies, along with the results of the present study are presented in Table 2-7. To facilitate comparison with the studies in Table 2-7, only the data on the younger subjects from the present study are included, as almost no simulation studies have tried to measure/estimate the maximal isometric force in older adults (besides the present study). One of the only studies to report maximal isometric muscle forces based on direct measurements is Arndt et al. (1998), who inserted an optic fiber through the Achilles tendon. Other studies have made direct force measurements, but during dynamic activities and not during maximal isometric contractions (Komi et al. 1992, Komi et al. 1987). Arndt et al. (1998) report a maximal isometric force of ~3000 N for the plantarflexors of a young male subject, which is very close to the average of the young male subjects in the present study. In contrast, it appears that many studies have used relatively large maximal isometric force values, which might be overestimate the strength of “average” individuals; especially for the plantarflexor muscles (see Table 2-7).

No studies have reported direct force measurements from the dorsiflexor muscles, presumably due to the difficulty of attaching a buckle transducer or inserting an optic fiber through the smaller dorsiflexor tendons. Nevertheless, based on the trends seen in estimating the plantarflexor maximal isometric force, values used for the dorsiflexors in the literature might be considered on the high side. However, it should be considered that the results of the present study were all taken from the left leg, which is likely the non-dominant side for most subjects - values for the dominant side may be larger.

Muscle maximal isometric force is one of the most influential muscle model parameters, as previously shown in models of individual joints (Maganaris 2004, Out et al. 1996), jumping (Nagano and Gerritsen 2001, Pandy et al. 1990), and running (Scovil and Ronsky 2006) have been shown to be sensitive to this parameter. Of note however, is that jumping and running are very vigorous movements, where many muscles would be expected to operate for brief periods near their maximal capacities. Simulations of submaximal movements, such as upright standing may not be as sensitive to maximal isometric muscle force, although the control signals sent to the muscles of a weaker older musculoskeletal model will necessarily be larger than if the muscle was stronger. In general, considering the age- and gender-related changes in the maximal isometric muscle force observed here, it is important to consider the implications of using general estimates rather than subject-specific values in musculoskeletal modeling and simulation.

Table 2-7. Maximal isometric force (P_0) for dorsi- and plantarflexor muscles reported in the literature and the present study.

	Subjects	Method	TA	DF	GA	SO	PF
Present Study	Males (21-30 yrs)	8	-	976	1432	1616	3048†
	Females (21-31 yrs)		-	679	873	1113	1986†
Arndt et al (1998)	Male (26 yrs)	2	-		-	-	~3000
Wickiewicz. et al. (1984)	Males & Females (20-38 yrs)	1	-	792	-	-	2769
Bobbert et al. (1986)	Males (23 ± 4 yrs)	4	-	-	3000[a]	3000[a]	6000†
Brand et al. (1986)	Male Cadaver (37 yrs)	7	535	1348[b]	688	1008	1696
Bobbert et al. (1990)	Males (23 ± 3 yrs)	4	-	-	2430	2430	4860†
Hoy et al. (1990)	None (Data taken from literature)	3	-	1400	2372	4234	6606†
Pandy et al. (1990)	None (Data taken from literature)	5	1400	-	2370	4235	6605
Raasch et al. (1997)	None (Data taken from literature)	9	1375	-	2225	3549	5774
Anderson et al. (1999)	Males (26 ± 3 yrs)	6	1003	-	1651	3016	4667

1: Divided measured torque by moment arm estimate (tendon-excursion method)
2: Measured using optic fiber through Achilles tendon
3: Maximum isometric force of muscle models predicted using CSA from Wickiewicz et al. (1983), multiplied by a scaling factor to match experimental torque from Sale et al. (1982) and Marsh et al. (1981)
4: Forces in muscle model predicted by best-fit to experimental torque-angle data (assigned GA and SO same value)
5: Estimated from data reported by Wickiewicz et al. (1983) and Brand et al. (1986)
6: Estimates from Delp (1990) were adjusted to fit experimental maximal isometric torques
7: Predicted using static nonlinear optimization, minimize muscle stresses, used measured PCSAs as inputs
8: See methods section.
9: Data from Delp (1990) were used

[a]Adjusted upwards from 2790 N based on submaximal activation
[b]Summed values given for all dorsiflexors (includes extensor hallucis longus, extensor digitorum longus, peroneus tertius)
†Added GA an SO values in table together
TA: tibialis anterior; DF: dorsiflexors; GA: gastrocmenius; SO: soleus; PF: plantarflexors

2.4.2.2 Force-Length

No differences in the parameters describing the force-length relation were found with respect to age. These parameters include the optimal contractile component length (L_0) and the width of the force-length relation (W). These results are supported by studies of isolated rat muscle and human skeletal muscle, which have shown that both the optimal fiber length and shape of the force-length relation are relatively unchanged with age (Brown et al. 1999, Larsson et al. 1997). However, many previous studies have shown that the performance of both Hill muscle models and locomotion simulations are sensitive to the values chosen for the optimal contractile component length (Lloyd and Besier 2003, Lloyd and Buchanan 1996, Manal and Buchanan 2004, Out et al. 1996, Scovil and Ronsky 2006, van den Bogert et al. 1998). Based on these past studies, the force-length properties of muscle should be selected with care when simulating human movement with musculoskeletal models; however, the data from the present study suggest that it may not be crucial to account for age-related differences in force-length properties.

2.4.2.3 Series Elasticity

There were age-related differences in the stiffness of the series elastic components of the muscle models, such that the rate of increase of stiffness (α) with increasing force was greater in the older male subjects. However, there were no such differences in stiffness in the female subjects, and no age-related differences in the degree of linearity of the force-extension relationship (β) or the series-elastic slack length (L_0) in either gender group. In general, these results are consistent with the data from the ultrasound

experiments, where the older subjects had stiffer torque-extension relationship, although there was no interaction with gender present in the ultrasound data. Our findings of increased stiffness with age are also supported by reports in the literature (Blanpied and Smidt 1993, Ochala et al. 2004a, Valour and Pousson 2003). Additional support is provided based on Ochala et al. (2007a), who demonstrated significant age-related increases in the stiffness of single muscle fibers obtained from muscle biopsies of the vastus lateralis.

The gender-related differences in stiffness may be explained by differences in the overall physical condition of the older subject gender groups. Although all of the older subjects were healthy, active, community-dwelling individuals, the older females may have been in better physical condition. This is supported by the different age-related changes in muscle strength (P_0) between the gender groups, such that the strength of the female subjects did *not* decrease with aging, compared to significant decreases in the male subjects. Therefore, the series elastic stiffness of the male subjects' muscles may have increased to offset the strength loss, allowing a tighter coupling between muscle activation and force production, "counterbalancing the effect of aging" (Ochala et al. 2007b). In the literature, results of studies on aging and gender differences in stiffness are equivocal. For instance, Ochala et al. (2004a) showed that the plantarflexor stiffness of older males is decreased compared to older females. However, Burgess et al. (2008) demonstrated no differences between genders in more active older adults - providing additional support for physical activity as a moderator of muscle stiffness in older adults. Along with the results of the present study, these observations suggest that age and

gender related differences in the stiffness of musculotendon complexes should be considered when modeling the movements of older individuals.

2.4.2.4 Force-Velocity

In the present study, there were no differences between the age groups or genders for a/P_0, which mainly controls the shape (concavity) of the concentric side of the force-velocity relationship (Figure 2-11). On the other hand, there were age-related changes in b/L_0, which was greater for the younger subjects compared with the older subjects. The parameter b/L_0 affects both concentric and eccentric portions of the force-velocity relation; a larger value of b/L_0 causes the force-velocity curve to "flatten out", increases the maximum shortening velocity, and enables larger forces to be produced at high velocities (Figure 2-11). The values for the eccentric plateau (ε) of the force velocity relation were lower for the older subjects, compared to the younger subjects, suggesting that the capacity to produce eccentric force is reduced with aging.

Although there were no differences between the age or gender groups for a/P_0, there were differences between the muscles, with a/P_0 being the largest on average for the GA (0.40), followed by the SO (0.27), and then the DF (0.15). Close (1972) stated that values of a/P_0 for mammalian muscles are generally in the range of 0.15 - 0.30 (Close 1969, 1964), and are higher in the faster contracting muscles compared to slower ones. However, other studies have suggested values that are higher than Close's upper limit. For instance, with regard to individual muscles, values for rat tibialis anterior of 0.36 were given by Wells (1965), while Phillips and Petrofsky (1980) reported values greater than 0.5 for cat lateral and medial gastrocnemius and soleus. Concerning

experiments on muscle groups, Wilkie (1950) reported values for ranging from 0.20 – 0.48 in five male and female subjects for the elbow flexors. Chow and Darling (1999) reported even larger values between 0.5 - 0.6 in male and female subjects performing wrist flexion. Finally Bobbert and Van Ingen Schenau (1990) used values as low as 0.12 for a "slow" model of the triceps surae, which they estimated from measurements made by Hof and Van Den Berg (1981). Thus, the average a/P_0 values for the GA and SO estimated in the present study seem reasonable, as the value for the GA should be higher than the SO, based on the proportion of fast-twitch Type II muscle fibers (GA has about 50/50 Type I and Type II) (Johnson et al. 1973); (SO has mostly Type I [89%]) (Gollnick et al. 1974, Johnson et al. 1973). The relatively low value for the DF also fits expectations, as the dorsiflexors have a large proportion of slower Type I muscle fibers (for TA: 76% young, 84% old) (Jakobsson et al. 1988).

In the literature, values for b/L_0 are reported far less frequently than a/P_0. Bobbert and Van Ingen Schenau (1990) used a value for b/L_0 of 5.2 s^{-1}, calculated from the data of Spector et al. (1980) for the cat medial gastrocnemius. Wells (1965) reported a values of 2.25 $s^{-1}$for rat tibialis anterior, and 0.40 s^{-1} for rat soleus. Unfortunately, as pointed out by Wickiewicz (1984), it is difficult to compare values across studies, since the value depends on the definition of muscle length. Both Spector et al. and Wells used the *in situ* lengths of the muscles as the "standard length". In the present study, the Hill b coefficient was normalized to the optimal contractile component length (L_0) of the Hill muscle model (b/L_0), which is very different than the lengths of the small animal muscles used in Spector et al. and Wells. Despite the significant age-related differences in b/L_0 in the present study, these may not have a large impact on the results of

simulation studies, as Scovil and Ronsky (2006) showed that the results of an isolated muscle model simulation and walking and running simulations were insensitive to the values of b/L_0.

Finally, the force-velocity eccentric plateau constant (ε) for the older subjects (average = 1.34) was lower than for the younger subjects (1.51), suggesting that the capacity to produce eccentric force is reduced with aging. This agrees with reports showing that eccentric strength is decreased with age both in absolute and relative (to the isometric maximum) units (Hortobagyi et al. 1995, Klass et al. 2005, Porter et al. 1995a, Porter et al. 1997, Poulin et al. 1992, Vandervoort et al. 1990).

2.4.2.5 Maximal Shortening Velocity

The results of the modeling and optimization revealed no age- or gender-related differences in the maximal shortening velocity (V_{MAX}), which is frequently expressed in optimal fiber lengths per second. Epstein and Herzog (1998) give typical values of 8 L_0/s or less for slow twitch muscles, and about 14 L_0/s for fast-twitch muscles in humans. These values are difficult to compare with our results (Averages: DF=5.8 L_0/s, GA = 2.4 L_0/s, SO = 1.4 L_0/s) for the same reasons discussed earlier for comparing b/L_0 between studies, as they are dependent on the definition of fiber length. Most phenomenological muscle models use a functionally equivalent contractile component; therefore, the length of this component is not equal to any physiological structure. An alternative is to express the maximal shortening velocity in terms of the total musculotendon length, which also poses problems. Close (1972) points out that maximal shortening speeds, whether expressed as the speed of shortening of the whole muscle or

in muscle lengths per second are of "…little use in estimating the properties of the contractile material unless they are converted to speed of individual fibers or sacromeres." Ideally, speed of shortening should be expressed in terms of the lengths of single sacromeres (Close 1972). For modeling studies using phenomenological models, this is not possible as there is no explicit representation of single sacromeres. However, if the model's contractile component can be considered to behave as a scaled-up version of a single sacromere, the best approach may be to scale V_{MAX} to the length of the contractile component (as done in this study), and not the length of the entire muscle model (contractile and series elastic component lengths).

2.4.3 Limitations

Every musculoskeletal model is a simplification of the human system. The degree of simplification depends largely on the research question, and a good philosophy is to use the simplest model possible (Winters and Stark 1987). Adhering to this, a number of simplifications and assumptions were made in the present study. Several simplifications were made of the lower leg anatomy, all of which are common in musculoskeletal modeling. The optimized mechanical properties of the dorsiflexors represent a lumped "equivalent" dorsiflexor muscle. Thus, the dorsiflexor properties may not represent any single dorsiflexor muscle, such as the tibialis anterior. Similarly, the plantarflexor muscle properties were found for the GA and SO muscles, which do not include the "other plantarflexors" (e.g. tibialis posterior) and do not separate the contributions of the medial and lateral heads of the GA muscle.

We assumed that once the muscle models were excited, the excitation level instantly rose to a maximum and remained at this level for the remainder of the simulation. For the isometric simulations, this occurred immediately; for the isovelocity simulations, the excitation onset time was based on experimental EMG data. We based this assumption on the appearance of the measured EMG, which appeared to remain relatively constant throughout the isometric and isovelocity contractions. Data from Klass et al. (2005) support this assumption, as they showed that there are no age-related differences in the ability of individual to maximally excite their muscles in either isometric or isovelocity movements. An alternative approach would have been to use the entire experimental EMG time-series as an input to the model, by computing the linear envelope and "driving" the simulation. However, there are a number of considerations with this approach: 1) there is movement between the surface EMG electrode and the underlying muscle during isometric and isovelocity contractions (Kamen and Caldwell 1996), which will alter the relationship between the linear envelope and the level of excitation, 2) the surface EMG activity detected from the SO is quasi-specific (i.e. there is substantial cross-talk present) (Cram et al. 1998). An additional consideration is that the isovelocity dynamometer data collections were done on separate days, complicating the normalization of EMG data due to daily variations in skin preparation and electrode placement.

We did not include pennation angle explicitly in the simulations; however, pennation angle was used in the PCSA calculations, which influenced the relative maximal isometric forces that the model could choose for the GA and SO muscles. By not including pennation angle, the predicted muscles forces would be slightly

overestimated. However, even with a relatively large pennation angle, as in the SO muscle, the effects would be minor (although noticeable, e.g. if the pennation angle is 25°, the force transmitted to the skeleton would be reduced by about 9%.). However, studies have shown that an accurate correction for pennation angle would be nonlinear, such that the pennation angle would change as a function of the muscle force (Kawakami et al. 1998). The addition of a pennation angle would also change the velocity of shortening, as it changes the orientation between the contractile and series elastic component. Thus, including an accurate pennation angle adjustment would have increased the complexity of the model considerably.

Finally, the muscle model does not have history dependence, such as force depression following muscle fiber shortening (Edman et al. 1993) or enhancement following lengthening (Edman et al. 1978, Rassier and Herzog 2002). This would have had minimal influence on the results of the isometric simulations, as the force level in the muscle models reached a plateau and remained at this level for at least a few seconds. In the isovelocity simulations on the other hand, it is expected that neglecting force depression/enhancement would have caused small errors in the predictions of muscle force. However, these errors would have been consistent across the subjects groups, as there have been no reports on age-related changes in force depression/enhancement.

2.4.4 Conclusions

This study developed a methodology to combine muscle imaging, dynamometer experiments, muscle modeling, and numerical optimization to arrive at subject-specific estimates of the mechanical properties of the dorsi- and plantarflexors in young and older

adults. Compared to the younger males, the older males had lower maximal isometric force capabilities and increased stiffness, while there were no age-related differences in strength and stiffness in the female subjects. Regardless of gender or muscle group, the older subjects had significant changes in the shape of the force-velocity relation, and had lower eccentric force capabilities. No differences were found for the parameters describing the force length relation. Based on these age-related related differences in muscle mechanical properties, consideration should be given to the values of these parameters when implementing musculoskeletal models to describe the movement of older individuals.

CHAPTER 3

MUSCULAR PROPERTIES AND POSTURAL CONTROL

3.1 Introduction

While standing upright, older adults are less stable than younger adults (Woollacott and Shumway-Cook 1990), as they exhibit increased center of pressure (CoP) and center of mass (CoM) motion (Brocklehurst et al. 1982, Colledge et al. 1994, Era and Heikkinen 1985, Redfern et al. 2001). These differences have been associated with an increased risk of falling (Shumway-Cook et al. 1997, Tinetti et al. 1988). Older adults also exhibit reduced temporal margins of stability, which can be measured through variables such as the CoP and CoM time-to-contact (Slobounov et al. 1998).

To maintain postural stability in humans, the sensory system must provide information about the body's orientation and relative stability, while the neuromuscular system must make necessary postural corrections. The sensory system includes the visual, vestibular, and somatosensory systems, while the neuromuscular system includes the motor unit pool and its interactions with the skeletal muscle system. The literature has shown that both systems are degraded with aging, negatively influencing the postural stability of older adults. Although the effects of age-related changes in the visual, vestibular, and somatosensory systems (Woollacott and Shumway-Cook 1990, Woollacott et al. 1986) as well as the neural system (Light 1990, Speers et al. 2002) have been well documented, the influence of age-related changes in muscular mechanical properties on postural stability is not clear.

The mechanical properties of muscle are those that influence force production. The amount of force produced by a muscle in response to a neural input (muscle excitation) is dependent on a number of factors, including the length and velocity of the muscle contractile elements, as expressed in the force-length (Gordon et al. 1966) and force-velocity (Hill 1938) relations, and the compliance of the series elastic structures as seen in its force-extension relation (Bahler 1967). The force-length relationship dictates how much force a muscle can produce at a given muscle length, and has been shown to remain unchanged with age (Chapter 2) (Brown et al. 1999, Larsson et al. 1997). However, with regard to the force-velocity relation, older individuals have shown a decrease in the maximum shortening velocity of plantarflexor muscles (Narici et al. 2005), as well as shifts in the torque-angular velocity relationship (Karamanidis and Arampatzis 2005, Lanza et al. 2003). In addition, the maximal contraction velocity of single muscle fibers reportedly decreases with age (Doherty and Brown 1997, Larsson et al. 1997, Thompson and Brown 1999). Age-related changes in these mechanical properties will alter the translation of neural commands into muscle force. This may in turn change the way in which the nervous system coordinates multiple muscles during postural control, and may at least partially explain the declines in balancing ability with aging.

In living humans, it is difficult to measure these mechanical properties for individual muscles. Therefore, it is common to use a combination of experimentation and modeling to estimate these muscular properties (Bobbert and van Ingen Schenau 1990, Garner and Pandy 2003, Koo and Mak 2005, Lloyd and Besier 2003, Winters and Stark 1988, Zajac 1989). Muscle behavior is often modeled using a two-component Hill model

(Hill 1938), consisting of a contractile component with nonlinear force-length and force-velocity relations and a series-elastic component possessing a nonlinear force-extension relation. The parameters that determine the shapes of the relations for the contractile component are the maximal isometric force capability (P_0), optimal length (L_0), slack length (L_S), width of the FL relation (W), and shape coefficients for the force-velocity relation $(a/P_0, b/L_0, \varepsilon)$. Finally, two coefficients define the shape of the force-extension relation of the series elastic component (α, β). A detailed explanation of these equations is provided in Appendix B.

In Chapter 2, these model parameters were estimated for the major muscles controlling the ankle joint (dorsiflexors [DF], gastrocnemius [GA], and soleus [SO]), for a group of young and old subjects. The results of this study provided evidence for age-related changes in the maximal isometric force, series elasticity, and force-velocity characteristics of the dorsi- and plantarflexor muscles. Compared to the younger subjects, the older male subjects had muscles with lower maximal isometric force capabilities $(\downarrow P_0)$ and increased series elastic stiffness $(\uparrow \alpha)$. Regardless of gender, the shape of the force-velocity relation was changed with age, such that older adults produced relatively less force during periods of either muscle shortening (concentric) or lengthening (eccentric) $(\downarrow b/L_0, \downarrow \varepsilon)$.

The purpose of this chapter is to evaluate the postural control of the same subjects from Chapter 2, and relate alterations in balance control with the changes seen in muscular properties. In particular, we sought to identify specific mechanical properties that are most predictive of the performance on various static and dynamic postural tests. It was hypothesized that the older adults would have poorer postural control than younger

subjects, and these deficits would be associated with the age-related changes in the muscle mechanical properties. Based on the age-related changes in muscle properties seen in Chapter 2, it was expected that the maximal isometric force, series elasticity, and force-velocity properties would be most predictive of age-related differences in balance performance.

3.2 Methods

3.2.1 Overall Experimental Design

Experimental postural control data were collected on the same young and old subjects who participated in the study described in Chapter 2. Their postural stability was evaluated under several static (quiet stance, leaning forward and backward) and dynamic conditions (swaying at preferred and imposed frequencies, reaching, and responding to an external perturbation).

3.2.2 Experimental Setup

3.2.2.1 Ground Reaction Forces and Marker Kinematics

A force platform (Model BP600, 1200 x 2000 mm, AMTI, Watertown, MA) was used to collect ground reaction forces and moments. For measurement of the total body center of mass (CoM) motion, whole-body kinematics were measured using passive reflective markers placed on anatomical landmarks (Figure 3-1) and an 8-camera infrared motion capture system (ProReflex MCU 240, Qualysis, Gothenburg, Sweden). Three-dimensional marker coordinates were captured, however only sagittal plane motion was analyzed.

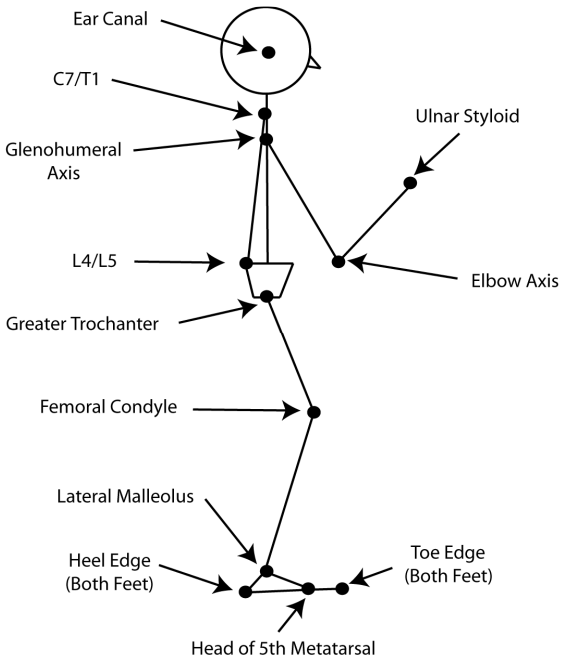

Figure 3-1. Subject marker setup.

3.2.2.2 External Perturbation Backboard / Pendulum System

For the balance perturbations, a backboard apparatus (Figure 3-2, Left) was constructed similar in concept to the one developed by Peterka and Loughlin (2004). The backboard acted to distribute the impact forces imparted by a swinging pendulum during the balance perturbations. The backboard was supported on two bearings aligned with the ankle joint, limiting motion to the sagittal plane. Straps secured the subject's upper body to the backboard, allowing movement only about the ankle joints, such that the subject's motion approximated that of an inverted pendulum. Concern that the backboard inertia might influence postural control was minimal based on Perteka and Loughlin (2002), who found no differences in the amplitude and frequency of the CoP or ankle torque generated in freestanding and backboard-restrained subjects.

A pendulum striker was used to ensure consistent external perturbations of known magnitudes. The pendulum was instrumented with a load cell (Figure 3-2, B) to measure the impact force, and a potentiometer (Figure 3-2, C) to measure the angular position of the pendulum. A shock absorber mounted to a load cell dampened the impact force (Figure 3-2, D). The shock absorber consisted of an outer brass tube attached to the load cell, and an inner spring-loaded telescoping brass tube attached to a padded strike plate (Figure 3-2, E). The pendulum angle was displayed on an LCD mounted on the pendulum (Figure 3-2, F), which allowed an investigator to easily release the pendulum from specific angles. The magnitude of the perturbation was fully determined by the release angle of the pendulum.

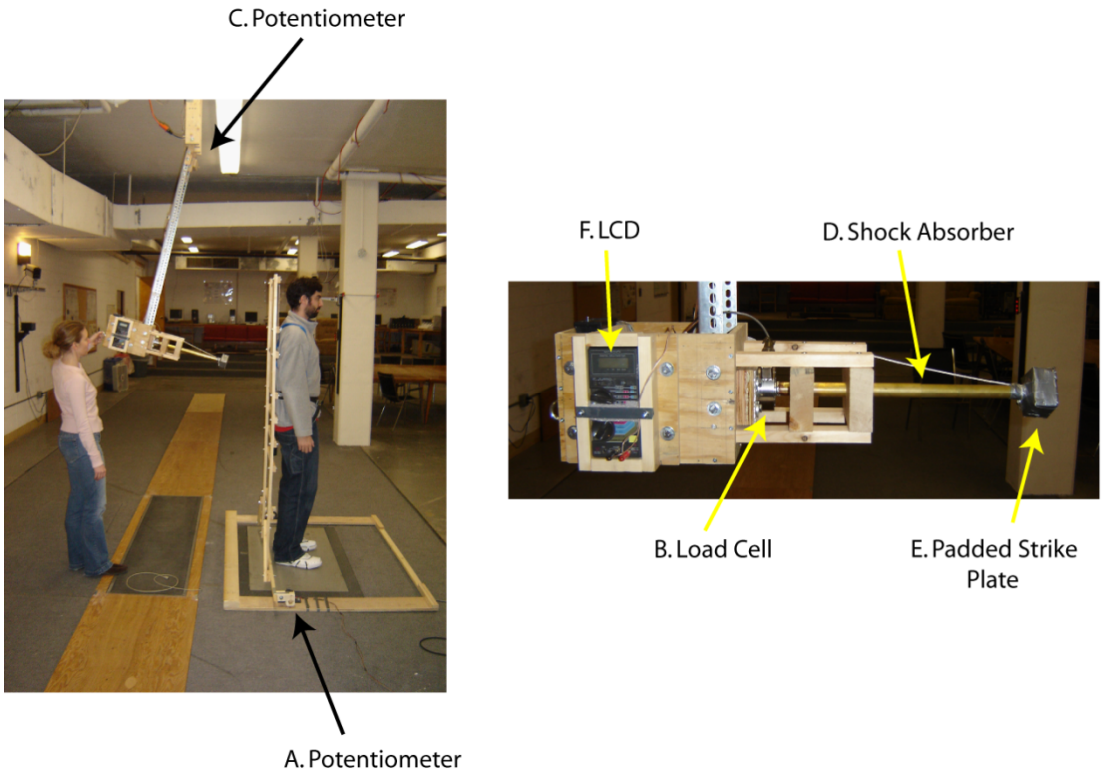

Figure 3-2. Left: Setup for the external perturbation condition. Right: Detail of the pendulum.

3.2.2.3 Safety Considerations

All of the older subjects wore a full-body safety harness anchored to the ceiling. The tether rope was adjusted for each subject to remain slack during all postural tests unless the subject fell. Although subjects lost their balance and needed to take compensatory steps during some of the postural tests, none of the subjects fell at any time. During the external perturbations, subjects were told that they could stop at any time if they felt uncomfortable or the magnitude of the perturbations was too large. None of the subjects reported any discomfort during these tests, and all subjects completed all aspects of the protocol successfully, with the exception of one older subject who chose not to do the external perturbation condition.

3.2.2.4 Sampling

Ground reaction forces, marker kinematics, pendulum angles, impact forces, and metronome signals (for Rhythmic Sway) were sampled using a 16-bit analog-to-digital card on a personal computer. The marker kinematics were sampled at 200 Hz, while all other data were sampled at 1000 Hz.

3.2.3 Protocol

The experimental conditions included: 1) quiet stance, 2) static leaning (forward and backward), 3) rhythmic sway (anterior-posterior sway at preferred and imposed frequencies), 4) maximum reach, and 5) an external pendulum perturbation. A schematic showing the flow of the experimental session is shown in Figure 3-3.

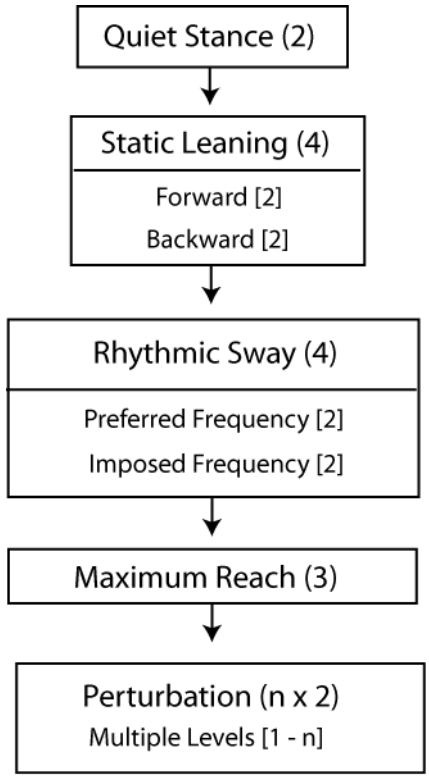

Figure 3-3. Diagram of the experimental protocol. Numbers in parenthesis indicate total number of trials performed for each condition; numbers in brackets indicate number of trials in different sub-conditions. For the external perturbations, the number of perturbations (n) varied between subjects (see text for details).

For all conditions, subjects were instructed to stand with their eyes open. The feet were positioned directly under the hips in line with the anterior-superior iliac spines, parallel with the sagittal plane. For most conditions, two trials were performed. Three trials were performed for the maximum reach, while a variable number of trials were performed for the external perturbations, until subjects needed to step.

3.2.3.1 Quiet Stance

For the quiet stance condition subjects were instructed to stand as still as possible for 30 s with their hands behind their back, keeping their gaze focused on a target placed at eye-level on a wall 10 ft in front of them.

3.2.3.2 Static Leaning

Subjects were instructed to lean as far forward (backward) as possible without bending at the waist, keeping their heels on the floor and their arms behind their back. Once data collection started, a 1-3 s delay was observed, after which subjects were given the cue to begin leaning. Upon achieving maximum lean, subjects were required to maintain the leaning position while data were collected for 30 s.

3.2.3.3 Rhythmic Sway

Subjects performed anterior-posterior sways at both their preferred frequency and an imposed frequency. In each condition two trials were performed. Subjects were instructed to sway forwards and backwards at the ankle joint as much as possible without stepping, keeping their feet flat on the floor and their body straight with the arms behind the back (Owings et al. 2000). In the preferred frequency condition, subjects were not given specific instructions on how fast to sway, but in the imposed condition they were instructed to entrain their sway to a metronome beating at 0.25 Hz. The analog audio metronome signal was amplified and output to both a speaker and an A/D converter. Data were collected for 30 s after the subject had successfully entrained their swaying for 4 consecutive cycles.

3.2.3.4 Maximum Reaching

The maximum reach of subjects was first determined by instructing them to reach as far forward as possible with their hands together without losing their balance. Each subject performed four trials, with their maximum distance reached used to determine the location for a reaching target. Next, data was collected while subjects performed three maximum reach trials, in which they were instructed to touch the target with both hands as quickly as possible upon hearing a verbal cue, and then return to quiet stance. The movement cue occurred after several seconds of quiet stance. In all reaching trials, subjects were told that they could lift their heels. Data were collected for 10 s, capturing the entire quiet stance/reach/quiet stance sequence.

3.2.3.5 External Perturbation

Subjects were strapped to the backboard apparatus, and their foot position was marked to ensure consistency across trials. Subjects were told to fix their gaze on a point located at eye-level on a wall 5 m away. They were instructed to resist the perturbations, resume quiet stance as quickly as possible, and only step if they felt a fall was imminent.

The pendulum was positioned at a static release angle with respect to vertical. A light signaled subjects to commence quiet stance; after a random delay of 2 to 6 s the pendulum was released to swing forward, contacting the backboard/subject in the upper back region, accelerating the body forward. Subjects listened to white noise through headphones to mask the sound of the pendulum release. The first pendulum release angle was 10°. In subsequent perturbation trials the release angle was increased sequentially in increments of 5° (light subjects, i.e. <70 kg) or 10° (heavier subjects) until subjects

needed to step to prevent a fall. Only one trial was performed at each perturbation level. The different increments were used so that subjects would receive a similar number of perturbations. The perturbations were impulsive; after the pendulum shock absorber made contact, it rebounded away and was caught, resulting in a singular perturbation of short duration (~0.25 s). Subjects received two sets of sequentially increasing perturbations.

3.2.4 Data Analysis

The center of pressure (CoP) was computed from the measured ground reaction forces and moments. Sagittal plane segment center of mass (CoM) locations and inertial properties were estimated using regression equations, and then combined to give the total body sagittal plane CoM motion (Winter, 1990). Kinematic and kinetic data were smoothed using a Butterworth digital filter, with optimal cut-off frequencies determined through spectral analysis and residual analysis (Winter 1990). The anterior-posterior displacements of the CoP and CoM were referenced to the position of the ankle joint, so that a value of zero indicated that the anterior-posterior CoP or CoM location was the same as the ankle joint center in the sagittal plane.

Only the second trial was analyzed for the quiet stance, leaning, and swaying postural conditions, and only the second set was analyzed in the perturbation condition. For the maximum reach, all three trials were processed and the performance measures were averaged together; this was done since there was only a singular event (e.g. maximum reach), compared with the other conditions which all included multiple events of interest (e.g. CoP position during 30 s of quiet stance).

In the literature, researchers have used an array of variables for the quantification of postural control. For example, Prieto et al. (1996) examined over 15 different measures of postural steadiness – just for the CoP. Considering that most methods of analyzing the CoP can be applied to the CoM, it is evident that there are many variables to choose from. For simplicity, we chose to use relatively basic variables in most cases, which have been shown to reliably distinguish between younger and older individuals (Prieto et al. 1993). For the different experimental conditions, we computed various measures related to the movement of both the CoP and CoM, which reflect different aspects of postural control (Figure 3-4). Displacements of the CoP are related to the modulation of ankle and/or hip torque, and therefore capture the neuromuscular control processes involved in postural control. On the other hand, the CoM is the key variable that needs to be controlled in order for stability to be maintained, and thus reflects how successful an individual is at performing a particular balance task. A more detailed description of the various measures for the different postural conditions follows.

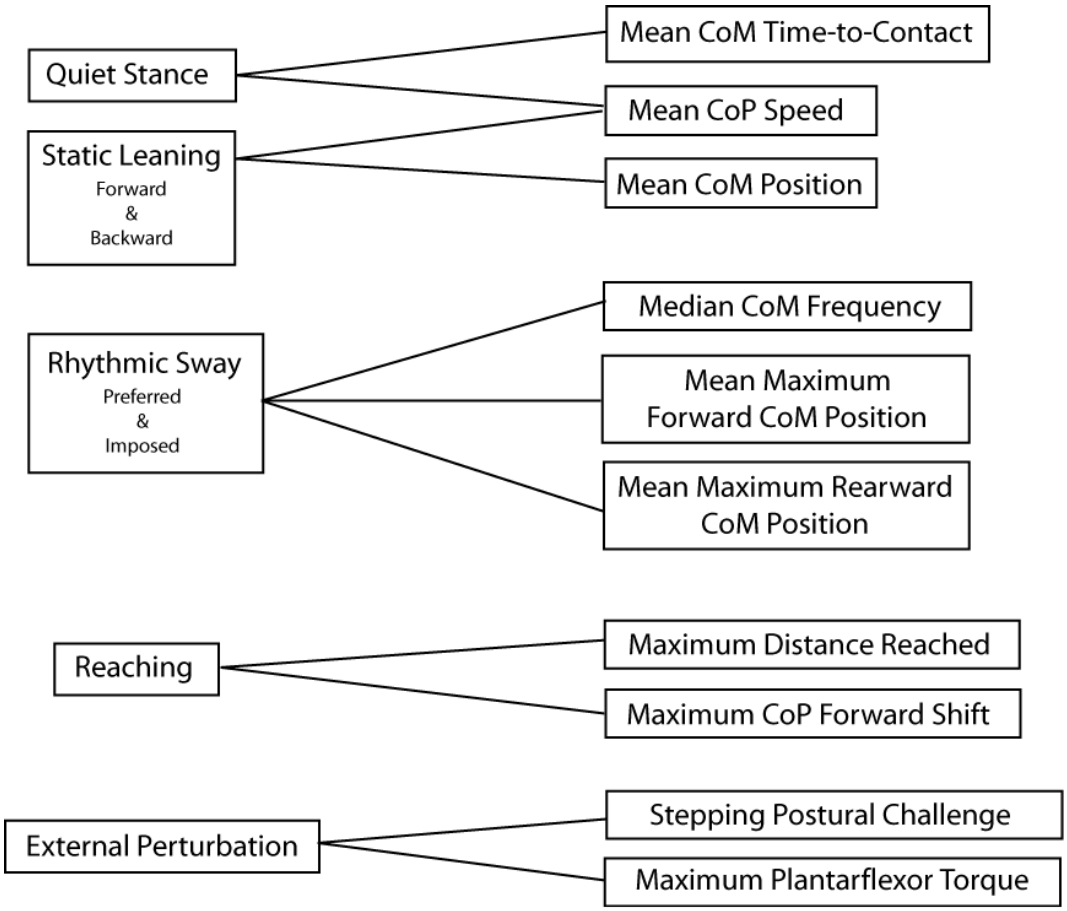

Figure 3-4. Summary of balance measures (right side) computed for the different postural conditions (left side). Abbreviations: CoP (center of pressure), CoM (center of mass), TtC (time-to-contact).

3.2.4.1 Quiet Stance and Leaning Variables

For the quiet stance and leaning conditions, only the last 20 s of the 30-second trial were used in the analysis. The mean CoP speed was computed as the average absolute value of the first time-derivative of the anterior-posterior CoP displacement. This measure was chosen because it reflects the overall amount of CoP movement, which might be greater in the older subjects if their postural control is poorer (i.e. more CoM

movement in the normal and leaning conditions). This measure has been shown to reliably distinguish between young and older individuals (Prieto et al. 1996).

For the quiet stance condition, the mean time-to-contact of the CoM was computed. Time-to-contact combines instantaneous CoM kinematics to predict a future time when it will contact the base of support boundary, akin to the "extrapolated CoM" described by Hof et al.(2005). This measure has been shown to decrease with age during quiet stance (Slobounov et al. 1998). The instantaneous CoM time-to-contact to the anterior (toe) and posterior (heel) support boundaries was calculated based on Slobounov et al. (1997):

$$\text{Time-to-Contact} = \left| \frac{-v \pm \sqrt{v^2 - 2a\left(p_{\max} - p\right)}}{a} \right| \tag{4.1}$$

where *p*, *v*, and *a* are the anterior-posterior positions, velocities, and accelerations of the CoM, respectively, and p_{max} is the anterior-posterior location of the toe (or heel) markers. This calculation was performed at each point in time, and the average CoM time-to-contact was calculated.

Finally, for the leaning conditions, the average anterior-posterior CoM position was computed, and expressed relative to the anterior-posterior position of the ankle joint center. Because subjects were asked to lean as far as they could, this variable reflects the postural control of the subjects at the extreme limits of their postural capabilities.

3.2.4.2 Rhythmic Sway Variables

In the swaying conditions, the entire 30 second trial was used in the analysis, as the data collection started after subjects established a stable swaying pattern. A fast-

Fourier transform was used to calculate the frequency and power spectrums of the CoM anterior-posterior displacement. The median CoM frequency was calculated, such that half of the total power was below and above the median frequency. This variable captures the basic requirements of the swaying task, which was to perform a stable oscillatory motion (Chiari et al. 2002). In the imposed swaying condition, subjects were required to match a target frequency, so the median frequency assessed how well subjects were able to perform the task.

The maximum forward and rearward positions of the CoM during each sway cycle were computed automatically using a local min/max detection algorithm; all identifications were manually checked and adjusted if misidentifications occurred. The maximum forward and rearward CoM positions were averaged across the 30 s swaying trial. Similar to the static leaning condition, these variables measured the postural control of the subject at the limits of their stability, but in a dynamic condition that required appropriate deceleration of the CoM as it approached the base of support boundary.

3.2.4.3 Reaching Variables

For the reaching condition, the maximum distance reached was indicated by the maximum anterior position of the wrist marker. This absolute distance was expressed relative to the anterior-posterior positions of the toe markers, and then divided by the height of the subjects to account for differences in stature. This variable reflects the basic task requirement of reaching as far forward as possible. The maximal anterior position of the CoP was also computed and expressed relative to the anterior-posterior position of the

ankle joint center, which reflects in part the maximum amount of ankle torque generated by the subjects during the reach.

3.2.4.4 External Perturbations Variables

In the external perturbation condition, sagittal plane pendulum angles were calculated and numerically differentiated to compute the pendulum angular velocity. To account for differing subject inertias, we computed the "postural challenge" for each perturbation level by dividing the peak pendulum velocity at impact by the subject's mass. The pendulum was adjusted to strike subjects at 78% of their standing height to account for varying CoM height. In the analysis, the postural challenge at which the subjects initiated a stepping response was used. This reflects the capacity of the subjects to resist the perturbations; subjects who perform better will step at a higher postural challenge level. Newton-Euler equations of motion were solved for the reaction forces and torque at the ankle (Elftman 1939). The maximum plantarflexor torque generated on the stepping perturbation level was calculated.

3.2.5 Statistics

3.2.5.1 Balance Measures

All statistical analyses were done with the software package R (2008). Separate two-way ANOVAs (age x gender) were performed on each of the dependent balance variables. Effect sizes for the ANOVAs were determined using Cohen's *f* statistic (Cohen 1969). Although the effect sizes will not be discussed explicitly, they are listed in tables so that the reader can make informed interpretations of the results (see Chapter 2 for

more details on interpreting effect sizes). Multiple comparisons were used for post-hoc analysis. A p-value of .05 was used as a guide for judging statistical significance for all tests.

3.2.5.2 Regression Analysis

3.2.5.2.1 Individual Mechanical Properties

Linear regression analysis was used to assess the relationship between the muscular mechanical properties measured in Chapter 2 and the 16 balance variables presented here. The first step was to perform linear regressions for each individual muscle mechanical property, for each of the three muscles (DF, GA, and SO), against each balance measure. The aim of this analysis was to determine the ability of each property to independently predict the performance of the subjects on the postural tests, and to determine whether there were differences between the age groups. The form of the regression model was:

$$BM = \beta_0 + \beta_1 Age + \beta_2 MP + \beta_3 \left(Age \cdot MP \right) \tag{4.2}$$

where *Age* is a dummy variable allowing the examination of the effect of age group (young or old), *MP* is a single mechanical property for one muscle, *BM* is the balance measure, and the βs are the coefficients describing the relationship.

The results of these regressions were screened for significance $\left(p \le .05 \right)$, and a subset of those with overall significance was created. This subset was further examined for significant differences in the y-intercepts – representing an effect of age only (Figure 3-5A), slopes – representing an effect of the balance measure only (Figure 3-5B), effects of age and the balance measure (Figure 3-5C), and the interaction between age and the balance measure (Figure 3-5D). Out of these possibilities, the interaction between age

and the balance measure was of most interest. Cases where there was an effect of age only were not examined further, as the age-only effects were tested in the ANOVA described in the previous section (3.2.5.1, Balance Measures). Specific muscles were not analyzed for postural conditions in which they would have little or no influence (e.g. the DF muscles during the forward lean).

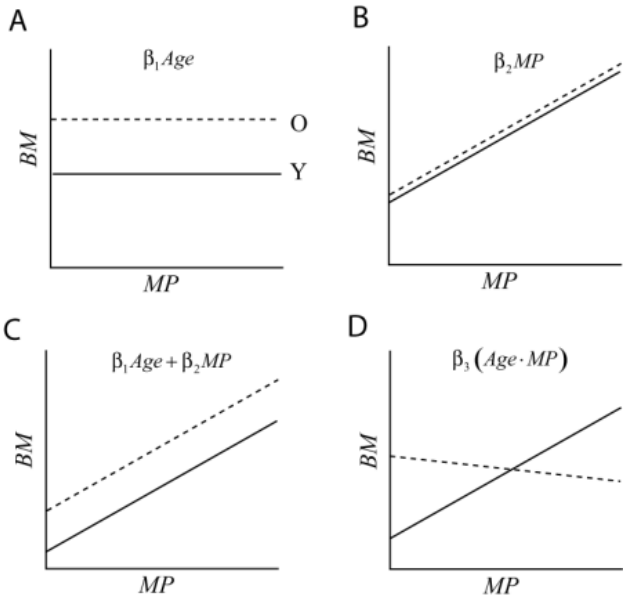

Figure 3-5. Hypothetical regression results between a muscle property (MP) and a balance measure (BM) for young (Y) and older (O) subject groups. See text for details.

3.2.5.2.2 Multiple Mechanical Properties

The second step of the regression analysis was to examine the ability of multiple mechanical properties, *considered together*, to predict the performance of the young and older subjects on the different postural tests. The form of the full linear regression model used in this analysis was:

$$BM = \beta_0 + \beta_1 Age + \beta_2 MP_1 + \beta_3 (Age \cdot MP_1) + \beta_4 MP_2 + \beta_5 (Age \cdot MP_2) \text{K}\ \beta_i MP_j + \beta_i (Age \cdot MP_j) \quad (4.3)$$

where j represents each of nine mechanical properties and i represents each of the β coefficients. In the full model, each mechanical property appeared as an independent term (9 terms) and as an interaction with age (9 terms). Thus, the 18 mechanical property terms, the y-intercept (β_0), and the age effect $(\beta_1 Age)$ gave a total of 20 terms in the full regression model (i = 0 to 19). As shown in the equation, the interaction of age with each mechanical property was included in the regression model. Separate regression models were created using the mechanical properties for each muscle (DF, GA, and SO).

A hybrid branch-and-bound/backward elimination procedure was used to find the best set of mechanical property predictors for the 16 balance variables, implemented with the *regsubsets* search algorithm in the R (2008). See Appendix D for a detailed example of this selection procedure. The search algorithm was configured to output the best models for different model sizes (one of each size up to nine mechanical properties), arranged according to their "adjusted" R^2 values $(\bar{R}^2)$, which weighs the predictive power of the models against the number of terms in each model (if two models have equal R^2 values, the one with fewer terms will have the higher $\bar{R}^2$). In the arranged model list, the break-point was manually identified. The break-point was the point at which the removal of any parameter caused a precipitous drop in $\bar{R}^2$. The model right before the breakpoint was selected as the final "best" model. If there were multiple models close to the breakpoint with similar $\bar{R}^2$ values, the one with the lowest Bayesian information criterion was selected (Schwarz 1978). For tractability in the interpretation of the results, and to help identify the most important mechanical properties, the final model was limited to a maximum of five predictors. Thus, no optimal model was selected if there were no significant $(p \leq .05)$ models with five or less predictors. The final models for

each muscle and balance measure were inspected and compared. In some cases, terms were added or subtracted manually to ensure that the final models were indeed optimal. As in the linear regression using independent mechanical properties, the interaction terms were of interest, as these signify that the effect of a mechanical property on predicting balance performance depends on the age of the subjects (young or old).

3.3 Results

3.3.1 Balance Measures

An example of representative young and older subject performance on the different postural tests is shown in Figure 3-6. In general, there were significant differences between the age groups in all postural conditions, with the exception of the backward leaning. There were main effects of age for most variables, main effects of gender for a few variables, and no age by gender interactions.

The results for the static postural tests of quiet stance and leaning are presented in Table 3-1. For quiet stance, the older adults had significantly higher CoP speeds ($p < .001$) and significantly shorter mean CoM times-to-contact ($p < .001$). In the forward lean, the older adults had higher CoP speeds ($p = .016$) and did not lean as far forward ($p < .001$).

Table 3-1. Balance measures for static postural tasks.

	Quiet Stance		Lean Forward		Lean Backward	
	CoP Speed (mm/s)	CoM TtC (s)	CoP Speed (mm/s)	CoM Pos. (mm)	CoP Speed (mm/s)	CoM Pos. (mm)
Young Male	6.5 ± 2.1	10.3 ± 0.7	19.4 ± 4.2	142 ± 14	20.6 ± 6.0	4.6 ± 13.8
Young Female	6.3 ± 1.6	9.5 ± 1.4	15.9 ± 6.6	119 ± 14	15.4 ± 5.6	-7.6 ± 12.2
Old Male	14.7 ± 5.7	7.4 ± 2.0	26.2 ± 7.7	101 ± 18	26.2 ± 9.1	4.4 ± 17.4
Old Female	10.3 ± 2.8	8.2 ± 1.0	22.3 ± 5.6	101 ± 18	19.5 ± 7.6	0.6 ± 8.8
Main Effects	A	A	A	A	-	-
Interactions	-	-	-	-	-	-
Cohen's *f*	0.99	0.85	0.62	1.04	0.53	0.37

Note: Main effect abbreviations: A = Age

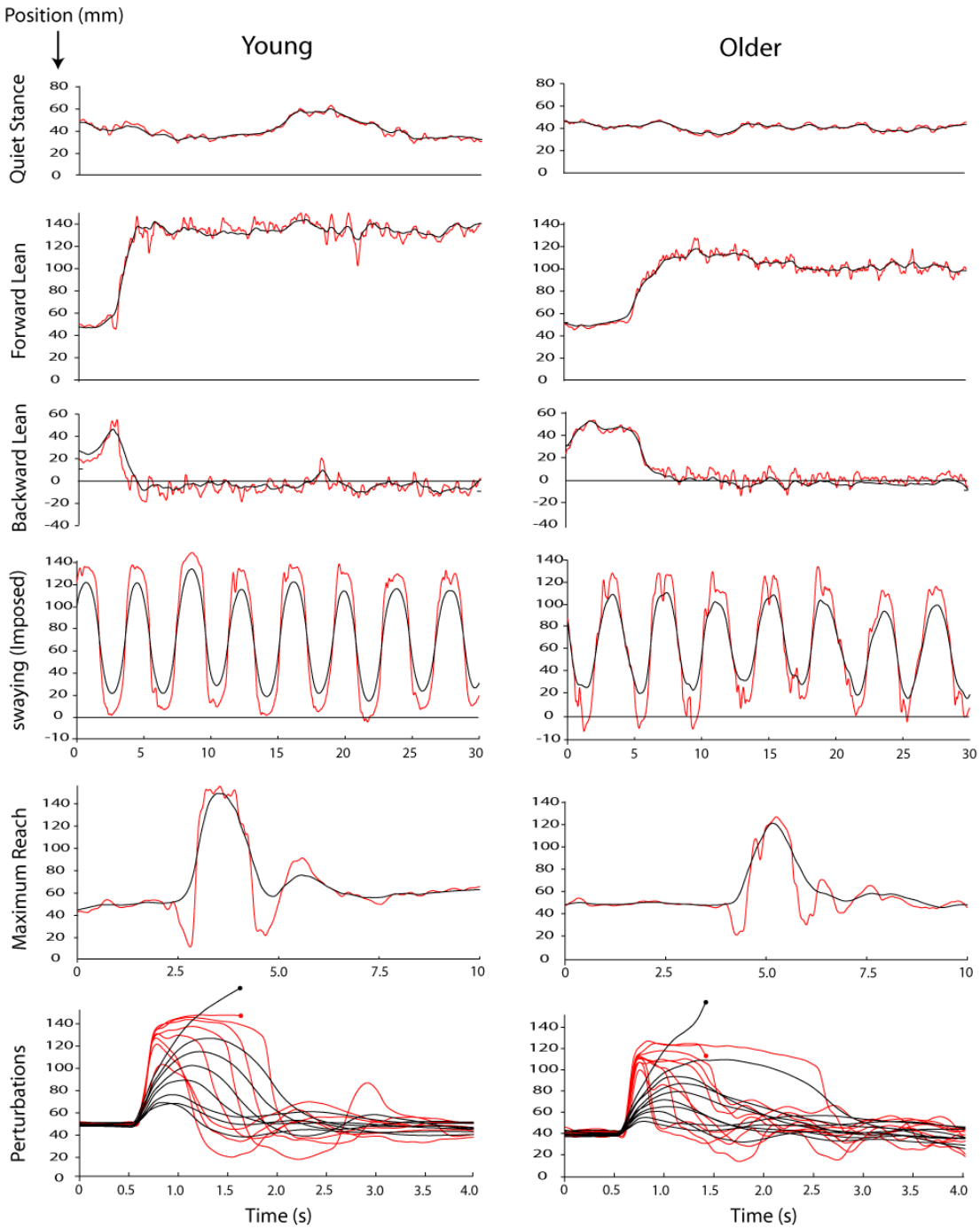

Figure 3-6. Representative young (left) and older (right) subject anterior-posterior center of mass (black lines) and center of pressure (red lines oscillating around black center of mass lines) for the different postural conditions. From top to bottom: quiet stance, forward lean, backward lean, imposed swaying (preferred swaying is not shown), maximum forward reach, and sequential external perturbations (the solid circles indicate trials in which the subjects stepped off the force platform). Positions are referenced to the ankle joint.

The results for the swaying postural tests are presented in Table 3-2. For both swaying conditions, the older adults did not sway forward (indicated by "+" in Table 3-2) as far as the younger subjects (preferred: $p = .005$; imposed: $p = .006$). In contrast, there were no age-related differences in the maximum posterior CoM displacement (indicated by "-" in Table 3-2) for either swaying condition (preferred: $p = .155$; imposed: $p = .302$). In the imposed swaying condition, the median frequency of the anterior-posterior CoM movements was closer to the target frequency for the younger subject group ($p = .023$). In the preferred swaying condition, males chose to sway at a lower frequency compared to females, regardless of age ($p = .039$).

Table 3-2. Balance measures for swaying.

	Swaying - Preferred			Swaying – Imposed		
	CoM Median Freq. (Hz)	+ CoM Pos. (mm)	- CoM Pos. (mm)	CoM Median Freq. (Hz)†	+ CoM Pos. (mm)	- CoM Pos. (mm)
Young Male	0.17 ± 0.06	136 ± 6	0.9 ± 17	0.23 ± 0.01	130 ± 12	11.6 ± 14
Young Female	0.23 ± 0.05	112 ± 11	-4.3 ± 18	0.22 ± 0.02	111 ± 13	-4.2 ± 12
Old Male	0.14 ± 0.08	106 ± 25	-10.2 ± 2	0.21 ± 0.03	100 ± 33	1.1 ± 21
Old Female	0.18 ± 0.04	98 ± 20	-5.9 ± 19	0.20 ± 0.01	91 ± 18	-7.8 ± 14
Main Effects	G	A, G	-	A	A	-
Interactions	-	-	-	-	-	-
Cohen's f	0.58	0.81	0.49	0.58	0.71	0.46

Note: Main effect and interaction abbreviations: A = Age, G = Gender
†Target median frequency was 0.25 Hz.
+ Anterior; - Posterior

Finally, the results of the reaching and perturbation postural conditions are shown in Table 3-3. In the reaching condition, the older subjects were able to reach farther ($p = .020$) than the younger subjects, but were not able to shift their CoP as far forward ($p < .001$). Males were able to shift their CoP farther than the females ($p < .001$). There were

no significant differences between the foot length of the young and older subjects ($p = .969$), although there were differences between the male and female subjects ($p < .001$). In the perturbation trials, the younger subjects were able to withstand a larger postural challenge level ($p < .001$), and the male subjects generated larger plantarflexor torques than females ($p < .001$).

Table 3-3. Balance measures for reaching and in response to a perturbation.

	Reaching		Perturbation	
	Max. Reach (% Height)†	Max. CoP Shift (mm)	Max. Challenge (deg/s/kg)	Peak Torque (Nm)
Young Male	13.0 ± 1.9	172 ± 8	1.92 ± 0.14	168 ± 21
Young Female	13.2 ± 2.7	139 ± 10	1.69 ± 0.27	105 ± 12
Old Male	14.5 ± 3.1	134 ± 19	1.17 ± 0.31	164 ± 25
Old Female	18.2 ± 4.3	122 ± 14	0.97 ± 0.27	99 ± 25
Main Effects	A	A, G	A	G
Interactions	-	-	-	-
Cohen's *f*	0.67	1.35	1.50	1.49

Note: Main effect and interaction abbreviations: A = Age, G = Gender
†Distance reached beyond toes, normalized to subject height.

3.3.2 Regression Analysis: Individual Mechanical Properties

The first part of the regression analysis was designed to determine the relationship between muscle mechanical properties, *considered individually*, and the performance of the young and older subjects on the postural tests. Muscle mechanical properties that had significant overall effects on the prediction of the static balance measures are shown in Figure 3-7, with the coefficients describing these relationships and statistical results displayed in Table 3-4.

Figure 3-8 and Table 3-5 report similar information for the dynamic tests. In most cases, the properties for only one muscle were significant for a given balance measure. The sole exception was the mean CoM position in the forward lean condition, which was predicted by both GA and SO muscular properties.

3.3.2.1 Static Balance Conditions

For the quiet stance condition, the prediction of mean center of pressure (CoP) speed included a significant interaction between age and the slope of the SO force-length width (W) vs. mean CoP speed relationship. In the older subjects, as the width of the force-length relation increased, the mean center of pressure speed decreased. In contrast, mean CoP speed tended to increase as the width of the force-length relationship increased for the young subjects.

In the forward lean condition, the relationship for mean CoP speed showed a significant interaction between age and the slope of the GA a/P_0 force-velocity coefficient. In the young subjects, a/P_0 increased with greater CoP speeds; however, the opposite was true for the older subjects, with increasing a/P_0 associated with decreasing CoP speed. For the prediction of mean CoM forward position, there were no significant age group interactions with any of the muscular mechanical properties, but there were significant overall relationships with both the GA slack length (L_S) and the SO a/P_0 coefficient. For both age groups, when the mean CoM position moved farther forward away from the ankle joint the GA slack length increased, and the SO a/P_0 decreased.

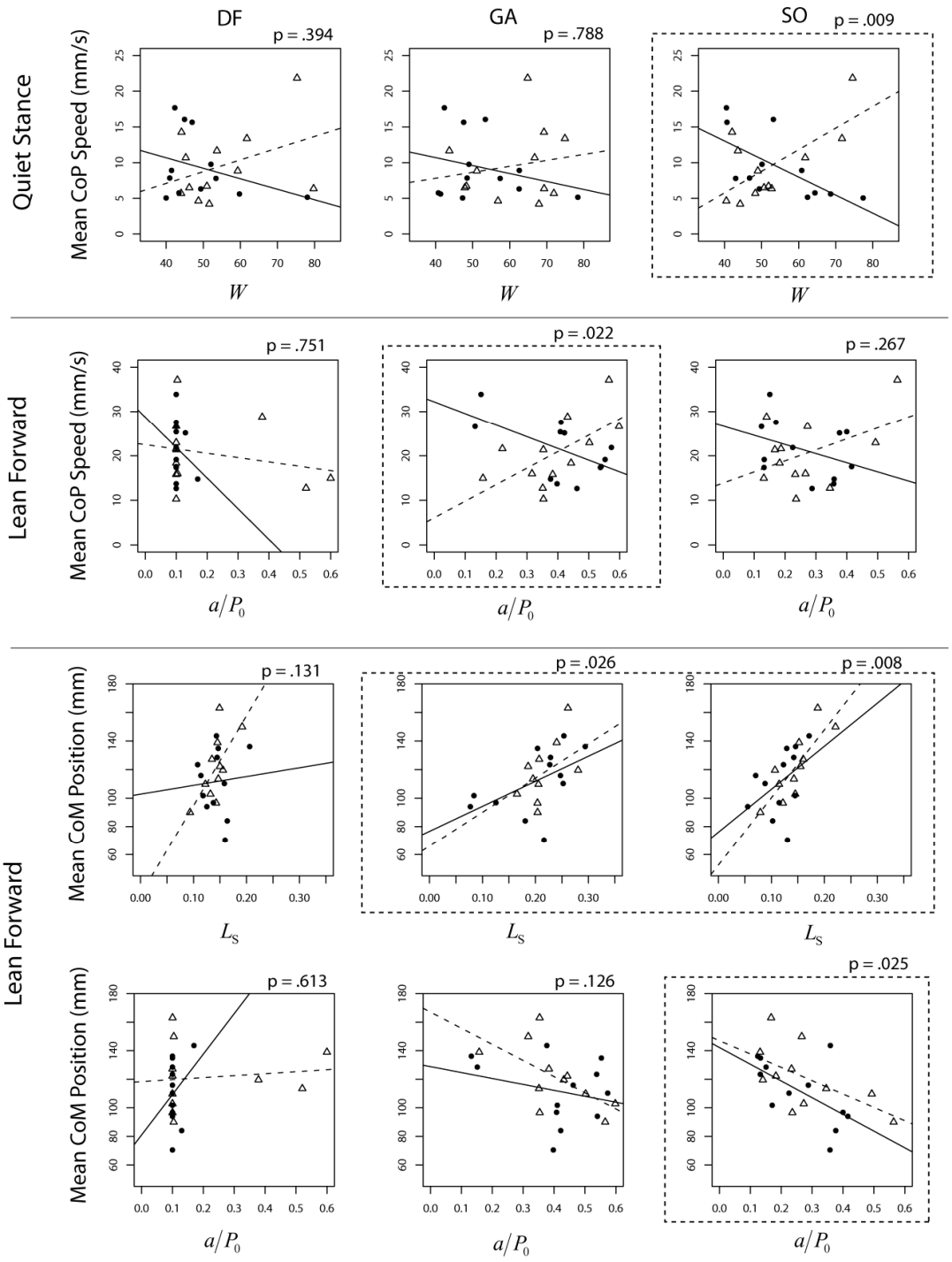

Figure 3-7. Relationships between static postural measures and muscle mechanical properties for the dorsiflexors (DFs), gastrocnemius (GA), and soleus (SO). Data sets with overall significance are outlined by a dashed rectangle. Older subjects are shown as solid circles and a solid fitted line; young subjects are represented by open triangles and a dashed fitted line.

Table 3-4. Linear regression results for static postural variables. Only those with an overall p-value below .05 are shown.

Balance Variable	Muscle Property	Muscle	Coefficient	Value	Error	p-value
Quiet Stance Mean CoP Speed	Force-Length Width (W)	SO	Age	-29.5	7.80	< .001*
			Slope	-0.253	7.80	.001*
			Interaction	0.555	0.143	.018*
			Multiple R^2		.432	
			Overall p-value		.009*	
Leaning Forward Mean CoP Speed	Force-Velocity Coefficient (a/P_0)	GA	Age	-26.1	7.75	.003*
			Slope	-26.4	12.3	.044*
			Interaction	63.5	18.4	.002*
			Multiple R^2		.376	
			Overall p-value		.022*	
Leaning Forward Mean CoM Position	Slack Length (L_S)	GA	Age	-10.6	29.5	.723
			Slope	175.7	83.4	.049*
			Interaction	64.3	130	.628
			Multiple R^2		.379	
			Overall p-value		.026*	
		SO	Age	-23.4	29.3	.434
			Slope	301	160.7	.076
			Interaction	174	217	.431
			Multiple R^2		.454	
			Overall p-value		.008*	
	Force-Velocity Coefficient (a/P_0)	SO	Age	4.79	19.3	.806
			Slope	-117	49.5	.029*
			Interaction	23.7	65.6	.072
			Multiple R^2		.382	
			Overall p-value		.025*	

*Significant at p <= .05

3.3.2.2 Dynamic Balance Conditions

In the preferred-frequency swaying balance test, there was a significant age-related interaction between the stiffness of the GA muscle (α) and the median swaying frequency, such that the higher median frequencies were associated with increased stiffness in the young subjects, while the opposite was true for the older subjects. There was also an age-related interaction between the maximal isometric force (P_0) of the SO

muscle and the median swaying frequency, such that the swaying frequency tended to decrease with greater muscle strength in the younger subjects, but in the older subjects higher SO (P_0) values were associated with higher swaying frequencies.

When asked to time their sways to a metronome in the imposed swaying condition, there was a significant age-related interaction between the GA slack length (L_S) and the mean forward sway position. Greater GA slack lengths were associated with greater forward positions in both age groups, in agreement with the results of the static forward leaning condition. However, the rate of increase (slope) in the forward CoM position relationship with slack length was larger for the younger subjects. For both age groups, there was an overall negative relationship between the SO a/P_0 coefficient and the mean forward CoM position, with less forward swaying associated with greater a/P_0 coefficients.

In the reaching test, there was an age-related interaction between the width of the SO force-length relation (W) and the maximum distance reached. The young subjects with greater SO force-length widths were able to reach farther forward, but this relation was not seen in the older subjects.

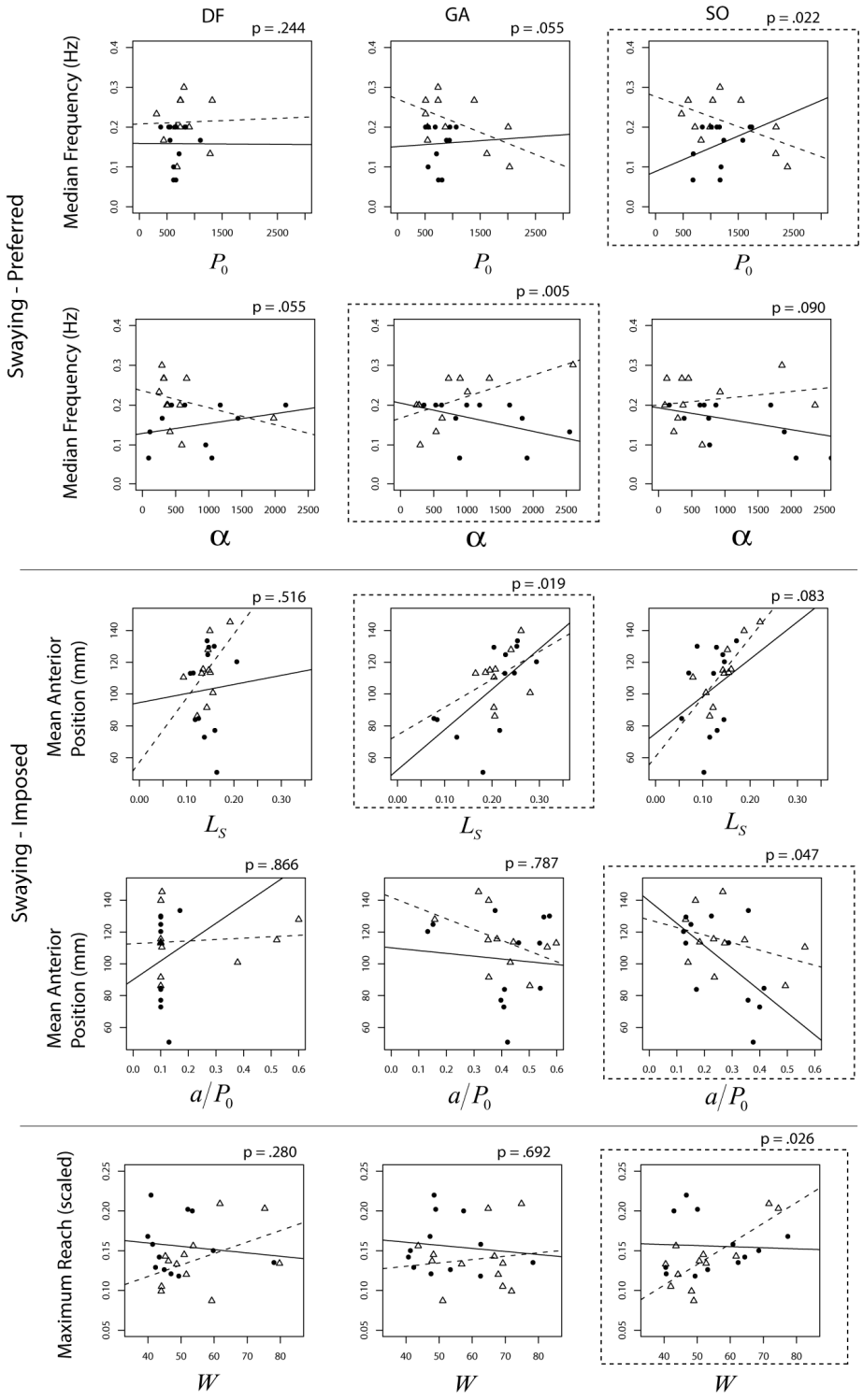

Figure 3-8. Relationships between dynamic postural measures and muscle mechanical properties for the dorsiflexors (DFs), gastrocnemius (GA), and soleus (SO). Data sets with overall significance are outlined by a dashed rectangle. Older subjects are shown as solid circles and a solid fitted line; young subjects are represented by open triangles and a dashed fitted line.

Table 3-5. Linear regression results for dynamic postural variables. . Only those with an overall p-value below .05 are shown.

Balance Variable	Muscle Property	Muscle	Coefficient	Value	Error	p-value
Swaying (Preferred) Median Frequency	Series Elasticity (α)	GA	Age	-0.038	0.036	.308
			Slope	-0.035	0.001	.078
			Interaction	0.001	0.001	.004*
			Multiple R^2		.488	
			Overall p-value		.005*	
	Maximum Isometric Force (P_0)	SO	Age	0.019	0.065	.009*
			Slope	0.001	0.045	.197
			Interaction	0.001	0.001	.043*
			Multiple R^2		.389	
			Overall p-value		.022*	
Swaying (Imposed) Mean Forward Position	Slack Length (L_S)	GA	Age	-0.024	0.131	.079
			Slope	-0.137	0.584	.030*
			Interaction	2.08	0.905	.033*
			Multiple R^2		.399	
			Overall p-value		.019*	
	Force-Velocity Coefficient (a/P_0)	SO	Age	-11.9	21.0	.579
			Slope	140	54.0	.018*
			Interaction	92.8	71.5	.210
			Multiple R^2		.336	
			Overall p-value		.047*	
Maximum Reach	Force-Length Width (W)	SO	Age	-0.161	0.063	.019*
			Slope	-0.001	0.001	.865
			Interaction	0.003	0.001	.027*
			Multiple R^2		.364	
			Overall p-value		.026*	

*Significant at p <= .05

3.3.3 Multiple Mechanical Properties

3.3.3.1 General Multiple Regression Results

To aid in interpreting the results of regression analyses incorporating *multiple* muscle mechanical properties, Table 3-6 lists the frequency of appearance of each mechanical property in the models of the static and dynamic tests (based on the final "best" regression models). For the static conditions, the slack length (L_S) and the stiffness coefficient α appear the most (4 or more times) in the regression models, suggesting that these properties are important for explaining the variance in static postural conditions. The maximal isometric strength (P_0) and optimal contractile component length (L_0) were also important predictors (3 appearances). For the dynamic postural conditions the most prominent muscle parameters were those describing the force-length relation (L_0, W), the force-extension relation (α, β, L_S), and the force-velocity relation $(a/P_0, b/L_0)$.

Table 3-6. Frequency of appearance of mechanical properties in regression models.

Postural Condition	Form in Model	Mechanical Properties									Total
		P_0	L_0	L_S	W	α	β	a/P_0	b/L_0	ε	
Static	Alone	2	2	2	2	3	0	2	0	0	13
	Age Interaction	1	1	3	0	1	1	0	0	0	7
	Total	3	3	5	2	4	1	2	0	0	20
Dynamic	Alone	0	4	2	5	3	3	3	5	0	25
	Age Interaction	0	2	1	1	1	1	2	1	2	11
	Total	0	6	2	6	4	4	5	6	2	36
Grand Total		3	9	8	8	8	5	7	6	2	56

Overall, there were regression models for individual muscles that demonstrated significant predictions of balance variables when incorporating multiple mechanical properties that were not significant by themselves. This is to be expected; mechanical properties of a single muscle have varying degrees of correlation (see Appendix C for correlations). The majority of the models include age as a separate factor or in an interaction with a mechanical property. In some cases, relatively few mechanical properties are needed to give moderately strong predictions ($R^2 > .40$) for some balance measures.

3.3.3.2 Static Postural Tests

The predictive abilities of the best regression models using multiple muscle mechanical properties for the static postural tests are shown in Figure 3-9 and the corresponding regression models are listed in Table 3-7. Regression models without overall significance are not shown, which meant that none of the independent measures accounted for the variability in the balance measure at the $p \leq .05$ significance level.

For quiet stance, regression models for the DF and SO muscles were significant when explaining the variance in the mean CoP speed, while the GA regression model was significant when explaining the variance in the mean CoM time-to-contact (Table 3-7). Age, stiffness (α), and slack length (L_S) of the DF and SO muscles were all important predictors of the mean CoP speed. In these models, α appeared independently, but L_S only appeared as an interaction with age. The maximal isometric force (P_0) was also an important predictor, but only for the DF muscle. In contrast, there was a different set of predictors for the for the mean CoM time-to-contact based on the GA muscle properties,

including the optimal fiber length (L_0), width of the force-length relation (W), and the interaction between age and the linearity of the force-extension relation (β). Together, these predictors accounted for almost 40% of the variance in the mean CoM time-to-contact.

In the forward lean condition, similar predictors were included in the GA and SO regression models for the mean CoP speed (Age, L_0, L_S, α). However, the a/P_0 coefficient of the force-velocity relation was also included in the model for the SO. For the mean CoM position, L_S, and a/P_0 were again important predictors, with the maximal isometric force (P_0) and the width or the force-length (W) relation also making contributions. No mechanical properties were significant predictors for the backward lean.

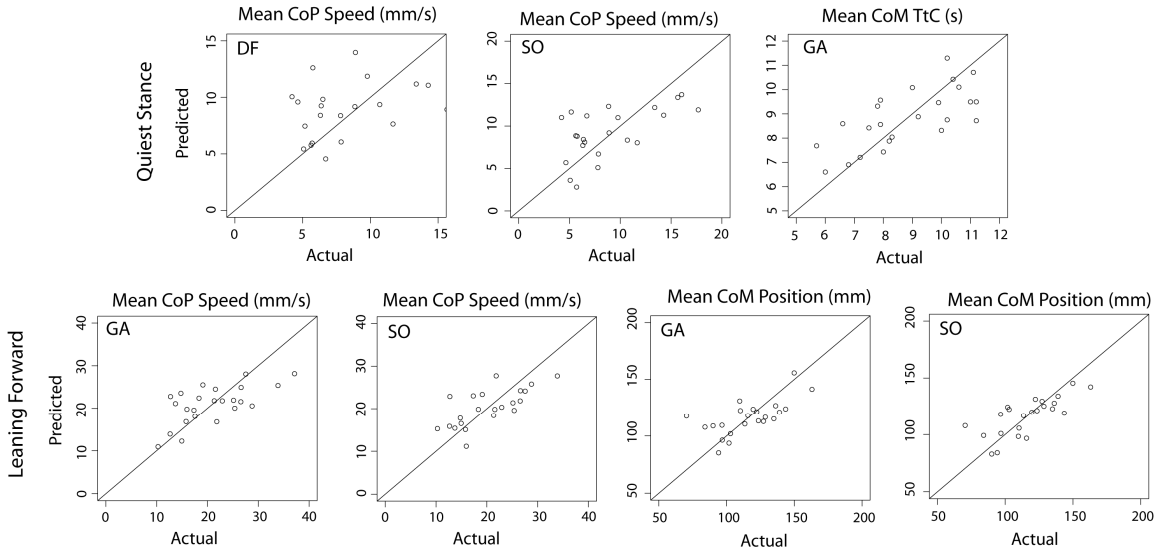

Figure 3-9. Actual vs. predicted static balance measures using the regression models.

Table 3-7. Multiple regression results for static postural tests.

Postural Condition	Balance Measure	Muscle	Independent Measures Included in Best Model	# Terms	R^2	p
Quiet Stance	Mean CoP Speed	DF	$P_0 + \alpha + (Age \cdot P_0) + (Age \cdot L_S)$	4	.34	.015
		GA	-	-	-	-
		SO	$Age + \alpha + (Age \cdot L_S) + (Age \cdot \alpha)$	4	.57	.039
	Mean CoM TtC	DF	-	-	-	-
		GA	$L_0 + W + (Age \cdot \beta)$	3	.40	.013
		SO	-	-	-	-
Lean Forward	Mean CoP Speed	DF	NA	NA	NA	NA
		GA	$L_0 + L_S$	2	.42	.004
		SO	$Age + a/P_0 + \alpha + (Age \cdot L_0)$	4	.47	.038
	Mean CoM Position	DF	NA	NA	NA	NA
		GA	$P_0 + L_S$	2	.45	.003
		SO	$Age + W + a/P_0 + (Age \cdot L_S)$	4	.59	.004
Lean Backward	Mean CoP Speed	DF	-	-	-	-
		GA	NA	NA	NA	NA
		SO	NA	NA	NA	NA
	Mean CoM Position	DF	-	-	-	-
		GA	NA	NA	NA	NA
		SO	NA	NA	NA	NA

Regressions including more than 9 terms and/or no significant regressions not shown, signified by "-".
NA: model not applicable; CoP: center of pressure; CoM: center of mass; TtC: time-to-contact

3.3.3.3 Dynamic Postural Tests

The predictive abilities of the best regression models using multiple muscle mechanical properties for the dynamic postural tests are shown in Figure 3-10 and the corresponding regression models are listed in Table 3-8. Again, regression models without overall significance are not shown.

Many of the same predictors were present in the dynamic balance conditions as in the static balance conditions. New parameters present in the dynamic conditions (but not in the static models) were the b/L_0 force-velocity coefficient and the eccentric plateau (ε). The regression models for the median CoM frequency in the preferred swaying included the optimal length (L_0), the α stiffness coefficient, the a/P_0 force-velocity coefficient, and ε; the majority of these properties appeared as an age interaction (except a/P_0). Only the DF and GA muscles were associated with significant regression models – none were found for the SO muscle. There were no significant regression models for the median CoM frequency in the imposed swaying condition.

There were significant plantarflexor regression models for the mean forward CoM position during both preferred and imposed frequency swaying, including the force-length properties (L_0 and W), the slack length (L_S), and the force-velocity coefficients (a/P_0 and b/L_0). Here, b/L_0 played a prominent role, but age did not. Similar properties were included in the mean rearward CoM position model for preferred swaying. However, different terms were included for imposed swaying, including the β stiffness coefficient and ε.

The regression models for the maximum reach were significant for only the plantarflexor muscles, and included both age and age-interaction terms. The predictors included the force-velocity coefficients $(a/P_0, b/L_0)$, the optimal fiber length (L_0), and the stiffness (α). The GA and SO muscles also had significant regression models for the maximum forward CoP shift during the maximum reach that included L_0, W, and β; the SO model also included a/P_0. There were no significant dorsiflexor regression models with respect to the maximum reach or the maximum CoP shift. Finally, the slack length L_S and force-velocity coefficient b/L_0 were significant predictors for the maximum ankle torque in the external perturbation condition, with age playing a prominent role. On the other hand, there were no significant models for the maximum postural challenge that caused subjects to take a compensatory step.

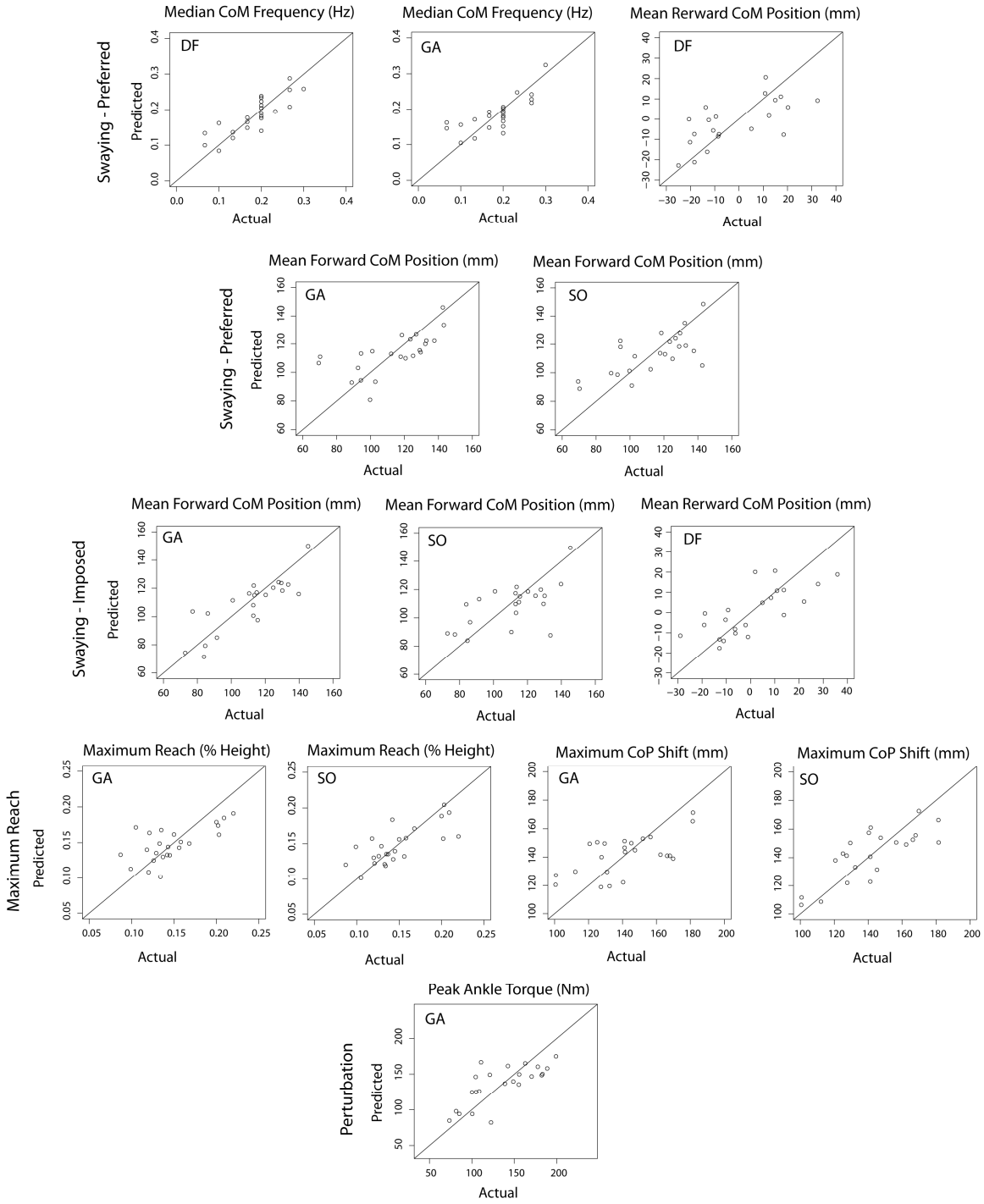

Figure 3-10. Actual vs. predicted dynamic balance measures using the regression models.

Table 3-8. Multiple regression results for dynamic postural tests.

Postural Condition	Balance Measure	Muscle	Independent Measures Included in Best Model	# Terms	R^2	P
Swaying (Preferred)	CoM Median Frequency	DF	Age + $(Age \cdot L_0)$	2	.43	.021
		GA	$a/P_0 + \alpha + (Age \cdot \varepsilon) + (Age \cdot \alpha)$	4	.65	.001
		SO	-	-	-	-
	Mean CoM Forward Position	DF	NA	NA	NA	NA
		GA	$L_S + b/L_0$	2	.41	.005
		SO	$W + a/P_0 + b/L_0$	3	.46	.007
	Mean CoM Rearward Position	DF	$L_0 + (Age \cdot L_S) + (Age \cdot W)$	3	.54	.022
		GA	NA	NA	NA	NA
		SO	NA	NA	NA	NA
Swaying (Imposed)	CoM Median Frequency	DF	-	-	-	-
		GA	-	-	-	-
		SO	-	-	-	-
	Mean CoM Forward Position	DF	NA	NA	NA	NA
		GA	$L_0 + W + b/L_0$	3	.60	.001
		SO	$a/P_0 + b/L_0$	2	.47	.009
	Mean CoM Rearward Position	DF	$W + \beta + (Age \cdot \varepsilon)$	3	.43	.013
		GA	NA	NA	NA	NA
		SO	NA	NA	NA	NA
Maximum Reach	Maximum Reach	DF	-	-	-	-
		GA	$Age + b/L_0 + \alpha + (Age \cdot L_0)$	4	.43	.050
		SO	$Age + \alpha + (Age \cdot a/P_0)$	3	.44	.005
	Maximum Forward CoP Shift	DF	-	-	-	-
		GA	$L_0 + W + \beta + (Age \cdot \beta)$	4	.38	.049
		SO	$L_0 + W + \beta + (Age \cdot a/P_0)$	4	.62	.005
External Perturbation	Maximum Challenge	DF	NA	NA	NA	NA
		GA	-	-	-	-
		SO	-	-	-	-
	Maximum Ankle Torque	DF	NA	NA	NA	NA
		GA	$Age + L_S + (Age \cdot b/L_0)$	3	.47	.006
		SO	-	-	-	-

Regressions including more than 9 terms and/or no significant regressions not shown, signified by "-".
NA: model not applicable; CoP: center of pressure; CoM: center of mass; TtC: time-to-contact

3.4 Discussion

The purpose of this chapter was to evaluate the postural control of a group of young and older subjects under a variety of static and dynamic balance conditions, and to determine if there were specific muscle mechanical properties (measured in Chapter 2) that could explain the age-related changes in postural control. The balance tests demonstrated that the older adults had poorer postural control. We hypothesized that the maximal isometric force, the series elasticity, and the force-velocity characteristics of the plantar- and dorsiflexor muscles would be predictive of the age-related changes in postural control. While maximal isometric force had less predictive power than expected, the series elasticity and force-velocity characteristics did indeed explain a significant proportion of the age-related variance in the balance tests. Muscle force-length properties were also important in predicting age-related differences in balance ability, even though they were not significantly different between the age groups in Chapter 2. The multiple linear regression analysis revealed that for most postural tests, a combination of mechanical properties was needed for good predictive power.

3.4.1 Age-Related Differences in Static and Dynamic Balance Conditions

Almost all postural conditions were associated with differences between the younger and older groups. In upright quiet stance conditions, the older subjects exhibited more CoP movement (greater mean CoP speed), reflecting greater modulation of active ankle torque. The older subjects also had lower mean CoM times-to-contact, indicating decreased spatio-temporal margins of stability. These findings agree with previous

studies that have shown increased CoP speed (Maki et al. 1990, Prieto et al. 1996) and lower time-to-contact values (Slobounov et al. 1998, van Wegen et al. 2002) in older individuals. Overall, the present results suggest that older subjects had an increased amount of postural modulation but still had more CoM movement (based on the shorter CoM TtC), indicating less stability than the younger subjects during upright quiet stance.

A maximum forward lean places increased demands on the plantarflexor muscles (Sinha and Maki 1996), and is therefore regarded as a more challenging postural task. The older adults could not lean as far and had more CoP movement than the younger subjects, supporting reports that older adults have smaller maximum recoverable lean angles (Cummings and Nevitt 1989, Grabiner et al. 2005). No age-related differences occurred in the maximal backward lean, perhaps due to the very small stability margins afforded to all subjects in this condition, where the CoM must be controlled by the dorsiflexors to be within a narrow range of positions (i.e. the ankle-heel distance is much shorter than the ankle-toe distance). The similar young and older responses may reflect the relatively few postural strategies from which to choose. In most balance studies involving older subjects, backward leaning is not included, as it is much more difficult to recover should a fall occur. An exception is a study by Van Wegen et al. (2002), who found that older subjects did indeed lean less far in the rearward direction, which contrasts with the results of the present study. This may be because the older subjects in the present study were all healthy and active individuals, who wore a safety harness to increase their confidence during the backward lean, which may have allowed them to more closely match the younger subjects.

In the dynamic maximal range swaying conditions, the older adults did not sway as far forward as the young when swaying at either preferred or imposed frequencies. Similar to the backward leaning, no age differences were found for the maximum rearward sway position. Thus, the results for the swaying kinematics and the static leaning are in agreement. Further, no age-related differences were seen in the preferred swaying frequencies, but the younger subjects were able to more closely match the target frequency (0.25 Hz) in the imposed swaying condition. This age-related decrement in entrainment performance is consistent with reports that errors in time estimation increase with age (Coelho et al. 2004, Rakitin et al. 2005). While several studies have examined voluntary swaying to study multi-muscle synergies (Danna-Dos-Santos et al. 2007, Krishnamoorthy and Latash 2005, Wang et al. 2006) or time-to-contact calculation methods (Haddad et al. 2006) in young healthy adults, this was the first comparison of voluntary swaying behavior between young and older adults of which we are aware.

Internal and external perturbations also showed age differences. In the rapid forward reach condition (an internal perturbation), the older subjects did not shift their CoP as far forward as the young subjects, but were able to reach farther forward than the young subjects. The age-related differences in the maximum CoP shifts are consistent with other studies (Duncan et al. 1992, Duncan et al. 1990, Weiner et al. 1992). But why were the older adults able to reach farther forward? An inspection of the reaching movement motion capture data revealed that the speed of the older reaching movements was slower than the younger subject; this allowed their CoM to come closer to their forward base of support boundary and thus enabled them to reach farther.

In the sequentially increasing postural perturbations, subjects were instructed to resist stepping if possible. The older adults used a stepping strategy at a lower postural challenge than the younger subjects, which agrees with other studies (Luchies et al. 1994, Mille et al. 2003, Thelen et al. 1996) . The maximum plantarflexor torque used to resist the perturbations was similar between the age groups, agreeing with studies that suggest that maximal torque capability does not limit the ability of older adults to recover from postural perturbations (Grabiner et al. 2005, Hall and Jensen 2002, Mille et al. 2003).

3.4.2 Muscle Mechanical Properties and Balance Control

The main purpose of this chapter was to relate sets of individual muscle mechanical properties to balance performance in young and older individuals. Although other studies have examined the effects of isolated properties on postural control, such as the strength or stiffness of the plantarflexors (Fitzpatrick et al. 1992, Loram and Lakie 2002a, Morasso and Sanguineti 2002, Winter et al. 1998, Winter et al. 2001), to our knowledge this is the first study to relate full sets of mechanical properties that describe the static and dynamic properties of the dorsi- and plantarflexor muscles.

A previous study by Onambele et al. (2006) examined the influence of plantarflexor muscle properties on postural control in the elderly, performing a multiple regression analysis similar to that reported here. Their study focused on total joint strength, muscle size, activation capacity, and Achilles tendon stiffness, rather than individual muscle properties. They found that age-related changes in these measures could explain a relatively large amount of the variance (> 70%) in balance performance during challenging postural tasks like tandem and single leg stance. In the present

chapter, age-related mechanical property alterations were significant predictors for a wide range of balance conditions, including mundane tasks such as quiet stance. In comparison to the Onambele study, the present regression models explained a lower proportion of the variance in the postural conditions, averaging ~40% when using specific independent mechanical properties to predict specific postural conditions, and increasing to ~50% when using multiple mechanical properties. The lower predictive power may be related to subject populations, as the Onambele study included many more subjects (n = 90), distributed across young, middle-aged, and older age groups. The smaller sample size in our study was associated with the involved experimental and computational aspects of our protocol, which included MRI and ultrasound imaging, multiple dynamometer experiments, musculoskeletal modeling, and computer optimization (Chapter 2).

3.4.3 Maximal Isometric Force

It is well established in the literature that muscle strength generally decreases with age (Bemben et al. 1991, Frontera et al. 2000a). Most studies providing this evidence have studied the strength of entire joints, due to the difficulty in measuring individual muscle forces directly in humans (Komi et al. 1987). While the torque-producing capability of a joint can be informative, knowledge of the maximal isometric strength of individual muscles is needed to fully understand the influence of age-related changes on balance performance. Individual muscles make unique contributions to the overall joint strength, as is the case for the gastrocnemius (GA) and soleus (SO), both of which are important in the control of upright posture (Nashner and McCollum 1985). For example, selective age-related atrophy of the faster-contracting Type II muscle fibers (Frey et al.

2000, Larsson and Ansved 1995, Lexell 1995) may cause the GA to be disproportionally weaker in older adults, changing the relative contributions of GA and SO to the control of posture in older individuals. The present study accounts for these possibilities, as the maximal isometric force (P_0) capabilities of the dorsiflexors and *individual* plantarflexor muscles were estimated in Chapter 2 for the young and old subjects.

In general, P_0 was weakly related to performance on the different static and dynamic postural tests. The regression analysis revealed that SO P_0 was a significant individual predictor of only one balance variable – the preferred swaying frequency (explaining ~40% of the variance overall). In this case, there was an age-related interaction, such that the preferred swaying frequency was inversely related to P_0 for the young, but directly related in the older subjects. One possible explanation could be that SO P_0 was a limiting factor in swaying speed for the older subjects, who may have needed stronger muscles to sway faster. Other mechanical properties may have been more important than P_0 in the younger subjects, such as series elasticity (which was included in the multiple regression models). Another possibility is that the younger subjects who had stronger muscles also tended to have larger masses, and therefore had a lower natural swaying frequency, which would explain the inverse relationship between P_0 and preferred swaying frequency in the young subjects. In the multiple regression analysis P_0 was an important predictor for only 3 of the 16 balance variables associated with the different balance conditions. These included the mean quiet stance CoP speed and mean forward leaning CoM position; P_0 did not appear in any of the multiple regression models for the dynamic conditions.

Compared to the other muscle properties, the sparse appearance of P_0 as a significant predictor indicates a relatively minor role in predicting age-related degradations in postural performance. We had expected that P_0 might be a more powerful predictor, especially in conditions that require large ankle torques, such as the maximal lean and perturbation conditions. This expectation was in part due to the large influence of muscle strength on other muscle properties (P_0 scales both the force-length and force-velocity relationships), the age-related decreases in P_0 with age found in Chapter 2, and other studies demonstrating that musculoskeletal models are highly sensitive to P_0 (Maganaris 2004, Out et al. 1996, Scovil and Ronsky 2006). Instead, the present results are consistent with other studies showing that maximal plantarflexor strength had little relation with age-related balance ability in tandem and single-leg stance (Onambele et al. 2006), and recovering from a maximal lean (Grabiner et al. 2005). It may be that the strength of the healthy older adults in the present study was well beyond the minimal values required for the performance of the various static and dynamic postural tasks, and that muscle strength may play a more important role in frail elderly individuals (Kuo and Zajac 1993).

3.4.4 Stiffness of the Series Elastic Components

The stiffness of the series-elastic component has a large influence on the behavior of muscle. As the contractile component of a muscle produces force, it is expressed across the series elastic component, causing it to stretch. This in turn alters the contractile component length and velocity, changing the time-course of force production due to the force-length and force-velocity relations. A variety of studies have shown an increase in

the stiffness of the series elastic components with aging (Chapter 2) (Blanpied and Smidt 1993, Ochala et al. 2007a, Ochala et al. 2005, Ochala et al. 2004b); although others have shown opposite trends in the stiffness of the external portion of the Achilles tendon, which decreased with age (Onambele et al. 2006). These different findings may be due to different measurement sites (overall series elasticity vs. external tendon), which have different adaptations with age (Galler and Hilber 1998, Higuchi et al. 1995, Kjaer 2004, Ochala et al. 2007a, Tuite et al. 1997) (see section *2.1 Introduction* for a brief discussion). The increase in series elastic stiffness is thought to be an adaptation to the aging process, as a stiffer musculotendon complex will allow a faster rise in force after a muscle is excited, as the contractile elements will not shorten as much compared to a more compliant musculotendon complex (Morasso and Sanguineti 2002). This adaptation may partially offset the decrease in the rate of tension development that occurs with aging (Clarkson et al. 1981). If this change in series elasticity is indeed an age-related adaptation, we expected that it would be predictive of the age-related changes in postural control. In general, this hypothesis was supported by the results of the regression analyses; however, series elastic stiffness was most predictive of age-related differences in balance performance when it was combined with other mechanical properties in the multiple regression analysis.

Series elastic stiffness was characterized by the force-extension relationship, expressed as a second order polynomial for each muscle. The two polynomial coefficients specified the rate of extension with increases in force (α), and the degree of linearity in the force-extension relation (β). A third parameter, the slack length (L_S), is the length at which the series-elastic component becomes "taut.". Independently, the α

stiffness coefficient for the GA explained ~50% of the variance in the preferred swaying frequency, with an age interaction. In the younger subjects, the preferred swaying frequency was directly related to α, perhaps because the stiffer series elasticity allows a faster rise in force that promotes a greater swaying frequency. It is not clear why increases in the GA stiffness of the older group were related to *lower* swaying frequencies. One possibility is that other age-related changes in mechanical properties play a role in determining the preferred swaying frequency. For instance, the older subjects with decreased plantarflexor maximal isometric muscle force capabilities tended to have lower swaying frequencies (see previous section). Therefore, gains in force rise time due to the increased stiffness may be offset by diminished force capacity, thus reducing the net muscular impulse and decreasing the ability to accelerate and decelerate the CoM during swaying.

In the multiple regression analysis, the series elastic stiffness coefficients were important predictors in the regression models for both static and dynamic balance conditions. The α coefficient was particularly important in predicting the mean CoP speed during quiet stance, while the β coefficient seemed to be most important in predicting the maximal forward CoP shift during a forward reach. The α coefficient appeared as an interaction with age in the multiple regression models for both median swaying frequency (as in the independent linear regression) and mean quiet stance speed. The β coefficient had age interactions for both mean CoM time-to-contact in quiet stance and the maximum forward CoP shift during reaching. In general, these results are consistent with the findings of Onambele et al. (2006), who showed that the stiffness and Young's modulus of the Achilles tendon are both important predictors for postural stance

ability, and suggested that ankle stiffness would be important in sinusoidal swaying movements.

In both age groups, subjects with longer GA and SO slack lengths (L_S) tended to lean further forward during the leaning task, and subjects with longer GA slack lengths reached more anterior positions during the imposed swaying task. The slack length of a muscle is an important factor in setting the operating range of a muscle. However, anatomical constraints dictate that the contractile fibers of a muscle with a long series elastic slack length will be relatively *shorter* than the fibers of a muscle with a shorter slack length, possibly placing the fibers on a different region of the force-length relation (Figure 3-11). Therefore, the series elastic slack length can alter plantarflexor force production indirectly due to its effect on the active force-length muscle property, and thus influence the degree to which subjects can lean forward. Although numerous studies have shown that slack length is an important property of human muscle based on modeling efforts (Buchanan et al. 2004, Hoy et al. 1990, Lloyd and Besier 2003, Manal and Buchanan 2004, Scovil and Ronsky 2006), this provides the first experimental evidence of a functional link between slack length and postural control of which we are aware.

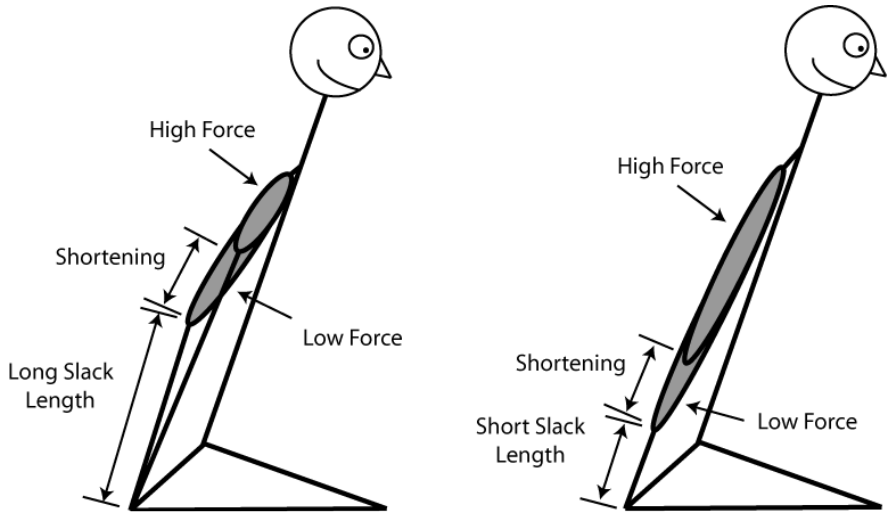

Figure 3-11. A schematic of the role of the series elastic slack length during upright posture using a simplified inverted pendulum model. A subject with a long (left) and short (right) series elastic slack length.

3.4.5 Force-Velocity Characteristics

The force-velocity relationship dictates that contractile elements produce less force than P_0 when shortening, and more force than P_0 when lengthening. In Chapter 2, the parameters that define the shape $(a/P_0, b/L_0)$ and the eccentric force plateau (ε) of this relationship were estimated for the young and older subjects. When each of these parameters was included in separate linear regression models, only the a/P_0 coefficient for the plantarflexor muscles was predictive of age-related differences in balance performance. The SO a/P_0 coefficient explained almost 40% of the variance in the mean CoP speed when leaning forward, with the younger subjects displaying a direct relation between CoP speed and a/P_0. In contrast, the older subjects had an indirect relationship, with *greater* mean CoP speeds associated with smaller a/P_0 values. A smaller SO a/P_0 coefficient produces a higher maximum shortening velocity.

We were initially surprised to find this age-related interaction of the SO a/P_0 coefficient with CoP speed in a static postural task such as quiet stance. However, as previous researchers have pointed out, quiet stance is actually quite dynamic (Loram et al. 2004). During quiet stance, the body is constantly making small corrections, "catching" the CoM when it moves too far, and "throwing" it back towards an equilibrium point (Loram and Lakie 2002b). During this process, the muscle fibers undergo small stretch and shortening cycles, in which the force-velocity properties of muscle would play an important role. This throw-and-catch behavior, combined with increased neural delays, may explain the association between greater mean CoP speeds and smaller (faster) a/P_0 values in the older subjects. To elaborate, in order to maintain posture with a minimal amount of effort the throws should be of just the right magnitude to bring the CoM velocity to zero at the equilibrium point, although in reality some overshoot is always present (Loram et al. 2005). The magnitude of the "throws" in the older subjects with faster contracting SO muscles (smaller a/P_0) may have been greater than those observed in the older subjects with slower muscles, causing the CoM to overshoot the equilibrium point, and therefore requiring an increased corrective action (increasing the CoP speed). This behavior could arise from the increased neural delays observed in older adults (Norris et al. 1953, Sato et al. 1985), causing the older adults with faster contracting muscles to have a harder time controlling the larger forces (impulses) that can be produced at concentric muscle velocities. Older subjects with slower muscles may not have "overcorrected" as much, which resulted in slower CoP speeds. On the other hand, the younger subjects may have been better able to control their postural adjustments due to shorter neural delays. Therefore, younger subjects with faster

contracting SO muscles were able to use smaller corrections resulting in slower CoP speeds through a more precise control of the throws and subsequent catches of the CoM during quiet stance.

In the multiple regression analysis, both force- velocity coefficients $(a/P_0, b/L_0)$ appeared often in the models for the dynamic balance tests, with a/P_0 also appearing as an age interaction. This reinforces the importance of the a/P_0 coefficient as a predictor of balance performance. The eccentric plateau coefficient ε also appeared as an interaction with age in predicting dynamic postural performance, albeit with less frequency than a/P_0 and b/L_0. Although to our knowledge this is the first study to examine the relation between age-related changes in individual muscle force-velocity properties and postural control, other studies have suggested that age-related decreases in the rate of torque development can explain performance differences in a variety of postural tasks (Chandler et al. 1990, Horak et al. 1989, Lord et al. 1991, Luchies et al. 1994, Wolfson et al. 1986). Together, this suggests that velocity-dependent muscle properties are important in explaining age-related differences in postural control, even during relatively static postural tasks.

3.4.6 Force-Length Properties

The contractile component force-length properties were described by parameters defining the optimal length (L_0) and the width (W) of this parabolic relation (see Appendix B for more details). Although the optimal contractile length (L_0) was not associated with balance ability independently, it was one of the most frequently appearing terms in the multiple regression analysis, appearing in models for both static

and dynamic postural tasks, and as an age-related interaction term. This suggests that L_0 has an influential performance on general postural control, and played a part in predicting age-related differences in balance ability.

The width of the SO force-length relation (W) was able to independently explain more than 35% of the variance associated with the age-related differences in both quiet stance CoP speed and the maximum forward reach, with significant age interactions in both cases. Younger subjects with wider force-length relations tended to have greater CoP speeds, while in the older group narrower force-length parabolas were associated with greater CoP speeds. Narrower force-length relations decrease the operating range of muscle, such that force is produced over a smaller range of motion; the force also decreases more sharply as the muscle fibers move away from the optimal length. This would cause greater changes in muscle force potential as the muscles repeatedly shorten and lengthen during quiet stance (Figure 3-12, Top). Therefore, in the older subjects the narrower force-length relations may have required greater neural inputs from the central nervous system to compensate for the greater changes in the force potential (Figure 3-12, Bottom). The greater neural inputs may have caused over-corrections (i.e. moving from one side of the force-length relation to the other), leading to repeated large inputs and corresponding changes in muscle force, which would be expected to increase the mean CoP speed. However, this does not explain the positive relationship between the force-length width and the CoP speed in the younger subjects. This may again be due to the influence of other mechanical properties, such as the series elastic slack length and stiffness, which were also terms in the multiple regression models for quiet stance CoP speed. When performing a maximal reach, younger subjects with wider force-length

relations could reach farther, but this association was absent in the older subjects. This absence may be related to the importance of multiple factors that dictate the maximum reach in older adults. Indeed, in the multiple regression analysis the series elastic stiffness and force-velocity shape parameters together accounted for more variance in the reaching task performance than the width of the force-length relation by itself.

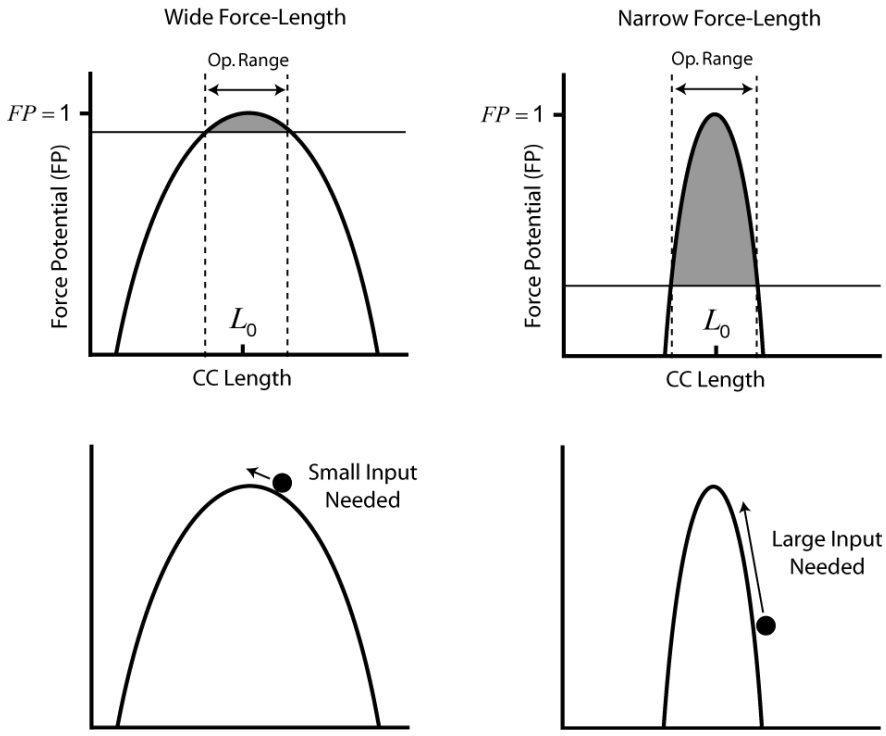

Figure 3-12. Top: Example of "wide" and "narrow" force-length relations, for a given operating range ("Op. Range"; vertical dashed lines). Bottom: For the wide force-length relation, the force potential changes gradually so only small inputs are needed to remain near optimal length. On the other hand, large inputs are needed to counteract the large changes in force potential when the force-length relation is narrow.

Based on the results of Chapter 2 and previous studies that reported no age-related changes in the force-length relationship of muscles (Brown et al. 1999, Larsson et al. 1997), we did not expect that the force-length parameters would be predictive of age-related differences in the performance of the postural tasks. On the contrary, the force-

length parameters of the dorsi- and plantarflexor muscles were indeed predictive of age-related differences in both static and dynamic balance performance, independently or when combined with other mechanical properties. The Chapter 2 analysis was designed to compare parameter differences between the young and old subject *groups*, but did not consider the relationship between the force-length properties and the balance variables for each subject within each group, as did the regression analysis performed in the present chapter. Although others have examined the influence of a variety of muscle characteristics (e.g. activation capacity, strength, stiffness) on postural control (Loram and Lakie 2002a, Onambele et al. 2006, Winter et al. 1998, Winter et al. 2001, Wolfson et al. 1995), few (if any) have examined the relationship between force-length properties and balance control in older adults.

3.4.7 Limitations

Although the regression results suggest that muscle mechanical properties are important in explaining age-related differences in balance control, they should be interpreted with a degree of caution due to the limitations imposed by the relatively small sample size and the inherent limitations of multiple regression. One such limitation is that of multicollineraity, as the mechanical property predictor variables exhibit varying amounts of correlation (see Appendix C). Although some mechanical properties exhibited moderate correlations ($R \approx .4$ to .5 between a few properties), most were very low - far below values for "strong" ($R > .8$) correlations (which may cause problems with model selection and interpretation) (Licht 1994).

Another caveat relates to the use of a specified significance cut-off of $p < .05$, which is the traditional approach for statistical analysis of data and served to simplify the reporting of results. However, there were cases where *p*-values were close, but not below the cut-off value. In particular, there were instances where one of the plantarflexor muscles had a significant predictive relationship with a balance variable, but the other plantarflexor did not – although the regression plot was qualitatively similar (e.g. median CoM frequency during preferred swaying vs. P_0; Figure 3-8).

Finally, because our subjects were all healthy, active, community-dwelling individuals, the results of this study may not extend to others with neurological or musculoskeletal disorders, who may have vastly different mechanical properties and postural abilities. It also unknown whether the present results are indicative for other postural conditions not examined here.

3.4.8 Conclusions

This study examined the performance of healthy young and older adults on a variety of static and dynamic balance tasks, and sought to determine whether the differences in balance performance could be explained by age-related changes in the mechanical properties of the dorsi- and plantarflexor muscles. The older adults performed more poorly on the balance tasks, and the series-elasticity, force-length, and force-velocity properties all made important contributions to the prediction of age-related differences balance control. Contrary to expectations, the maximal isometric force capability of the muscles had relatively little predictive power. For some balance tests, a

combination of mechanical properties was needed to explain the variance in postural performance.

CHAPTER 4

MUSCULOSKELETAL MODEL OF POSTURAL CONTROL

4.1 Introduction

In upright standing posture, older individuals are generally considered less stable than younger adults (Woollacott and Shumway-Cook 1990). This conclusion is often based on increases in the amount center of mass (CoM) and center of pressure (CoP) movement in older adults. This decrease in stability has been linked to degradation of the sensory and neuromuscular systems (Horak et al. 1989, Hughes et al. 1996, Lord et al. 1991), and have been associated with increased sway and increased risk of falling (Lord et al. 1991, Lord et al. 1994).

There have been a number of prospective studies designed to elucidate cause and effect relationships between age-related changes in components of the neuromuscular system and postural stability (Baloh et al. 1998, Brauer et al. 2000, Maki 1997, Maki et al. 1994). However, these studies follow subjects for only a few years at most, making it difficult to assess changes occurring over a human life span. An inherent difficulty is that a multitude of anatomical, physiological, and neural changes occur as a person ages, making it difficult to draw causal relationships between specific neuromuscular changes and their effect on posture. An alternate approach is the use of musculoskeletal models, where simulated age-related changes in the neuromuscular system can be invoked instantaneously, and the effects of individual changes can be evaluated systematically.

Human standing posture is often modeled as a two-segment inverted pendulum (Karlsson and Lanshammer 1997, Loram and Lakie 2002b, Winter 1995b, Winter et al.

1997), which is appropriate when the amplitude of body sway is small and movement occurs about the ankle joint (Gage et al. 2004). Such models can be controlled through regulation of "ankle" joint torque (Fitzpatrick et al. 1996, Peterka and Loughlin 2004, Winter et al. 1998), but these "torque controlled" models are unable to address the role of individual muscles in postural control. A musculoskeletal model incorporating individual muscle forces rather than net ankle torque is more useful for studying the effects of age-related changes of muscle properties on postural control. This is because there may be changes specific to certain muscles, such as the preferential loss of fast-twitch Type II fibers in the gastrocnemius (Frey et al. 2000, Larsson and Ansved 1995, Lexell 1995).

The mechanical behavior of muscle can be represented by a Hill muscle model that delineates the nonlinear relationships affecting the force produced when neural control signals are input to a muscle (Hill 1938). The Hill model is comprised of an active contractile component that is responsible for producing force, and a passive series elastic component that accounts for the series elasticity within a muscle-tendon complex. The mechanical properties defining contractile component behavior include force-length, and force-velocity relations, while a force-extension relation defines the series-elastic component (see Chapters 2 & 3 and Appendix B for more details).

The major muscles contributing to ankle torque and the control of sway in the sagittal plane include the dorsiflexors (DF) and the gastrocnemius (GA) and soleus (SO) plantarflexor muscles (Nashner and McCollum 1985). These muscles can be represented as Hill-type actuators with unique sets of parameters describing the Hill muscle properties. For the contractile component these include the maximal isometric force capability $\left(P_0\right)$, the optimal contractile component length $\left(L_0\right)$, the width of the force-

length relation (W), and shape coefficients for the force-velocity relation $(a/P_0, b/L_0, \varepsilon$). For the force-extension relation of the series elastic component, parameters include the slack length (L_S), and stiffness coefficients (α, β) (see Chapters 2 & 3 Appendix B for details). These parameters define the mechanical behavior of muscle, and have been shown to be important for the dynamic stability of the musculoskeletal system during simulations of locomotion (Gerritsen et al. 1998). Although muscular properties are a fundamental part of neuromuscular control, they are difficult to measure in living humans. As a result, many studies measure the properties of joints as a whole, where the behavior is the result of a complex combination of individual muscle mechanical properties. For example, studies have reported that in older individuals the maximum muscle shortening velocity decreases (Doherty and Brown 1997, Lanza et al. 2003, Larsson et al. 1997, Narici et al. 2005, Thompson and Brown 1999), and musculotendinous stiffness increases (Blanpied and Smidt 1993, Ochala et al. 2004a). However, these studies have focused on estimating the "net" mechanical properties of joints; few have investigated age-related changes in individual muscles (Thelen 2003).

The role of musculotendinous stiffness in the control of posture has received much attention (Loram and Lakie 2002a, Morasso and Sanguineti 2002, Winter et al. 1998, Winter et al. 2001). Conversely, little research has examined the impact of other muscle mechanical properties on posture. Changes in muscle mechanical properties may influence the effective operating range of the muscles controlling posture (e.g. the width of the force-length relation), and may alter the ability of muscle to react to changing postural conditions (e.g. the coefficients of the force-velocity relation). Indeed, the results of Chapter 2 showed that with aging there are declines in the maximal isometric force of

the dorsi- and plantarflexor muscles, increases in musculotendinous stiffness, and altered force-velocity characteristics. In Chapter 3, it was shown that age-related changes in muscle mechanical properties can account for a significant amount of the variability in the balancing abilities of young and older adults. However, one limitation of this experimental research is that the contributions of age-related changes in individual muscle properties to balance control cannot be isolated, as many properties changed together with aging. A musculoskeletal model of postural control will assist in delineating the relations between muscle mechanical properties and postural control by allowing independent changes in muscle property values.

In previous chapters, the mechanical properties of the DF, GA, and SO muscles have been estimated for a group of young and old individuals (Chapter 2), and the postural stability of the same subjects has been evaluated through a series of static and dynamic postural tasks (Chapter 3). The present chapter extends this work by using an inverted pendulum model of sagittal plane postural dynamics that incorporates sets of subject-specific “young” and “old” muscle mechanical properties. The model integrates the muscle models with a feedback-based neural controller and uses numerical optimization to simulate postural control when maintaining upright “quiet” stance. The mechanical properties of the postural model are then systematically changed to investigate how age-related alterations in these properties affect postural control.

4.2 Methods

4.2.1 Overall Study Design

Initially, a musculoskeletal model of postural control that includes sub-models of the skeleton, foot-floor interaction, and individual muscles is described. This is followed by a description of the simulation and optimization procedures, consisting of two parts: 1) the performance of the model in quiet stance using sets of "young" and "older" mechanical properties is compared with the results of young and old subjects in the Chapter 3 experiments; and 2) a sensitivity analysis is performed to assess effects of changes in individual muscle mechanical properties on the performance of quiet stance.

4.2.2 Skeletal Model

The skeletal model comprised two rigid segments linked by a frictionless hinge ankle joint, confined to sagittal plane movement (Figure 4-1). One segment represented the head, arms, trunk, and legs (the "body"); the other combined both feet into a single rigid foot segment. Although the model includes a landmark representing the metatarsal-phalangeal joint (Figure 4-1, 5^{th} Met.), no movement was permitted at this joint. The mass of the body and foot segments were concentrated at single points, CoM_{Body} and CoM_{Foot}, respectively. The mass and inertial properties of the segments was scaled to that of an average adult male, based on Maurer and Perterka (2005). See Appendix E for details on the skeletal model parameters. For consistency, the same skeletal model parameters were used for the "young" and "older" quiet stance models, so that any differences in the behavior of the model would be solely due to the muscle mechanical properties and the magnitudes of the control signals.

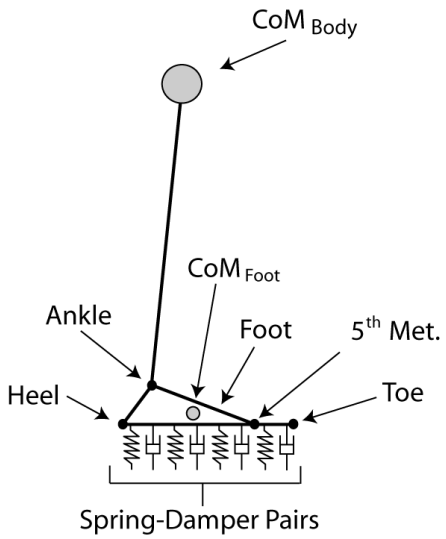

Figure 4-1. Schematic of the skeletal and foot-floor model. See text for details.

4.2.3 Foot-Floor Model

The foot-floor interaction was modeled with a series of 21 spring-damper elements, spaced uniformly along the length of the foot. Thus, the foot was not rigidly attached to the ground, but was allowed to have translational and rotational movement as dictated by the spring-damper elements. Each spring-damper could apply force in the vertical and anterior-posterior directions. The vertical force exerted by each spring was an exponential function of the vertical displacement of the foot relative to the ground (Anderson and Pandy 1999). The net ground reaction force was computed by summing the forces exerted by the springs on the foot segment. See Appendix E for more details.

4.2.4 Muscle Model

The skeletal model was actuated by three two-component Hill-type (1938) muscle models representing the DF, GA, and SO. Each muscle model included a contractile

component with nonlinear stimulation-activation, force-length, and force-velocity properties, and a series elastic component with a nonlinear force-extension relationship. Details about the equations representing these relationships and the muscle model algorithm can be found in Appendix B. The combined parallel elasticity of the muscle-tendon complexes, ligaments, and other tissues was represented by a nonlinear passive torque-angle relation, based on Riener and Edrich (1999):

$$T_{PASSIVE} = \exp(2.1016 - 0.0843\theta_{ANK}) - \exp(-7.9763 + 0.1949\theta_{ANK}) - 1.792 \qquad (5.1)$$

where θ_{ANK} is the ankle angle, and $T_{PASSIVE}$ is the passive ankle torque, which contributed to the net ankle torque. Although passive ankle torque contributions were measured using a dynamometer in Chapter 2, we chose to use the literature-based equation to facilitate comparison with studies in the literature, and also the ankle angle vs. passive torque relationships were similar (i.e. equations based on the Chapter 2 results vs. the Riener and Edrich equation).

4.2.5 Anatomical Model

The software package SIMM (Delp et al. 1990) was used to construct an anatomical model that included the body and foot segments, and could generate the DF, GA, and SO muscle kinematical relationships. The model anthropometric measurements were scaled to that of an average man (see Appendix E). For each of the three muscles, fourth-order polynomials were used to describe the relationships between the length and moment arms of the muscles and the ankle flexion-extension joint angle.

4.2.6 Neural Controller

The motor commands for postural stabilization were generated using a type of proportional-derivative (PD) feedback control based on existing models (Barin 1989, Johansson et al. 1988, Masani et al. 2003, Morasso and Sanguineti 2002, Peterka 2002, Peterka and Loughlin 2004). These studies all used PD feedback to control an active joint torque generator, but in the present model the control scheme was modified to include models of the individual muscle model actuators. An outline of the control scheme is shown in Figure 4-2.

A single proportional controller was used to modulate the excitation signals of the plantarflexor muscles (GA and SO). This was done for simplicity, and also due to reports indicating that the GA and SO are modulated together during quiet stance. (Loram et al. 2005, 2004). The proportional controller responded linearly to the horizontal deviation of the CoM from a position in line with the anterior-posterior position of the ankle joint center $\left(X_{CoM}^{REF}\right)$. Separate plantar- and dorsiflexor derivative controllers based on the CoM time-to-contact (see below) were also included. When the CoM was moving forward (+ *v*) the plantarflexors were excited, while the dorsiflexors were excited whenever the CoM was moving rearward (- *v*). No dorsiflexor proportional controller was needed, because it would only be active when the CoM was behind the ankle joint. Since one of the criteria for the optimization was for the model to maintain its position about an equilibrium point *in front* of the ankles (see 4.2.8 Optimization Procedure), dorsiflexor proportional control would be of no benefit.

A novel aspect of the feedback control system is that the derivative control was based on the CoM time-to-contact, a spatiotemporal variable that includes information

about CoM kinematics (position, velocity and acceleration) relative to the base of support boundaries (see Chapter 3 for computational details). Previous feedback-control models used the segmental angular velocity as a basis for the derivative controller (Masani et al. 2003, Maurer and Peterka 2005, Peterka 2002, Peterka and Loughlin 2004). Knowledge of the putative time before the CoM would cross (contact) a base of support boundary provides information concerning the urgency of the postural situation, and introduces nonlinearities into the derivative control. These nonlinearities arise from the constraint imposed by the finite foot length distance over which the CoM can travel before stability is lost. The inverse of time-to-contact (1/time-to-contact was used as the input to the derivative controllers, meaning that decreased stability (i.e. shorter time-to-contact) would cause an increase in the excitation level of the appropriate muscle models. In contrast, the excitation signal generated by the derivative controllers would be very small if the time-to-contact to the base of support boundary was large.

The postural control model also accounted for various delays and noise that are found in the transmission of control signals within the neural system (Eurich et al. 2000, Faisal et al. 2008). A time delay of 50 ms (τ_d) was chosen to represent the cumulative time delay due to sensory transduction, neural transmission, and nervous system processing (Masani et al. 2003, Peterka and Loughlin 2004). An additional delay was due to the excitation-activation properties of the muscles, in which the activation increased or decreased exponentially following changes in the excitation signal (see Appendix B for details). The time constants were 10 and 70 ms for rising and falling excitation levels, respectively (Winters 1995). A noise source was injected into the control model by generating white noise with a maximum range of ±20 Nm with a pseudo-random number

generator (the noise gain K_N was equal to 20). The white noise was filtered with a moving average from the previous 2 s of data (thus, the noise level was zero for the first 2 s). This filtering removed the higher frequency components of the white noise, leaving a more prominent lower frequency oscillation, reproducing the "random walk" behavior of human postural control (Collins and Deluca 1993). The resulting noise was introduced into the model as a disturbance torque (maximum range ~ ±2 Nm, standard deviation ~ 0.7 Nm; Figure 4-2). This disturbance torque ($T_{Disturb}$) represented the combined effects of noise throughout the neuromuscular system. The pseudo-random number generator was started with the same seed for each simulation, causing each simulation to receive identical disturbance torque-time series.

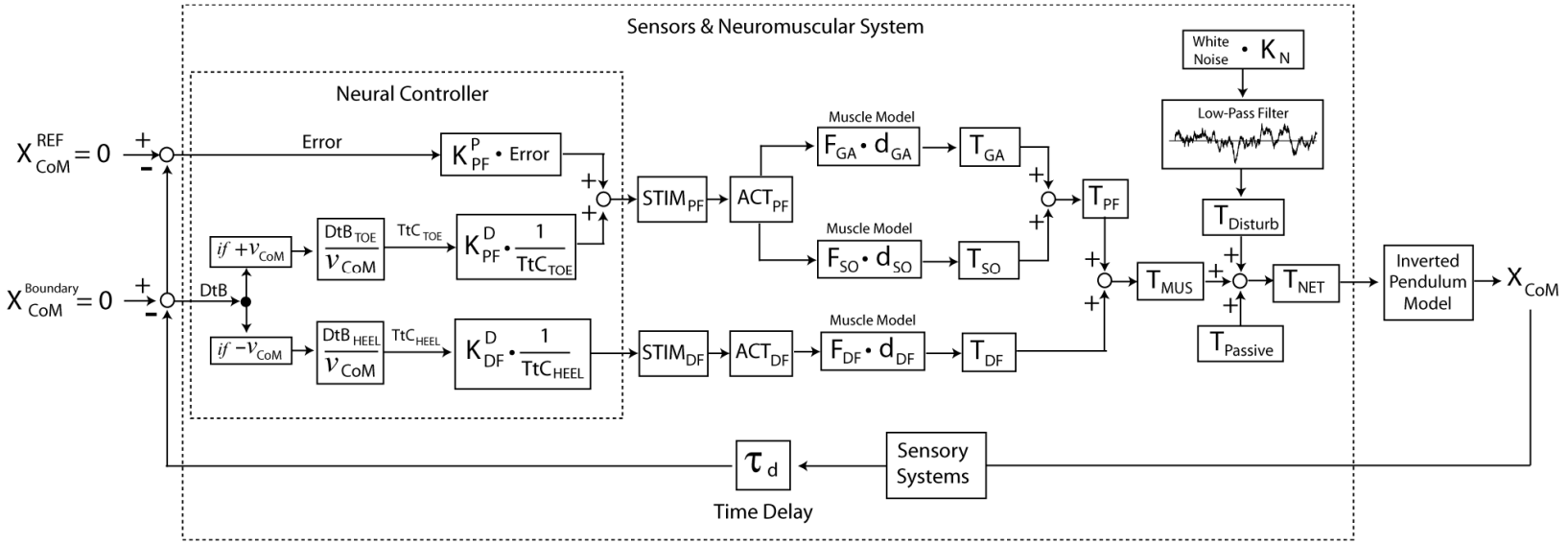

Figure 4-2. Schematic of the postural control model. Subscripts DF, GA, and SO refer to the dorsiflexors, gastrocnemius, and soleus muscles, respectively. X_{CoM}: the anterior-posterior (AP) position of the body center-of-mass (CoM), X_{CoM}^{REF}: the AP position of the ankle joint center, $X_{CoM}^{Boundary}$: the AP position of the base of support boundaries, v_{CoM}: AP velocity of CoM, DtB: distance from CoM to toe or heel boundaries, depending on the CoM velocity direction (v_{CoM}), TtC_{CoM}: CoM time-to-contact to toe or heel boundaries depending on the CoM velocity direction (v_{CoM}), K_{PF}^{P}: proportional control gain for a the plantarflexors, K^{D}: derivative control gain for a given muscle (DF or PF), STIM: neural excitation signal, ACT: muscle activation, F: muscle force, d = muscle moment arm at the ankle, T: ankle torque produced by each muscle, T_{MUS}: net muscle torque produced at ankle, $T_{Passive}$: passive torque contributions, K_N: noise gain, $T_{Disturb}$: disturbance torque, T_{NET}: net ankle torque, τ_d: time delay.

4.2.7 Equations of Motion

The equations of motion for the two-segment inverted pendulum model were derived symbolically using Autolev (Version 4, OnLine Dynamics, Inc., Sunnyvale CA), software, which is based on Kane's method (Kane and Levinson 1985). The model had four degrees of freedom, as it was not pinned to the ground. A variable step-size Runge–Kutta–Merson integrator (Fox 1962) was used to integrate the model state equations (maximum step size = 0.01 s, maximum absolute & relative error $\leq 10^{-7}$).

4.2.8 Optimization Procedure

Numerical optimization was used to find the values of the unknown gains for the PD controller $\left(K_{PF}^{P}, K_{DF}^{D}, K_{PF}^{D} \right)$ that would allow the model to maintain quiet stance. A genetic algorithm (Storn and Price 1995) was used to find the solution to the optimization problem (see Chapter 2 for details). In the experimental quiet stance condition (Chapter 3), subjects were asked to stand "as still as possible", analogous to the task of minimizing the amount of CoM motion. Other implicit goals included maintenance of upright stance and minimal muscular effort, which would be reflected by reduced muscle excitations, relatively low muscle forces, and small CoP movements - as seen in experimental quiet stance data. Therefore, a multi-component fitness criterion (cost function) that takes all these goals into account was specified.

Maximal fitness $f\left(\overset{\mathrm{r}}{X}\right)$ was obtained by minimizing a function comprised of four components related to the time the model could stand without losing its balance

(C_{FALL}), the total muscle force produced (C_{FORCE}), the deviation from a target equilibrium point (C_{EQ}), and the total CoM-CoP difference $(C_{CoM-CoP})$:

$$f(\vec{X}) = w_1 C_{FALL} + w_2 C_{FORCE} + w_3 C_{EQ} + w_4 C_{CoM-CoP} \tag{5.2}$$

where w is a weighting factor, such that $w_1 = 1$, $w_2 = 1$, $w_3 = 7.5$, and $w_4 = 10$. These weighting factors were obtained through pilot work, and resulted in the fastest and most robust convergence to an optimal solution. The vector $\vec{X}$ consisted of the neural controller gains:

$$\vec{X} = \left[K_{PF}^{P}, K_{DF}^{D}, K_{PF}^{D} \right] \tag{5.3}$$

where K_{PF}^{P} is the gain of the proportional controller for the plantarflexor muscles, and K_{DF}^{D} and K_{PF}^{D} are the derivative gains for the dorsi- and plantarflexors, respectively.

The first cost (C_{FALL}) was associated with the time until the model lost stability because the CoM moved outside of the base of support:

$$C_{FALL} = \left[10\left(T_{FINAL} - T_{FALL} \right) \right]^2 \tag{5.4}$$

where T_{FINAL} is the selected duration of the simulation and T_{FALL} is the instant at which stability was lost. This cost was much greater than the other cost components, to drive the optimization procedure away from unacceptable solutions where the model falls. Once this cost was brought to zero, the optimization then focused on reducing the other three costs. The inclusion of this stability cost was preferred to simply adding a large fixed penalty if the model fell because it improved the performance of the optimization procedure.

The second cost (C_{FORCE}) was based on the cumulative sum of the muscle forces, scaled to each muscle's maximal isometric force P_0:

$$C_{FORCE} = \sum_{i=1}^{n}\left[\left(\frac{P^{DF}}{P_0^{DF}}\right)+\left(\frac{P^{GA}}{P_0^{GA}}\right)+\left(\frac{P^{SO}}{P_0^{SO}}\right)\right] \tag{5.5}$$

where P is the muscle force at time step i for a given muscle. Since P_0 is a function of a muscle's physiological cross-sectional area, this cost function is identical to one which minimizes the net muscle stress (Crowninshield and Brand 1981). This cost component encouraged optimal solutions associated with a minimal level of muscle activity, as exhibited during quiet stance in humans. In pilot work, a nonlinear cost component associated with minimizing the sum of the squared muscle forces was also explored. The results were virtually identical, so the simpler linear cost function, which produced realistic solutions, was employed.

The third cost component $\left(C_{EQ}\right)$ was associated with the cumulative sum of the CoM distance from the target equilibrium point. Previous modeling studies implementing feedback control of an inverted pendulum model have used a target position directly above the ankle joint (Masani et al. 2003, Maurer and Peterka 2005). However, humans normally keep their CoM about 50 mm in front of the ankle joint during quiet stance (Winter et al. 1998), which agrees with our results from Chapter 3 (young 52 mm; older 43 mm; see Table 4-1). Based on our experimental data, the target equilibrium point was set to 47 mm, and the cost component defined as:

$$C_{EQ} = \sum_{i=1}^{n}\left|X_{CoM} - X_{EQ}\right| \tag{5.6}$$

where X_{CoM} is the anterior-posterior position of the CoM at time step i, and X_{EQ} is the equilibrium point (47 mm). This cost component introduces a constant plantarflexor muscle activity bias to maintain this forward-leaning position, and encourages the model

to limit excessive CoM motion. The same target equilibrium point was used for both young and old models so both would have identical optimization goals.

The final cost $\left(C_{CoM-CoP}\right)$ included the cumulative difference between the positions of the CoM and CoP, which is proportional to the horizontal acceleration of the CoM during quiet stance (Winter 1995a). A small CoM-CoP difference has been suggested as indicative of more efficient postural control (Benvenuti et al. 1999):

$$C_{CoM-CoP} = \sum_{i=1}^{n} \left| X_{CoM} - X_{CoP} \right| \tag{5.7}$$

where X_{CoM} is the anterior-posterior position of the CoP at time step i.

4.2.9 Assessment of Quiet Stance Model

The model was evaluated by assessing how well its behavior reproduced the experimental data of the young and old subjects in the 30 s quiet stance balance condition in Chapter 3. Separate optimizations were performed using the average DF, GA, and SO mechanical properties of the young and older subjects, estimated for each age group in Chapter 2. The maximal isometric force capabilities were doubled to represent the combined muscle strengths in both legs together in the inverted pendulum model. The simulation time was set for 90 s but only the middle 30 s was compared with the 30 s long experimental data time-series. The beginning of the model data series was ignored to ensure that initial transients decayed. Each simulation required ~18 hours of computing time on a Pentium 4 processor to converge to an optimal solution. Several postural control variables were computed for the CoM and CoP, including the mean position and its standard deviation, the total path length, mean speed, maximum range, and median frequency. To test the long-term stability of the quiet stance model, the optimized young

model was simulated for 10 min (600s). Ignoring the first 10 s due to transients, a linear equation was fit to the CoM position data. The y-offset of this equation represents the effective equilibrium point of the model, and the slope represents the long-term trend, such that a slope of zero would mean that the model always tends to return to the same equilibrium point over time (did not drift).

4.2.10 Sensitivity Analysis

The initial sensitivity analysis was designed to examine the behavior of the young quiet stance model in response to age-related changes in muscle mechanical properties. The young quiet stance model was simulated multiple times using the optimized proportional and derivative controller gains; however, for each simulation one of the nine plantarflexor (GA and SO) muscle mechanical properties was independently "aged" by changing the value to the mean of the older male subjects. Although the dorsiflexor muscles contribute to postural control, the mechanical properties of the dorsiflexor muscle model were not changed as the analysis was designed to focus on the plantarflexor muscles since they have a dominate role in postural control (Nashner and McCollum 1985). Investigated parameters were the maximal isometric force (P_0), the force-length relationship (L_0, W), the force-extension relationship (α, β, L_S), and the force-velocity relationship ($a/P_0, b/L_0, \varepsilon$), all of which were described in Chapter 2. For this initial sensitivity analysis, the gains of the controllers were not re-optimized. Each simulation lasted for 180 s, with all other model parameters and mechanical properties kept constant. A final 180 s simulation was performed with all of the

mechanical properties changed to the older values, again with the same control gains as in the optimal young model solution.

A further sensitivity analysis was performed by systematically altering each plantarflexor muscle model parameter to assess the general nature of their influence on the control of quiet stance. In this case the model was re-optimized each time so the gains of the neural controllers could change, adapting to the change in mechanical properties. The initial model parameters were the average values of the young male subjects estimated in Chapter 2. The nine parameters were then varied systematically across six levels (±5%, ±10%, and ±15%), based on a similar sensitivity analysis by Maurer and Perterka (2005). After each change the model was re-optimized to find the proportional and derivative controller gains that minimized the fitness criteria, for a total of 54 separate optimizations.

Some of the older subjects had mechanical properties that were outside of the investigated range of ±15%. Thus additional optimizations were performed where each of the mechanical properties was independently changed to the mean older value. For all of the sensitivity analysis re-optimizations, the simulation time was set to 50 s, followed by a model simulation using the new optimized parameters for 180 s. For these re-optimizations, a subset of the balance variables was calculated, including the mean position, standard deviation of the mean position, mean speed, and median frequency. These variables were only computed for the CoM, as preliminary data analysis showed that the changes in the variables computed using CoM and CoP were virtually identical.

4.3 Results

4.3.1 Assessment of Quiet Stance Model

The model and experimental performances are compared in Figure 4-3. The models were able to achieve stable postural states and qualitatively capture the basic structure of the CoM and CoP motion during quiet stance. Quantitatively, summary measures from the "older" postural model more closely matched the older subject group data than did the "younger" model for the younger subjects (Table 4-1). For the older model, the CoM and CoP path lengths and mean speeds were similar for the model and subjects, while the younger model displayed longer CoM and CoP path lengths and higher mean speeds than the young subjects (Table 4-1).

Figure 4-3 (bottom graphs) clearly shows that the older model needed more excitation to the muscles than did the young model. In both young and old models, the dorsiflexor muscle excitation displayed higher frequencies and more phasic activity than the plantarflexors, associated with the exclusive derivative control of the dorsiflexors versus the combined proportional/derivative plantarflexor control. The young model exhibited stable long-term behavior when simulated to stand for a total time of 10 min. This stability was assessed by fitting an equation to the CoM position data:

$$y = 0.0031t + 46.9 \tag{5.8}$$

where t is time (s), and y is the anterior-posterior CoM position (mm). The y-offset of 46.9 indicates that the model remained very close to the target equilibrium point of 47 mm, and the very small slope of 0.0031 *mm/s* indicates that in the long term, the model did not drift away from the equilibrium point (Figure 4-4).

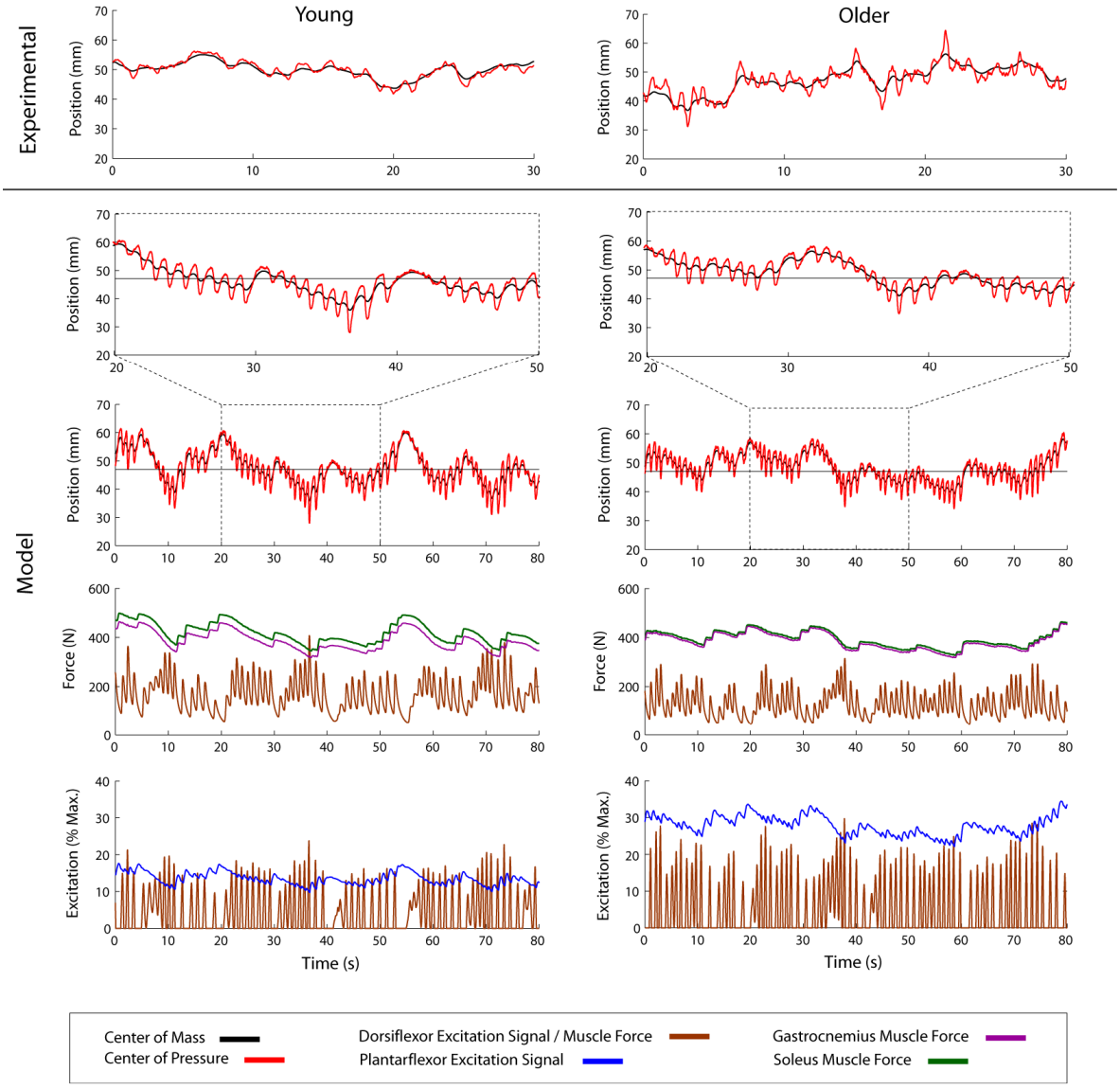

Figure 4-3. Performance of the optimized quiet stance postural control models using muscle mechanical properties measured for young (left) and older (right) subjects. For comparison, experimental data from representative young and older male subjects are shown (top graphs).

Table 4-1. Balance measures characterizing the performance of young and old subjects and the postural control model using sets of young and old mechanical properties.

Balance Measure		Young			Old		
		Subjects	Model	% Diff.	Subjects	Model	% Diff.
Mean Position (mm)	CoM	51.3	47.4	-7.6	43.1	52.6	22.0
	CoP	51.1	47.5	-7.0	42.6	52.5	23.2
SD of Position (mm)	CoM	5.8	4.8	-17.2	6.9	5.1	-26.1
	CoP	6.2	5.5	-11.3	7.7	5.8	-24.7
Path Length	CoM	68.6	108.7	58.5	108.6	101.8	-6.3
	CoP	206.5	330.9	60.2	385.3	398.2	3.3
Mean Speed (mm/s)	CoM	2.3	3.6	56.5	3.6	3.4	-5.6
	CoP	6.9	11.0	59.4	12.8	13.3	3.9
Max. Range (mm)	CoM	21.4	19.7	-7.9	27.1	18.8	-30.6
	CoP	26.2	24.2	-7.6	36.1	24.3	-32.7
Median Frequency (Hz)	CoM	0.04	0.03	-25.0	0.05	0.01	-80.0
	CoP	0.05	0.04	-20.0	0.11	0.03	-72.7

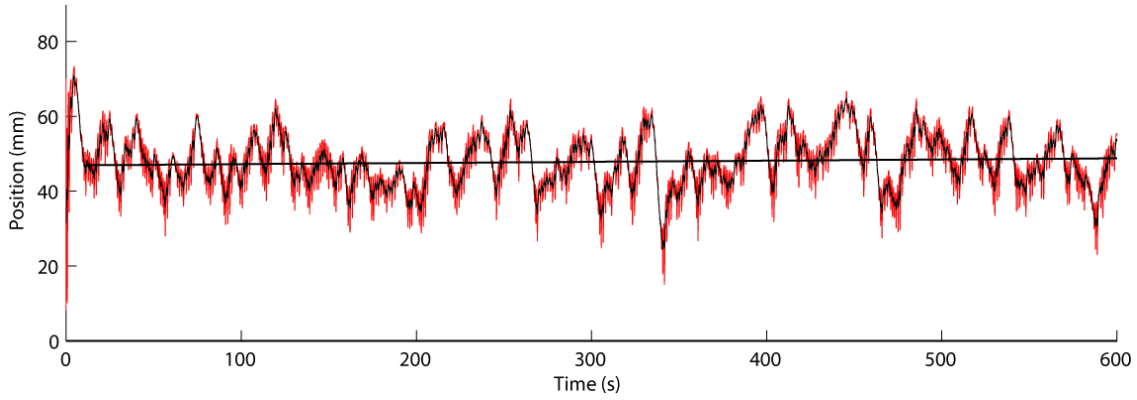

Figure 4-4. Long duration behavior of the optimized young postural model (10 min). The center of pressure (red) is shown oscillating around the center of mass (black). The linear trend is shown (not including the first 10 s).

With the musculoskeletal model we can observe variables that we are unable to measure in the human subjects, such as the individual muscle forces (Figure 4-3). The length and velocity of the muscle fibers are important as they dictate the force that the muscle can produce for a given excitatory input. Figure 4-5 shows the operating lengths of the DF, GA and SO contractile components for the optimized young and older models. The DF and GA muscles were very close to the optimum lengths of their force-length relations in the young model, but in the older model the DF was further on its ascending limb (shorter lengths), and the GA was positioned further on the descending limb (longer lengths). The SO muscle was operating on the ascending limb of its force-length relationship for both young and old models, with a shorter length in the older model. The shortening and lengthening actions of the plantarflexor contractile components were largely synchronous with the kinematics of the total musculotendon complex, with zero-lag cross-correlations of .73 and .89 for the GA and SO muscles, respectively, in the optimized young model (Figure 4-6).

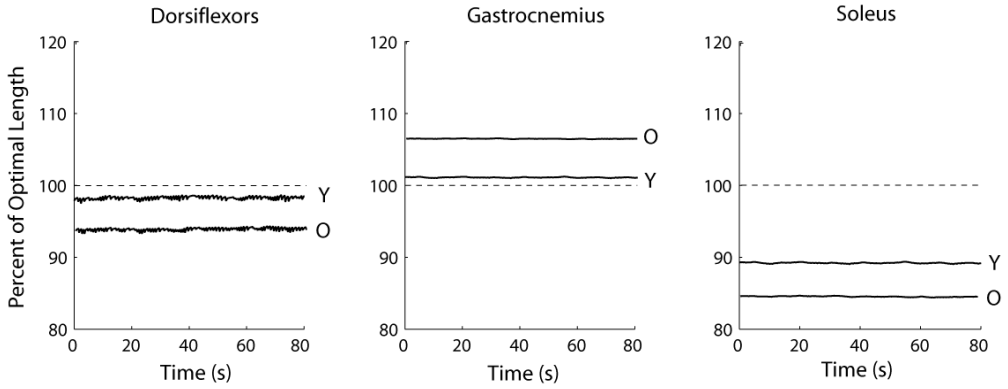

Figure 4-5. Lengths of the contractile components of the young (Y) and older (O) optimized quiet stance models, relative to the optimum contractile component length (dashed line).

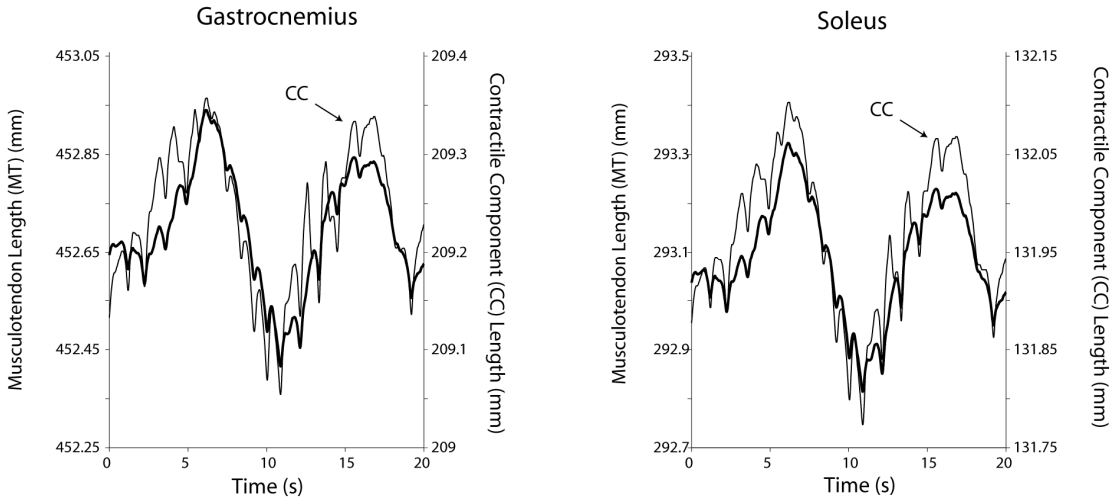

Figure 4-6. Total musculotendon (thick line) and contractile component (thin line) lengths for the gastrocnemius (left) and soleus (right) muscles for the optimized young model during 20 s of quiet stance.

4.3.2 Sensitivity Analysis

For the initial sensitivity analysis, the young quiet stance model was simulated nine times using the optimized values for the proportional and derivative controller gains. In each simulation, one of the nine plantarflexor mechanical properties was changed to the value of the older subjects. The model quickly fell forward after only a few seconds when the maximal isometric force (P_0), optimal fiber length (L_0), and slack length (L_S) were changed to the older values. Conversely, the model was able to stand for the entire 180 s simulation time when the other six mechanical properties were changed (Figure 4-7). When an additional simulation was performed with *all* of the young mechanical properties changed to the older values simultaneously, the model fell forward.

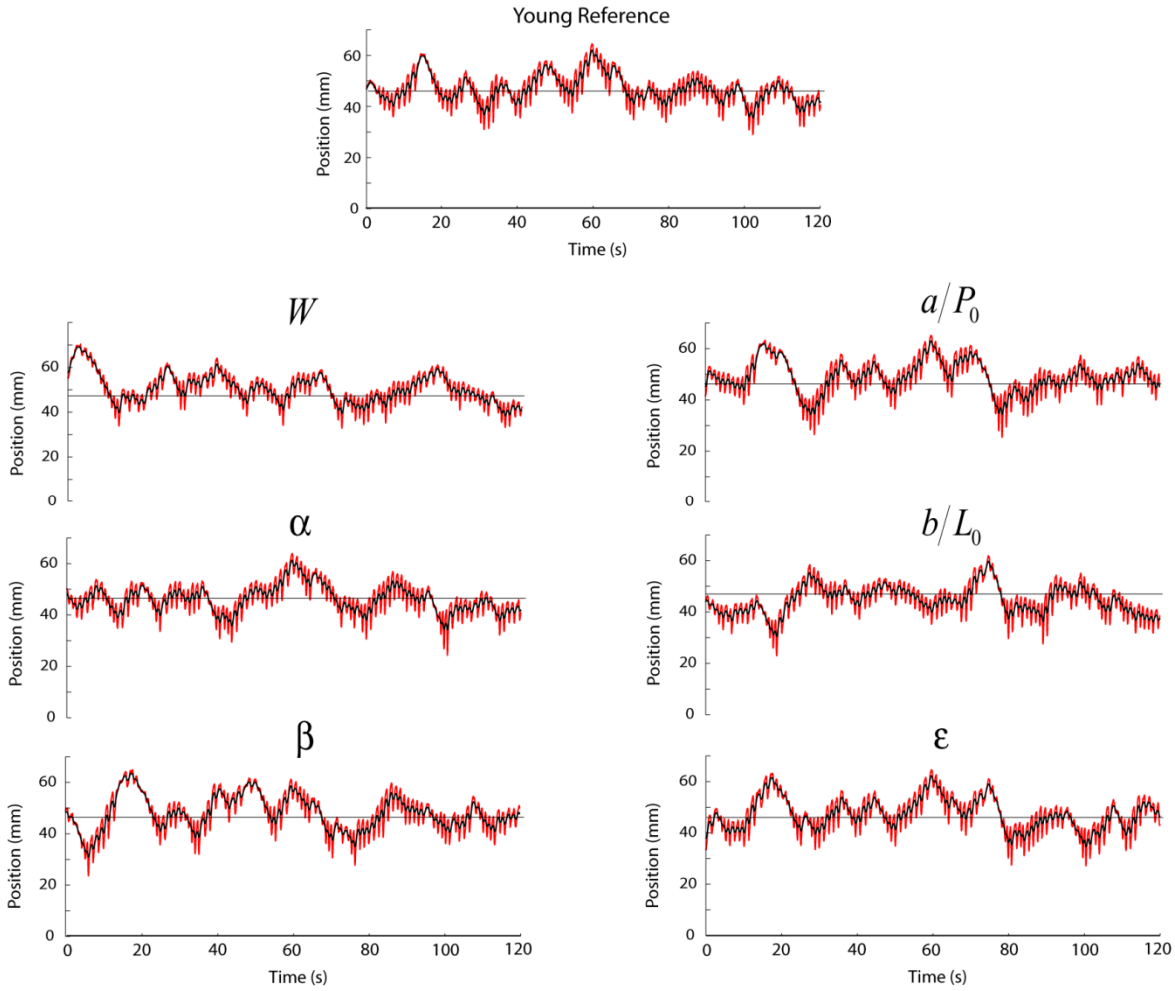

Figure 4-7. Results of the optimized young quiet stance model (top), and after each of six of the mechanical properties were independently changed to the mean value of the older subjects. The center of pressure (red) is shown oscillating around the center of mass. The models were simulated for 180 s, the first 60 s of data are not shown. For three of the mechanical properties, the model was unable to maintain balance for 180 s. See text for an explanation of nomenclature.

For the second sensitivity analysis each of the nine plantarflexor mechanical properties was systematically changed by ±15%, and the model was re-optimized with the altered properties. Because some of the older mechanical properties were outside of the ±15% range, additional optimizations were performed with each mechanical property shifted by the average difference between the mean plantarflexor young and old property

values (Table 4-2). Six of the nine mechanical properties fell outside the ±15% range, including: $P_0, L_0, L_S, \alpha, \beta$, and b/L_0.

Table 4-2. Differences between average mechanical properties for young and older subjects. (Data are from Chapter 2).

Mus.	Group	P_0 (N)	L_0 (cm)	W (%L_0)	α	β	L_S (cm)	a/P_0	b/L_0 (s^{-1})	ε
GA	Young Males	1423	20.7	58.6	630	19.2	24.2	0.38	.854	1.42
	Old Males	718	23.0	54.3	1575	.395	20.6	.395	.594	1.27
	Difference	-705	2.3	-4.3	945	-8.9	-3.6	0.015	-0.260	-0.15
	Ratio (Change)	-0.50	0.11	-0.07	1.50	-0.46	-0.15	0.04	-0.30	-0.11
SO	Young Males	1616	14.8	53.2	404	13.3	16.0	0.267	0.532	1.31
	Old Males	1053	21.5	52.5	1800	8.7	11.0	0.237	0.270	1.28
	Difference	-563	6.7	-0.7	1396	-4.6	-5.0	-0.03	-0.262	-0.03
	Ratio (Change)	-0.35	0.45	-0.01	3.46	-0.35	-0.31	-0.11	-0.49	-0.02
Mean GA&SO	Ratio (Change)	-0.42*	0.30*	0.04	2.48*	-0.40*	-0.20*	-0.04	-0.40*	-0.06

*Average older plantarflexor mechanical properties more than ±15% different than young.

After re-optimization, the model was able to maintain quiet stance successfully for all modification levels of the mechanical properties, with two exceptions. The model fell forward after a few seconds when the slack length of the series elastic component was increased by 15% from the young optimal value. This was because the change in slack length caused the length of the SO contractile component to be outside of its force-length relation, and therefore the SO was unable to contribute to postural stabilization (Figure 4-8). The model also fell forward when the optimal length of the contractile component was increased to the value of the older subjects (+30%); however in this case the integration process was very unstable as the SO muscle was completely outside its force-length relation, and the GA muscle remained on the very edge of its force-length relation, causing numerical instabilities.

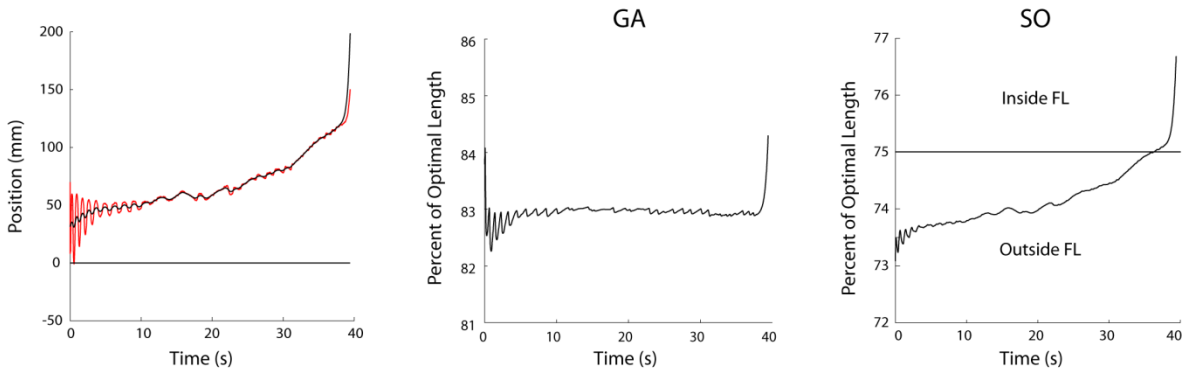

Figure 4-8. Left Panel: Center of mass (black) and center of pressure kinematics (red line oscillating around black) when the slack length was increased by 15% from the reference young value, where the model fell after about 40 s. Right Panels: Corresponding length of the GA and SO contractile components. The GA length remained within the force-length (FL) relation, while the SO began outside of the force-length (FL) relation, but moved inside right before falling forward.

In the majority of the simulations, the model oscillated around a position that was close to the equilibrium position of 47 mm in front of the ankle joint center. In a few simulations, the model either drifted forward and maintained quiet stance at a much more forward position without falling over (L_0 at -5% and +10%, a/P_0 at -15%, and ε at +10%) or exhibited a pattern that was very unstable (L_0 at +15%) (Figure 4-9).Because this behavior was very different from the rest of the simulations, variables computed for these trials were not included in the presentation of the results of the sensitivity analysis.

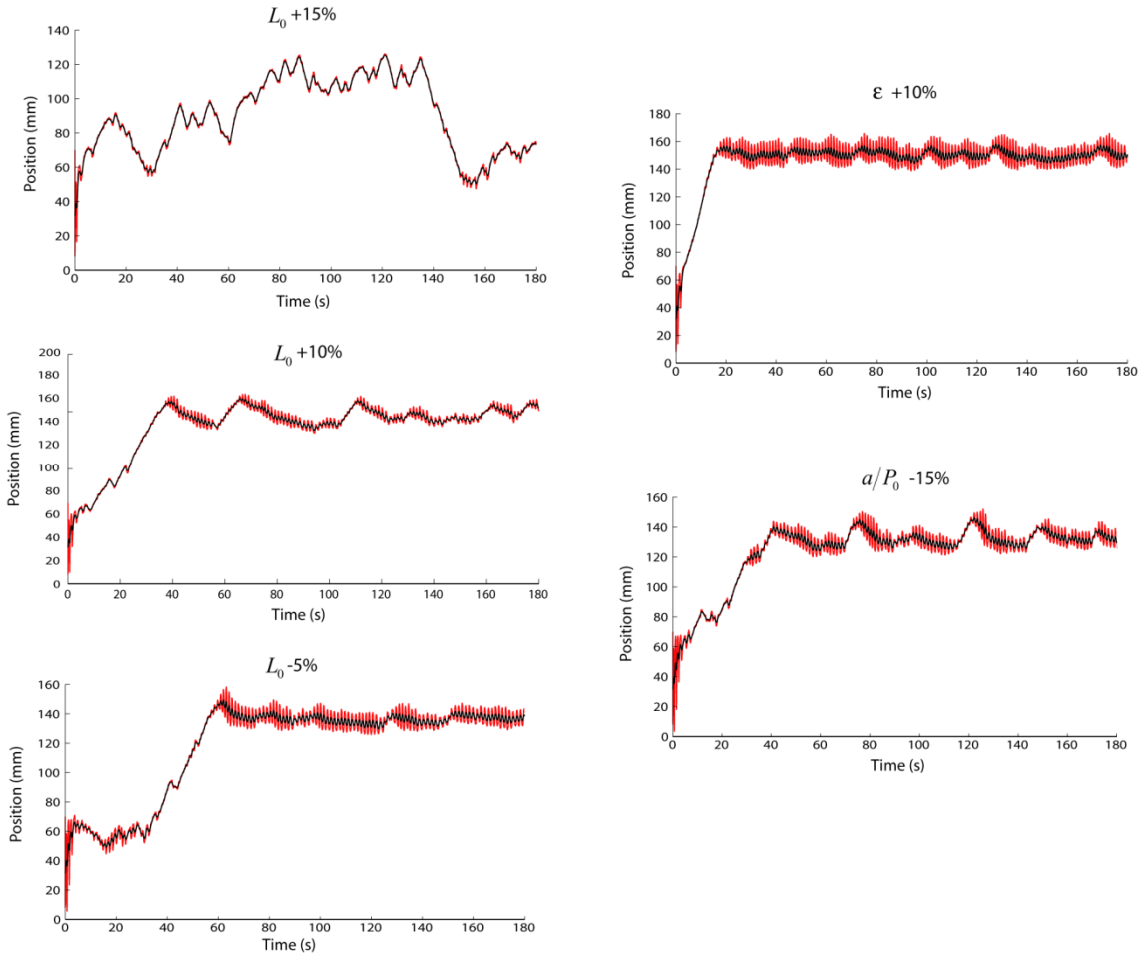

Figure 4-9. Center of mass (black) and center of pressure (red line oscillating around black) kinematics for the simulations in which the model had qualitatively different behavior compared to the rest of the simulations. The percentages represent the amount each muscle mechanical property was changed from the young reference values, while all other model parameters remained constant.

As the model was re-optimized with each parameter change, new proportional and derivative controller gains were found. The changes in the plantarflexor proportional gain had very well defined trends for changes in the maximal isometric force capability (P_0), the optimal contractile component length (L_0), and the slack length (L_S) (Figure 4-10 A). As P_0 increased, the gain of the plantarflexor proportional controller decreased

linearly. Changes in L_0 and L_S from the optimal young model values produced nonlinear increases in the controller gain. In contrast, there were no well-defined patterns of change in the dorsi- and plantarflexor derivative controllers (Figure 4-10B).

When the model parameters were changed to the values for the older subjects, the resulting changes in the controller gains were consistent with patterns established from the standardized increments of ±5%, ±10%, and ±15%. The results of these optimizations are also displayed in Figure 4-10 (squares, dashed lines). The gain values for these extreme changes were all close to the ±15% range, except for two cases (not shown in Figure 4-10). The plantarflexor derivative controller gain was set very low when the stiffness coefficient α was increased by 248% (meaning a stiffer series elastic component). When the maximal isometric strength of the plantarflexors was decreased by 42%, there was a corresponding increase in the plantarflexor proportional control gain, which was higher than would be predicted based on a linear extrapolation of the ±15% range data (Figure 4-11).

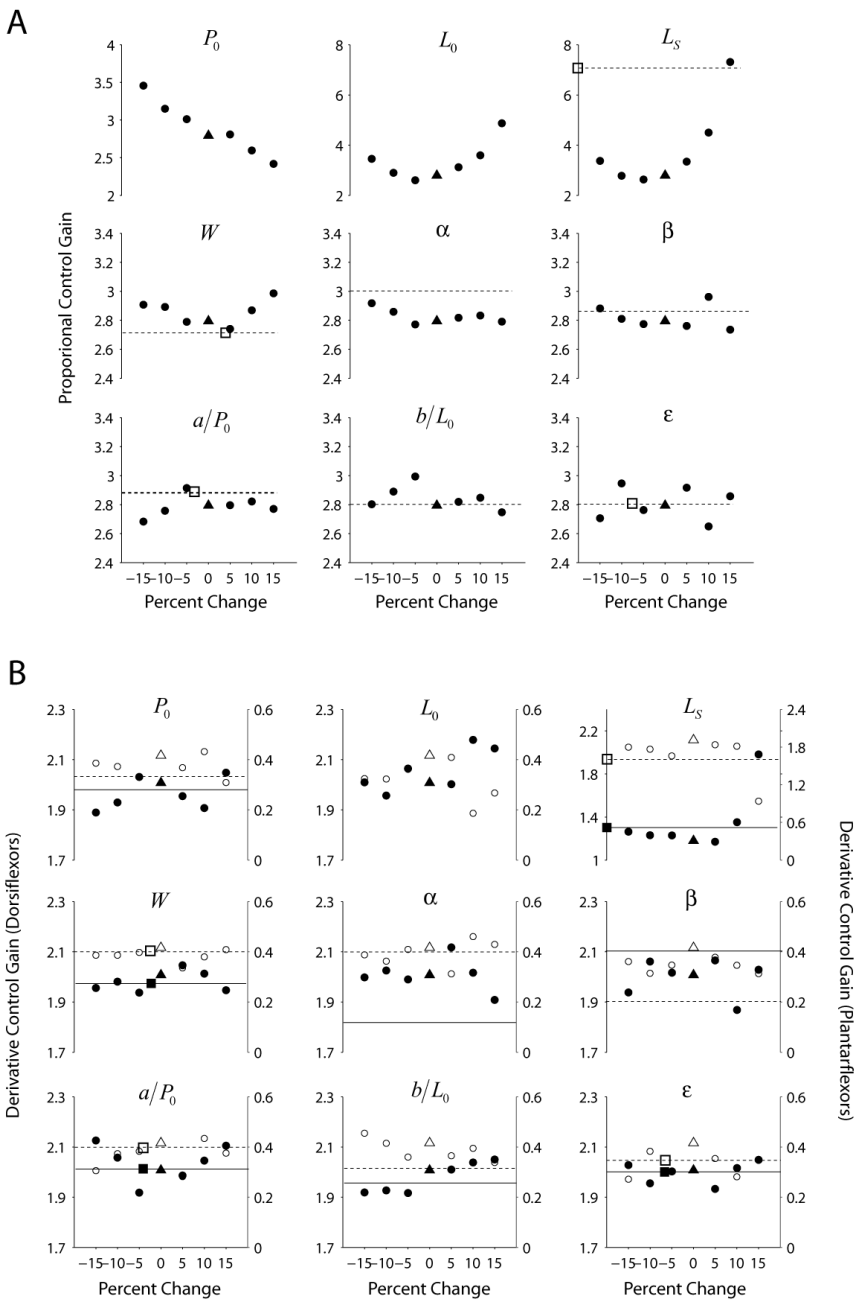

Figure 4-10. Results of the sensitivity analysis for each of the muscle mechanical properties. A: Effects on the gains of the plantarflexor proportional controller). B: Effects on the gains of the derivative controllers for the dorsi- (open data points) and plantarflexor (closed data points) muscle models. The results for the optimized model using the original mechanical property values are shown as triangles. Proportional and derivative controller gains for the older parameter values are identified by square data points and horizontal lines. Note that some of the changes for the older parameters were very large; these values are indicated by horizontal lines, but do not have the data points identified.

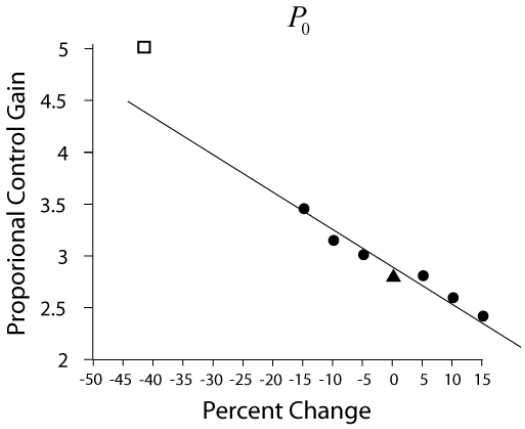

Figure 4-11. Result of decreasing the strength of the plantarflexors by 42% (open square).

Changing the mechanical properties had relatively small effects on the mean and standard deviation of the model's CoM position (Figure 4-12 and Figure 4-13, respectively). At most, changes in the mechanical properties resulted in a shift of about ±10 mm in the mean CoM position, excluding the few notable exceptions mentioned earlier. The optimal contractile component length (L_0), had a relatively strong positive correlation with the mean and standard deviation of the CoM position; however, in half of these simulations the model maintained balance in a much forward-shifted position (and were therefore not included in the correlation).

The slack length (L_S) had relatively large and systematic effects on CoM speed (Figure 4-14), with the mean CoM speed decreasing linearly as slack length increased. Increasing maximal isometric force (P_0) caused an increase in mean CoM speed. The optimal contractile component length (L_0) had a strong negative relationship with both mean CoM speed and median CoM frequency (Figure 4-15), but again there were relatively few data points due to the excluded far-forward simulations.

In almost all cases where the mechanical properties were changed to the older values, even when the changes were relatively large, the resulting performance of the model was similar to that observed when the properties were manipulated within the standardized ±15% range (Figure 4-12 to Figure 4-15).

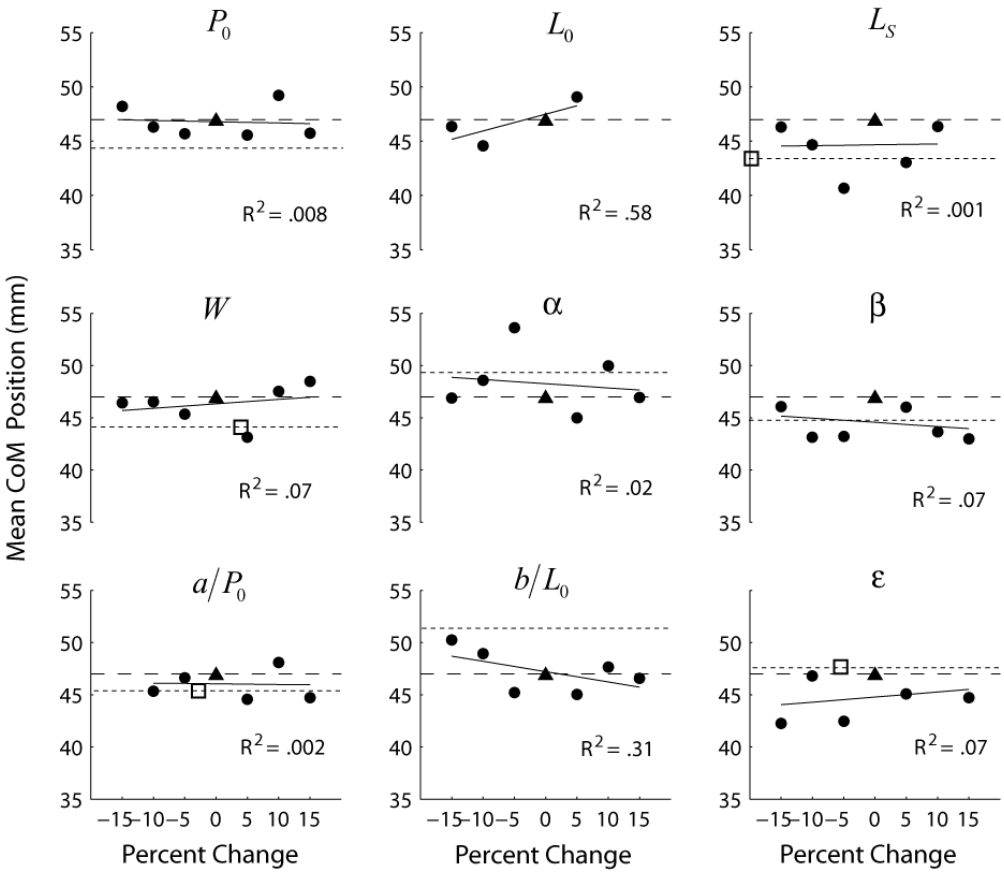

Figure 4-12. Mean center of mass (CoM) position with changes in the mechanical properties. The horizontal line with wide dashes represents the postural set point. The results from changing the properties to the older values are indicated by horizontal lines with small dashes, and where possible, are indicated by hollow squares. Note that some of the changes for the older parameters were very large; these values are indicated by horizontal lines, but do not have the data points identified.

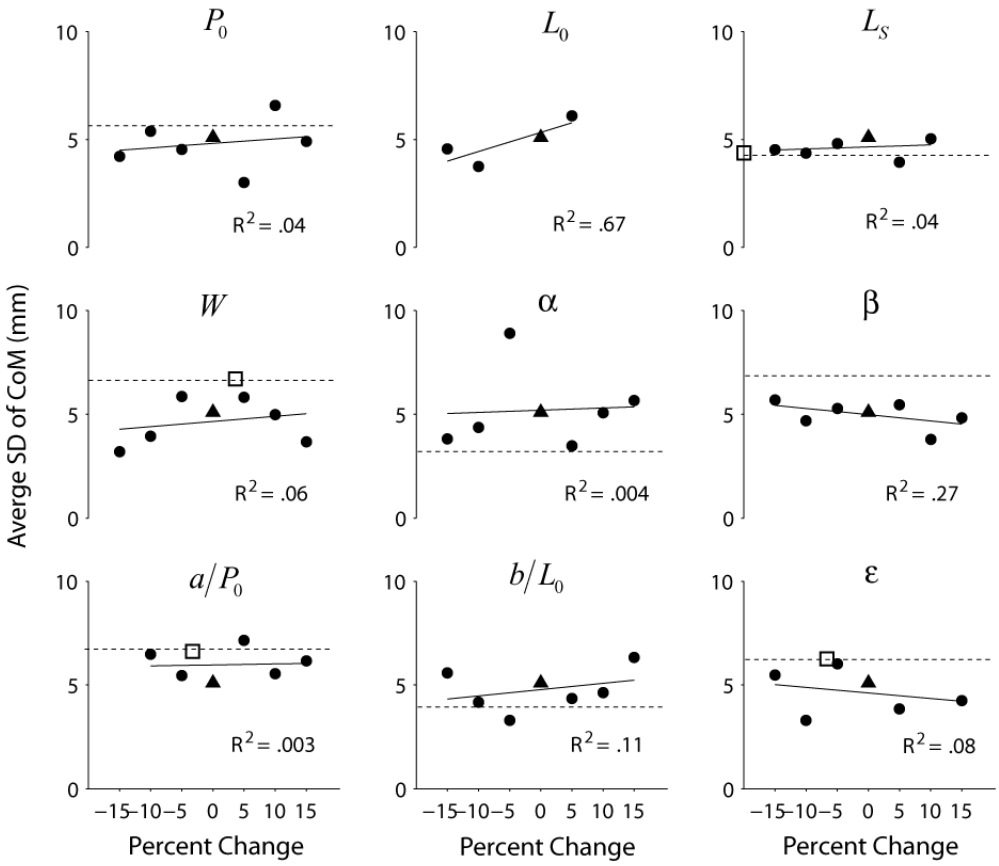

Figure 4-13. Average standard deviation of the center of mass (CoM) position with changes in the mechanical properties. The results from changing the properties to the older values are indicated by dashed horizontal lines, and where possible, are indicated by hollow squares. Note that some of the changes for the older parameters were very large; these values are indicated by horizontal lines, but do not have the data points identified.

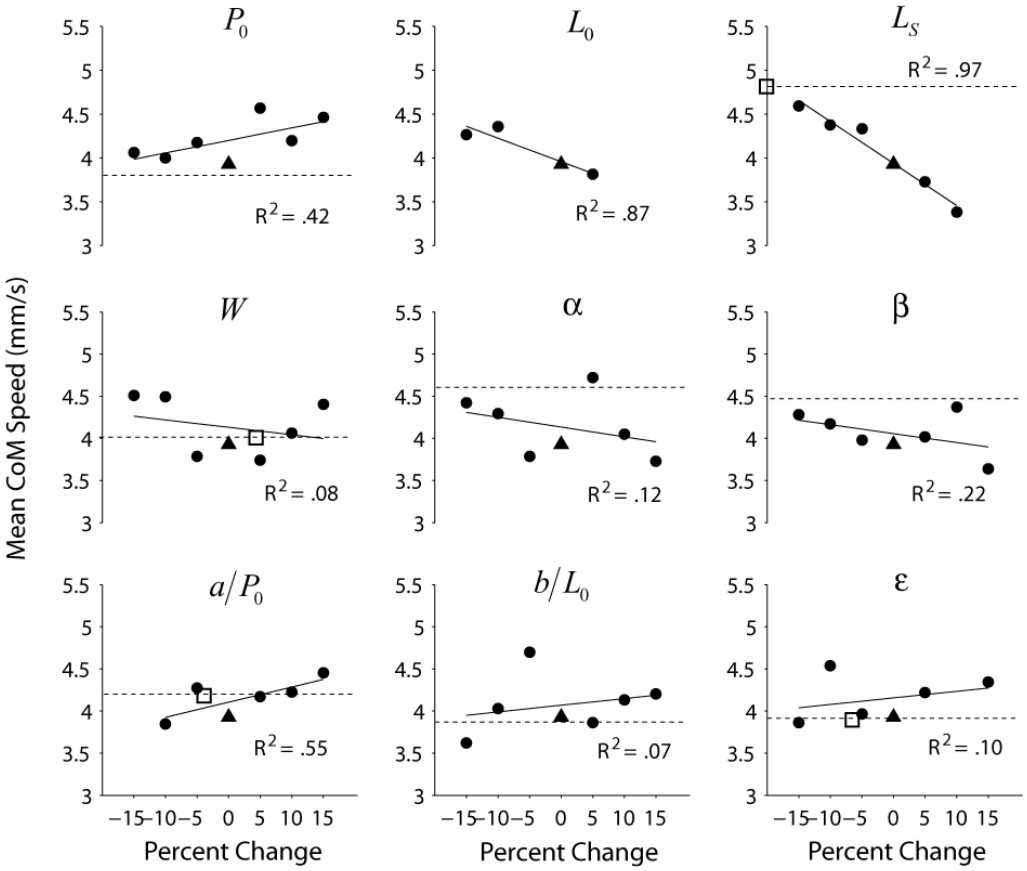

Figure 4-14. Mean center of mass (CoM) speed with changes in the mechanical properties. The results from changing the properties to the older values are indicated by dashed horizontal lines, and where possible, are indicated by hollow squares. Note that some of the changes for the older parameters were very large; these values are indicated by horizontal lines, but do not have the data points identified.

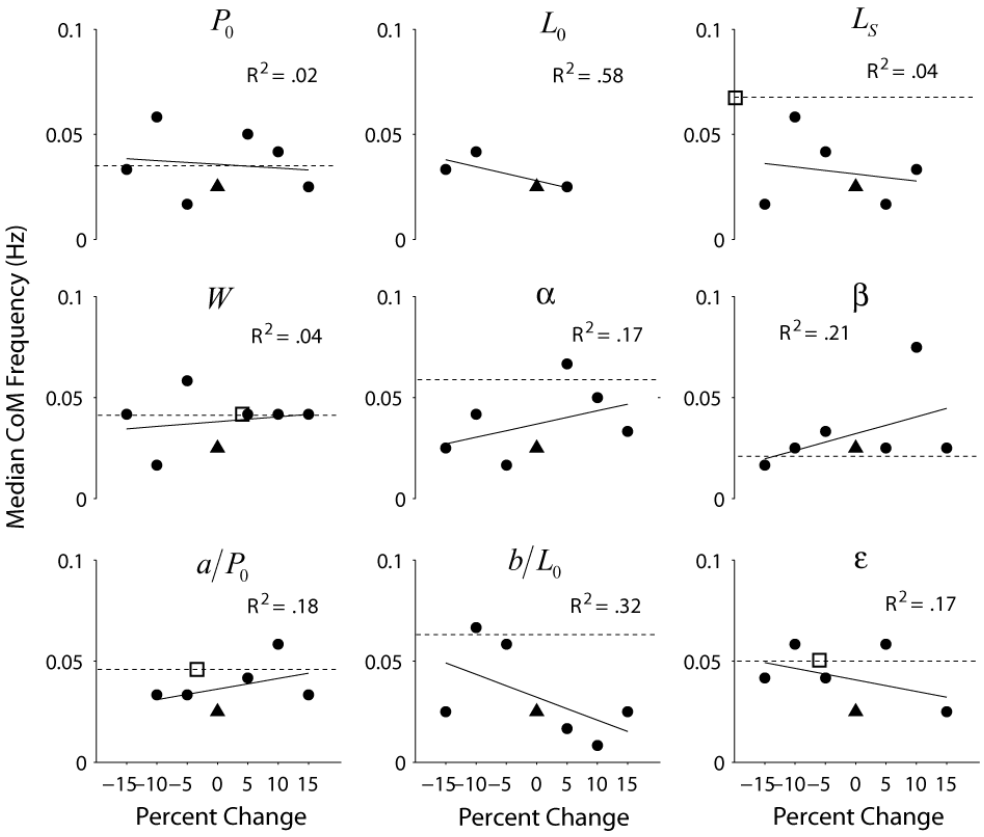

Figure 4-15. Median center of mass (CoM) frequency with changes in the mechanical properties. The results from changing the properties to the older values are indicated by dashed horizontal lines, and where possible, are indicated by hollow squares. Note that some of the changes for the older parameters were very large; these values are indicated by horizontal lines, but do not have the data points identified.

4.4 Discussion

In this chapter we developed a feedback-driven postural control model of quiet stance that included estimates of dorsi- and plantarflexor mechanical properties measured from the young and older adults in Chapter 2. The model was able to balance using either the young or older mechanical properties, and predicted age-related changes in muscle activity consistent with experimental studies. A sensitivity analysis demonstrated that the maximal isometric force, the optimal contractile component length, and the slack length of the series elastic component had the most influence on the behavior of the model in quiet stance.

4.4.1 Comparison of Optimized Young and Old Model Behavior

In general, the model described the basic characteristics of quiet stance postural control, as described by the random walk theory of Collins and DeLuca (1993). This theory suggests that over short-time intervals during quiet standing, the postural system tends to drift away from an equilibrium point (persistence). In contrast, over longer time intervals the system returns to the equilibrium point (anti-persistence). A major factor contributing to the persistent model behavior was the disturbance torque, generated by low-pass filtering white noise, which tended to “push” the model away from the equilibrium point. Although both age-related models exhibited similar quiet stance behaviors, they did so with unique levels of muscle model excitations and contractile forces, which caused differences in the postural kinematics.

When the optimized model responses were compared with the age-appropriate experimental quiet stance data, the “older” model was a better match than the “young”

model. This was because the optimization process was unable to reduce the amplitude of the corrective actions of the young and older models beyond a specific level (a floor effect). Therefore the end result was closer to the older subject data that had larger CoM and CoP fluctuations, since the young model couldn't reduce its corrective actions enough to match the younger subject data with smaller CoM and CoP movements. One reason for this may be due to the relatively simple skeletal model, which assumed inverted pendulum-like dynamics. The inertial properties of all body segments (except the feet) were lumped together into a single inertial mass (the "body" segment), which could only be controlled by a single ankle torque. This could have caused the model to need larger control inputs, which were needed to accelerate the large inertial mass. On the other hand, the minute motions occurring in the numerous linked body segments in humans may serve to dampen the various intrinsic postural disturbances (e.g. the random noise torque introduced at the ankle joint in the model). Thus, smaller control inputs may be needed in humans, compared with the simplified model.

In the postural model, the control signals represent the nervous system excitations sent to the dorsi- and plantarflexor muscles. The synchronized control signals for both muscle groups were larger in the older model, indicating more antagonistic co-activation than in the younger model. This agrees with the experimental results of Laughton et al. (2003) whose elderly non-fallers demonstrated significantly greater muscle activation and co-activation during quiet stance compared to younger subjects. In the model, one explanation is that the older muscle models were weaker, so muscle excitations needed to be higher because the masses and inertial properties of the two age-appropriate models

were the same. Therefore, the muscles of the older model were operating at a greater percentage of their maximum capacity (although still well below the maximum).

An interesting observation is that for both the young and older optimized postural models, the GA and SO muscle model forces were similar (SO-GA Avg. Force Difference: Y = 31 Nm; O = 8 Nm), despite differences in the maximal isometric strength of the muscles (P_0: Y = 192 Nm; Old = 335 Nm). The reason for this is that although both plantarflexor muscles received the same control inputs, the GA muscle was closer to its optimal length than the SO muscle (Figure 4-5). This served to offset the force capability discrepancies, such that the weaker muscle (GA) was able to produce a greater proportion of its "rated" maximal force output.

4.4.2 Model Sensitivity to Changes in Muscle Mechanical Properties

Previous studies on postural control have investigated the ability of different types of neural controllers to regulate posture (Maurer and Peterka 2005, Micheau et al. 2003, Peterka 2002, Peterka and Loughlin 2004), and others have focused on the effects of ankle joint stiffness (Loram and Lakie 2002a, Morasso and Sanguineti 2002, Winter et al. 1998, Winter et al. 2001). In the same vein, the present study investigated the sensitivity of a postural control model to changes in muscle mechanical properties. The mechanical properties of each muscle model were defined by a set of parameters describing nonlinear force-length $\left(L_0, L_S, W\right)$, force-velocity $\left(a/P_0, b/L_0, \varepsilon\right)$, and force-extension $\left(\alpha, \beta\right)$ relationships. A unique aspect of the postural model was that the values of these parameters were based on age-appropriate estimates from the experimental and modeling work done in Chapter 2.

One issue addressed in the sensitivity analysis was the consequence of replacing all of the plantarflexor mechanical properties in the young postural model with the properties of the older subjects, while maintaining the optimized control gains from the younger model. In other words, what if the plantarflexor muscles of a younger subject were instantly aged, but the basic "settings" of their nervous control were unchanged? The outcome was that the postural model was unable to stand and promptly fell forward. This provides evidence that the postural model is sensitive to the muscle mechanical properties, and that the gains of the neural controllers must be changed if the model is to remain standing with the altered muscle properties. This is in line with other studies showing that the maximum vertical jumping height of an optimized musculoskeletal model is reduced when the muscles are strengthened without adjusting (re-optimizing) the control signals (Bobbert and van Soest 1994).

Perhaps it is not surprising that the model fell when all of the muscle mechanical properties were simultaneously aged, as this could be seen as a drastic perturbation, and it was not clear whether there were particular muscle properties that were causing the instability. Thus, further simulations were performed where each muscle property was "aged" independently (i.e. one-at-a-time), and in most cases the model was able to remain standing with kinematics similar to the original unaltered model. However, the model quickly fell forward when the maximal isometric strength (P_0), optimal fiber length (L_0), or the slack length (L_S) were changed, suggesting that model performance is sensitive to these three parameters. However, in the face of an instant change in a muscle property of a young human, it is likely that the nervous control settings would adapt to the change to maintain adequate postural control. To account for this, a sensitivity

analysis was performed where each mechanical property was changed and the model was re-optimized to find the combination of neural controller gains for optimal quiet stance performance.

The results of the re-optimizations demonstrated that in general, the model was quite robust to changes in muscle mechanical properties if new controls could be used, and achieved stable balance in many cases. However, model behavior was sensitive to changes in P_0, L_0, and L_S, with large changes in the gains of the proportional controllers needed to maintain balance, and in some cases the model was unable to remain standing no matter what the control adjustments.

Changes in plantarflexor muscle maximal isometric strength (P_0) were inversely related to the optimal gains of their proportional controller (i.e. gain increased as P_0 decreased). The plantarflexor proportional gain almost doubled when the muscle strength was decreased by 42% from the young to the older value, undoubtedly because the weaker muscles required an increase in excitatory drive to compensate. Although the control gains changed in response to changes in P_0, the model was able to perform quiet stance well as long as the plantarflexor P_0 did not decrease too much. Even when P_0 was changed to the older value the model was able to remain standing – provided the control gains were allowed to change. This suggests that quiet stance performance is not sensitive to changes in P_0; however, there is a lower limit beyond which upright stance cannot be achieved (Winter et al. 1998).

Although changes in P_0 had an approximately linear effect on the plantarflexor proportional controller gains, the optimal length (L_0) and the slack length (L_S) had nonlinear effects. The proportional controller gains were close to their minimum values

using the original set of young muscle mechanical properties, but the control gains increased as L_0 and L_S were either increased or decreased. This suggests that the combination of L_0 and L_S in the younger subjects was close to optimal in terms of minimizing the level of excitatory drive to the muscles.

The performance of the model was particularly sensitive to changes in the optimal contractile component length L_0, producing quite different behaviors depending on the specific value. In some cases, the model initially drifted forward towards the toes, and then remained balanced in this forward position. This behavior also occurred for specific values of the force-velocity shape coefficient a/P_0 and the eccentric plateau ε. Curiously, this behavior did not only occur at the extreme parameter values. For instance, the forward shift occurred when the eccentric plateau was increased by 10%, but did not occur at +15%. It is plausible that certain combinations of controller gain levels and mechanical properties caused "bifurcations" in model behavior, due to the control delays, model nonlinearities, and uncertainty from the random disturbance torque. For example, on a given forward sway, the noise could randomly "bump" the model forward in a state where the neural controllers can't immediately stop its motion. The plantarflexor proportional controller alone might be insufficient to bring the model back to the target equilibrium position, and therefore the model continues to drift forward due to the destabilizing gravitational torque. As the model drifts forward the SO muscle will lengthen, moving its contractile component *closer* to optimal length, allowing it to produce more force for the same control input. Eventually, the increase in force potential will be enough to counteract the gravitational torque, and therefore the model consolidates its motion around this forward equilibrium point to take advantage of this

stronger, near optimal length position. Such behavior highlights the importance of the force-length properties of muscle in the control of quiet stance, and aligns well with the spring-like behavior of muscle proposed by equilibrium point theory (Bizzi et al. 1992).

Changes in series elastic component slack length (L_S) prompted large changes in the gain of the plantarflexor proportional controller, and altered model balance performance, especially the mean CoP speed. As the slack length decreased, CoP speed also decreased; when the slack length was increased by 15%, the model fell. The slack length dictates the length at which the series elastic component becomes "taut" when the contractile component produces force. Because the contractile component force-length characteristics (L_0 and W) were *not* changed in concert with the changes in L_S in the sensitivity analysis, the contractile component would have operated on a different portion of its force-length relation (Figure 4-16, left panel). For the optimal young model, both the GA and SO were near their optimal lengths (L_0) during quiet stance. Thus, increasing (decreasing) the slack length would shift the contractile component operating ranges to shorter (longer) lengths and thus weaker positions, based on the parabolic force length relation (Figure 4-16, right panel).

This conjecture is supported by the (inverted) parabolic shape seen in the plantarflexor proportional controller gain with changes in the slack length (Figure 4-10). At long slack lengths, the contractile component is shifted to the ascending limb of the force-length curve, which is a stable configuration since a forward sway would move the contractile component towards a more optimal length (Figure 4-16, right panel). Note that when the slack length was increased past 15% the model fell since the contractile component length shifted completely off the force-length curve (Figure 4-8). On the other

hand, short slack lengths would shift the contractile component to the descending limb of the force-length curve, which is a more unstable situation as a forward sway would move the contractile component *further away* from the optimal length. As pointed out by Rassier et al. (1999), the negative slope of the descending limb is representative of a softening material and is therefore unstable. Therefore, we conclude that the shorter slack lengths shifted the contractile component to an unstable force-length region, causing greater sway magnitudes and therefore a larger mean CoP speed. Of note, is that Rassier et al. also point out that in humans there are two reasons why this instability may not be observed experimentally: 1) the phenomenon known as "force enhancement" following a muscle stretch (Edman et al. 1978) has the potential stabilize muscles that operate on the descending limb of the force-length relationship, and 2) in-homogeneity of sarcomere lengths (Edman and Reggiani 1984), which causes the force transmitted across sarcomeres to be close to the force capabilities of the shorter sarcomeres which remain on the ascending limb of the force-length relation at the expense of other lengthening sarcomeres on the descending limb. The quiet stance model utilized in the present study did not include force enhancement or non-uniform sarcomere lengths, so these stabilizing mechanisms did not influence the model's behavior.

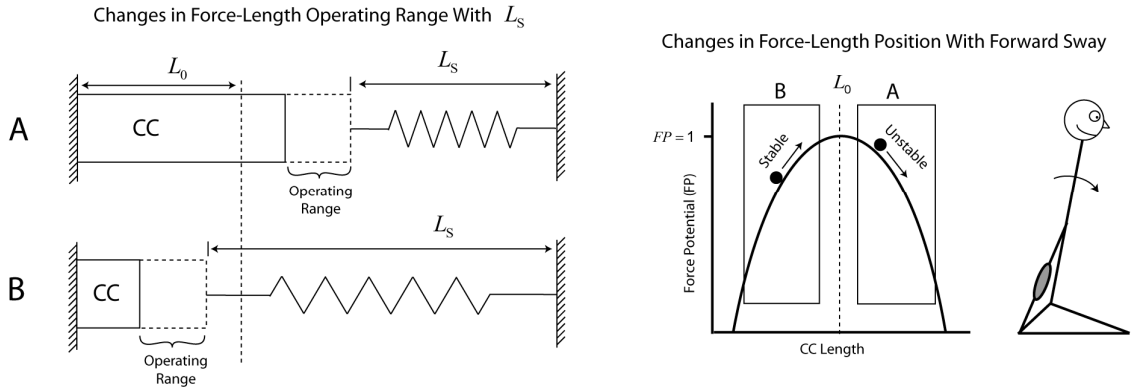

Figure 4-16. Left panel: schematic showing the effect of changing the series elastic component slack length (L_S) on the force-length operating range of the contractile component (CC). The optimal CC length (L_0) is indicated by the vertical dashed line. If the CC is near L_0, increasing L_S (B) will shift the CC to the ascending region of the force-length curve, while decreasing L_S (A) will shift the CC to the descending region of the force-length curve. Right panel: when the CC lengthens during forward sway, case B will be "stable" as the CC will move to a more optimal length, while case A is "unstable" as the CC will move to a less optimal length and thus the force-potential will reduce.

Previous modeling studies on jumping (van Soest and Bobbert 1993) and locomotion (Gerritsen et al. 1998) have shown that muscle mechanical properties contribute to the stability of the musculoskeletal system with respect to the influences of static and dynamic movement perturbations. These studies employed purely open-loop control, and focused on stability related to relatively dynamic multi-joint movements, with the goal of the model being to either maximize vertical jumping height (van Soest and Bobbert 1993) or to match experimental locomotion data (Gerritsen et al. 1998). The present study used feed-back control to stabilize an inverted pendulum model, which had the goal of maintaining quiet stance with a minimal amount of control (i.e. muscle force). The force-length relationship of the SO muscle had a great influence on behavior of the quiet stance model, as the optimal contractile component length largely determined the

equilibrium point of the model, and the series elastic slack length was an important factor in the determining the amplitude of the control inputs required for stabilization. Therefore, despite the differences in model design and control, the results of this study agree with the previous studies (Gerritsen et al. 1998, van Soest et al. 1993), and provide support for the importance of muscle mechanical properties for the stabilization of human movement.

4.4.3 Different Control for Young and Older Adults?

An interesting result was that when the model of quiet stance was optimized using the young and older sets of muscle mechanical properties, the model behavior more closely matched older subject experimental data. This could suggest that the postural control of the older subjects was more like the simple feedback control used with our inverted pendulum model. The younger subjects may rely more on predictive (feed-forward) control mechanisms that were not included in the postural model, leading to poorer agreement between model and subject behavior. Morasso and Sanguineti (2002) point out that reliable sensory information is necessary for anticipatory or feed-forward control, and that age-related sensory deficits would reduce its efficacy. They suggest that decreased use of predictive control would result in an increase in ankle stiffness through an “energetically expensive co-activation of the ankle muscles”. Our modeling results provide support for this notion, as do the results from Chapters 2 and 3 that demonstrated increased stiffness of the series elastic components of the older subjects, which was an important predictor of balance ability. However, we did not perform measurements for possible sensory deficits or explore possible uses of different control (feedback/forward)

in our experimental subjects, so we are only able to speculate on these age-related adaptations in feed-back/forward control.

Another possible reason for the difference in how well the young and old models matched their experimental counterparts was the use of the same absolute perturbation torque for both models. This caused the perturbation to be relatively larger for the older model, which had reduced muscular strength parameters (i.e. P_0 values). While there is evidence for increased noise and uncertainty with aging (Poliakov et al. 1996), which would support the relatively larger disturbance torque in the older model, the exact magnitude of such age-related changes in noise levels for postural control is unknown.

4.4.4 Novel Aspects of the Postural Model

A novel aspect of this study was the inclusion of individual muscle models that incorporated age-appropriate estimates of the muscle mechanical properties, driven by a proportional-derivative feedback neural controller. Numerous studies have used postural models with feedback control, however most have used hypothetical torque generators to control the model (Barin 1989, Johansson et al. 1988, Masani et al. 2003, Maurer and Peterka 2005, Micheau et al. 2003). Studies that have used musculotendon actuators have all used parameters from the literature to define the behavior of their muscle models (Menegaldo et al. 2003, Ramos and Stark 1990, Verdaasdonk et al. 2004). Our results indicate the behavior of postural control models is influenced by the mechanical properties of the individual muscles.

Another novel aspect was the use of time-to-contact information in the neural controller. Previous studies have used feedback derivative controllers based solely on the

angular velocity of a body segment (Barin 1989, Johansson et al. 1988, Masani et al. 2003, Maurer and Peterka 2005, Micheau et al. 2003). From an engineering perspective, the use of velocity as input to proportional-derivative (and proportional-integral-derivative) controllers is prudent to help stabilize unstable mechanical systems. However, our approach is based on studies that have suggested humans may use time-to-contact information for controlling posture (Riccio 1993, Slobounov et al. 1997). Time-to-contact information has been shown to differentiate between balance abilities in young vs. elderly and diseased populations (Forth et al. 2007, Hertel and Olmsted-Kramer 2007, Slobounov et al. 1998, van Wegen et al. 2002), and also to predict stepping behavior in response to perturbations (Hasson et al. 2008). The time-to-contact estimate includes information about the distance, velocity and acceleration of the CoM relative to the base of support boundary, such that time-to-contact decreases nonlinearly as the CoM approaches the boundary. The present results demonstrate that time-to-contact control is able to produce realistic simulations of human postural control. Future modeling work should examine time-to-contract control under different simulated postural conditions, and make comparisons between the time-to-contact control and other putative control schemes.

4.4.5 Conclusions

A feedback-driven postural control model was developed that incorporated realistic models of young and older dorsi- and plantarflexor muscles. The model reproduced the basic characteristics of human postural control in quiet stance, and was most sensitive to changes in the maximal muscle strength, optimal contractile component length, and series elastic slack length. The results highlight the importance of the muscle

model parameter accuracy in models of postural control, given the evidence for age-related changes in muscle characteristics established in Chapter 2 and in the literature.

CHAPTER 5

GENERAL DISCUSSION

The main goal of this dissertation was to understand how age-related changes in the mechanical properties of muscle influence postural control. With aging, we found lower maximal isometric strength and increased series elastic stiffness in the male subjects, and decreased velocity-dependent force capabilities in both gender groups. These properties were predictive of age-related differences in the performance of subjects on the postural tests. However, the maximal isometric force was less influential than expected, and the length-dependent muscular properties also contributed to prediction of balance performance. When the estimated young and older mechanical properties were used in a musculoskeletal model of quiet stance, the balancing ability of the model was most sensitive to the contractile component optimal length and series elastic slack length of the muscle models.

To put these findings in perspective, the main hypotheses of this dissertation can be restated in the form of several general questions: How can we estimate subject-specific muscle mechanical properties? Do muscle mechanical properties change as we age? How important is it that researchers use subject-specific muscle properties when simulating human movement? How do age-related changes in muscle properties influence postural control? What can a musculoskeletal model tell us about the influence of muscle properties on postural control? Of what clinical use are the results? This dissertation contributes to each of the areas of musculoskeletal modeling, aging, and postural control, and provides answers to these six questions.

Estimating subject-specific muscle mechanical properties. The first study developed methods for estimating subject-specific muscle mechanical properties that incorporated imaging techniques, dynamometer experiments, musculoskeletal modeling, and numerical optimization. Although many of these ideas are not new, they are often implemented in separate experiments to determine specific mechanical properties of interest. This study combined all of these techniques, and by doing so was able to estimate full sets of subject-specific mechanical properties describing the force-length, force-velocity, and force-extension properties of human muscle. Moreover, these properties were determined for an agonist/antagonist muscle pair (the dorsi- and plantarflexors) instead of just a single muscle group. The computational methods that were developed provided realistic estimates of muscle mechanical properties for both young and older adults.

Age-related changes in muscle mechanical properties. After using the developed methodology to estimate the mechanical properties of the dorsi- and plantarflexor muscles, significant differences were found between the young and older subjects. The older male subjects had lower maximal isometric strength and increased stiffness; both gender groups had decreased velocity-dependent force capabilities. Although similar findings have been shown before for older joint properties, a unique contribution here is that these changes were shown in *individual* muscles. This has important implications for musculoskeletal modeling, and suggests that not only should the strength of muscle models be altered when modeling the behavior of older adults, but other properties need to be changed as well.

Importance of subject-specific mechanical property measurements. The degree to which subject-specific estimates are needed when modeling human movement depends on the nature of the research question. For example, when investigating tasks that are predominately static, such as the quiet stance task used in this dissertation, it may not be necessary to have extremely accurate force-velocity properties, as it was shown that the quiet stance model was not sensitive to changes in these properties. However, other tasks such as locomotion have been shown to be sensitive to the force-velocity properties of muscle (Gerritsen et al. 1998). Subject-specific estimates may be especially important when trying to explain the behavior of individuals that vary from the normally used healthy young male subject group. In this dissertation a variety of muscular characteristics of older muscles were found to differ from younger muscles, including increased stiffness and decreased velocity-dependent force capabilities.

Influence of age-related changes in muscle properties on postural control. The second study of the dissertation was designed to assess the balance abilities of the young and older subjects, and to determine whether there were specific muscle mechanical properties that would be predictive of the differing balance abilities of the two age groups. Despite being healthy and relatively active, older adults displayed poorer postural control than the younger subjects. Age-related differences were found in both static and dynamic balance, and were found on even relatively unchallenging tasks such as quiet stance. Contrary to our initial expectations, the maximal isometric strength of the muscles had comparatively little predictive power. However, the contractile force-length and force-velocity characteristics, and the series elastic force-extension parameters were all able to explain a significant proportion of the age-related variance in the balance tests.

Some muscle properties that were not predictive of balance ability when examined individually did reveal significant predictive abilities when combined with other mechanical properties. Thus, it seems important to consider multiple mechanical properties together when trying to understand their influence on postural control.

Sensitivity of musculoskeletal models of postural control to muscle mechanical properties. The third study developed a feedback-driven inverted pendulum model of postural control that incorporated realistic representations of young and old dorsi- and plantarflexor muscles. Novel aspects of the model included the use of proportional-derivative controllers to drive subject-specific Hill two-component muscle models, and the use of time-to-contact information as input to the derivative controllers. The balancing ability of the model was most influenced by the optimal length of the contractile components and the slack length of the series elastic components within the muscle models. This study highlighted the importance of the force-length relation of muscle to the stabilization of upright posture.

Clinical significance. Musculoskeletal modeling is widely used for understanding human movement, and also as an invaluable tool for clinicians to assist in the treatment of musculoskeletal disorders. For example, a rectus femoris tendon transfer is used in patients with cerebral palsy to improve knee flexion during walking (Asakawa et al. 2002). Prior to such a surgery, a musculoskeletal model can be used to simulate the effects of the transfer on movements such as walking. In this case, it is imperative to use subject-specific muscle properties to minimize the errors in the model predictions, especially in these cases where the individual may be differ from the norm. The

methodology developed in Chapter 2 can be used to obtain subject-specific muscle property measurements, and will be useful in such pre-surgery simulations.

Although ankle joint strength is routinely measured in humans, this dissertation showed that the strength of individual dorsi- and plantarflexor muscles has relatively little power in predicting age-related changes in balance ability. This suggests that clinical tests of strength may be of little use in assessing the risk of postural instability in *healthy* older adults. This dissertation highlighted the importance of other muscle properties, including those related to series elastic stiffness and active force capabilities at different lengths and velocities. This is important information for clinicians, may provide clues to the origin of balance problems in the elderly, and may also lead to balance improvement in older adults. For example, strength training has been shown to increase the stiffness of muscles in older adults (Reeves et al. 2003a, Reeves et al. 2003b), which may provide benefits by changing the dynamics of the force response in the muscles that control posture. Although stiffness was an important predictor of age-related changes in balance ability in the static and dynamic balance experiments, the quiet stance model was not particularly sensitive to the muscle stiffness. However, stiffness may be more important under more dynamic conditions, such as a responding to a postural perturbation. Future work with the postural control model can address this issue and other questions.

5.1 Future Study

With regard to future work, there are two aspects of this dissertation that should prove particularly fruitful. The first is related to further improvement of the methods to estimate subject-specific muscle mechanical properties, and the other is related to

improving the physiological realism of the postural control model and evaluating the model's sensitivity on other more challenging postural tasks.

Improvements in subject-specific parameter estimation. A significant amount of time and effort was required for the determination of subject-specific mechanical properties, from both participants and researchers. The subjects were required to attend numerous experimental sessions with various physical and psychological demands. For the MRI experiments, subjects needed to travel to a hospital and lie motionless for a half-hour while images were taken. Individuals with metal in their body were unable to participate. In the ultrasound and dynamometer sessions, the subjects needed to perform numerous maximal effort muscle contractions. The dynamometer contractions were particularly taxing for the older subjects, requiring the dynamometer experiments to be spread out over multiple experimental sessions. Collectively, this produced a significant amount of data for post-processing. The ultrasound data produced many large video files that required "tracking", and the MRI data produced multiple images (up to 80 per muscle) that required manual processing by outlining the muscles in each image, requiring considerable analysis time.

Thus, one objective of future studies will be to reduce the amount of data and data processing needed to obtain accurate subject-specific mechanical property estimates. For example, fewer MRI slices may be needed to obtain muscle volumes. Alternatively, MRI may not be needed at all, as studies have shown that ultrasound can be used to estimate muscle volumes (Esformes et al. 2002). However, one advantage of using MRI is that non-contractile tissue (e.g. fat, tendon) can be identified and accounted for in the measurements of contractile tissue. This is currently not possible with ultrasound, and is

an important consideration when studying older adults. It may also be possible to reduce the number of trials performed in the dynamometer data collection sessions; however this depends on the nature of the research questions being investigated.

A more physiological basis for postural control models. Another area that is in need of further research is the improvement of physiological realism in postural control models. Currently, an engineering perspective dominates, such that postural control models are commonly controlled by fictitious torque generators (Johansson et al. 1988; Barin 1989; Masani et al. 2003; Micheau et al. 2003; Maurer and Peterka 2005). The amount of torque generated is frequently based on the angular deviation of the body from a vertical reference line passing through the ankle joint and the time rate of change of this deviation (i.e. proportional-derivative [PD] control). Although we do not know the precise way in which sensory information is integrated in the human nervous system and the way this information is represented as an internal model, it is likely that *strict* PD control is *not* used. In other words, the PD control may be combined with other control schemes, such as a forward internal model that predicts future behavior (Morasso et al. 1999). In the current study, we used "time-to-contact" as a control input to the postural model. Time-to-contact is a measure that includes information about the kinematic relation between the center-of-mass and the base of support boundary, and is based on experiments that have provided evidence that humans may use time-to-contact information to control posture (Riccio 1993, Slobounov et al. 1997). Future work should investigate this further, and should compare the two control schemes (traditional PD vs. time-to-contact), to examine how postural control models respond to different types of control.

An obvious shortcoming of torque-controlled postural models is that humans use muscles that have complex and nonlinear mechanical properties. These properties will drastically alter the relationship between the control signal and the resulting actively generated torque. As shown in this dissertation, small changes in some muscle mechanical properties will cause nonlinear changes in the gains of the control signals. Other studies have shown that muscle acts as a damping element, and therefore can reduce the sensitivity of models to perturbations (Gerritsen et al. 1998). More work is needed in developing musculoskeletal models of postural control that include accurate representations of muscle mechanical properties, to help our understanding of the role these properties play in controlling balance under different conditions.

Future applications of the postural control model. The postural control model developed in this dissertation holds much promise for future improvements and modifications. Most previous postural control models have been artificially pinned to the ground (Barin 1989, Johansson et al. 1988, Masani et al. 2003, Maurer and Peterka 2005, Micheau et al. 2003), which simplifies the numerical complexities of the model. This assumption limits the validity in investigations of many postural tasks. Even the simple act of leaning forward is associated with some degree of heel rise. The postural model used in the present study was not pinned directly to the ground, using a visco-elastic interface found in other models of locomotion and jumping (Anderson and Pandy 2001, 1999). This model formulation should prove useful for future work on postural control in various situations. For example, it will allow the study of how the mechanical properties of muscle influence the way in which a postural model responds to a perturbation.

5.2 Final Thoughts

Apart from the scientific contributions of this dissertation, it is useful to step back and take a more introspective viewpoint. If nothing else, this dissertation has reinforced a sense of wonderment at the complexities of human muscle. Muscles exhibit a wide spectrum of nonlinear behaviors that have taken researchers decades to fully appreciate – but are still not completely understood. Most fascinating of all is the extreme adaptability of muscle, which is constantly changing to best suit the demands placed upon it by the human body. The challenge for future research is to understand the nature of these adaptations, and how they influence the control of human movement.

APPENDIX A

ISOVELOCITY AND CO-ACTIVATION ADJUSTMENTS

Adjusting Isovelocity Data for Torque-Angle Effects

Adjustments were made to the measured experimental torque-angular velocity data to account for torque-angle effects and to ensure agreement between the torque-angle and torque-angular velocity data. First, the relationships between the joint angles and angular velocities coinciding with the peak isovelocity joint torques were assessed using linear regression (Figure A-1B). Each peak isovelocity torque data point was then adjusted by the following procedure (outlined in Figure A-1):

1) The angular velocity at which the peak torque occurred (in original data set; Figure A-1C, #1) was input into the joint angle-angular velocity regression, giving a predicted joint angle (Figure A-1B, #2). This predicted joint angle was then mapped onto the original fit of the torque-angle data, giving the predicted isometric torque at that angle.
3) Each isovelocity peak torque data point was divided by the predicted isometric joint torque, giving a scaled isovelocity peak torque (Figure A-1C, #3). A scaled isovelocity value of 1 would be equal to the maximum isometric joint torque at the predicted joint angle.
4) A Hill equation was fit to the scaled isovelocity peak torque data. However, due to subject variability and experimental error, when evaluated at zero angular velocity, the fitted Hill equation did not pass exactly through 1. Therefore, the scaled data points were shifted so that the fitted Hill equation was equal to 1 at zero velocity (Figure A-1C, #4).
5) The scaled isovelocity data were then multiplied by the predicted peak torque from the torque-angle data, converting the units back to Nm (Figure A-1C, #5).

The result of this procedure was to have "matching" torque-angle and torque-angular velocity relationships, so that the torque at zero angular velocity equals the peak torque form the torque-angle relation (curve #5 in Figure A-1A and 2C).

Adjustments for Co-Activation (Isometric & Isovelocity Data)

Next, the torque-angle and torque-angular velocity data were adjusted for the effects of antagonist co-activation. The relationships between agonist muscle torque and the percentage of antagonist muscle co-activation were based on the data of Simoneau et al. (2005), which showed similar linear relationships for young and older adults. From the data of Simoneau et al., we estimated the linear equations to be

$$y_{PF} = 0.270x_{DF} + 2 \quad \text{(A.1)}$$

$$y_{DF} = 0.177x_{PF} \quad \text{(A.2)}$$

where y is the percentage of antagonist co-activation as a function of the agonist torque level (x). To adjust the dorsiflexor torque-angle data, each measured torque data point (x_{DF}) was adjusted using the following procedure:

1) Determining the corresponding percentage of plantarflexor co-activation (y_{PF}),
2) Taking the maximum agonist plantarflexor torque at the same ankle angle ($\tau_{PF}^{Max@\theta}$)
3) Shifting the dorsiflexor torque-angle data point upwards by $y_{PF}/100 \cdot \tau_{PF}^{Max@\theta}$.

A similar procedure was then used to adjust the plantarflexor torque-angle data; however, the *adjusted* dorsiflexor torque-angle data were used for the antagonistic contribution. Each original dorsiflexor torque-angle data point was re-adjusted using the adjusted plantarflexor torque-angle data; this procedure continued iteratively until the results stabilized (which occurred after only a few iterations at the most). An example of the final co-activation adjusted isometric torque angle data is shown in Figure A-1A (#6). Finally, the torque-angular velocity data were adjusted so that the torque produced at zero angular velocity equaled the peak co-activation adjusted isometric torque (Figure A-1, #6).

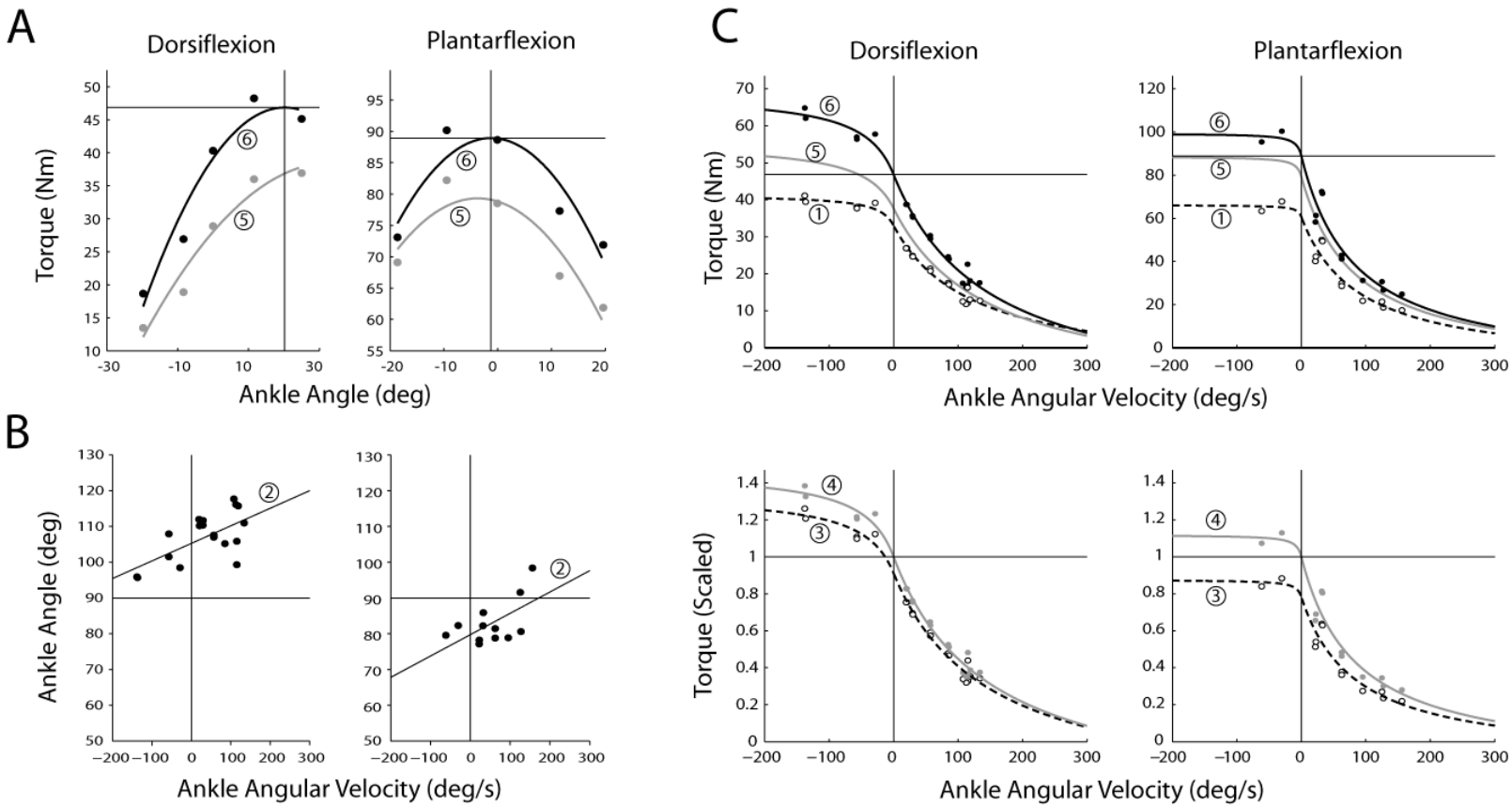

Figure A-1. Example of the procedure for adjusting the experimental torque-angle (A) and torque-angular velocity data (C) data for a representative subject. The torque-angular velocity data were adjusted for the effects of the torque-angle relationship, based on the angle at which the peak torques occurred (B), and also adjusted for the effects of antagonistic co-contraction. See text for details.

APPENDIX B

MUSCLE MODEL

Nomenclature

CC	Contractile component
SEC	Series elastic component
MT	Musculotendon actuator
l_{CC}, l_{SEC}, l_{MT}	Length of CC, SEC, and MT
v_{CC}, v_{SEC}, v_{MT}	Velocity of CC, SEC, and MT
P_{CC}, P_{SEC}, P_{MT}	Force expressed across the CC, SEC, and MT
SA	CC stimulation-activation relation
FL	CC force-length relation
FV	CC force-velocity relation
$F\Delta L$	SEC force-extension relation
τ_{Rise}, τ_{Fall}	Time constants for rise and fall of activation
μ	CC excitation level
λ	CC activation level
W	Width of force-length parabola
L_0	Optimal CC length
L_S	SEC slack length
α, β	SEC $F\Delta L$ shape coefficients
a,b	Hill coefficients for CC FV relation
$a/P_0, b/L_0$	Normalized Hill coefficients for CC FV relation
ε	CC eccentric force plateau
P_0	Maximal CC isometric force
FP	Force potential of CC based on location on FL curve
$\hat{P}_0$	Maximal isometric CC force adjusted for λ, FP, and P_0
V_{MAX}	Maximal CC shortening velocity

Muscle Model Design

Each muscle-tendon unit will be represented by a Hill-type (1938) model. This phenomenological lumped-parameter model incorporates a contractile component (CC) in series with an elastic component (SEC) (Figure B-1).

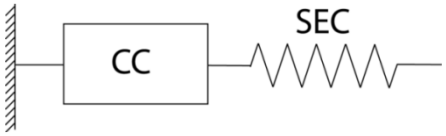

Figure B-1. Components of the musculotendon model.

The behavior of the SEC is defined by a force-extension ($F\Delta L$) relation. The behavior of the CC is defined by stimulation-activation (SA), force-length (FL) and force-velocity (FV) relations. Both the FL and FV relations are linearly scaled with activation level. Note that in the present model:

$$P_{MT} = P_{CC} = P_{SEC} \tag{B.1}$$

$$l_{MT} = l_{CC} + l_{SEC} \tag{B.2}$$

$$v_{MT} = v_{CC} + v_{SEC} \tag{B.3}$$

Conceptually, the muscle models act as transducers of neural stimulation into force. What follows, is a description of the model algorithm as it is implemented in a dynamic simulation of musculoskeletal movement (Figure B-2).

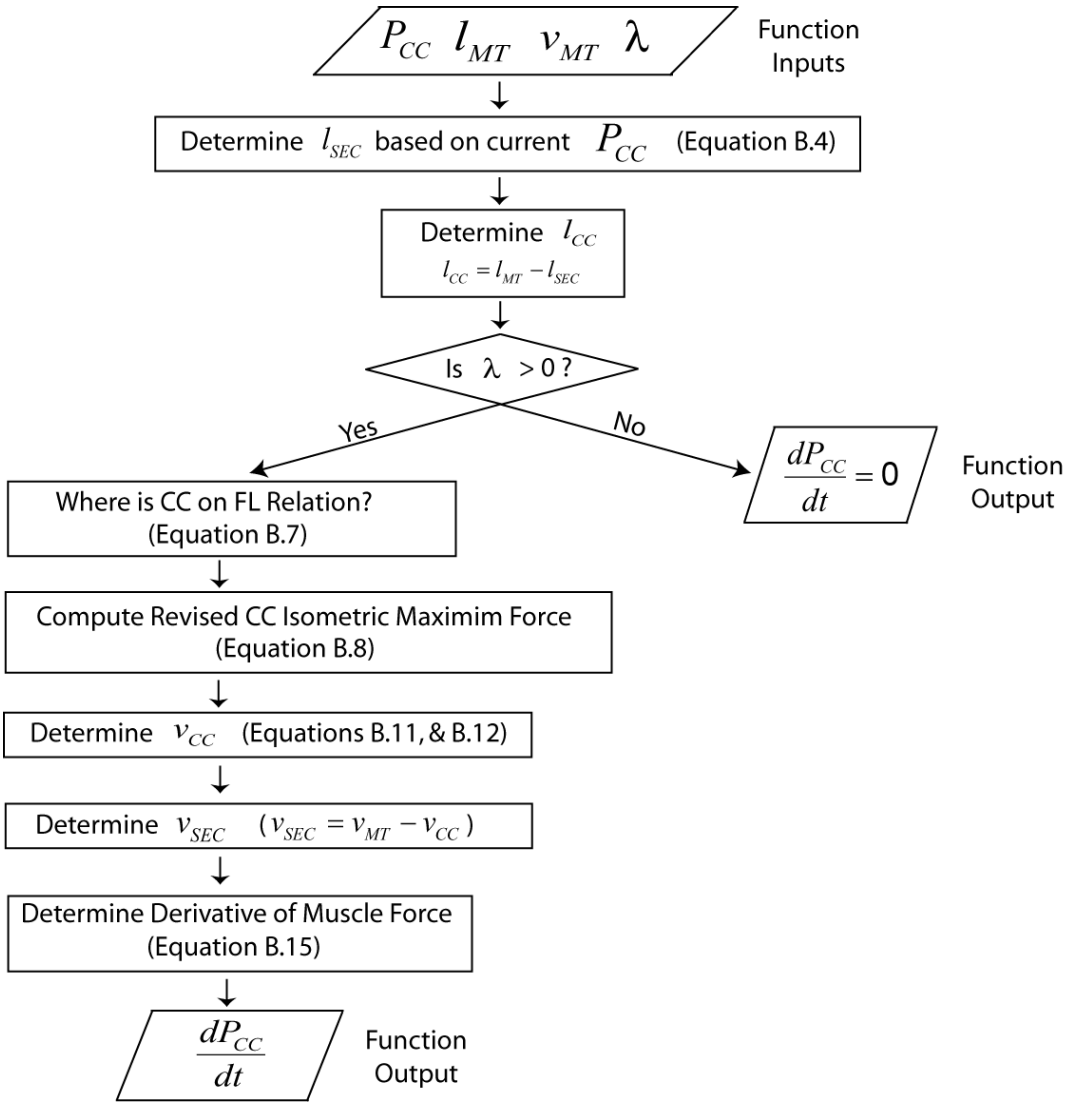

Figure B-2. Flowchart of the musculotendon model algorithm as implemented within a simulation.

Force-Extension Relationship

When a force is expressed across the SEC, the length of the SEC changes by a given amount. The length of the SEC (l_{SEC}) was given by a second-order polynomial, which defined the amount of extension for a given force relative to the slack length of the SEC (L_S) and the maximal isometric force capability of the CC (P_0):

$$l_{SEC} = \frac{L_0}{2P_0}\left[2P_0\alpha - P_0\beta + \sqrt{P_0^2\beta^2 + 4P_0\alpha P_{CC}}\right] \quad \text{(B.4)}$$

where P_{CC} is the force generated by the CC (and is thus expressed across the SEC), and α and β are coefficients defining the shape of the polynomial (Figure B-3.).

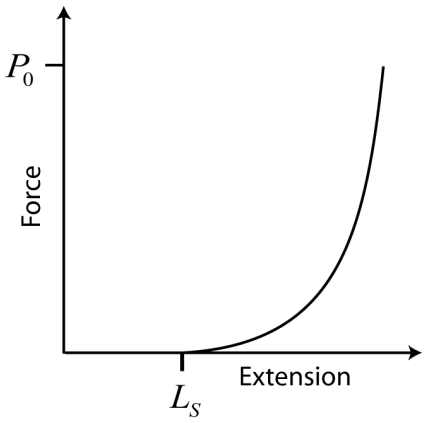

Figure B-3. Illustration of the force-extension relation.

Stimulation-Activation Relationship

An exponential (Figure B-4) characterizes the relationship between the stimulation input to the muscle model and the activation of the CC. When the current stimulation level (μ_i) is greater than the previous activation level (λ_{i-1}) (rising activation):

$$\lambda_i = \lambda_{i-1} + \left[\mu_i \left(1 - e^{\left(-\frac{\Delta t}{\tau_{Rise}} \right)} \right) \left(\mu_i - \lambda_{i-1} \right) \right] \tag{B.5}$$

When the current stimulation level (μ_i) is less than the previous activation level (λ_{i-1}) (falling activation):

$$\lambda_i = \lambda_{i-1} + \left[\left(\lambda_{i-1} - \mu_i \right) \left(1 - e^{\left(-\frac{\Delta t}{\tau_{Fall}} \right)} \right) \left(\lambda_{i-1} \right) \right] \tag{B.6}$$

where i denotes the sample number, Δt is the integration step-size, and τ_{Rise} and τ_{Fall} are time constants specifying the rate muscle activation and deactivation, respectively.

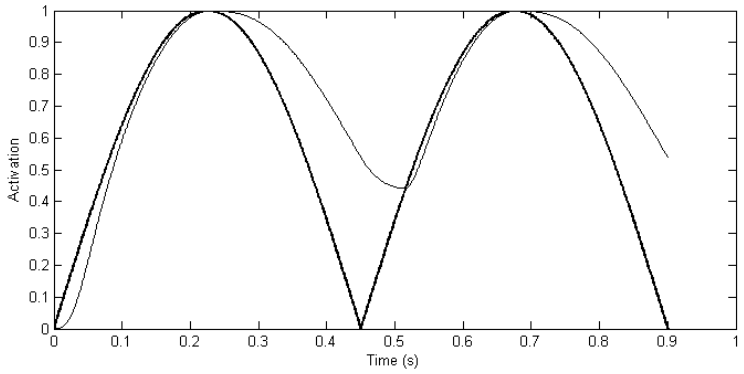

Figure B-4. Example of the exponential relation between stimulation (thick line) and activation (thin line) using hypothetical data. Δt = 0.001, τ_{Rise} = 5 ms, and τ_{Fall} = 80ms.

Force-Length Relationship

The force producing potential of the CC (*FP*) is based on the normalized CC length (l_{CC}/L_0 , where $l_{CC} = l_{MT} - l_{SEC}$) and modeled as an inverted parabola (van Soest and Bobbert 1993), with width determined by the coefficient *W*. The force-length relationship is scaled with activation (Figure B-5). Based on Woittiez (1983):

$$FP = 100 \cdot W \cdot \left(\frac{l_{CC}}{L_0} - 1 \right)^2 + 1 \qquad \text{(B.7)}$$

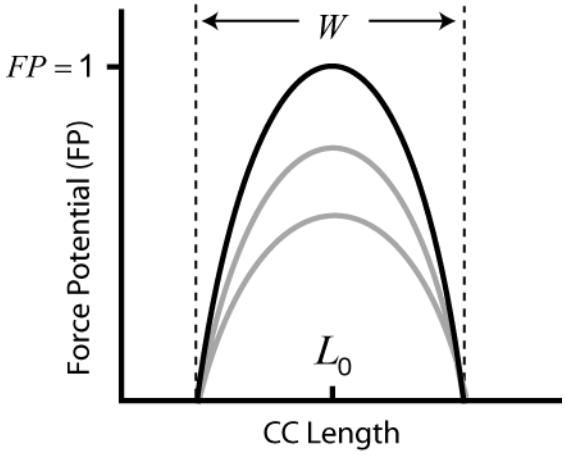

Figure B-5. Illustration of the force-length relation. The black line is when the CC is at full activation, while the gray lines show the CC at below-maximal activation.

Force-Velocity Relationship

An adjusted maximal isometric CC force ($\hat{P}_0$) can be determined based on the activation level of the CC (λ), the current location on the force-length relation, and the isometric force potential of the CC (*FP*):

$$\hat{P}_0 = \lambda \cdot FP \cdot P_0 \tag{B.8}$$

with λ and *FP* ranging from 0 to 1, and P_0 in units of Newtons. The Hill constants a/P_0 and b/L_0 determine the shape of the rectangular hyperbola describing the force-velocity relation (Figure B-6). These values are best expressed as dimensionless numbers (Hill 1970) for use in subsequent equations:

$$a = a/P_0 \cdot \hat{P}_0 \tag{B.9}$$

$$b = b/L_0 \cdot L_0 \tag{B.10}$$

If the force generated by the CC (P_{CC}) is *less* than the adjusted isometric maximum CC force ($\hat{P}_0$), the CC must be shortening. Therefore, based on Hill (1970):

$$v_{CC} = -\left[\frac{\left(\hat{P}_0 + a\right)b}{\left(P_{CC} + a\right)} - b\right] \tag{B.11}$$

If P_{CC} is *greater* than the adjusted isometric maximum CC force ($\hat{P}_0$), the CC must be lengthening. Therefore, based on FitzHugh (1977):

$$v_{CC} = \frac{b\left[\left(\hat{P}_0 \cdot \varepsilon\right) - P_0\right]\left(\hat{P}_0 - P_{CC}\right)}{\left(\hat{P}_0 + a\right)\left[P_{CC} - \left(\hat{P}_0 \cdot \varepsilon\right)\right]} \tag{B.12}$$

Where ε is the saturation force for an eccentric contraction (eccentric plateau). The velocity of the CC is constrained by the maximum shortening velocity (V_{MAX}):

$$V_{MAX} = -\frac{\hat{P}_0 b}{a} \tag{B.13}$$

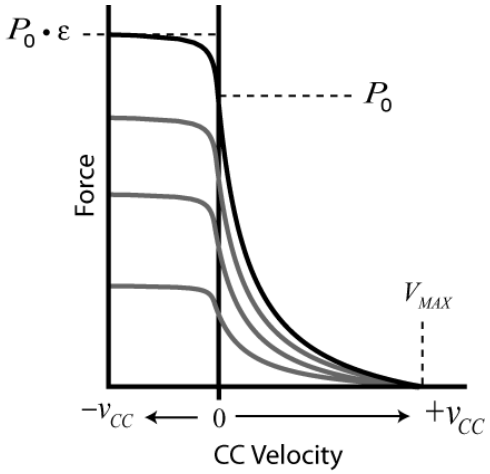

Figure B-6. Illustration of the CC force-velocity relationship used. The black line is when the CC is fully activated at optimal fiber length, while the gray lines show the CC at sub-maximal activation and/or at a non-optimal fiber length.

Final Muscle Model Output

The output of the muscle model is the rate of change of muscle force with respect to time:

$$\frac{dP_{CC}}{dt} = \frac{\sqrt{P_0^2 b^2 + 4P_0 a P_{CC}}}{L_S} \cdot v_{SEC} \tag{B.14}$$

where the velocity of the SEC is $v_{SEC} + V_{MT} - V_{CC}$. This allows the derivative to be sent to the integration routine, which is integrated along with the other model state variables to give the P_{CC} for the next iteration.

APPENDIX C

OPTIMIZATION COSTS AND MUSCLE PROPERTY CORRELATIONS

Optimization Costs

The individual costs for the Phase 1 and 2 optimizations are listed in Table C-1. Note that the statistical analysis was performed on the *net* isometric and isovelocity costs, which are displayed in Figure C-1. For the net costs, there was a significant main effect for muscle (p = .018) and contraction type (p = .001), indicating that overall the costs were greater for the plantarflexion simulations, and were greater for the isometric simulations (Cohen's f = 0.14). There was also an interaction between muscle and contraction type (p = .030), such that for the isovelocity optimizations (Figure C-1, Right) the costs were higher for plantarflexion compared with dorsiflexion (p < .001); however, for the isometric optimizations the costs were similar for dorsi- and plantarflexion (p = .906).

Table C-1. Optimization Costs

Group	Mus.	Isometric Costs (Nm)			Isovelocity Costs (Nm)	
		$C_{T\theta}$	$C_{T\Delta L}$	$C_{SOL/GA}$	$C^1_{T\omega}$	$C^2_{T\omega}$
Young Male	DF	0.02 ± 0.04	0.25 ± 0.07	-	0.97 ± 1.16	1.64 ± 0.48
	PF	0.81 ± 0.43	0.47 ± 0.65	0.42 ± 0.38	1.01 ± 0.90	1.78 ± 2.43
Young Female	DF	0.19 ± 0.44	0.40 ± 0.06	-	0.85 ± 0.48	0.62 ± 0.62
	PF	0.92 ± 1.53	0.43 ± 0.39	0.33 ± 0.28	0.96 ± 1.44	0.62 ± 0.43
Older Male	DF	0.14 ± 0.05	0.40 ± 0.05	-	0.90 ± 0.85	0.85 ± 0.29
	PF	0.66 ± 0.19	0.71 ± 0.18	0.76 ± 0.49	0.64 ± 0.45	2.00 ± 0.90
Older Female	DF	0.15 ± 0.06	0.33 ± 0.20	-	1.24 ± 0.41	0.76 ± 3.11
	PF	1.03 ± 0.35	0.49 ± 0.21	0.70 ± 0.08	0.31 ± 0.40	1.50 ± 1.34

†Non-normal distribution.
[a]Dorsiflexion = Negative; Plantarflexion = Positive

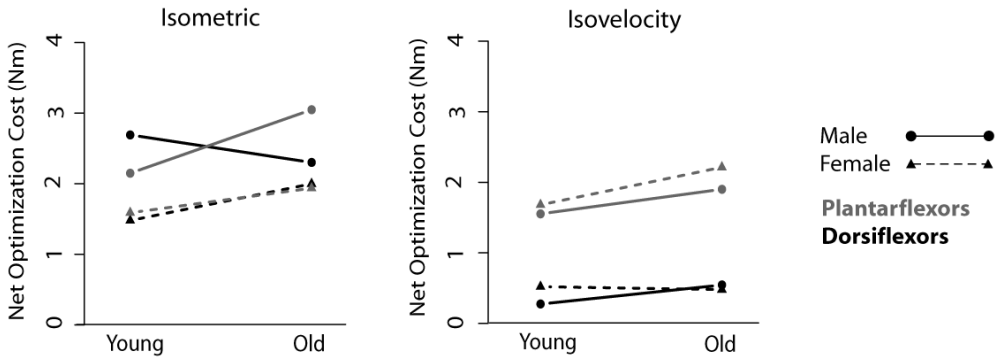

Figure C-1. Interaction plots for costs associated with isometric and isovelocity optimizations.

Table C-2. Correlations (*R*) between muscle mechanical properties.

Muscle Property		P_0	Force-Length (FL)			Force-Extension (FΔL)			Force-Velocity (FV)			
			L_0	L_S	W	α	β	ΔL_{MAX}	a/P_0	b/L_0	ε	V_{MAX}
	P_0	1										
FL	L_0	-0.11	1									
	L_S	0.11	-0.31*	1								
	W	0.03	0.41*	-0.07	1							
FΔL	α	-0.34*	0.25	-0.07	-0.15	1						
	β	0.00	0.12	0.16	0.15	-0.05	1					
	ΔL_{MAX}	0.38*	-0.23	-0.10	-0.16	-0.59*	-0.53*	1				
FV	a/P_0	0.01	0.48*	0.16	0.36*	-0.02	0.18	-0.21	1			
	b/L_0	-0.04	-0.24	0.56*	0.01	-0.08	0.04	-0.07	0.03	1		
	ε	0.08	-0.06	-0.04	0.11	-0.16	-0.08	0.08	0.07	0.11	1	
	V_{MAX}	0.23	0.16	-0.06	0.14	-0.09	0.18	-0.07	0.56*	-0.55*	-0.04	1

* Denotes at least a moderately strong relationship.

APPENDIX D

MULTIPLE REGRESSION MODELING PROCEDURE

The form of the full regression model used in this analysis was:

$$BM = \beta_0 + \beta_1 Age + \beta_2 MP_1 + \beta_3 \left(Age \cdot MP_1 \right) + \beta_4 MP_2 + \beta_5 \left(Age \cdot MP_2 \right) \text{K} \ \beta_i MP_j + \beta_i \left(Age \cdot MP_j \right)$$

where *j* represents each of nine mechanical properties and *i* represents each of the β coefficients. In the full model, each mechanical property appeared as an independent term (9 terms) and as an interaction with age (9 terms). Thus, the 18 mechanical property terms, the y-intercept β_0 and the age effect ($\beta_1 Age$) gave a total of 20 terms in the full regression model (i = 0 to 19).

The multiple regression analyses was done with the software package R (2008). The function "regsubsets" from the "leaps" package was used to select the best regression models using a "branch-and-bound" search algorithm. In short, the algorithm constructs a search tree and "prunes" the tree in a backward stepwise fashion by removing variables that increase the residual sum-of-squares (which quantifies the discrepancy between the model and the data). For more details, see Miller (2002).

The output of the model selection algorithm for an example model is presented in Table D1. The example model included the mechanical properties of the DF muscle as predictors, and the mean rearward CoM position during imposed swaying as the response variable. The algorithm outputs the best model for each number of terms (up to 9), and arranges them according to the adjusted $R^2 \left(\bar{R}^2 \right)$ values (Table D1).

Before defining $\bar{R}^2$, the coefficient of determination $\left(R^2 \right)$ needs to be defined. The R^2 is a measure of the global fit of a regression model, representing the proportion of the variability in the observed values that can be attributed to a particular linear combination of the predictor variables, and is defined as

$$R^2 = 1 - \frac{SS_{ERR}}{SS_{TOT}}$$

$$\text{where } SS_{TOT} = \sum_i \left(y_i - \bar{y} \right)^2 \text{ and } SS_{ERR} = \sum_i \left(y_i - f_i \right)^2$$

In the above equations, y_i and $\bar{y}$ are the observed values and mean of the observed values, and f_i are the predicted values. SS_{TOT} is the total sum of squares, which is proportional to the sample variance, and SS_{ERR} is the sum of squared errors (residual sum of squares).

The $\bar{R}^2$ weighs the predictive power of the models against the number of terms in each model and is defined as

$$\bar{R}^2 = 1-\left(1-R^2\right)\frac{n-1}{n-p-1}$$

where p is the number of terms in the model and n is the sample size.

In the output of the model selection algorithm, there is usually a "cluster" of models with similar adjusted R^2 values (in this example, the top seven models in Table D1), and then a break where the removal of terms is associated with a large drop in $\bar{R}^2$ (bottom two models). The goal is to select a model that has the least number of terms, but still has good predictive power (i.e. only the most important predictors are included). Three candidates are highlighted in bold in Table D1, which have similar $\bar{R}^2$ values and appear just before the break. In this example the $\bar{R}^2$ values of the candidate models are very similar so an additional criterion is used to select the appropriate model, the Bayesian information criterion (BIC). The BIC measure is similar to $\bar{R}^2$, as it measures the efficacy of the model in its predictions and applies a penalty for an overly complex model (one that has many terms); however the BIC is based upon a Bayesian statistical framework. Given two models, the one with the lower BIC is preferred (Schwarz 1978). The BIC is computed as

$$BIC = n\ln\left(\frac{SS_{ERR}}{n}\right) + p\ln\left(n\right)$$

where SS_{ERR} is the residual sum of squares, n s the number of fitted data points, and p is the number of parameters in the model. For this example, the model with three terms [$W + \beta + (Age\cdot\varepsilon)$] was chosen as the best model since the BIC was the lowest. There is high confidence that this is the best model, as dropping any of the terms (e.g. β) results in a large change in the $\bar{R}^2$ (e.g. from .318 to .176).

Table D-1. Best regression models (one of each size up to 9) for predicting the mean rearward CoM position during imposed swaying based on the mechanical properties of the DF muscle.

#	Model	$\bar{R}^2$	R^2	BIC
8	$L_0 + L_S + W + b/L_0 + \beta + (Age\cdot L_0) + (Age\cdot\varepsilon) + (Age\cdot\beta)$	.507	.715	1.9
9	$L_0 + L_S + W + b/L_0 + \beta + (Age\cdot P_0) + (Age\cdot L_0) + (Age\cdot\varepsilon) + (Age\cdot\beta)$	.476	.724	4.2
7	$L_0 + L_S + W + b/L_0 + \beta + (Age\cdot L_0) + (Age\cdot\varepsilon)$	.373	.604	5.4
6	$L_0 + W + b/L_0 + \beta + (Age\cdot L_0) + (Age\cdot\varepsilon)$	.362	.563	4.4
4	**$W + b/L_0 + \beta + (Age\cdot\varepsilon)$**	**.322**	**.465**	**2.5**
3	**$W + \beta + (Age\cdot\varepsilon)$**	**.318**	**.426**	**0.9***
5	**$W + b/L_0 + \beta + (Age\cdot L_0) + (Age\cdot\varepsilon)$**	**.316**	**.496**	**4.3**
2	$W + (Age\cdot\varepsilon)$	.176	.263	2.9
1	Age	.053	.102	3.8

*Best Model

APPENDIX E

QUIET STANCE INVERTED PENDULUM MODEL PROPERTIES

A schematic illustrating the inverted pendulum model, which includes the dimensions of the segments is shown in Figure E-1. The mass and inertial properties of the model were defined as:

Mass of body segment = 76 kg
Mass of foot segment = 2.01 kg
Mass moment of inertia of body segment about segment CoM = 8.48 kg m^2
Mass moment of inertia of foot segment about segment CoM = 0.148 kg m^2

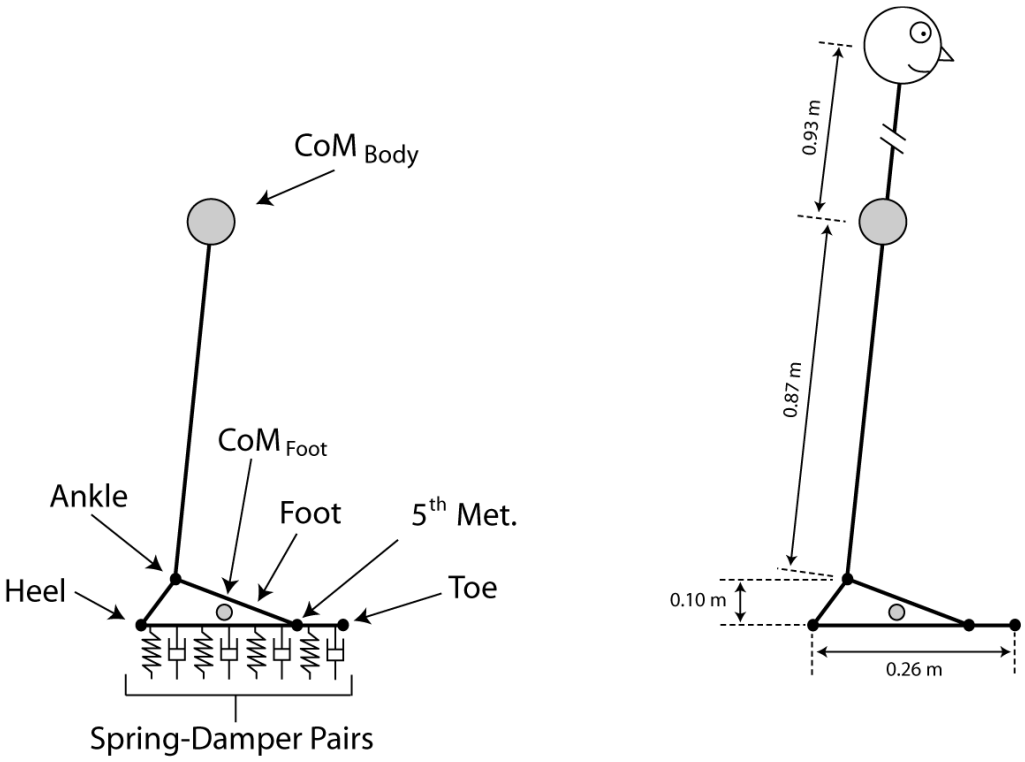

Figure E-1. The inverted pendulum model.

The force applied by each spring-damper elements was an exponential function of the height of the foot above the ground (Anderson and Pandy 1999):

$$F_{y_i} = 0.5336e^{-1150\left(p_{y_i} - y_0\right)} - 1000v_{y_i}\, g\left(p_{y_i}\right) \tag{D.1}$$

$$g\left(p_{y_i}\right) = \frac{1}{1 + 10e500\left(p_{y_i} - g_0\right)} \tag{D.2}$$

where i represents each of the 21 spring-damper elements, v_{yi} is the vertical velocity of the point of application of the spring force, p_y is the vertical position of the point of application of the spring force, y_0 is a parameter (0.0065905 m) that determines when the magnitude of the spring force becomes significant (> 0.5 N), $g(p_{yi})$ is a function that brings damping into effect as the foot approaches the ground, and g_0 is a parameter that determines the point at which the damping force is applied. The horizontal forces exerted by the spring-damper elements were defined as:

$$F_{x_i} = -1000v_{x_i} \tag{D.3}$$

If the horizontal force becomes greater their limiting value, the foot will slip:

$$If\ F_{x_i} > 0.7F_{y_i}\ then\ F_{x_i} = F_{y_i} \tag{D.4}$$

The center-of-pressure in the anterior-posterior direction (CoP_X) was computed as:

$$CoP_X = \frac{\sum_{i=1}^{N} p_X^i\, f_Y^i}{\sum_{i=1}^{N} f_Y^i} \tag{D.5}$$

where i = 1 to the number of springs (N = 21), p_X^i is the horizontal position of spring i, and f_Y^i is the vertical force exerted by spring i on the foot. Although the foot is not constrained from vertical or rotational movement, it was assumed that frictional forces were sufficient so that the foot did not slip horizontally.

BIBLIOGRAPHY

1. **Anderson DE, Madigan ML, and Nussbaum MA.** Maximum voluntary joint torque as a function of joint angle and angular velocity: model development and application to the lower limb. *J Biomech* 40: 3105-3113, 2007.

2. **Anderson FC and Pandy MG.** Dynamic optimization of human walking. *J Biomech Eng* 123: 381-390, 2001.

3. **Anderson FC and Pandy MG.** A Dynamic Optimization Solution for Vertical Jumping in Three Dimensions. *Comput Methods Biomech Biomed Engin* 2: 201-231, 1999.

4. **Aniansson A, Grimby G, and Rundgren A.** Isometric and isokinetic quadriceps muscle strength in 70-year-old men and women. *Scand J Rehabil Med* 12: 161-168, 1980.

5. **Arndt AN, Komi PV, Bruggemann GP, and Lukkariniemi J.** Individual muscle contributions to the in vivo achilles tendon force. *Clin Biomech (Bristol, Avon)* 13: 532-541, 1998.

6. **Asakawa DS, Blemker SS, Gold GE, and Delp SL.** In vivo motion of the rectus femoris muscle after tendon transfer surgery. *J Biomech* 35: 1029-1037, 2002.

7. **Bahler AS.** Series elastic component of mammalian skeletal muscle. *Am J Physiol* 213: 1560-1564, 1967.

8. **Baloh RW, Corona S, Jacobson KM, Enrietto JA, and Bell T.** A prospective study of posturography in normal older people. *J Am Geriatr Soc* 46: 438-443, 1998.

9. **Barin K.** Evaluation of a generalized model of human postural dynamics and control in the sagittal plane. *Biol Cybern* 61: 37-50, 1989.

10. **Basmajian JV and De Luca CJ.** *Muscles Alive: Their Functions Revealed by Electromyography*. Baltimore, MD: Williams & Wilkins, 1985.

11. **Belanger AY, McComas AJ, and Elder GB.** Physiological properties of two antagonist human muscle groups. *Eur J Appl Physiol Occup Physiol* 51: 381-393, 1983.

12. **Bemben MG, Massey BH, Bemben DA, Misner JE, and Boileau RA.** Isometric muscle force production as a function of age in healthy 20- to 74-yr-old men. *Med Sci Sports Exerc* 23: 1302-1310, 1991.

13. **Benvenuti F, Mecaaci R, Gineparari I, Bandinelli S, Benvenuti E, and Ferrucci L.** Kinematic characteristics of standing disequilibrium: reliability and validity of a posturographic protocol. *Arch Phys Med Rehabil* 80: 178-287, 1999.

14. **Bernstein N.** *The co-ordination and regulation of movements*. London: Pergamon Press, 1967.

15. **Bizzi E, Hogan N, Mussa-Ivaldi FA, and Giszter S.** Does the nervous system use equilibrium-point control to guide single and multiple joint movements? *Behavioral and Brain Sciences* 15: 603-613, 1992.

16. **Blanpied P and Smidt GL.** The difference in stiffness of the active plantar flexors between young and elderly human females. *J Gerontol* 48: 58-63, 1993.

17. **Bobbert MF and van Ingen Schenau GJ.** Isokinetic plantar flexion: experimental results and model calculations. *J Biomech* 23: 105-119, 1990.

18. **Bobbert MF and van Soest AJ.** Effects of muscle strengthening on vertical jump height: a simulation study. *Med Sci Sports Exerc* 26: 1012-1020, 1994.

19. **Brand RA, Pedersen DR, and Friederich JA.** The sensitivity of muscle force predictions to changes in physiologic cross-sectional area. *J Biomech* 19: 589-596, 1986.

20. **Brauer SG, Burns YR, and Galley P.** A prospective study of laboratory and clinical measures of postural stability to predict community-dwelling fallers. *J Gerontol A Biol Sci Med Sci* 55: M469-476, 2000.

21. **Bressler BH and Clinch NF.** Cross bridges as the major source of compliance in contracting skeletal muscle. *Nature* 256: 221-222, 1975.

22. **Brocklehurst JC, Robertson D, and James-Groom P.** Clinical correlates of sway in old age--sensory modalities. *Age Ageing* 11: 1-10, 1982.

23. **Brown M, Fisher JS, and Salsich G.** Stiffness and muscle function with age and reduced muscle use. *J Orthop Res* 17: 409-414, 1999.

24. **Buchanan TS, Lloyd DG, Manal K, and Besier TF.** Neuromusculoskeletal modeling: estimation of muscle forces and joint moments from measurements of neural comand. *Journal of Applied Biomechanics* 20: 367-395, 2004.

25. **Burgess KE, Pearson SJ, Breen L, and Onambele GN.** Tendon structural and mechanical properties do not differ between genders in a healthy community-dwelling elderly population. *J Orthop Res*, 2008.

26. **Chandler JM, Duncan PW, and Studenski SA.** Balance performance on the postural stress test: comparison of young adults, healthy elderly, and fallers. *Phys Ther* 70: 410-415, 1990.

27. **Chiari L, Rocchi L, and Cappelo A.** Stabilometric parameters are affected by anthropometry and foot placement. *Clinical Biomechanics* 17: 666-677, 2002.

28. **Chow JW and Darling WG.** The maximum shortening velocity of muscle should be scaled with activation. *J Appl Physiol* 86: 1025-1031, 1999.

29. **Clarkson PM, Kroll W, and Melchionda AM.** Age, isometric strength, rate of tension development and fiber type composition. *J Gerontol* 36: 648-653, 1981.

30. **Close R.** Dynamic properties of fast and slow skeletal muscles of the rat after nerve cross-union. *J Physiol* 204: 331-346, 1969.

31. **Close R.** Dynamic Properties of Fast and Slow Skeletal Muscles of the Rat During Development. *J Physiol* 173: 74-95, 1964.

32. **Close RI.** Dynamic properties of mammalian skeletal muscles. *Physiol Rev* 52: 129-197, 1972.

33. **Coelho M, Ferreira JJ, Dias B, Sampaio C, Pavao Martins I, and Castro-Caldas A.** Assessment of time perception: the effect of aging. *J Int Neuropsychol Soc* 10: 332-341, 2004.

34. **Cohen J.** *Statistical power analysis for the behavioral sciences.* San Diego, CA: Academic Press., 1969.

35. **Colledge NR, Cantley P, Peaston I, Brash H, Lewis S, and Wilson JA.** Ageing and balance: the measurement of spontaneous sway by posturography. *Gerontology* 40: 273-278, 1994.

36. **Collins JJ and Deluca CJ.** Open-loop and closed-loop control of posture: a random walk analysis of center-of-pressure trajectories. *Exp Brain Res* 95: 308-318, 1993.

37. **Cram JR, Kasman GS, and Holtz J.** *Introduction to Surface Electromyography*. Gaithersburg, Maryland: Aspen Publishers, 1998.

38. **Crowninshield RD and Brand RA.** The prediction of forces in joint structures: distribution of intersegmental resultants. *Exerc Sport Sci Rev* 9: 159-181, 1981.

39. **Cummings SR and Nevitt MC.** A hypothesis: the causes of hip fractures. *J Gerontol Med Sci* 44: M107-111, 1989.

40. **Danna-Dos-Santos A, Slomka K, Zatsiorsky VM, and Latash ML.** Muscle modes and synergies during voluntary body sway. *Exp Brain Res* 179: 533-550, 2007.

41. **D'Antona G, Pellegrino MA, Adami R, Rossi R, Carlizzi CN, Canepari M, Saltin B, and Bottinelli R.** The effect of ageing and immobilization on structure and function of human skeletal muscle fibres. *J Physiol* 552: 499-511, 2003.

42. **Delbono O.** Neural control of aging skeletal muscle. *Aging Cell* 2: 21-29, 2003.

43. **Delp SL.** *Surgery simulation: A computer grphics system to analyze and design musculoskeletal reconstructions of the lower limb* (Ph.D.). Stanford, CA: Stanford University, 1990.

44. **Delp SL, Loan JP, Hoy MG, Zajac FE, Topp EL, and Rosen JM.** An interactive, graphics-based model of the lower extremity so study orthopaedic surgical procedures. *IEEE Trans Biomed Engng* 37: 757-767, 1990.

45. **Delp SL, Ringwelski DA, and Carroll NC.** Transfer of the rectus femoris: effects of transfer site on moment arms about the knee and hip. *J Biomech* 27: 1201-1211, 1994.

46. **Doherty TJ.** Invited review: Aging and sarcopenia. *J Appl Physiol* 95: 1717-1727, 2003.

47. **Doherty TJ and Brown WF.** Age-related changes in the twitch contractile properties of human thenar motor units. *J Appl Physiol* 82: 93-101, 1997.

48. **Duncan PW, Studenski S, Chandler J, and Prescott B.** Functional reach: predictive validity in a sample of elderly male veterans. *J Gerontol* 47: M93-98, 1992.

49. **Duncan PW, Weiner DK, Chandler J, and Studenski S.** Functional reach: a new clinical measure of balance. *J Gerontol* 45: M192-197, 1990.

50. **Edman KA, Caputo C, and Lou F.** Depression of tetanic force induced by loaded shortening of frog muscle fibres. *J Physiol* 466: 535-552, 1993.

51. **Edman KA, Elzinga G, and Noble MI.** Enhancement of mechanical performance by stretch during tetanic contractions of vertebrate skeletal muscle fibres. *J Physiol* 281: 139-155, 1978.

52. **Edman KA and Reggiani C.** Redistribution of sarcomere length during isometric contraction of frog muscle fibres and its relation to tension creep. *J Physiol* 351: 169-198, 1984.

53. **Epstein M and Herzog W.** *Theoretical models of skeletal muscle.* New York: Wiley, 1998.

54. **Era P and Heikkinen E.** Postural sway during standing and unexpected disturbance of balance in random samples of men of different ages. *J Gerontol* 40: 287-295, 1985.

55. **Esformes JI, Narici MV, and Maganaris C.** Measuremetn of human muscle volume using ultrasonography. *Eur J Appl Physiol* 87: 90-92, 2002.

56. **Eurich CW, Pawelzik K, Ernst U, Thiel A, Cowan JD, and Milton JG.** Delay adaptation in the nervous system. *Neurocomputing* 32-33: 741-748, 2000.

57. **Faisal AA, Selen LP, and Wolpert DM.** Noise in the nervous system. *Nat Rev Neurosci* 9: 292-303, 2008.

58. **Ferri A, Scaglioni G, M. P, Capodaglio P, Van Hoecke J, and Narici MV.** Strength and power changes of the human plantarflexors and knee extensors in response to resistance training in old age. *Acta Physiol Scand* 177: 69-78, 2003.

59. **FitzHugh R.** A model of optimal voluntary muscular control. *J Math Biol* 4: 203-236, 1977.

60. **Fitzpatrick R, Burke D, and Gandevia SC.** Loop gain of reflexes controlling human standing measured with the use of postural and vestibular disturbances. *J Neurophysiol* 76: 3994-4008, 1996.

61. **Fitzpatrick RC, Taylor JL, and McCloskey DI.** Ankle stiffness of standing humans in response to imperceptible perturbation: reflex and task-dependent components. *J Physiol* 454: 533-547, 1992.

62. **Forth KE, Metter EJ, and Paloski WH.** Age associated differences in postural equilibrium control: a comparison between EQscore and minimum time to contact (TTC_{min}). *Gait & Posture* 25: 56-62, 2007.

63. **Fox L.** *Numerical solutions of ordinary and partial differential equations*. Palo Alto: Addison-Wesley, 1962.

64. **Frey D, Schneider C, Xu L, Borg J, Spooren W, and Caroni P.** Early and selective loss of neuromuscular synapse subtypes with low sprouting competence in motoneuron diseases. *J Neurosci* 20: 2534-2542, 2000.

65. **Frijns CJ, Laman DM, van Duijn MA, and van Duijn H.** Normal values of patellar and ankle tendon reflex latencies. *Clin Neurol Neurosurg* 99: 31-36, 1997.

66. **Frontera WR, Hughes VA, Fielding RA, Fiatarone MA, Evans WJ, and Roubenoff R.** Aging of skeletal muscle: a 12-yr longitudinal study. *J Appl Physiol* 88: 1321-1326, 2000a.

67. **Frontera WR, Hughes VA, Lutz KJ, and Evans WJ.** A cross-sectional study of muscle strength and mass in 45- to 78-yr-old men and women. *J Appl Physiol* 71: 644-650, 1991.

68. **Frontera WR, Suh D, Krivickas LS, Hughes VA, Goldstein R, and Roubenoff R.** Skeletal muscle fiber quality in older men and women. *Am J Physiol Cell Physiol* 279: C611-618, 2000b.

69. **Gage WH, Winter DA, Frank JS, and Adkin AL.** Kinematic and kinetic validity of the inverted pendulum model in quiet standing. *Gait Posture* 19: 124-132, 2004.

70. **Gajdosik RL, Vander Linden DW, and Williams AK.** Concentric isokinetic torque characteristics of the calf muscles of active women aged 20 to 84 years. *J Orthop Sports Phys Ther* 29: 181-190, 1999.

71. **Galler S and Hilber K.** Tension/stiffness ratio of skinned rat skeletal muscle fiber types at various temperatures. *Acta Physiol Scand* 162, 1998.

72. **Gans C.** Fiber architecture and muscle function. *Ex Sci Sport Rev* 10: 160-207, 1982.

73. **Garner BA and Pandy MG.** Estimation of musculotendon properties in the human upper limb. *Ann Biomed Eng* 31: 207-220, 2003.

74. **Gerritsen KG, van den Bogert AJ, Hulliger M, and Zernicke RF.** Intrinsic muscle properties facilitate locomotor control - a computer simulation study. *Motor Control* 2: 206-220, 1998.

75. **Gollnick PD, Sjodin B, Karlsson J, Jansson E, and Saltin B.** Human soleus muscle: a comparison of fiber composition and enzyme activities with other leg muscles. *Pflugers Arch* 348: 247-255, 1974.

76. **Gordon AM, Huxley AF, and Julian FJ.** The variation in isometric tension with sarcomere length in vertebrate muscle fibres. *J Physiol* 184: 170-192, 1966.

77. **Grabiner MD, Owings TM, and Pavol MJ.** Lower extremity strength plays only a small role in determining the maximum recoverable lean angle in older adults. *J Gerontol* 60A: 1447-1450, 2005.

78. **Gray H.** *Anatomy of the Human Body*. Philadelphia, PA: Lea & Febiger, 1973.

79. **Haddad JM, Gagnon JL, Hasson CJ, Van Emmerik RE, and Hamill J.** Evaluation of time-to-contact measures for assessing postural stability. *Journal of Applied Biomechanics* 22: 155-161, 2006.

80. **Hall CD and Jensen JL.** Age-related differences in lower extremity power after support surface perturbations. *J Am Geriatr Soc* 50: 1782-1788, 2002.

81. **Harries UJ and Bassey EJ.** Torque-velocity relationships for the knee extensors in women in their 3rd and 7th decades. *Eur J Appl Physiol Occup Physiol* 60: 187-190, 1990.

82. **Hasson CJ, Van Emmerik RE, and Caldwell GE.** Predicting dynamic postural instability using center of mass time-to-contact information. *J Biomech* 41: 2121-2129, 2008.

83. **Heine R, Manal K, and Buchanan TS.** Using Hill-type muscle models and EMG data in a forward dynamic analysis of joint moment: evaluation of critical parameters. *journal of Mechanics in Medicine and Biology* 3: 169-186, 2003.

84. **Hertel J and Olmsted-Kramer LC.** Deficits in time-to-boundary measures of postural control with chronic ankle instability. *Gait & Posture* 25: 33-39, 2007.

85. **Herzog W.** *Individual muscle force prediction in athletic movements*. Calgary: University of Calgary Printing, 1985.

86. **Higuchi H, Yanagida T, and Goldman YE.** Compliance of thin filaments in skinned fibers of rabbit skeletal muscle. *Biophys J* 69, 1995.

87. **Hill AV.** *First and last experiments in muscle mechanics.* London: Cambridge Press, 1970.

88. **Hill AV.** The heat of shortening and the dynamic constants of muscle. *Proceedings of the Royal Society of London Series B, Containing Papers of a Biological Charachter* 126B: 136-195, 1938.

89. **Hof AL.** Muscle mechanics and neuromuscular control. *J Biomech* 36: 1031-1038, 2003.

90. **Hof AL, Gazendam MG, and Sinke WE.** The condition for dynamic stability. *Journal of Biomechanics* 38: 1-8, 2005.

91. **Hof AL and Van den Berg J.** EMG to force processing II: Estimation of parameters of the Hill muscle model for the human triceps surae by means of a calfergometer. *J Biomech* 14: 759-770, 1981.

92. **Hook P, Sriramoju V, and Larsson L.** Effects of aging on actin sliding speed on myosin from single skeletal muscle cells of mice, rats, and humans. *Am J Physiol Cell Physiol* 280: C782-788, 2001.

93. **Horak FB, Shupert CL, and Mirka A.** Components of postural dyscontrol in the elderly: a review. *Neurobiol Aging* 10: 727-738, 1989.

94. **Hortobagyi T, Zheng D, Weidner M, Lambert NJ, Westbrook S, and Houmard JA.** The influence of aging on muscle strength and muscle fiber characteristics with special reference to eccentric strength. *J Gerontol A Biol Sci Med Sci* 50: B399-406, 1995.

95. **Hoy MG, Zajac FE, and Gordon ME.** A musculoskeletal model of the human lower extremity: the effect of muscle, tendon, and moment arm on the moment-angle relationship of musculotendon actuators at the hip, knee, and ankle. *J Biomech* 23: 157-169, 1990.

96. **Hughes MA, Duncan PW, Rose DK, Chandler JM, and Studenski SA.** The relationship of postural sway to sensorimotor function, functional performance, and disability in the elderly. *Arch Phys Med Rehabil* 77: 567-572, 1996.

97. **Ito M, Kawakami Y, Ichinose Y, Fukashiro S, and Fukunaga T.** Nonisometric behavior of fascicle during isometric contractions of a human muscle. *J Appl Physiol* 80: 1235-1235, 1998.

98. **Jakobsson F, Borg K, Edstrom L, and Grimby L.** Use of motor units in relation to muscle fiber type and size in man. *Muscle Nerve* 11: 1211-1218, 1988.

99. **Johansson R, Magnusson M, and Akesson M.** Identification of human postural dynamics. *IEEE Trans Biomed Eng* 35: 858-869, 1988.

100. **Johnson MA, Polgar J, Weightman D, and Appleton D.** Data on the distribution of fibre types in thirty-six human muscles. An autopsy study. *J Neurol Sci* 18: 111-129, 1973.

101. **Kamen G and Caldwell GE.** Physiology and interpretation of the electromyogram. *J Clin Neurophysiol* 13: 366-384, 1996.

102. **Kane TR and Levinson DA.** *Dynamics: Theory and applications*. New York: McGraw-Hill Book Company, 1985.

103. **Karamanidis K and Arampatzis A.** Mechanical and morphological properties of different muscle-tendon units in the lower extremity and running mechanics: effect of aging and physical activity. *J Exp Biol* 208: 3907-3923, 2005.

104. **Karlsson A and Lanshammer h.** Analysis of postural sway strategies using an inverted pendulum model and force plate data. *Gait & Posture* 5: 198-203, 1997.

105. **Kawakami Y, Ichinose Y, and Fukunaga T.** Architectural and functional features of human triceps surae muscles during contraction. *J Appl Physiol* 85: 398-404, 1998.

106. **Kent-Braun JA and Ng AV.** Specific strength and voluntary muscle activation in young and elderly women and men. *J Appl Physiol* 87: 22-29, 1999.

107. **Kjaer M.** Role of extracellular matrix in adaptation of tendon and skeletal muscle to mechanical loading. *Physiol Rev* 84: 649-698, 2004.

108. **Klass M, Baudry S, and Duchateau J.** Aging does not affect voluntary activation of the ankle dorsiflexors during isometric, concentric, and eccentric contractions. *J Appl Physiol* 99: 31-38, 2005.

109. **Komi PV, Fukashiro S, and Jarvinen M.** Biomechanical loading of Achilles tendon during normal locomotion. *Clin Sports Med* 11: 521-531, 1992.

110. **Komi PV, Salonen M, Jarvinen M, and Kokko O.** In vivo registration of Achilles tendon forces in man. I. Methodological development. *Int J Sports Med* 8 Suppl 1: 3-8, 1987.

111. **Koo TK and Mak AF.** Feasibility of using EMG driven neuromusculoskeletal model for prediction of dynamic movement of the elbow. *J Electromyogr Kinesiol* 15: 12-26, 2005.

112. **Korhonen MT, Cristea A, Alen M, Hakkinen K, Sipila S, Mero A, Viitasalo JT, Larsson L, and Suominen H.** Aging, muscle fiber type, and contractile function in sprint-trained athletes. *J Appl Physiol* 101: 906-917, 2006.

113. **Krishnamoorthy V and Latash ML.** Reversals of anticipatory postural adjustments during voluntary sway in humans. *J Physiol* 565: 675-684, 2005.

114. **Kubo K, Kanehisa H, and Fukunaga T.** Gender differences in the viscoelastic properties of tendon structures. *Eur J Appl Physiol* 88: 520-526, 2003.

115. **Kuo AD and Zajac FE.** A biomechanical analysis of muscle strength as a limiting factor in standing posture. *J Biomech* 26: 137-150, 1993.

116. **Lanza IR, Russ DW, and Kent-Braun JA.** Age-related enhancement of fatigue resistance is evident in men during both isometric and dynamic tasks. *J Appl Physiol* 97: 967-975, 2004.

117. **Lanza IR, Towse TF, Caldwell GE, Wigmore DM, and Kent-Braun JA.** Effects of age on human muscle torque, velocity, and power in two muscle groups. *J Appl Physiol* 95: 2361-2369, 2003.

118. **Larsson L and Ansved T.** Effects of ageing on the motor unit. *Prog Neurobiol* 45: 397-458, 1995.

119. **Larsson L, Li X, and Frontera WR.** Effects of aging on shortening velocity and myosin isoform composition in single human skeletal muscle cells. *Am J Physiol* 272: C638-649, 1997.

120. **Laughton CA, Slavin M, Katdare K, Nolan L, Bean JF, Kerrigan DC, Phillips E, Lipsitz LA, and Collins JJ.** Aging, muscle activity, and balance control: physiologic changes associated with balance impairment. *Gait & Posture* 18, 2003.

121. **Lexell J.** Human aging, muscle mass, and fiber type composition. *J Gerontol A Biol Sci Med Sci* 50 Spec No: 11-16, 1995.

122. **Licht MH.** Multiple Regression and Correlation. In: *Reading and understanding multivariate statistics*, edited by Grimm LG and Yarnold PR. Washington, D.C.: American Psychological Association, 1994, p. 19-64.

123. **Light KE.** Information processing for motor performance in aging adults. *Phys Ther* 70: 820-826, 1990.

124. **Lloyd DG and Besier TF.** An EMG-driven musculoskeletal model to estimate muscle forces and knee joint moments in vivo. *J Biomech* 36: 765-776, 2003.

125. **Lloyd DG and Buchanan TS.** A model of load sharing between muscles and soft tissues at the human knee during static tasks. *J Biomech Eng* 118: 367-376, 1996.

126. **Loram ID and Lakie M.** Direct measurement of human ankle stiffness during quiet standing: the intrinsic mechanical stiffness is insufficient for stability. *J Physiol* 545: 1041-1053, 2002a.

127. **Loram ID and Lakie M.** Human balancing of an inverted pendulum: position control by small, ballistic-like, throw and catch movements. *J Physiol* 540: 1111-1124, 2002b.

128. **Loram ID, Maganaris CN, and Lakie M.** Human postural sway results from frequent, ballistic bias impulses by soleus and gastrocnemius. *J Physiol* 564: 295-311, 2005.

129. **Loram ID, Maganaris CN, and Lakie M.** Paradoxical muscle movement in human standing. *J Physiol* 556: 683-689, 2004.

130. **Lord SR, Clark RD, and Webster IW.** Physiological factors associated with falls in an elderly population. *J Am Geriatr Soc* 39: 1194-1200, 1991.

131. **Lord SR, Ward JA, Williams P, and Anstey KJ.** Physiological factors associated with falls in older community-dwelling women. *J Am Geriatr Soc* 42: 1110-1117, 1994.

132. **Luchies CW, Alexander NB, Schultz AB, and Ashton-Miller J.** Stepping responses of young and old adults to postural disturbances: kinematics. *Journal of the American Geriatrics Society* 42: 506-512, 1994.

133. **Lynch NA, Metter EJ, Lindle RS, Fozard JL, Tobin JD, Roy TA, Fleg JL, and Hurley BF.** Muscle quality. I. Age-associated differences between arm and leg muscle groups. *J Appl Physiol* 86: 188-194, 1999.

134. **Maganaris CN.** A predictive model of moment-angle characteristics in human skeletal muscle: application and validation in muscles across the ankle joint. *J Theor Biol* 230: 89-98, 2004.

135. **Maganaris CN, Baltzopoulos V, and Sargeant AJ.** Changes in the tibialis anterior tendon moment arm from rest to maximum isometric dorsiflexion: in vivo observations in man. *Clin Biomech (Bristol, Avon)* 14: 661-666, 1999.

136. **Maganaris CN and Paul JP.** In vivo human tendon mechanical properties. *J Physiol* 521 Pt 1: 307-313, 1999.

137. **Magnusson SP, Aagaard P, Dyhre-Poulsen P, and Kjaer M.** Load-displacement properties of the human triceps surae aponeurosis in vivo. *J Physiol* 531: 277-288, 2001.

138. **Maki BE.** Gait changes in older adults: predictors of falls or indicators of fear. *J Am Geriatr Soc* 45: 313-320, 1997.

139. **Maki BE, Holliday PJ, and Fernie GR.** Aging and postural control: A comparison of spontaneous- and induced-sway balance tests. *J Am Geriatr Soc* 38: 1-9, 1990.

140. **Maki BE, Holliday PJ, and Topper AK.** A prospective study of postural balance and risk of falling in an ambulatory and independent elderly population. *J Gerontol* 49: M72-84, 1994.

141. **Manal K and Buchanan TS.** Subject-specific estimates of tendon slack length: a numerical method. *Journal of Applied Biomechanics* 20: 195-203, 2004.

142. **Marsh E, Sale D, McComas AJ, and Quinlan J.** Influence of joint position on ankle dorsiflexion in humans. *J Appl Physiol* 51: 160-167, 1981.

143. **Masani K, Popovic MR, Nakazawa K, Kouzaki M, and Nozaki D.** Importance of body sway velocity information in controlling ankle extensor activities during quiet stance. *J Neurophysiol* 90: 3774-3782, 2003.

144. **Maurer C and Peterka RJ.** A new interpretation of spontaneous sway measures based on a simple model of human postural control. *J Neurophysiol* 93: 189-200, 2005.

145. **McDonagh MJ, White MJ, and Davies CT.** Different effects of ageing on the mechanical properties of human arm and leg muscles. *Gerontology* 30: 49-54, 1984.

146. **Menegaldo LL, Fleury Ade T, and Weber HI.** Biomechanical modeling and optimal control of human posture. *J Biomech* 36: 1701-1712, 2003.

147. **Merletti R, Farina D, Gazzoni M, and Schieroni MP.** Effect of age on muscle functions investigated with surface electromyography. *Muscle Nerve* 25: 65-76, 2002.

148. **Metter EJ, Conwit R, Tobin J, and Fozard JL.** Age-associated loss of power and strength in the upper extremities in women and men. *J Gerontol A Biol Sci Med Sci* 52: B267-276, 1997.

149. **Micheau P, Kron A, and Bourassa P.** Evaluation of the lambda model for human postural control during ankle strategy. *Biol Cybern* 89: 227-236, 2003.

150. **Mille ML, Rogers MW, Martinez K, Hedman LD, Johnson ME, Lord SR, and Fitzpatrick RC.** Thresholds for inducing protective stepping responses to external perturbations of human standing. *Journal of Neurophysiology* 90: 666-674, 2003.

151. **Miller A.** *Subset selection in regression*: Chapman & Hall/CRC, 2002.

152. **Morasso PG, Baratto L, Capra R, and Spada G.** Internal models in the control of posture. *Neural Netw* 12: 1173-1180, 1999.

153. **Morasso PG and Sanguineti V.** Ankle muscle stiffness alone cannot stabilize balance during quiet standing. *J Neurophysiol* 88: 2157-2162, 2002.

154. **Nagano A and Gerritsen KG.** Effects of neuromuscular strength training on vertical jumping performance - a computer simulation study. *Journal of Applied Biomechanics* 17: 113-128, 2001.

155. **Narici MV, Maganaris C, and Reeves N.** Myotendinous alterations and effects of resistive loading in old age. *Scand J Med Sci Sports* 15: 392-401, 2005.

156. **Narici MV, Maganaris CN, Reeves ND, and Capodaglio P.** Effect of aging on human muscle architecture. *J Appl Physiol* 95: 2229-2234, 2003.

157. **Nashner L and McCollum G.** The organization of human postural movements: a formal basis and experimental synthesis. *Behavioral and Brain Sciences* 8: 135-172, 1985.

158. **Norris AH, Shock NW, and Wagman IH.** Age changes in the maximum conduction velocity of motor fibers of human ulnar nerves. *J Appl Physiol* 5: 589-593, 1953.

159. **Oberg B, Bergman T, and Tropp H.** Testing of isokinetic muscle strength in the ankle. *Med Sci Sports Exerc* 19: 318-322, 1987.

160. **Ochala J, Frontera WR, Dorer DJ, Van Hoecke J, and Krivickas LS.** Single skeletal muscle fiber elastic and contractile characteristics in young and older men. *J Gerontol A Biol Sci Med Sci* 62: 375-381, 2007a.

161. **Ochala J, Lambertz D, Pousson M, Goubel F, and Hoecke JV.** Changes in mechanical properties of human plantar flexor muscles in ageing. *Exp Gerontol* 39: 349-358, 2004a.

162. **Ochala J, Lambertz D, Van Hoecke J, and Pousson M.** Changes in muscle and joint elasticity following long-term strength training in old age. *Eur J Appl Physiol* 100: 491-498, 2007b.

163. **Ochala J, Lambertz D, Van Hoecke J, and Pousson M.** Effect of strength training on musculotendinous stiffness in elderly individuals. *Eur J Appl Physiol* 94: 126-133, 2005.

164. **Ochala J, Valour D, Pousson M, Lambertz D, and Van Hoecke J.** Gender differences in human muscle and joint mechanical properties during plantar flexion in old age. *J Gerontol A Biol Sci Med Sci* 59: 441-448, 2004b.

165. **Onambele GL, Narici MV, and Maganaris CN.** Calf muscle-tendon properties and postural balance in old age. *J Appl Physiol* 100: 2048-2056, 2006.

166. **Out L, Vrijkotte TG, van Soest AJ, and Bobbert MF.** Influence of the parameters of a human triceps surae muscle model on the isometric torque-angle relationship. *J Biomech Eng* 118: 17-25, 1996.

167. **Owings TM, Pavol MJ, Foley KT, and Grabiner MD.** Measures of postural stability are not predictors of recovery from large postural disturbances in healthy older adults. *J Am Geriatr Soc* 48: 42-50, 2000.

168. **Pandy MG, Anderson FC, and Hull DG.** A parameter optimization approach for the optimal control of large-scale musculoskeletal systems. *J Biomech Eng* 114: 450-460, 1992.

169. **Pandy MG, Zajac FE, Sim E, and Levine WS.** An optimal control model for maximum-height human jumping. *J Biomech* 23: 1185-1198, 1990.

170. **Peterka RJ.** Sensorimotor integration in human postural control. *J Neurophysiol* 88: 1097-1118, 2002.

171. **Peterka RJ and Loughlin PJ.** Dynamic regulation of sensorimotor integration in human postural control. *J Neurophysiol* 91: 410-423, 2004.

172. **Phillips CA and Petrofsky JS.** Velocity of contraction of skeletal muscle as a function of activation and fiber composition: a mathematical model. *J Biomech* 13: 549-558, 1980.

173. **Poliakov AV, Powers RK, Sawczuk A, and Binder MD.** Effects of background noise on the response of rat and cat motoneurones to excitatory current transients. *J Physiol* 495 (Pt 1): 143-157, 1996.

174. **Porter MM, Myint A, Kramer JF, and Vandervoort AA.** Concentric and eccentric knee extension strength in older and younger men and women. *Can J Appl Physiol* 20: 429-439, 1995a.

175. **Porter MM, Vandervoort AA, and Kramer JF.** Eccentric peak torque of the plantar and dorsiflexors is maintained in older women. *J Gerontol A Biol Sci Med Sci* 52: B125-131, 1997.

176. **Porter MM, Vandervoort AA, and Lexell J.** Aging of human muscle: structure, function and adaptability. *Scand J Med Sci Sports* 5: 129-142, 1995b.

177. **Poulin MJ, Vandervoort AA, Paterson DH, Kramer JF, and Cunningham DA.** Eccentric and concentric torques of knee and elbow extension in young and older men. *Can J Sport Sci* 17: 3-7, 1992.

178. **Prieto TE, Myklebust JB, Hoffmann RG, Lovett EG, and Myklebust BM.** Measures of postural steadiness: differences between healthy young and elderly adults. *IEEE Trans Biomed Eng* 43: 956-966, 1996.

179. **Prieto TE, Myklebust JB, and Myklebust BM.** Characterization and modeling of postural steadiness in the elderly: a review. *IEEE Transactions on Rehabilitation Engineering* 1: 26-34, 1993.

180. **R_Development_Core_Team.** R: A languague and environment for statistical computing. Vienna, Austria: R Foundation for Statistical Computing, 2008.

181. **Raasch CC, Zajac FE, Ma B, and Levine WS.** Muscle coordination of maximum-speed pedaling. *Journal of Biomechanics* 30: 595-602, 1997.

182. **Raikova RT and Prilutsky BI.** Sensitivity of predicted muscle forces to parameters of the optimization-based human leg model revealed by analytical and numerical analyses. *J Biomech* 34: 1243-1255, 2001.

183. **Rakitin BC, Stern Y, and Malapani C.** The effects of aging on time reproduction in delayed free-recall. *Brain Cogn* 58: 17-34, 2005.

184. **Ramos CF and Stark LW.** Postural maintenance during mocement: simulations of a two joint model. *Biol Cybern* 63: 363-375, 1990.

185. **Rassier DE and Herzog W.** Force enhancement following an active stretch in skeletal muscle. *J Electromyogr Kinesiol* 12: 471-477, 2002.

186. **Rassier DE, MacIntosh BR, and Herzog W.** Length dependence of active force production in skeletal muscle. *J Appl Physiol* 86: 1445-1457, 1999.

187. **Redfern MS, Jennings JR, Martin C, and Furman JM.** Attention influences sensory integration for postural control in older adults. *Gait Posture* 14: 211-216, 2001.

188. **Reeves ND, Maganaris CN, and Narici MV.** Effect of strength training on human patella tendon mechanical properties of older individuals. *J Physiol* 548: 971-981, 2003a.

189. **Reeves ND, Narici MV, and Maganaris CN.** Strength training alters the viscoelastic properties of tendons in elderly humans. *Muscle Nerve* 28: 74-81, 2003b.

190. **Riccio GE.** Information in movement variability about the qualitative dynamics of posture and orientation. In: *Variability and Motor Control*, edited by Newell KM and Corcos DM. Champaign, IL: Human Kinetics, 1993, p. 317-358.

191. **Riener R and Edrich T.** Identification of passive elastic joint moments in the lower extremities. *J Biomech* 32: 539-544, 1999.

192. **Rugg SG, Gregor RJ, Mandelbaum BR, and Chiu L.** In vivo moment arm calculations at the ankle using magnetic resonance imaging (MRI). *J Biomech* 23: 495-501, 1990.

193. **Sale D, Quinlan J, Marsh E, McComas AJ, and Belanger AY.** Influence of joint position on ankle plantarflexion in humans. *J Appl Physiol* 52: 1636-1642, 1982.

194. **Sato A, Sato Y, and Suzuki H.** Aging effects on conduction velocities of myelinated and unmyelinated fibers of peripheral nerves. *Neurosci Lett* 53: 15-20, 1985.

195. **Schwarz GE.** Estimating the dimension of a model. *Annals of Statistics* 6: 461-464, 1978.

196. **Scovil CY and Ronsky JL.** Sensitivity of a Hill-based muscle model to perturbations in model parameters. *J Biomech* 39: 2055-2063, 2006.

197. **Shumway-Cook A, Baldwin M, Polissar NL, and Gruber W.** Predicting the probability for falls in community-dwelling older adults. *Phys Ther* 77: 812-819, 1997.

198. **Siegler S, Moskowitz GD, and Freedman W.** Passive and active components of the internal moment developed about the ankle joint during human ambulation. *J Biomech* 17: 647-652, 1984.

199. **Simoneau E, Martin A, and Van Hoecke J.** Muscular performances at the ankle joint in young and elderly men. *J Gerontol A Biol Sci Med Sci* 60: 439-447, 2005.

200. **Sinha T and Maki BE.** Effect of forward lean on postural ankle dynamics. *IEEE Trans Rehab Eng* 4: 348-359, 1996.

201. **Sipila S and Suominen H.** Knee extension strength and walking speed in relation to quadriceps muscle composition and training in elderly women. *Clin Physiol* 14: 433-442, 1994.

202. **Slobounov SM, Moss SA, Slobounova ES, and Newell KM.** Aging and time to instability in posture. *J Gerontol A Biol Sci Med Sci* 53: B71-78, 1998.

203. **Slobounov SM, Slobounova ES, and Newell KM.** Virtual Time-to-Collision and Human Postural Control. *Journal of Motor Behavior* 29: 263-281, 1997.

204. **Spector SA, Gardiner PF, Zernicke RF, Roy RR, and Edgerton VR.** Muscle architecture and force-velocity characteristics of cat soleus and medial gastrocnemius: implications for motor control. *J Neurophysiol* 44: 951-960, 1980.

205. **Speers RA, Kuo AD, and Horak FB.** Contributions of altered sensation and feedback responses to changes in coordination of postural control due to aging. *Gait Posture* 16: 20-30, 2002.

206. **Spoor CW, van Leeuwen JL, van der Meulen WJ, and Huson A.** Active force-length relationship of human lower-leg muscles estimated from morphological data: a comparison of geometric muscle models. *Eur J Morphol* 29: 137-160, 1991.

207. **Storn R and Price K.** Differential evolution - a simple and efficient adaptive scheme for global optimization over continuous spaces. *Technical Report TR-95-012, International Computer Science Institute*, 1995.

208. **Thelen DG.** Adjustment of muscle mechanics model parameters to simulate dynamic contractions in older adults. *J Biomech Eng* 125: 70-77, 2003.

209. **Thelen DG, Schultz AB, Alexander NB, and Ashton-Miller JA.** Effects of age on rapid ankle torque development. *J Gerontol A Biol Sci Med Sci* 51: M226-232, 1996.

210. **Thompson LV and Brown M.** Age-related changes in contractile properties of single skeletal fibers from the soleus muscle. *J Appl Physiol* 86: 881-886, 1999.

211. **Tinetti ME, Speechley M, and Ginter SF.** Risk factors for falls among elderly persons living in the community. *N Engl J Med* 319: 1701-1707, 1988.

212. **Titler M, Dochterman J, Picone DM, Everett L, Xie XJ, Kanak M, and Fei Q.** Cost of hospital care for elderly at risk of falling. *Nurs Econ* 23: 290-306, 279, 2005.

213. **Tuite DJ, Renstrom PA, and O'Brien M.** The aging tendon. *Scand J Med Sci Sports* 7: 72-77, 1997.

214. **Valour D and Pousson M.** Compliance changes of the series elastic component of elbow flexor muscles with age in humans. *Pflugers Arch* 445: 721-727, 2003.

215. **van den Bogert AJ, Gerritsen KG, and Cole GK.** Human muscle modelling from a user's perspective. *J Electromyogr Kinesiol* 8: 119-124, 1998.

216. **van Soest AJ and Bobbert MF.** The contribution of muscle properties in the control of explosive movements. *Biol Cybern* 69: 195-204, 1993.

217. **van Soest AJ and Casius LJ.** The merits of a parallel genetic algorithm in solving hard optimization problems. *J Biomech Eng* 125: 141-146, 2003.

218. **van Soest AJ, Schwab AL, Bobbert MF, and van Ingen Schenau GJ.** The influence of the biarticularity of the gastrocnemius muscle on vertical-jumping achievement. *Journal of Biomechanics* 26: 1-8, 1993.

219. **van Wegen EE, van Emmerik RE, and Riccio GE.** Postural orientation: age-related changes in variability and time-to-boundary. *Human Movement Science* 21: 61-84, 2002.

220. **Vandervoort AA.** Aging of the human neuromuscular system. *Muscle Nerve* 25: 17-25, 2002.

221. **Vandervoort AA, Kramer JF, and Wharram ER.** Eccentric knee strength of elderly females. *J Gerontol* 45: B125-128, 1990.

222. **Verdaasdonk BW, Koopman HFJM, Van Gils SA, and van der Helm FCT.** Bifurcation and stability nalysis in musculoskeletal systems: a study in human stance. *Biol Cybern* 91: 48-62, 2004.

223. **Wang Y, Asaka T, Zatsiorsky VM, and Latash ML.** Muscle synergies during voluntary body sway: combining across-trials and within-a-trial analyses. *Exp Brain Res* 174: 679-693, 2006.

224. **Weiner DK, Duncan PW, Chandler J, and Studenski SA.** Functional reach: a marker of physical frailty. *J Am Geriatr Soc* 40: 203-207, 1992.

225. **Wells JB.** Comparison of Mechanical Properties between Slow and Fast Mammalian Muscles. *J Physiol* 178: 252-269, 1965.

226. **Wickiewicz TL, Roy RR, Powell PL, and Edgerton VR.** Muscle architecture of the human lower limb. *Clin Orthop Relat Res*: 275-283, 1983.

227. **Wickiewicz TL, Roy RR, Powell PL, Perrine JJ, and Edgerton VR.** Muscle architecture and force-velocity relationships in humans. *J Appl Physiol* 57: 435-443, 1984.

228. **Wilkie DR.** The relation between force and velocity in human muscle. *J Physiol* 110: 249-280, 1950.

229. **Winter DA.** *A.B.C of balance during standing and walking*. Waterloo, Ontario: Waterloo Biomechanics, 1995a.

230. **Winter DA.** *Biomechanics and Motor Control of Human Movement*: John Wiley & Sons, 1990.

231. **Winter DA.** Human balance and posture control during standing and walking. *Gait & Posture* 3: 193-214, 1995b.

232. **Winter DA, Patla AE, Prince F, Ishac M, and Gielo-Perczak K.** Stiffness control of balance in quiet standing. *J Neurophysiol* 80: 1211-1221, 1998.

233. **Winter DA, Patla AE, Rietdyk S, and Ishac MG.** Ankle muscle stiffness in the control of balance during quiet standing. *J Neurophysiol* 85: 2630-2633, 2001.

234. **Winter DA, Prince F, and Patla AE.** Validity of the inverted pendulum model of balance in quiet standing. *Gait & Posture* 5: 153-154, 1997.

235. **Winters JM.** An improved muscle-reflex actuator for use in large-scale neuro-musculoskeletal models. *Ann Biomed Eng* 23: 359-374, 1995.

236. **Winters JM and Stark L.** Estimated mechanical properties of synergistic muscles involved in movements of a variety of human joints. *J Biomech* 21: 1027-1041, 1988.

237. **Winters JM and Stark L.** Muscle models: what is gained and what is lost by varying model complexity. *Biol Cybern* 55: 403-420, 1987.

238. **Woittiez RD, Huijing PA, and Rozendal RH.** Influence of muscle architecture on the length-force diagram. A model and its verification. *Pflugers Arch* 397: 73-74, 1983.

239. **Wolfson L, Judge J, Whipple R, and King M.** Strength is a major factor in balance, gait, and the occurrence of falls. *J Gerontol A Biol Sci Med Sci* 50 Spec No: 64-67, 1995.

240. **Wolfson LI, Whipple R, Amerman PM, and Kleinberg A.** Stressing the postural response: a quantitative method for testing balance. *J Am Geriatr Soc* 34: 845-850, 1986.

241. **Woollacott MH and Shumway-Cook A.** Changes in posture control across the life span--a systems approach. *Phys Ther* 70: 799-807, 1990.

242. **Woollacott MH, Shumway-Cook A, and Nashner LM.** Aging and posture control: changes in sensory organization and muscular coordination. *Int J Aging Hum Dev* 23: 97-114, 1986.

243. **Young A, Stokes M, and Crowe M.** The size and strength of the quadriceps muscles of old and young men. *Clin Physiol* 5: 145-154, 1985.

244. **Young A, Stokes M, and Crowe M.** Size and strength of the quadriceps muscles of old and young women. *Eur J Clin Invest* 14: 282-287, 1984.

245. **Zajac FE.** Muscle and tendon: properties, models, scaling, and application to biomechanics and motor control. *Crit Rev Biomed Eng* 17: 359-411, 1989.